THE UNIVERSITY
of EDINBURGH

Phospho-regulation of the spindle assembly checkpoint

Onur Sen

Thesis presented for the degree of Doctor of Philosophy

Wellcome Trust Centre for Cell Biology

University of Edinburgh

August 2015

Declaration

I declare that this thesis is composed entirely by myself and that the work presented is my own, except where contributions by others are clearly stated. The work has not been submitted for any other degree or professional qualification.

Onur Sen

August 2015

Abbreviations

APC/C	Anaphase promoting complex/cyclosome
ATP	Adenosine Triphosphate
bp	base pair
Bub	Budding uninhibited by benzimidazoles
DAPI	4',6-diamidino-2-phenylindole
DMSO	Dimethyl sulfoxide
FRAP	Fluorescence recovery after photobleaching
GFP	Green fluorescent protein
kDa	kilo Dalton
KT	Kinetochore
LB	Luria-Bertani
Mad	Mitotic arrest deficient
MCC	Mitotic checkpoint complex
PAGE	Polyacrylamide Gel Electrophoresis
PCR	Polymerase chain/Pure chance reaction
PMG	*Pombe* minimal medium
RNA	Ribonucleic acid
SDS	Sodium Dodecyl Sulphate
SPB	Spindle pole body
TAP	Tandem Affinity Purification
TE	Tris-EDTA
WT	Wild type
YES	Yeast extract supplemented

Abstract

Mitosis is a highly regulated process by which a cell duplicates and distributes its chromosomal DNA into two identical daughter cells equally. Equal distribution of the chromosomes is crucial for accurate propagation of genetic information. This is essential for maintaining viability and preventing genomic instability that can potentially lead to cancer. In order to avoid unequal distribution of chromosomes, cells employ a surveillance mechanism called the spindle assembly checkpoint (SAC). The SAC is an inhibitory signalling network, which delays segregation of chromosomes, until they have stably attached to spindle microtubules through their multi-protein platforms, known as kinetochores. The main target of the SAC is the anaphase promoter complex/ cyclosome (APC/C), an E3 ubiquitin ligase. Specifically APC/C and its activator Cdc20 are inhibited by the main effector of the SAC, called the mitotic checkpoint complex (MCC). The MCC consists of Cdc20, Mad2, Mad3 and Bub3 (except *S. pombe*) proteins, which are recruited to the unattached kinetochores to promote MCC assembly. Once the chromosomes stably attach to the spindle, the SAC is turned off, MCC disassembles, and APC/C^{Cdc20} is released from the inhibition. Activated APC/C^{Cdc20} then targets its two main substrates, securin and cyclin B, for proteasomal degradation, and thereby triggers anaphase onset and mitotic exit.

SAC signalling involves many protein components, whose activities are essentially regulated by direct protein-protein interactions and/ or post-translational modifications. One of these major modifications is phosphorylation, which is mediated by the SAC kinases such as Aurora B, Mps1 and Bub1. A number of studies have characterised SAC related substrates of Aurora B and Mps1 kinases in several model organisms. On the other hand, Bub1 kinase activity has been thought to play a key role in chromosome bi-orientation and more of an auxiliary role in SAC activation.

The aim of this study is to investigate the importance of Bub1 kinase activity for SAC response in fission yeast *Schizosaccharomyces pombe (S. pombe).* SAC activation assays, using various degrees of spindle perturbation, have demonstrated that Bub1 kinase activity plays an important role in SAC maintenance. In order to examine the pathways downstream of Bub1, we set out to indicate Bub1 substrates which may be involved in SAC signalling. According to studies in various species, Cdc20 appears to be a prominent candidate, whose phosphorylation by Cdk1 and Bub1 kinases has been reported to regulate its mitotic activity.

To investigate whether Cdc20 is phosphorylated by Bub1 *in vitro,* we purified recombinant *S. pombe* proteins from insect cells. Subsequent kinase assays identified Cdc20 as an *in vitro* substrate of Bub1, and the phosphorylated sites in Cdc20 were mapped by mass spectrometry. To address if this phospho-modification is involved in SAC regulation, phosphorylation mutants of Cdc20 were analysed in terms of their abilities to activate and silence SAC *in vivo*. Results show that phosphorylation of Cdc20 C-terminus promotes SAC maintenance in response to spindle damage. Furthermore, the mutations mimicking Bub1-mediated phosphorylation of Cdc20 C-terminus restore the SAC defects in the absence of Bub1 kinase activity.

In addition, we purified *S. pombe* mitotic checkpoint complex (MCC) from insect cells, and analysed the interactions between its components (Cdc20, Mad2 and Mad3) by cross-linking mass spectrometry. Crystal structure of *S.pombe* MCC has been determined recently, which lacks Mad3 C-terminus and flexible C-terminal tail of Cdc20. Using an MCC with full length Mad3, we identified novel interactions between the C-terminal tails Mad3 and Cdc20, which are in close proximity to the identified Cdc20 phosphorylation sites.

Briefly, in this study we confirm the previously known roles of Bub1 kinase activity (chromosome bi-orientation). Moreover, we propose a new pathway (in addition to the well-established H2A pathway) mediated by Cdc20, that may be important to maintain the SAC response.

List of Figures

Chapter 1: Introduction

1.1 The cell cycle of higher eukaryotes and fission yeast cell cycle 4

1.2 EM reconstructions of the human APC/C and its interaction with the MCC 6

1.3 Crystal structure of *S. pombe* MCC trimer 12

1.4 Expression of Cdc20 is dynamically regulated during the cell cycle 18

Chapter 3: Roles of Bub1 kinase activity in the SAC

3.1 Bub1 kinase activity is important for maintaining the SAC in *nda3-KM311* block 53

3.2 Bub1 kinase activity is required to ensure equal chromosome segregation 56

3.3 Bub1 kinase activity is required to delay premature anaphase in response to the microtubule drug CBZ 60

3.4 Bub1 kinase function is required to maintain the kinetochore localization of MCC components in response to CBZ 61

3.5 Bub1 kinase activity is not necessary for MCC formation in an unperturbed mitosis 65

3.6 Bub1 kinase activity is required to maintain the MCC-APC/C interaction in response to the microtubule drug CBZ 67

3.7 Speculative model for the regulation of SAC signalling by multiple factors in response to various degrees of spindle damage 73

Chapter 4: *In vitro* analysis of Bub1 kinase activity and interactions between the MCC components

4.1 Baculovirus transfer vectors cloned with MCC ΔN-term or Bub1 79

4.2 Purification of recombinant *S. pombe* SAC proteins from insect cells 80

4.3 Bub1 kinase autophosphorylates and phosphorylates Cdc20 *in vitro* 84

4.4 Cdc20 is phosphorylated *in vivo* during mitosis and *in vitro* by Bub1 87

List of Figures

Chapter 4: *In vitro* analysis of Bub1 kinase function and interactions between the MCC components

4.5 *In vivo* and *in vitro* phosphorylated Cdc20 sites are well-conserved 88

4.6 Recombinant MCC efficiently inhibits APC/C activity *in vitro* 91

4.7 Linkages between the regions of MCC components which were resolved in the crystal structure 95

4.8 MCC cross-linking data are consistent with the MCC crystal structure 96

4.9 Novel linkages between the regions of MCC components which were absent in the crystal structure 100

4.10 Mad2 and Mad3 may cooperate to sequester the APC/C activation domains of Cdc20 103

4.11 Marking of cdc20+ gene with an antibiotic resistance gene and inserting an internal tag 106

4.12 Cdc20 C-terminal mutants and the *bub1 kinase-dead* (*kd*) mutant used in this study. 110

Chapter 5: Roles of $Cdc20^{Slp1}$ phospho-regulation in the SAC

5.1 APC/C activating function of Cdc20 is not affected by either absent or constitutive phosphorylation of its C-terminus in an unperturbed mitosis 116

5.2 MCC formation is not affected by the absence of Cdc20 C-terminus phosphorylation in an unperturbed mitosis 118

5.3 MCC-APC/C interaction is not affected by the absence of Cdc20 C-terminus phosphorylation in an unperturbed mitosis 120

5.4 Constitutive phosphorylation of Cdc20 C-terminus results in a hyperactivated SAC response that is dependent on Mad2 124

5.5 Constitutive phosphorylation of Cdc20 C-terminus significantly increases the frequency of Mad3 kinetochore recruitment 125

List of Figures

Chapter 5: Roles of Cdc20^{Slp1} phospho-regulation in the SAC

5.6	MCC-APC/C interaction is not affected by the absence of Cdc20 C-terminus phosphorylation in response to the microtubule drug CBZ	128
5.7	Constitutive phosphorylation of Cdc20 C-terminus enhances MCC-APC/C interaction in response to the microtubule drug CBZ	129
5.8	Constitutive phosphorylation of Cdc20 C-terminus slightly enhances SAC activity in response to nda3-KM311 block	133
5.9	IR-motif of Cdc20 is required for an efficient Mad3-APC/C interaction	134
5.10	Constitutive phosphorylation of Cdc20 C-terminus does not impair Cdc20 function, yet slows down the SAC recovery	138
5.11	Lack of Cdc20 C-terminus phosphorylation does not affect Cdc20 turnover rate during metaphase arrest	140
5.12	Constitutive phoshorylation of Cdc20 C-terminus decreases Cdc20 turnover rate during metaphase arrest	141
5.13	Mimicking the phosphorylation of a putative Bub1 site in Cdc20 C-terminus rescues the anaphase delay defect of *bub1-kinase dead*	145
5.14	Mimicking the phosphorylation of a putative Bub1 site in Cdc20 C-terminus rescues the Mad3 kinetochore localization defect of *bub1-kinase dead*	146, 147

List of Tables

Chapter 2: Materials and Methods

2.1	Fission yeast strains used in this study	41
2.2	Plasmids used in this study	42
2.3	Primers used in this study	43

Chapter 4: *In vitro* analysis of Bub1 kinase function and interactions between the MCC components

4.1	Linkages between the regions of MCC components which were resolved in the crystal structure	97
4.2	Novel linkages through BS3 between the regions of MCC components which were absent in the crystal structure	101
4.3	Novel linkages through EDC between the regions of MCC components which were absent in the crystal structure	102

Table of Contents

Abbreviations ..... **I**

Abstract ..... **II**

List of Figures ..... **IV**

List of Tables ..... **VII**

Chapter 1: Introduction **1**

1.1 The cell division cycle 1

1.2 Mitosis 2

1.3 Anaphase promoting complex/cyclosome (APC/C) 5

1.4 The spindle assembly checkpoint (SAC): overview 7

1.4.1 Spindle assembly checkpoint activation at kinetochores 8

1.4.2 Assembly of the mitotic checkpoint complex (MCC) 10

1.4.3 Is the SAC response dependent on kinetochores? 11

1.5 Mechanisms underlying APC/C^{Cdc20} inhibition by the SAC 13

1.5.1 Inhibition of APC/CCdc20 through MCC 13

1.5.2 Inhibition of APC/C^{Cdc20} through Cdc20 turnover 15

1.5.3 Regulation of APC/C^{Cdc20} activity through phosphorylation 16

1.6 Roles of Bub1 kinase in mitosis 19

1.6.1 Roles of Bub1 that do not require its kinase activity 19

1.6.2 Roles of Bub1 that require its kinase activity 20

1.6.2.1 Bub1 kinase activity for chromosome bi-orientation 20

1.6.2.2 Bub1 kinase activity for a robust SAC response 21

1.6.2.2.1 Bub1 kinase activity in budding yeast SAC 21

1.6.2.2.2 Bub1 kinase activity in fission yeast SAC 22

1.6.2.2.3 Bub1 kinase activity in *Xenopus* SAC 23

Table of Contents

1.6.2.2.4 Bub1 kinase activity in human SAC 25

1.7 SAC silencing and recovery from a SAC mediated arrest 27

Aims 29

Chapter 2: Materials and Methods 30

2.1 Buffers and solutions 30

2.2 Growth media 31

2.3 Insect cell methods 33

2.3.1 Cloning target DNAs into a transfer vector 33

2.3.2 Integration of the transfer vector into the baculoviral genome 33

2.3.3 Initial insect cell infection with bacmid and generation of virus 34

2.3.4 Virus amplification and test expression 34

2.3.5 Protein expression 35

2.3.6 Protein purification 36

2.4 DNA methods 37

2.4 Fission yeast methods 38

2.4.1 Yeast transformation 38

2.4.2 Yeast genomic DNA extraction 39

2.4.3 Mitotic arrests 39

2.5 Protein methods 44

2.5.1 Immunoprecipitations 44

2.5.2 SDS-PAGE 44

2.5.3 Immunoblotting 45

2.5.4 *In vitro* kinase assays 46

2.5.5 Mass-spectrometry 47

2.5.6 APC/C ubiquitination assays 47

Table of Contents

Chapter 3: Roles of Bub1 kinase activity in the spindle assembly checkpoint... 49

3.1 Overview 49

3.2 Analysis of Bub1 kinase function in response to microtubule depolymerisation by *nda3-KM311* allele 51

3.2.1 Analysis of Bub1 kinase function in maintaining SAC arrest at metaphase 51

3.2.2 Analysis of Bub1 kinase function in recovering from the SAC arrest at metaphase 54

3.3 Analysis of Bub1 kinase function in response to microtubule depolymerisation by an anti-microtubule drug 57

3.3.1 Analysis of mitotic progression rate and kinetochore localization of MCC components in the presence of an anti-microtubule drug 58

3.3.2 Analysis of MCC formation in an unperturbed mitosis 64

3.3.3 Analysis of MCC-APC/C interaction in the presence of an anti-microtubule drug 66

3.4 Discussion 68

3.4.1 Bub1 kinase activity is important but not necessary for the SAC response to prolonged spindle damage 68

3.4.2 Bub1 kinase activity is necessary for chromosome bi-orientation..... 69

3.4.3 Bub1 kinase activity is necessary to maintain anaphase delay and kinetochore recruitment of SAC proteins in response to the anti-microtubule drug CBZ 70

3.4.4 Bub1 kinase activity is not necessary for MCC assembly, yet essential to maintain MCC-APC/C interaction 75

Table of Contents

Chapter 4: *In vitro* analysis of Bub1 kinase activity and interactions between the MCC components 76

4.1 Overview 76

4.2 Identification of Bub1 kinase substrates *in vitro* 78

4.2.1 Purification of Bub1 kinase and its putative substrates from insect cells 78

4.2.2 *In vitro* Bub1 kinase assay 83

4.2.3 Identification of *in vitro* phosphorylation sites using mass spectrometry 85

4.3 Analysis of interactions between the recombinant MCC components: Cdc20, Mad2 and Mad3 89

4.3.1 *In vitro* analysis of recombinant MCC as an APC/C inhibitor 89

4.3.2 Cross-linking mass spectrometry analysis of the interactions between the MCC components 92

4.4 Marking of cdc20+ gene with an antibiotic resistance and inserting an internal tag 104

4.5 Generating phosphorylation site mutants of Cdc20 107

Chapter 5: Roles of $Cdc20^{Slp1}$ phospho-regulation in the SAC 111

5.1 Overview 111

5.2 Analysis of Cdc20 C-terminal phosphorylation mutants under unperturbed conditions 114

5.2.1 Progression through an unperturbed mitosis 114

5.2.2 MCC formation in an unperturbed mitosis 117

5.2.3 MCC-APC/C interaction in an unperturbed mitosis 119

5.3 Analysis of Cdc20 C-terminal phosphorylation site mutants in the context of the SAC activated by an anti-microtubule drug 121

Table of Contents

5.3.1 Analysis of mitotic timing and Mad3 kinetochore localisation in the presence of an anti-microtubule drug 121

5.3.2 Analysis of the MCC-APC/C interaction in the presence of an anti-microtubule drug 126

5.4 Analysis of Cdc20 C-terminal phosphorylation mutants under *nda3-KM311*-mediated microtubule depolymerisation 130

5.4.1 Metaphase arrest mediated by *nda3-KM311* 131

5.4.2 Recovery from *nda3-KM311*-mediated metaphase arrest 135

5.4.3 Turnover rates of Cdc20 phospho – mutants during *nda3-KM311*-mediated metaphase arrest 139

5.5 Can the Cdc20 C-terminal phospho-mimicking mutation rescue the SAC defects of *bub1-kd* allele? 142

Chapter 6: Final discussion 151

6.1 Cdc20 C-terminal phosphorylation mutants retain their mitotic functions in an unperturbed mitosis 152

6.2 Constitutive phosphorylation of Cdc20 C-terminus slightly enhances the SAC arrest in response to penetrant spindle damage (*nda3-KM311*) 153

6.3 IR-motif of Cdc20 is required for recovering from the SAC arrest (*nda3-KM311*) and progressing into anaphase 154

6.4 Constitutive phosphorylation of Cdc20 C-terminus enhances the SAC response to the microtubule depolymerising drug CBZ 157

6.5 Mimicking phosphorylation of Cdc20 C-terminus by Bub1 rescues the SAC defects in the absence of Bub1 kinase activity 161

6.6 Relevance of Bub1 kinase activity and Cdc20 to therapeutic approaches 165

References 166

Acknowledgements 178

Chapter 1: Introduction

1.1 The cell division cycle

To grow and proliferate, all organisms require to produce genetically identical daughter cells through a process known as cell division. To maintain genetic identity, accurate duplication of cell contents and an equal distribution of those contents into two daughter cells must be ensured during every cell division. The sequence of events between two successive cell divisions is called the cell cycle.

The eukaryotic cell cycle can be split up into four distinct phases: G1, S, G2 and M (Hartwell & Weinert, 1989). Each cell division leads to G1 phase (gap 1), during which the cell monitors its mass and the environmental conditions before deciding whether to stay in the cell cycle or to enter a prolonged non-dividing phase (G_0).

Once the cell reaches a certain size in the availability of nutrients, it commits to a new cell cycle and progresses into S phase (synthesis) (Sherlock & Rosamond, 1993). In S phase, the genetic content of the cell is replicated through DNA synthesis and centrosomes are duplicated (Adams & Kilmartin, 2000), which is followed by G2 phase. G1, S and G2 phases define interphase, which form the majority of the cell cycle. In G2 (gap 2) the cell prepares for the M phase, in which segregation of duplicated chromosomes and their distribution into two daughter cells take place.

Transition between cell cycle phases is largely unidirectional. This requires the activity of a family of enzymes called cyclin-dependent kinases (Cdks), which regulate progression through the cell cycle (Hartwell, Culotti, Pringle, & Reid, 1974). Cdks are conserved serine/threonine protein kinases, which are present at constant levels throughout the cell cycle. Cdks are activated by binding to proteins called cyclins. The abundance of cyclins at a given time in the cell are tightly regulated by gene expression and proteolysis (Morgan 1997; Murray 2004).

In higher eukaryotes, there are cyclins that activate different Cdks during particular phases of the cells cycle: G1 (cyclin D), S phase (cyclins E and A) and mitosis (cyclins B and A) (Diffley, 2004) (Figure 1.1A). On the other hand fission yeast *Schizosaccharomyces pombe* (*S. pombe*) has only one type of Cdk ($Cdk1^{Cdc2}$) that is involved in G1/S and G2/M transition (Figure 1.1B) and three type of cyclins: G1 (cig1), G1/S (cig2), G2/M and M (cyclin B^{cdc13}) (Nurse et al., 1976, Nurse and Bissett,

1981). Although Cdc2 is constitutively expressed throughout the cell cycle, its activity is regulated by binding of cyclin B^{Cdc13}, phosphorylation by Wee1 kinase and dephosphorylation by Cdc25 phosphatase. Early in G2 phase, low levels of Cyclin B, and inhibitory phosphorylation by Wee1 keep Cdk1 inactive (Fattaey & Booher, 1997). Towards the end of G2 phase, Cyclin B levels and Cdc25 phosphatase activity increase. Hence, binding of Cyclin B and reversal of Wee1 mediated inhibitory phosphorylation by Cdc25 phosphatase activate Cdk1, which leads to the entry into mitosis. Moreover, the active Cdk1-Cyclin B complex then phosphorylates Wee1 kinase (to inhibit) and Cdc25 phosphatase (to further activate), in order to generate a positive-feedback loop for its own activation (Enoch & Nurse, 1990). In mitosis, Cdk1-Cyclin B complex catalyses the main events. Before the duplicated chromosomes separate, Cyclin B levels decrease through proteasomal degradation, thereby Cdk1 becomes inactive again (Sullivan & Morgan, 2007).

1.2 Mitosis

Mitosis is a short, but highly regulated process which results in the generation of two identical daughter cells. Mitosis comprises six stages in higher eukaryotes: prophase (not in yeast), pro-metaphase, metaphase, anaphase (anaphase A and anaphase B) and telophase/cytokinesis.

After S phase, replicated chromosomes (sister chromatids) are linked together by sister DNA catenation and protein complexes called cohesin (Uhlmann, Wernic, Poupart, Koonin, & Nasmyth, 2000). Upon entry into prophase chromosomes condense. Then duplicated centrosomes (spindle pole bodies in yeast) move apart and nucleate the mitotic spindle. The mitotic spindle is a bipolar structure comprising microtubules, which rapidly polymerise and depolymerise until stabilised end-on attachments (microtubule plus ends) are formed with protein assemblies called kinetochores (Cheeseman and Desai, 2008). Kinetochores are protein complexes that are found on centromeric regions of chromosomes and connect with microtubules emanating from each of the two poles. In prometaphase, the nuclear envelope breaks down (unlike fission yeast that has a closed mitosis, in which contents of the nucleus remain compartmentalised from the cytoplasm throughout the cell cycle), thereby the mitotic spindle attaches to sister-chromatids through their kinetochores (Sazer, Lynch, &

Needleman, 2014). With this stabilised attachment, captured chromatids are tethered to the centrosomes/ spindle pole bodies. During metaphase, sister chromatids align at the metaphase plate. Once all sister chromatids are bi-oriented, they are captured by microtubules emanating from opposite spindle poles, the cell progresses into anaphase. In anaphase A, the cohesin complex that links sister-chromatids together disassembles. In anaphase B, centrosomes/spindle pole bodies move apart from each other. Thereby, sister-chromatids are pulled to opposite spindle poles, which results in their separation (Elmore, Beckley, Chen, & Gould, 2014). During telophase the spindle is disassembled, chromosomes de-condense and the nuclear envelope begins to reform. Finally in cytokinesis, the cell is divided into two daughter cells with identical genetic material (David, 2010).

However, during prometaphase chromosomes are not bi-oriented straightaway. Until attaining bi-orientation, erroneous associations between microtubules and sister kinetochores occur, such as syntelic (kinetochores attach to microtubules from the same pole) and merotelic (a kinetochore attaches to microtubules from both poles) attachments (Musacchio & Salmon, 2007). If the cell fails to correct these attachment errors, chromosomes will segregate unequally, which results in aneuploidy (abnormal number of chromosomes). To establish bi-orientation, erroneous kinetochore-microtubule attachments are destabilized (error correction) by Aurora B kinase (Kalantzaki et al., 2015), which leads to formation of unattached kinetochores. Then unattached kinetochores are detected by a surveillance mechanism called the spindle assembly checkpoint (SAC) that delays chromosome segregation (anaphase onset), until all kinetochores attain biorientation (Conly L. Rieder, Cole, Khodjakov, & Sluder, 1995).

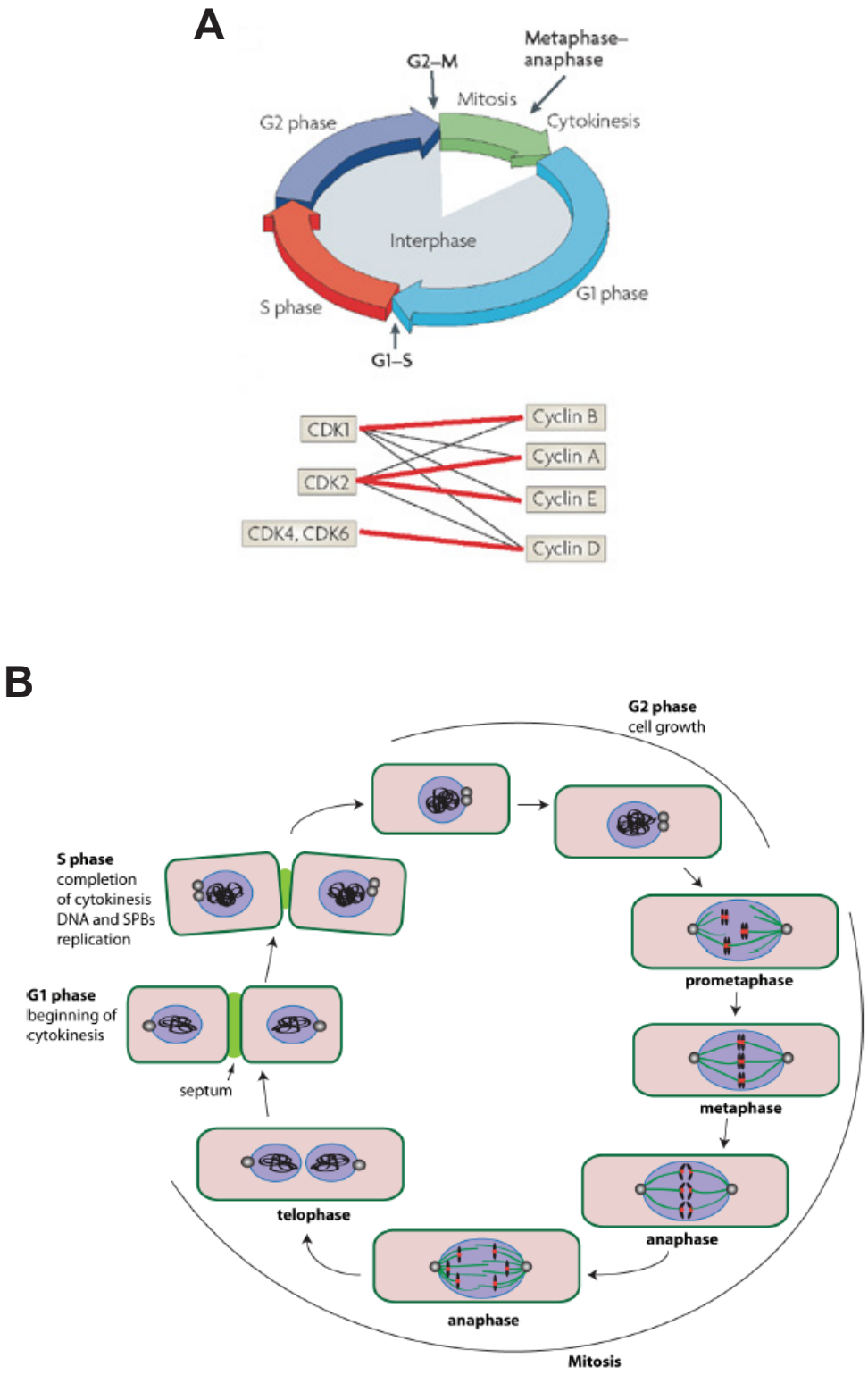

Figure 1.1 The cell cycle of higher eukaryotes and fission yeast cell cycle

(A) An overview of the cell division cycle of higher eukaryotes controlled by multiple cyclin-dependent kinases (Cdk) and cyclins. Model was adapted from Hochegger, Takeda, & Hunt, 2008 (B) An overview of fission yeast (S. pombe) cell cycle, which is driven by the activity of a single Cdk (cdc2). Note that fission yeast G2 phase takes up 70 % of its cell cycle, which is not reflected in the model. (See the text for details on the cyclin-dependent kinase and cyclins). Model was adapted from A. Sochaj, Hardwick lab, PhD thesis, 2013.

1.3 Anaphase promoting complex/cyclosome (APC/C)

The anaphase promoting complex/cyclosome (APC/C) is a large (1.5-MDa) multi-subunit (13 subunits) E3 ubiquitin ligase (Figure 1.2A) that regulates progression through, and exit from mitosis. In the absence of APC/C activity, cells cannot separate their sister chromatids in anaphase, exit from mitosis or divide into two daughter cells (D. Barford, 2011). The APC/C triggers anaphase onset by ubiquitinating two inhibitors of the transition to anaphase: securin and Cyclin B. Securin is a protein inhibitor of separase, a protease that cleaves the Cohesin subunit SCC1 (Uhlmann et al., 2000). Once securin is degraded, separase cleaves SCC1 which results in disassembly of Cohesin and sister chromatid segregation. Reduction in cyclin B levels are also required for entry into anaphase, (to relieve inhibition of separase by Cdk1) and exit from mitosis, that is maintained by Cyclin B- Cdk1 complex (Holland & Taylor, 2006).

The temporal regulation of APC/C activity is achieved through a combination of two structurally related activator proteins, Cdc20 and Cdh1 (Kraft et al., 2003). Cdc20 activates the APC/C during early mitosis, when APC/C is phosphorylated by Cdk1, which enhances its affinity for Cdc20 (Rudner & Murray, 2000). However, Cdk1-mediated phosphorylation of Cdc20 prevents it from activating APC/C in a C-box dependent manner; therefore dephosphorylation of Cdc20 is required for its interaction with and activation of APC/C (Labit et al., 2012). Cdh1 activity is low during mitosis due to its Cdk1 dependent phosphorylation. Cdh1 activates APC/C in late mitosis and G1 phase (Kramer, Scheuringer, Podtelejnikov, Mann, & Peters, 2000). APC/C activators utilise two conserved sequence motifs for APC/C binding: the C-box, located toward the N-terminus and a C-terminal IR motif (Figure 1.2A) (D. Barford, 2011; Chang, Zhang, Yang, McLaughlin, & Barford, 2015; Thornton et al., 2006). Upon binding, the activators recruit APC/C substrates to the catalytic site of APC/C. The recognition of APC/C substrates by co-activators is predominantly achieved through two destructions motifs (degrons) found on the substrates: D-box and KEN-boxes (J. L. Burton & Solomon, 2001). Cyclin B and securin are included in the APC/C substrates recognized through D-box and KEN-box, which is the reason for APC/C to be the main target of the SAC.

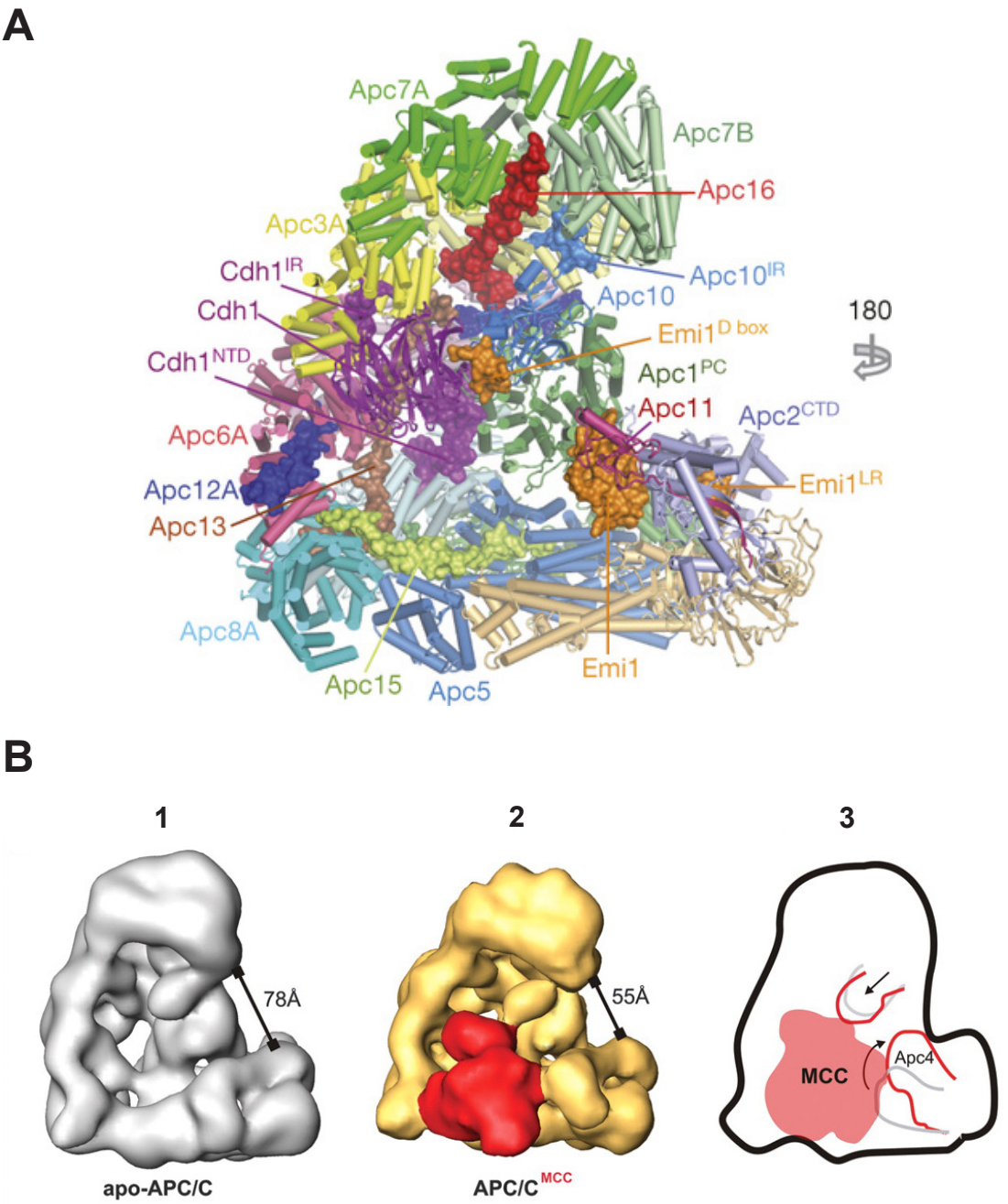

Figure 1.2 EM reconstructions of the human APC/C and its interaction with the MCC

(A) Atomic structure of the human anaphase promoting complex (APC/C) interacting with Cdh1 (APC/C coactivator) and Emi1 (APC/C inhibitor), indicated by electron microscopy (EM). Large subunits are shown in cartoon, whereas the four small subunits, Emi1, Cdh1NTD, Cdh1IR and Apc10IR, are shown as surface representations. Emi1 interacts with the substrate-recognition and catalytic modules Note that both Cdh1 and Apc10 (APC/C subunit) contain the IR (isoleucine, arginine) motif. The figure was taken from (Chang, Zhang, Yang, McLaughlin, & Barford, 2015). **(B)** APC/C subunit topology and structural changes upon MCC binding indicated by electron microscopy (EM): (1) The apo-APC/C structure in its most open conformation; (2) The APC/C-MCC structure with a closed conformation; (3) Conformational changes induced by MCC binding to APC/C. The figure was adapted from (Herzog, 2009).

1.4 The spindle assembly checkpoint (SAC): overview

Components of the spindle assembly checkpoint (SAC) were first identified in budding yeast (*Saccharomyces cerevisiae*) screens for mutants that failed to delay chromosome segregation upon treatment with a microtubule depolymerising drug, called benomyl (Hoyt et al., 1991; Li and Murray, 1991).

Major components of the SAC are the Bub (budding uninhibited by benzimidazole) proteins: the kinase Bub1 (Bernard et al., 1998; Roberts et al., 1994) and Bub3 (Taylor et al., 1998; Vanoosthuyse et al., 2004) and the Mad (mitotic arrest deficient) proteins: Mad1 (Hardwick and Murray, 1995), Mad2 (Chen et al., 1999; He et al., 1997), Mad3 (Hardwick et al., 2000; Millband and Hardwick, 2002). Another kinase component of the SAC is Mps1 (mono polar spindle 1) that was first identified in a budding yeast screen for mutants with spindle pole duplication defects (Winey et al., 1991).

The SAC proteins are recruited to unattached kinetochores, where the assembly of a diffusible checkpoint effector, known as mitotic checkpoint complex (MCC), is catalysed (Sudakin, Chan, & Yen, 2001). MCC consists of Mad2, Mad3 (BubR1 in animals) and Cdc20 (Slp1 in *S. pombe*) (plus Bub3 in budding yeast and animals). Once assembled, MCC delays anaphase onset through the inhibition of Anaphase promoting complex/cyclosome (APC/C). APC/C mediates poly-ubiquitination of cyclin B and securin (inhibitors of anaphase onset and mitotic exit), and thereby targeting them for degradation by 26S proteasome. By inhibiting APC/C, the SAC delays anaphase onset, and provides time for the aberrant kinetochore-microtubule attachments to be corrected. When the last kinetochore is stably attached in a bi-oriented manner, the SAC is satisfied, and the MCC disassembles (SAC silencing). Once the APC/C is active again, it targets cyclin B and securin for proteasomal degradation, which results in chromosome segregation and mitotic exit (Musacchio & Salmon, 2007).

1.4.1 Spindle assembly checkpoint activation at kinetochores

Laser ablation studies have indicated that even a single unattached kinetochore is sufficient to activate the "wait anaphase" signal mediated by the SAC (C L Rieder, Cole, Khodjakov, & Sluder, 1995). Kinetochore localization of checkpoint proteins has been reported to be important for SAC activation by many studies (London & Biggins, 2014a; Mchedlishvili et al., 2012; Rischitor, May, & Hardwick, 2007; Sharp-Baker & Chen, 2001; Taylor & McKeon, 1997; Vanoosthuyse, Valsdottir, Javerzat, & Hardwick, 2004). However, the precise mechanisms regulating their recruitment was unknown until recently. Recent studies have demonstrated that the core kinetochore protein KNL1 (Spc7 in fission yeast, Spc105 in budding yeast) recruits BUB proteins: Bub1, BubR1 (Mad3 in *S. pombe*) and Bub3 at unattached kinetochores (Kiyomitsu, Obuse, & Yanagida, 2007; London, Ceto, Ranish, & Biggins, 2012; Shepperd et al., 2012a; Yamagishi, Yang, Tanno, & Watanabe, 2012).

KNL1 contains conserved 'MELT'- like ([M/I/ L/ V]-[E/D]-[M/I/L/V]-T) motifs. It has been shown that the phosphorylation of the threonine residues on the MELT-like motifs by Mps1 (and polo-like kinase 1, plk1, in humans (von Schubert et al., 2015)) is required for kinetochore localization of Bub3, Bub1 and Mad3 (London et al., 2012; Shepperd et al., 2012a; Yamagishi et al., 2012). Additional crystallisation studies revealed that this phosphorylation is required for a tight interaction between KNL1 and Bub3, suggesting that Bub3 recruitment to KNL1 may be the key step in localizing Bub1-Bub3 complex at kinetochores (Primorac et al., 2013). Furthermore, Bub1 contributes to stabilizing the KNL1-Bub3 interaction *in vitro* (Primorac et al., 2013), which is in line with the finding that Bub1 is important for *in vivo* localization of Bub3 (Vanoosthuyse et al., 2004).

On the other hand, the mechanism of BubR1 (Mad3 in yeast) kinetochore recruitment remains unsolved. BubR1 (Mad3) may not be localising through the Bub3-KNL1 interaction, as it has not been found to stabilize the KNL1-Bub3 interaction (Krenn, Overlack, Primorac, Van Gerwen, & Musacchio, 2014). Instead, Mad3 recruitment has been demonstrated to depend on Bub1 in fission yeast (Millband & Hardwick, 2002). This raises the possibility that Mad3 may be directly recruited by Bub1 through heterodimerization (D'Arcy, Davies, Blundell, & Bolanos-Garcia, 2010).

This is consistent with the observation that ectopically localized fission yeast Bub1 recruits Mad3 (Rischitor et al., 2007). On the other hand, a Mad3-Bub3 complex at high levels has been observed in budding yeast (Hardwick, Johnston, Smith, & Murray, 2000).

Even though Bub3–Bub1 recruitment to kinetochores is required for the spindle assembly checkpoint (except in fission yeast), this localization does not always correlate with SAC activation. For instance, Bub1 has been observed on early anaphase kinetochores, which do not signal the SAC anymore (Sharp-Baker & Chen, 2001). On the other hand, kinetochore recruitment of Mad1-Mad2 heterodimer has been reported to strictly correlate with the SAC signalling (Maldonado & Kapoor, 2011). This implies that association of Mad1-Mad2 heterodimer with kinetochores is an important step in the SAC activation.

As for the kinetochore receptor of Mad1-Mad2, a budding yeast study reported that Mad1 interacts with Bub1, and is dependent on an RLK motif that is present in Mad1 (Brady & Hardwick, 2000). Mutation of this Mad1 motif or Bub1 depletion abrogated kinetochore recruitment of Mad1 in budding yeast and *Caenorhabditis elegans* (London & Biggins, 2014a; Moyle et al., 2014). Moreover, *in vitro* association of budding yeast Mad1 with kinetochores was found to require Mps1-mediated phosphorylation of Bub1 (London & Biggins, 2014a). Taken together, these findings imply that Mps1-mediated phosphorylation of KNL1 (Spc7, Spc105) and Bub1 may be responsible for establishing a link between Bub (Bub1, Bub3, BubR1 – Mad3 -) and Mad (Mad1 and Mad2) proteins at unattached kinetochores in budding yeast.

Once localized at unattached kinetochores, Mad1 recruits Mad2 and induces a conformational change; Mad1 converts it to closed Mad2 (C-Mad2), which is one of the two distinct conformations that Mad2 adopts. When unbound to Mad1, it adopts an open conformation (O-Mad2), whereas upon binding to Mad1 (or Cdc20) closed conformation (C-Mad2) is created through the movement of two β-sheets across the face of Mad2. Upon mitotic entry, Mad1-C-Mad2 complex localizes at kinetochores, recruits O-Mad2 from cytosol, and converts it to C-Mad2 that has a higher affinity for binding Cdc20 (De Antoni et al., 2005). This leads to the formation of C-Mad2-Cdc20 complex (Vink et al., 2006), which is the first step in MCC assembly. A fluorescence

recovery after photobleaching (FRAP) analysis in human cells has demonstrated that Cdc20 localizes at kinetochores with a fast turnover rate (Bonnie J Howell et al., 2004).

1.4.2 Assembly of the mitotic checkpoint complex (MCC)

MCC is the ultimate effector of the SAC that inhibits the APC/C in the cytoplasm (nucleoplasm in yeast which have closed mitosis). It has been suggested to be assembled from two sub-complexes, the C-Mad2-Cdc20 complex and the Mad3/BubR1-Bub3 complex (Musacchio & Salmon, 2007). While formation of C-Mad2-Cdc20 complex is catalysed by unattached kinetochores, Mad3/BubR1-Bub3 complex exists throughout the cell cycle in budding yeast (Hardwick et al., 2000). Recently, the crystal structure of the fission yeast MCC, that consists of Cdc20, Mad2 and Mad3, has been solved (Chao, Kulkarni, Zhang, Kong, & Barford, 2012a).

It has been established that Mad2 is essential for Cdc20 to bind Mad3/BubR1 (Janet L. Burton & Solomon, 2007; Hardwick et al., 2000; Nilsson, Yekezare, Minshull, & Pines, 2008). In addition, it has been demonstrated in yeast, flies and human cells that the N-terminal KEN box in Mad3/BubR1 (KEN20 in fission yeast) is necessary for MCC formation (King, van der Sar, & Hardwick, 2007; Pablo Lara-Gonzalez & Taylor, 2012; Sczaniecka et al., 2008).

The MCC crystal structure has revealed that the N-terminal KEN box of Mad3 adopts a helix-loop-helix structure, and exhibits direct interactions with both Mad2 and Cdc20 (Figure 1.3A and B) (Chao et al., 2012a). This is consistent with the findings that Mad2 is required for the Mad3/BubR1-Cdc20 interaction. In addition, the N-terminal TPR domains in Mad3 also directly interact with Cdc20. This is in line with the observation that mutating these domains in Mad3/BubR1 abolishes its binding to Cdc20 (P. Lara-Gonzalez, Scott, Diez, Sen, & Taylor, 2011). It was observed that only the closed conformation of Mad2 (C-Mad2) is capable of binding to Mad3. Intriguingly, the C-Mad2 bound to Cdc20 interacts with Mad3 through the same surface that it dimerises with O-Mad2 (Chao et al., 2012a). In other words, when Mad2 incorporates into the MCC, it is not able to bind O-Mad2 anymore, as Mad3 competes for the same region of C-Mad2. This implies that, once formed part of the MCC, C-Mad2 is not likely to catalyse formation of additional Mad2-Cdc20 complexes.

1.4.3 Is the SAC response dependent on kinetochores?

Although the SAC signalling network is widely associated with unattached kinetochores, some observations argue against the strict requirement for kinetochore localization of checkpoint proteins for a SAC response. For instance, MCC can still assemble in budding yeast strains with mutated Ndc10, a protein necessary for kinetochore function (Fraschini et al., 2001). Moreover, in fission yeast although Bub3 is required for kinetochore recruitment of Bub1, Mad3, Mad1 and Mad2, it is not essential for MCC-APC/C interaction in the presence of a microtubule depolymerising drug (S. Heinrich, Windecker, Hustedt, & Hauf, 2012; Vanoosthuyse, Meadows, van der Sar, Millar, & Hardwick, 2009; Windecker, Langegger, Heinrich, & Hauf, 2009). However, although SAC signals can be amplified without kinetochore recruitment of the checkpoint proteins, their kinetochore localisation is still required for a full SAC response, as 15% of *bub3* null cells failed to maintain a robust SAC arrest upon complete microtubule depolymerization (Vanoosthuyse et al., 2009). On the other hand Bub3 is essential for the SAC signalling in budding yeast (Hardwick et al., 2000).

Similar observations have been made in mammalian cells. Although BubR1 (Mad3) interacts with Bub3 throughout the cell cycle, Bub3 is not necessary either for the MCC assembly, or for the ability of Mad2 and BubR1 to inhibit APC/C^{Cdc20} activity *in vitro* (P. Lara-Gonzalez et al., 2011; Tang, Bharadwaj, Li, & Yu, 2001). Even though Bub3 may not be essential for *in vitro* interaction of BubR1 (Mad3) with Mad2 and Cdc20, or APC/C inhibition, in cellular context the ability of BubR1 to bind Bub3 (and to localize at kinetochores) is required for an efficient SAC response (Elowe et al., 2010; P. Lara-Gonzalez et al., 2011).

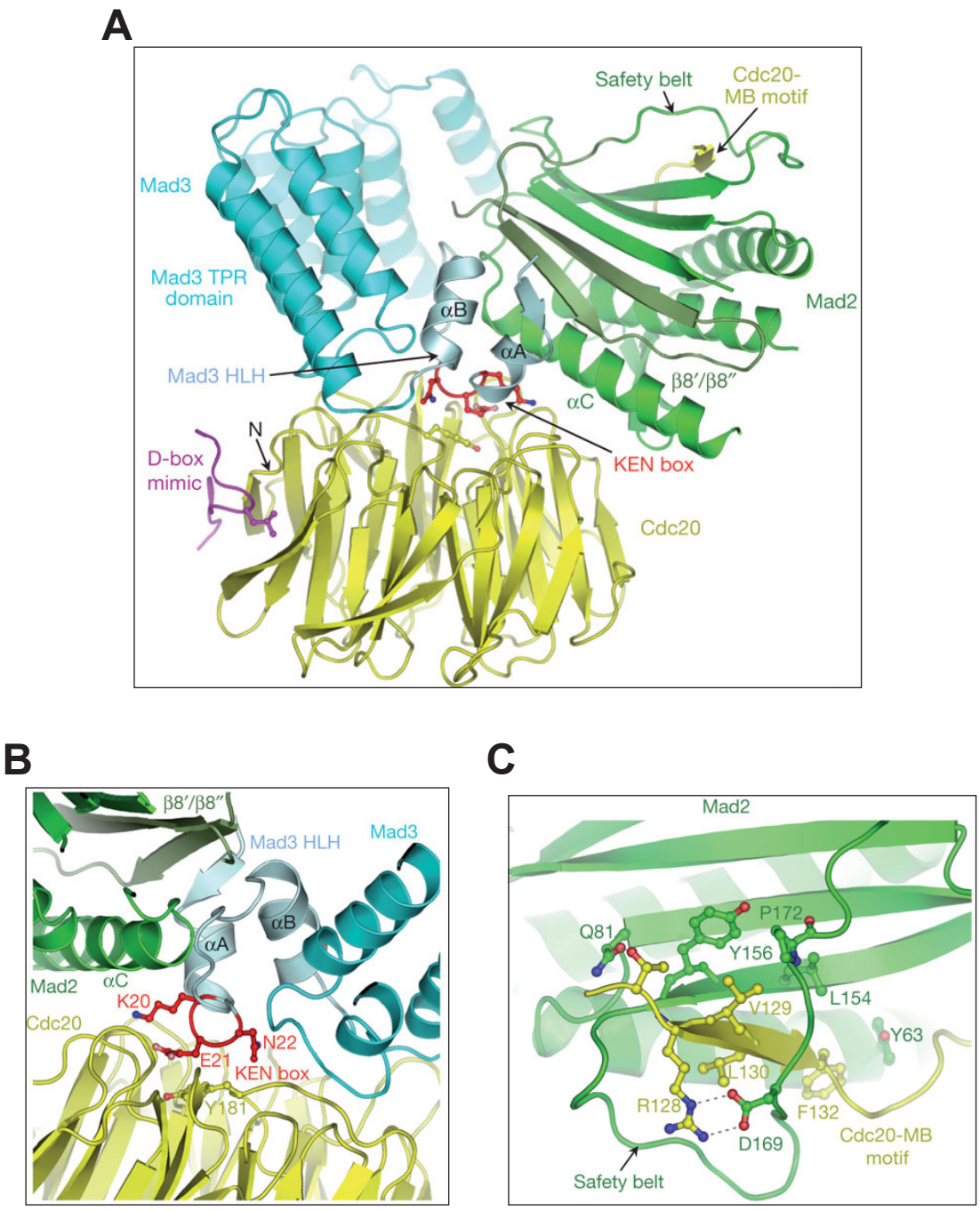

Figure 1.3 Crystal structure of *S. pombe* MCC trimer

(A) Cartoon representation of the fission yeast mitotic checkpoint complex: Cdc20 ΔN-term (yellow) lacking the first 86 amino acids; closed Mad2 (C-Mad2) (green) and Mad3 ΔC-term (blue) lacking last 87 amino acids, 224-310. The N-terminal KEN box is shown in red, located in the helix-loop-helix (HLH) motif of Mad3. The N-terminus of the WD40 domain is indicated. **(B)** Details of the Mad3 HLH interaction with Mad2 and Cdc20. **(C)** Mad2-binding motif (MB motif) of Cdc20 bound to the Mad2 safety belt**.** Cartoon images were adapted from Chao, Kulkarni, Zhang, Kong, & Barford, 2012.

1.5 Mechanisms underlying APC/C^{Cdc20} inhibition by the SAC

1.5.1 Inhibition of APC/C^{Cdc20} through MCC

According to the early observations Mad2 has been considered as a key inhibitor of anaphase onset, as it binds Cdc20 directly and prevents it from activating APC/C (Fang, Yu, & Kirschner, 1998; Li, Gorbea, Mahaffey, Rechsteiner, & Benezra, 1997). Consistent with this, Mad2 overexpression has been reported to activate the SAC in several model organisms (He, Patterson, & Sazer, 1997; Li et al., 1997). Indeed, a recent experiment in budding yeast has demonstrated that tethering Mad2 to Cdc20 delayed anaphase onset, which was partially dependent on Mad3 (Lau & Murray, 2012).

On the other hand, recent investigations have indicated that Mad3/BubR1 may be the key APC/C inhibitor, instead of Mad2. First of all, Mad2 alone requires to be added in very high amounts with respect to Cdc20, to be able to inhibit the APC/C *in vitro* (Fang et al., 1998; Tang et al., 2001). Moreover, Mad2 has been observed to bind APC/C^{Cdc20} *in vitro* without significantly affecting its activity (P. Lara-Gonzalez et al., 2011). Importantly, Mad2 is not always present at the same amounts as the other components of the MCC (Mad3/ BubR1 and Cdc20) are under different mitotic conditions. For example, in the presence of nocodazole (many kinetochores are unattached in response to microtubule depolymerisation) Mad2 is easily detectable as an MCC component. Whereas in the presence of taxol (only a few kinetochores are activating the SAC in response to stabilized microtubules) much less Mad2 is detected in the MCC. This finding suggests that as well as the MCC (Mad2, Mad3/BubR1, Cdc20), the Mad3/BubR1-Cdc20 complex is also a viable APC/C inhibitor in human cells (Westhorpe, Tighe, Lara-Gonzalez, & Taylor, 2011).

There is growing evidence that Mad3/BubR1 may be acting as a ‘pseudosubstrate’ to inhibit APC/C^{Cdc20} (Janet L. Burton & Solomon, 2007). Recent structural studies have demonstrated that D-box substrates bind at the bi-partite D-box receptor formed between the activator (Cdc20 or Cdh1) and the small APC/C subunit Apc10 (Buschhorn et al., 2011; da Fonseca et al., 2011). In addition, when the APC/C is bound by the MCC, its ability to recruit cyclin B and securin is reduced (Herzog, 2009).

These observations suggest that Mad3/BubR1 may inhibit substrate recruitment to the APC/C by either inducing a conformational change on the bi-partite D-box receptor of APC/C, or by directly occupying the substrate binding site, acting as a pseudosubstrate. This view has been supported by observations in yeast that Mad3 binds to Mad2-Cdc20 via its N-terminal KEN box (KEN20 in fission yeast) (Janet L. Burton & Solomon, 2007; King et al., 2007; Sczaniecka et al., 2008). Accordingly, Mad3 has been reported to compete with Cdc20 for substrate binding, which is dependent on the N-terminal KEN box (Janet L. Burton & Solomon, 2007). In agreement with these findings, the fission yeast MCC structure has demonstrated that the N-terminal KEN box of Mad3 occupies the KEN-box receptor on the WD40 domain of Cdc20 (Figure 1.3B) (Chao, Kulkarni, Zhang, Kong, & Barford, 2012b). This strengthens the possibility that Mad3 does indeed appear to act as a pseudosubstrate to block recognition of KEN box-containing substrates by APC/C^{Cdc20}.

Intriguingly, Mad3/ BubR1 contains a second KEN box (KEN271 in fission yeast) (Janet L. Burton & Solomon, 2007; King et al., 2007), which is essential for SAC function, although is not required for MCC assembly (P. Lara-Gonzalez et al., 2011; Sczaniecka et al., 2008). Moreover, BubR1 inhibits the recruitment of D-box-containing substrates to APC/C^{Cdc20} *in vitro*, in a second KEN box dependent manner (P. Lara-Gonzalez et al., 2011). These observations imply that, while the N-terminal KEN box inhibits the recruitment of KEN-box containing substrates to APC/C^{Cdc20}, C-terminal second KEN box might occupy the bi-partite D-box receptor. This possibility is supported by the MCC structure; docking of the fission yeast MCC structure onto that of the APC/C indicates that Mad3 binding displaces Cdc20 from Apc10, thus disrupting the bi-partite D-box receptor between them (Chao et al., 2012b). These data are in line with cryo-EM studies demonstrating that MCC binding changes the position of Cdc20 within the APC/C (Figure 1.2B) (Herzog, 2009). In addition, a study in human cells has demonstrated that Mad2 inhibits Cdc20 by binding directly to a site required to bind the APC/C (Izawa & Pines, 2012). This is consistent with the MCC crystal structure that safety belt domain of Mad2 sequesters the Mad2 binding domain of Cdc20, which is also required for its binding to APC/C (Figure 1.3C).

Taken together, Mad2 and the two KEN boxes of Mad3/BubR1 appear to cooperate for inhibiting APC/C^{Cdc20}.

1.5.2 Inhibition of APC/C^{Cdc20} through Cdc20 turnover

Cdc20 is an activator (along with Cdh1) of APC/C that associates with the APC/C in early mitosis and triggers anaphase onset by promoting the destruction of cyclin B and securin. Cdc20 is related to the β subunit of trimeric G proteins and contains seven WD40 repeats. These repeats form a seven-bladed β propeller structure which efficiently mediates protein-protein interactions (Chao et al., 2012b).

Although Cdh1 protein and transcript levels are constitutive, both Cdc20 mRNA and protein levels oscillate throughout the cell cycle: absent in G1, begin to accumulate in S phase, and reach their peak levels in mitosis. (Pan & Chen, 2004) (Figure 1.4). During the normal cell cycle, Cdc20 levels are regulated both by transcription and proteolytic degradation. Expression of *CDC20* gene is driven by a hybrid promoter that bears Yox1-, Mcm1- and Fkh-binding sites (Liang, Lim, Venkitaraman, & Surana, 2011).

Cdc20 is degraded by multiple APC/C-dependent mechanisms in budding yeast (Foe et al., 2011). It has been reported that late in mitosis and early in G1, Cdc20 degradation is largely mediated by APC/C^{Cdh1}. On the other hand, even though Cdh1-mediated degradation of Cdc20 is likely important, recent studies have proposed Cdh1-independent mechanisms for Cdc20 turnover (Foe et al., 2011). Consistent with this, a budding yeast study has demonstrated that the majority of Cdc20 turnover does not involve a second activator molecule but instead is mediated by *in cis* Cdc20 auto-ubiquitination while it binds to the activator binding site of the APC/C (Foe et al., 2011).

Studies in fission yeast, budding yeast and human cells have reported that Cdc20 turnover is promoted by SAC activation, leading to lower Cdc20 levels (King et al., 2007; Nilsson et al., 2008; Pan & Chen, 2004) to ensure that MCC (Mad2 and Mad3) levels are not overridden by Cdc20 hyper-accumulation.
These data are in agreement with the recent findings in fission yeast that $Cdc20^{Slp1}$ overexpression leads to a defective SAC response, whereas reduced Cdc20 expression

rescues the SAC defects caused by lower abundance of Mad2 and Mad3 (Stephanie Heinrich et al., 2013).

Interestingly, a budding yeast study has demonstrated that Cdk1 activity promotes recovery from SAC-induced mitotic arrest by sustaining Cdc20 expression during mitosis (Liang et al., 2011). It has been shown that Cdk1 activity silences Yox1, a transcription repressor of the *CDC20* gene, and thereby maintains Cdc20 levels high enough during SAC recovery, which contributes to the rapid anaphase onset upon chromosome bi-orientation.

Taken together, these observations suggest that the SAC keeps levels of Cdc20 low enough for its stoichiometric inhibition by the MCC until chromosome biorientation, yet high enough (by the indirect promotion of Cdk1 activity through stabilized Cyclin B) for APC/C^{Cdc20} to start anaphase rapidly (recover from the SAC) once chromosomes are bioriented.

1.5.3 Regulation of APC/C^{Cdc20} activity through phosphorylation

The association of APC/C and its activators is also subject to control by phosphorylation. Cdh1 can activate both interphase and mitotic APC/C, independent of APC/C phosphorylation, however its own activity is inhibited by Cdk1 mediated phosphorylation. On the other hand, Cdc20 binds and activates mitotically phosphorylated APC/C by Cdk1 (Kramer et al., 2000; Rudner & Murray, 2000; Yudkovsky, Shteinberg, Listovsky, Brandeis, & Hershko, 2000). This suggests that Cdc20 is the predominant activator of the APC/C when Cdk1 activity is high in mitosis.

Phospho-regulation of Cdc20 by different kinases has also been reported in different model organisms. However, unlike the activating phosphorylation of APC/C, phosphorylation of Cdc20 has largely been suggested to inhibit its APC/C activator function.

Studies in *Xenopus* egg extracts and human cells have reported that the SAC requires mitotic Cdk1 activity. Indeed, inhibition of Cdk1 activity disrupts the interaction of Cdc20 with other MCC components (Mad2 and Mad3/BubR1), and thereby overrides the SAC dependent arrest (D'Angiolella, Mari, Nocera, Rametti, & Grieco, 2003;

Yudkovsky et al., 2000). Moreover, the Cdc20 that is phosphorylated by Cdk1 *in vitro* has been shown to interact with Mad2 rather than APC/ C (D'Angiolella et al., 2003).

Another *Xenopus* egg extract study has reported that Cdk1 does not account for all of the phosphorylation on Cdc20. Indeed, mitogen-activated protein kinase (MAPK) and Cdk1 mediated phosphorylation of Cdc20 is required for the interaction between MCC components (Cdc20, Mad2 and Mad3/BubR1) and a functional SAC response to spindle perturbation by nocodazole (Chung & Chen, 2003). It has been suggested that the SAC delays anaphase onset by inhibiting a fully-phosphorylated Cdc20.

Consistent with these observations, a recent study in *Xenopus* egg extracts has demonstrated that the antagonistic activities of Cdk1 and protein phosphatase 2A (PP2A) regulate APC/C^{Cdc20} in mitosis (Labit et al., 2012). Upon mitotic entry, both APC/C and N-terminus of Cdc20 are phosphorylated by Cdk1. Phosphorylation of APC/C increases its affinity for Cdc20, whereas Cdc20 phosphorylation has the opposite effect on its affinity for the APC/C. During the metaphase- anaphase transition, dephosphorylation of Cdc20 N-terminus by PP2A promotes the binding of its C-box to Apc8 and the subsequent APC/C activation. Importantly, when Cdc20 remains hyper-phosphorylated through the inhibition of PP2A by ocadaic acid, it fails to activate APC/C-mediated ubiquitination.

In addition to Cdk1 and MAPK mediated phosphorylation of Cdc20, Bub1 kinase has also been reported to regulate Cdc20 in human cells (Tang, Shu, Oncel, Chen, & Yu, 2004). *In vitro* kinase assays have demonstrated that Bub1 directly phosphorylates Cdc20, which catalytically (at sub-stoichiometric amounts) inhibits APC/C. Moreover, *in vivo* phosphorylation of Cdc20 by Bub1 is required for a full SAC response, as the expression of a non-phosphorylatable Cdc20 mutant results in slippage from the SAC arrest upon spindle damage. Consequently, in addition to the APC/C^{Cdc20} inhibition by MCC that is mediated by protein-protein interactions, a catalytic inhibition of Cdc20 by Bub1 may contribute to the sensitivity of the SAC response.

***S. pombe* Cdc20**

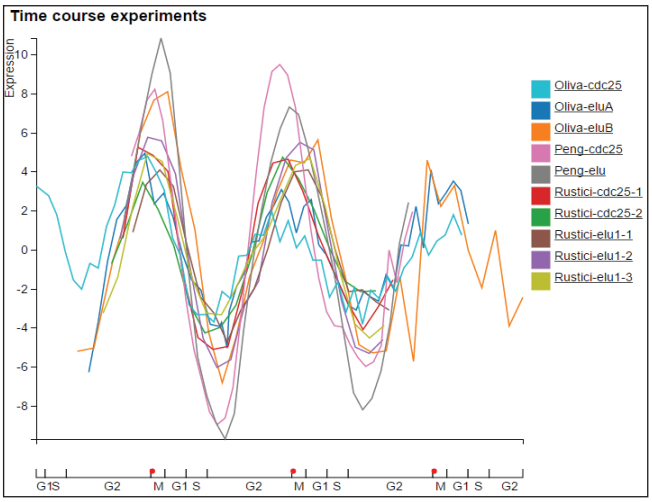

***S. cerevisiae* Cdc20**

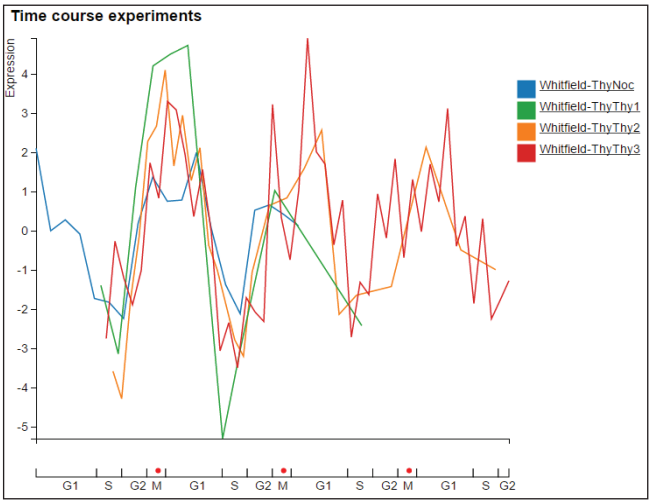

***H. sapiens* Cdc20**

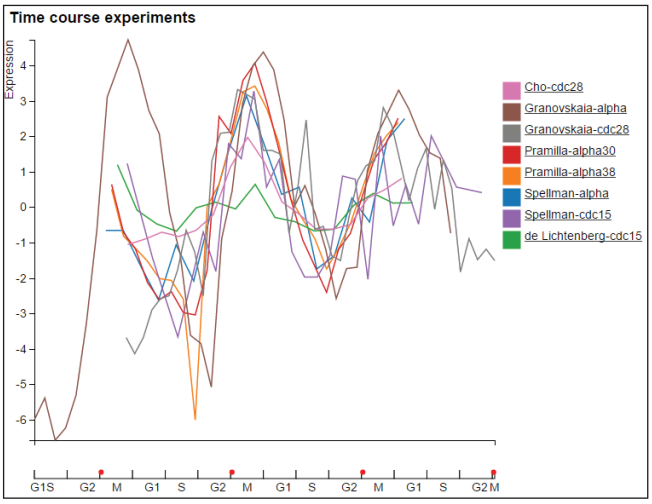

Figure 1.4 Expression of Cdc20 is dynamically regulated during the cell cycle

Oscillations in protein levels of Cdc20 orthologs from fission yeast (Slp1) (*S. pombe*), budding yeast (*S. cerevisiae*) and humans (*H. sapiens*) during the cell cycle progression. Each curve represents results of an independent time course experiment from different research groups (or from the same group if labeled with the same name). Red dots indicate the cell cycle phase, in which a particular Cdc20 ortholog reaches its peak levels. Oscillation graphs were adapted from Cyclebase 3.0.

1.6 Roles of Bub1 kinase in mitosis

Bub1 (budding uninhibited by benzimidazole 1) is a serine/threonine-protein kinase containing a conserved kinase domain at its C-terminus. Bub1 is recruited to unattached kinetochores during mitosis, and its slow FRAP recovery rates suggest that it is a more stable component of kinetochores than the other two Bub proteins (Bub3 and BubR1/Mad3) (Bonnie J Howell et al., 2004). Bub1 has been reported to have multiple roles in mitosis, either performed by its non-kinase region (N-terminal and middle) or the kinase domain (C-terminal).

1.6.1 Roles of Bub1 that do not require its kinase activity

Non-kinase roles of Bub1, for which its kinase function is dispensable, were previously mentioned in the section we described the SAC activation at kinetochores (1.4.1). In brief, Bub1 is recruited to the phosphorylated (by Mps1) kinetochore protein KNL1 (Spc7 in fission yeast) through Bub3, where it functions as a scaffold for the subsequent localization of downstream SAC proteins, such as Mad1, Mad2, Mad3 (BubR1 in animals) and Cdc20 (Klebig, Korinth, & Meraldi, 2009; Rischitor et al., 2007; Shepperd et al., 2012a; Vanoosthuyse et al., 2004; Mathijs Vleugel et al., 2013). In this way Bub1 significantly contributes to the activation and maintenance of a robust SAC response upon spindle damage.

A recent study in human cells has proposed that although Bub1 promotes Mad1 recruitment to unattached kinetochores, its ability to activate the SAC correlates more strongly with its ability to recruit Cdc20 (M. Vleugel et al., 2015). This function of Bub1 is dependent on its ABBA motif (A-box-like motif) and BubR1 (Mad3). Consequently, the kinetochore recruitment of Cdc20 by Bub1 has been suggested to activate the SAC by bringing the Cdc20 in close proximity to newly formed C-Mad2. In addition, Bub1 dependent kinetochore recruitment of Cdc20 may also promote the SAC response by mediating a kinetochore-driven modification of Cdc20 (such as phosphorylation), that may further increase its affinity for C-Mad2 and BubR1 (Mad3).

1.6.2 Roles of Bub1 that require its kinase activity

In this section we summarise observations in different model organisms which suggest two major roles for Bub1 kinase activity that are relevant to mitosis: (i) roles in maintaining accurate chromosome bi-orinetation; (ii) roles in the SAC signalling.

1.6.2.1 Bub1 kinase activity for chromosome bi-orientation

In mitosis, Bub1 kinase has been shown to recruit the Shugoshin protein (Sgo2 in fission yeast; Sgo1 in budding yeast and human cells) to inner centromere through direct phosphorylation of H2A (Kawashima, Yamagishi, Honda, Ishiguro, & Watanabe, 2010). By catalysing the centromere localization of Shugoshin, Bub1 kinase contributes to ensuring chromosome bi-orientation through two downstream mechanisms:

1. Sgo1 has been reported to protect centromere cohesion from premature separation by associating with PP2A phosphatase that counteracts kinases targeting the cohesin complex (Tang, Sun, Harley, Zou, & Yu, 2004).

2. Sgo1 (in mammalian cells and budding yeast), and Sgo2 (in fission yeast) have been demonstrated to recruit Aurora B to the inner centromere, where it destabilizes erroneous kinetochore–microtubule attachments (error correction) (Ruchaud, Carmena, & Earnshaw, 2007). Through the disruption of aberrant attachments, Aurora B promotes SAC signalling by creating unattached kinetochores. In addition, Aurora B is required for the recruitment of $Mps1^{Mph1}$ to unattached kinetochores in fission yeast (S. Heinrich et al., 2012), which is of vital importance for a stable SAC response. These two observations suggest that Bub1 kinase activity appears to contribute to the SAC signalling through the H2A-Shugoshin-Aurora B pathway. In the next section, we summarise the importance of Bub1 kinase activity for the SAC response in various species.

1.6.2.2 Bub1 kinase activity for a robust SAC response

Unlike its chromosome bi-orientation roles described above, requirement of the Bub1 kinase activity for the SAC response is less well understood. Contribution of Bub kinase activity to delaying anaphase onset in response to spindle damage has been investigated in different model organisms (fission yeast, budding yeast, *Xenopus* egg extracts and cultured human cells) and under various experimental conditions (such as different levels of spindle perturbation to induce SAC activation).

1.6.2.2.1 Bub1 kinase activity in budding yeast SAC

An early study in budding yeast reported that Bub1 is a kinase protein that is able to autophosphorylate and to catalyze phosphorylation of Bub3 (Roberts, Farr, & Hoyt, 1994). This study also suggested that the kinase activity of Bub1 is required for the SAC response, as a Bub1 kinase-dead mutant (*bub1-K733R*) fails to rescue the benomyl sensitivity exhibited by a *bub1* null strain. However, *bub1-K733R* was later found to be less stable than the wild type Bub1 in mitotically arrested cells (Cheryl, Johnston, Joseph, Hardwick & Spencer, 2003), which might have caused the SAC deficiency observed previously (Roberts et al., 1994).

Another budding yeast study investigated the kinase activity of Bub1 extensively, using a truncated Bub1 kinase allele (*bub1ΔK*) that lacks the whole kinase domain, yet is as stable as the wild type Bub1 (Fernius & Hardwick, 2007). *Bub1ΔK* was tested using different degrees of spindle perturbation. First, *bub1ΔK* cells were demonstrated to have growth defects when exposed to anti-microtubule drugs (benomyl); *bub1ΔK* cells are more sensitive than mad3*Δ* cells, but not as sensitive as *bub1* null cells. Moreover, *bub1ΔK* cells die rapidly (at similar rates to *bub1* null and mad2*Δ* cells) when they are first grown in the presence of nocodazole (microtubule depolymerisation), and then plated on a rich media. This sensitivity of *bub1ΔK* cells is not due to a defect in arresting at metaphase in the presence of unattached kinetochores. Instead, it is mainly caused by a defect in chromosome bi-orientation, as *bub1ΔK* cells mis-segregated chromosomes during recovery from the SAC arrest.

Subsequent experiments demonstrated that whilst the Bub1 kinase domain is not essential for the SAC response to unattached or defective kinetochores, it is essential for the SAC response to lack of tension at sister kinetochores (Fernius & Hardwick, 2007).

1.6.2.2.2 Bub1 kinase activity in fission yeast SAC

Fission yeast Bub1 has been reported to be hyperphosphorylated by Cdk1 *in vitro* and in cells arrested at metaphase upon spindle damage. This phosphorylation of Bub1 is required to activate the SAC (Yamaguchi, Decottignies, & Nurse, 2003). In addition, Bub1 kinase activity is also required for a complete SAC function, as both the *bub1-K762R* allele (equivalent of the budding yeast *bub1-K733R*) and a Bub1 truncation allele lacking the entire kinase domain (both of them are as stable as the wild type Bub1) failed to delay anaphase onset in response to the anti-microtubule drug carbendazim (CBZ). Importantly, the double mutant Bub1 allele (*bub1*P Cdk1, bub1Δkinase*), which both lacks its kinase domain and is refractory to Cdk1 mediated phosphorylation, exhibits a more severe SAC defect than the single mutants. This suggests that Cdk1-mediated phosphorylation of Bub1 and the kinase activity of Bub1 itself promote the SAC response non-redundantly, as losing them simultaneously results in an additive SAC defect (Yamaguchi et al., 2003).

Another fission yeast study analysed Bub1 kinase activity by mutating the invariant lysine 762 into methionine to generate the *bub1-K733M* allele (Vanoosthuyse et al., 2004). When the microtubules are depolymerized by the cold sensitive tubulin mutant *nda3-KM311, bub1-K733M* cells exhibit cut (**c**ell **u**ntimely **t**orn) phenotype more frequently than wild type, in which cells exit mitosis forming septa without equal chromosome segregation. This suggests that Bub1 kinase activity in response to unattached kinetochores is required for a complete SAC response. More importantly, upon recovery from the *nda3-KM311* arrest, *bub1-K733M* cells exhibit lagging chromosomes very frequently, which suggests that Bub1 kinase activity is necessary for bi-orientation and accurate segregation of chromosomes (Vanoosthuyse et al., 2004).

Bub1 kinase activity was further investigated in a recent fission yeast study, in which a different kinase-dead Bub1 allele (*bub1-K762R D900N*) was constructed through two point mutations: one in its ATP binding motif (lysine 762 to arginine) and another in the catalytic site (aspartate 900 to asparagine) (Kawashima et al., 2010). This group generated the *bub1-K762R D900N* allele because they have demonstrated that the previously reported (Yamaguchi et al., 2003) canonical 'kinase-dead' protein (*bub1-K762R*) still retains residual kinase activity *in vitro* (< 1/100 of wild type Bub1 activity) and *in vivo*. On the other hand, the *bub1-K762R D900N* allele has been shown to have no kinase activity. In addition, wild type Bub1 was shown to autophosphorylate (*in vitro*) as well as it catalyses the phosphorylation of H2A (*in vitro* and *in vivo*). Experiments with the *bub1-K762R D900N* allele demonstrated that lack of Bub1 kinase activity only slightly impairs the SAC response to unattached kinetochores (through the *nda3-KM311* mutation depolymerizing microtubules). However, when the tension between sister chromatids is lost, (through the *psc3-1T* temperature-sensitive cohesin mutation disrupting sister cohesion) Bub1 kinase activity is essential for a SAC response to delay anaphase. As described above, Bub1 phosphorylates H2A, and thereby recruits Sgo2 to inner centromeres, which is mainly required for chromosome bi-orientation. Forced enrichment of Sgo2 at centromeres is able to rescue only half of the SAC defect observed in the absence of Bub1 kinase activity when the tension between chromatids is lost (Kawashima et al., 2010).

1.6.2.2.3 Bub1 kinase activity in *Xenopus* SAC

An early study in *Xenopus* egg extracts reported that Bub1 is a kinase protein that autophosphorylates as well as it catalyses phosphorylations of Bub3 and Mad1 *in vitro* (Sharp-Baker & Chen, 2001). *In vivo* immunoprecipitations show that Bub1 is phosphorylated during interphase, mitosis, and SAC mediated arrest. Sharp-Baker and colleagues constructed a kinase-dead Bub1 allele (K872R) by mutating the invariant lysine 872 to arginine, which does not autophosphorylate. Catalytically inactive *Bub1 K872R* (transcribed *in vitro* and translated in egg extracts) was shown to be capable of restoring the SAC response and the kinetochore recruitment of Mad1, Mad2 and Bub3 proteins in Bub1-depleted egg extracts in response to high density of sperm nuclei (9000-15000/ µl extract) and high dose nocodazole

(10 ng/µl). (Sharp-Baker & Chen, 2001). However, it is worth noting that the kinase inactive *Bub1 K872R* mutant was translated at a noticeably higher level than the wild type Bub1. This might have accounted for the capability of the kinase inactive mutant in the SAC response. In other words, non-kinase SAC functions of the kinase-dead Bub1 mutant (that was more abundant than the wild type) might have compensated for its missing kinase activity. Importantly, to activate the SAC Sharp-Baker and colleagues perturbed spindle by exposing the egg extracts to high numbers of sperm nuclei and high dose nocodazole (10ng/µl) (optimal conditions to activate the SAC). Among components of the SAC machinery, the role of Bub1 kinase activity may be maintaining the SAC response by fine-tuning it, rather than being directly responsible for the assembly of the ultimate inhibitor of APC/C (**m**itotic **c**heckpoint **c**omplex, MCC). During such severe spindle perturbation, Bub1 kinase activity may not be detectable; as cells are expected to assemble high amounts of MCC, which might delay anaphase onset regardless of Bub1 kinase activity.

A similar *Xenopus* study from the same group has addressed this hypothesis (Chen, 2004), that any subtle difference in the SAC function between wild type and kinase-dead Bub1 may be revealed only under suboptimal conditions for the SAC activation. Chen tested this possibility by treating the egg extracts with lower concentrations of nocodazole (or sperm nuclei) to disrupt microtubule-kinetochore attachment to different degrees. First, they confirmed that Bub1 becomes hyperphosphorylated in mitosis; and demonstrated that Bub1 phosphorylation by MAPK promotes its further phosphorylation by other kinases, which collectively induce Bub1 kinase activity specifically on unattached chromosomes. Second, analysis of the kinase-dead Bub1 mutant (*Bub1 K872R*) revealed that although the kinase-dead Bub1 is fully SAC proficient under optimal spindle perturbation conditions (high concentration of nocodazole, 10 ng/µl; and sperm nuclei 10000/ µl extract), it is compromised in the SAC function under sub-optimal spindle perturbation conditions (low concentration of nocodazole, 1 ng/µl; and sperm nuclei 7500/ µl extract). This suggests that the kinase activity of Bub1 does not function as an on-off switch of the SAC; instead, it modulates the strength of the SAC signal generated from each kinetochore, and appears to become more important for the maintenance of the SAC when the number of unattached chromosomes are lower in the cell (mimicked by low dose of nocodazole).

1.6.2.2.4 Bub1 kinase activity in human SAC

As described in the previous sections, Bub1 kinase activity has been suggested to contribute to the SAC response in various species, by employing different methods/ conditions to activate the SAC. However, a substrate of Bub1 kinase, whose phosphorylation may directly promote the SAC signalling (other than H2A, as its role is indirect and mainly through the Aurora B recruitment to centromeres (S. Heinrich et al., 2012)), had not been implied until a report published in 2004 (Tang, Shu, et al., 2004).

Tang and colleagues demonstrate that six residues of human Cdc20 (N-terminal), phosphorylated *in vitro* by Bub1, are phosphorylated *in* vivo in a Bub1-dependent manner. In addition, expression of a Cdc20 mutant that is nonphosphorylatable on these residues has a dominant-negative effect, which results in 50% of the cells leaking through the SAC arrest in the lack of microtubule-kinetochore attachments (generated through nocodazole treatment) or the tension between chromatids (generated through taxol treatment). On the other hand, this mutation does not affect either Cdc20 recruitment to kinetochores or its binding to the other components of mitotic checkpoint complex (Mad2 and BubR1). Moreover, both Mad2 and BubR1 are capable of inhibiting the Cdc20 mutant (nonphosphorylatable on the six N-terminal residues by Bub1) by direct binding at least *in vitro* (Tang, Shu, et al., 2004).

It is worth noting that the mutation of the six serine/ threonine sites on Cdc20 does not completely abolish its Bub1 mediated phosphorylation *in vitro*. This residual phosphorylation of Cdc20 is not due to a co-purified kinase contaminant, as it is not observed in the presence of a kinase-inactive Bub1. This suggests that there may be other sites of Cdc20 which are likely to be phosphorylated by Bub1. On the basis of these findings, Tang and colleagues conclude that Bub1 kinase activity towards Cdc20 is crucial for a complete SAC response and full inhibition of APC/C activity (Tang, Shu, et al., 2004).

Another study from the same group addressed whether the Bub1 kinase activity is required for the SAC response to spindle damage (Kang et al., 2008). They showed that in Bub1 depleted HeLa cells (by Bub1 RNAi) exposed to nocodazole, expression of the Bub1 kinase-dead mutant is 30% less efficient than the wild type Bub1 in

delaying premature anaphase onset. This suggests that the kinase activity of Bub1 is required for a full SAC response in human cells.

Kang and colleagues next solved the crystal structure of the C-terminal domain of Bub1, consisting of its kinase domain and a 60 residue fragment N-terminal to it. The structure reveals that the extension fragment organizes the activation segment and the ATP-binding pocket of Bub1 in a similar way to the activation of cyclin- dependent kinases (Cdks) by cyclins. Mutations in the N-terminal extension disrupt the kinase activity of Bub1 (Kang et al., 2008).

Interestingly, compared to other kinases, Bub1 has an extended substrate recognition loop that limits the access of non-specific substrates by blocking the active site of Bub1. Bub1 contains two KEN boxes in its central region, which mediate its degradation by APC/C^{Cdh1} in G1 phase (Qi & Yu, 2007). In addition, Kang and colleagues demonstrated that these KEN boxes of Bub1 are also required for Cdc20 binding, efficient phosphorylation of Cdc20 by Bub1, and the SAC response (Kang et al., 2008). These data suggest that Bub1 has a considerable specificity toward Cdc20, because Cdc20 is one of only two known KEN box receptors. The other KEN box receptor is Cdh1 (the other activator of the APC/C); however, Cdh1 is not efficiently phosphorylated by Bub1 *in vitro* (Tang, Shu, et al., 2004) presumably because it lacks an optimal phospho-acceptor residue that can interact with the Bub1 kinase domain.

1.7 SAC silencing and recovery from a SAC mediated arrest

While it is essential to inhibit APC/C when kinetochores are unattached, the ability to alleviate APC/C inhibition once the SAC is satisfied is equally crucial for mitotic progression. Once all sister kinetochores stably attach to microtubules emanating from opposite poles, the 'wait anaphase' signal mediated by the SAC is extinguished. The major downstream consequence of the SAC silencing is the disassembly of the mitotic checkpoint complex (MCC), and the subsequent activation of the APC/C by Cdc20. SAC silencing is regulated by multiple mechanisms.

The most widely conserved silencing mechanism is the phosphatase activity of protein phosphatase 1 (PP1; Dis2 in *S. pombe*). PP1 is required for mitotic exit (Vanoosthuyse et al., 2009). KNL1 (Spc7 in fission yeast) cooperates with the kinesins Klp5/6 to recruit PP1/Dis2 to kinetochores (Meadows et al., 2011). In the absence of kinetochore tension, Aurora B phosphorylates KNL1, and inhibits it from recruiting PP1. Once kinetochores are under tension, KNL1 leaves the phosphorylation range of Aurora B, thus is relieved from the inhibitory phosphorylation (Liu et al., 2010). This enables the localisation of PP1 to the kinetochores, whereupon it counteracts the checkpoint kinase activity. PP1 activity removes Bub1-Bub3 from kinetochores, which subsequently removes Mad1 and Mad2 (London et al., 2012), yet direct targets (substrates) of PP1 remain to be discovered.

Another model for the SAC silencing suggests that a vertebrate protein known as $p31^{comet}$ interacts with closed Mad2 (C-Mad2; the only state of Mad2 that can recognize Mad3 in fission yeast (Chao et al., 2012a)) in a way similar to interactions of C-Mad2 with open Mad2 (O-Mad2), Cdc20 or Mad3. Binding of $p31^{comet}$ to Mad2 has been found to promote MCC disassembly (Westhorpe et al., 2011). It has been suggested that binding of $p31^{comet}$ to MCC through Mad2 may trigger a conformational change in Cdc20, facilitating its phosphorylation by Cdk1, which subsequently promotes dissociation of Cdc20 from BubR1 (Miniowitz-Shemtov et al., 2012).

Another SAC silencing mechanism is known as 'dynein-mediated stripping' of checkpoint proteins, albeit it has only been reported by vertebrate studies. Dynein localizes to kinetochores (not in all eukaryotes), and the attachment of microtubules to kinetochores allows Dynein to transport Mad1, Mad2 and BubR1 to spindle poles,

which contributes to silencing of the SAC (Gassmann et al., 2010; B. J. Howell et al., 2001).

Aims

In this study, we aim to further our understanding of the phospho-regulation of the spindle assembly checkpoint (SAC), specifically by investigating roles of Bub1 kinase activity in fission yeast SAC signalling. In order to investigate that:

1. We examine roles of Bub1 kinase activity in:
    1.1 Maintaining a SAC mediated metaphase arrest in response to various degrees of spindle perturbation
    1.2 Recovering from the SAC arrest and progressing into anaphase, once spindle reforms and chromosomes are bioriented.
2. We investigate the protein(s) downstream of Bub1 kinase activity by:
    2.1 Identifying the substrate(s) of Bub1 kinase (Cdc20)
    2.2 Mapping phosphorylated sites of Cdc20 by Bub1
    2.3 Analysing interactions between the MCC components by cross-linking mass spectrometry analysis (Cdc20, Mad2 and Mad3) to determine Cdc20 phosphorylation sites that may be important for SAC regulation.
    2.4 Engineering the cdc20+ gene at its endogenous locus (inserting an antibiotic resistance marker and an internal epitope tag) for using in subsequent experiments.
    2.5 Generating phosphorylation mutants of Cdc20 to analyse its regulation through putative Bub1-phosphorylated sites.
3. We examine roles of Cdc20 phosphorylation (C-terminal) by analysing phospho-deficient or phospho-mimicking mutants of Cdc20 in:
    3.1 Unperturbed mitosis or various degrees of spindle perturbation in terms of their abilities to maintain a SAC response.
    3.2 Prolonged spindle destabilisation followed by re-polymerisation of microtubules, in terms of their abilities to recover from the SAC and progress into anaphase.
    3.3 The absence of Bub1 kinase activity to test whether Cdc20 phospho-mimicking mutants can rescue the SAC defects exhibited by the Bub1 kinase-inactive mutant.

Chapter 2: Materials and Methods

2.1 Buffers and solutions

10 x TBE

Tris 445 mM

Boric acid 445 mM

EDTA (pH 8) 100 Mm

SDS gel running buffer (1x)

Tris 50 mM

Glycine 384 mM

SDS 2 %

Coomassie Blue stain

0.16 % Coomassie Blue in 4 volumes methanol

4 volumes acetic acid

5 volumes ddH20

PonceauS stain

PonceauS 0.25 g

Acetic acid 12.5 ml

ddH20 to 250 ml

Semi-dry transfer buffer (1x)

Tris-Cl 25 mM

Glycine 129 mM

Methanol 10 %

2.2 Growth media

Bacteria media (LB)

Component	Final conc.
Bacto-tryptone	1 % (w/v)
Bacto-yeast extract	0.5 % (w/v)
NaCl	0.5 % (w/v)
pH adjusted to pH 7.2 with NaOH	

Yeast media

Yeast extract supplemented (YES)

Component	Final conc.
Yeast extract	0.5 % (w/v)
D-glucose, anhydrous	0.5 % (w/v)
Supplements mix	1x

Pombe minimal medium (PMG)

Component	Final conc.
Phtalic acid	14.7 mM
Di-sodium hydrogen orthophosphate, anhydrous	15.5 mM
L-glutamic acid, monosodium salt	25.4 mM
D-glucose, anhydrous	2 % (w/v)

Vitamins mix	*1x*
Minerals mix	*1x*
Supplements mix	*1x*

Supplements mix (20x)

Component	**Mass**
Adenine	0.4 g
Arginine	0.4 g
Histindine	0.4 g
Leucine	0.4 g
Uracil	0.4 g
Lysine	0.4 g
Distilled water	*to 250 ml*

Vitamins mix (1000x)

Component	**Final conc.**
Biotin	10 mg/l
Pantothenic acid	1 g/l
Nicotinic acid	10 g/l
Inositol	10 g/l

2.3 Insect cell methods

This section describes the methods used in baculovirus/insect cell experiments. Expression and purification of protein complexes were carried out in five steps:

2.3.1 Cloning target DNAs into a transfer vector

Genes encoding the components of a protein complex were cloned into pFL using the multiple cloning site of the transfer vector. The efficiency of cloning was checked by analytical digestion and sequencing.

2.3.2 Integration of the transfer vector into the baculoviral genome

The Transfer vector carrying the insert was integrated into the baculovirus genome through transformation into engineered *E.coli* cells (DH10EMBacY) (a gift from Ken Sawin) containing this genome as a bacterial artificial chromosome (bacmid). This integration is performed using Tn7- dependent transposition. To enable the transposition, DH10EMBacY cells contain a helper plasmid (Tet resistant) that expresses the Tn7 transposon complex upon induction with IPTG. Selection of positive colonies occurs via blue-white screening. Insertions of the mini-Tn7 into the mini-*att*Tn7 attachment site on the bacmid disrupt the expression of the LacZα peptide. Hence, colonies containing the recombinant bacmid are white and colonies that harbor the unaltered bacmid are blue. Moreover, DH10EMBacY cells are kanamycin resistant and the integrated part of transfer vector (pFL) carries a gentamicin resistance gene. Thus, to select for the right transformants, LB plates were prepared with the following markers: kanamycin (50 μg/ml), gentamicin (7 μg/ml), tetracycline (10 μg/ml), bluo-gal (100 μg/ml), IPTG (40 μg/ml). Furthermore, DH10EMBacY cells carry a YFP reporter gene in the bacmid that is expressed by the same promoter as the insert gene. This enabled us to screen the expression of our gene of interest by examining YFP expression under UV light. Transformed cells were selected by blue/ white screening. Bacmid was isolated from white cells using PureLink HiPure Plasmid DNA Miniprep Kit (Invitrogen) and checked by PCR and sequencing.

2.3.3 Initial insect cell infection with bacmid and generation of virus

Recombinant bacmids containing the genes of interest were used to transfect insect cells in order to produce recombinant baculovirus. On the first day, an exponentially growing monolayer Sf9 culture (1-1.5 x 10^6 cells/ml) with 95% viability was diluted in serum and antibiotic free SF-900 II media (Invitrogen) to 0.4 x 10^6 cells/ml. One hour prior to transfection 2.5 ml cells (1 x 10^6) were added to each well of a 6- well plate. Cells were allowed to attach the plate for one hour at 27°C. Meanwhile the transfection mixture was prepared. For each well to be transfected, 2 μg bacmid DNA and 10 μl transfection reagent (Insect GeneJuice, Novagen) were diluted with 100 μl media (serum and antibiotic free) in separate tubes. The diluted DNA was added to the diluted transfection reagent and mixed. The mixture was incubated at room temperature for 30 minutes followed by addition of 0.8 ml media (serum and antibiotic free). After the cells attached the plate, media was aspirated from the cells and replaced with the transfection mixture (~1 ml). Cells were incubated at 27°C for 5 hours and then the transfection media was replaced with 2 ml medium (serum and antibiotic free). Approximately in 48- 72 hours, transfected insect cells start to demonstrate characteristics of very late infection (cessation of cell growth, granular appearance and release from the plate) as well as a YFP expression. 2 ml media was collected from wells with visibly infected cells. This medium contains the released virus. This is the high quality budded virus (P1) that has not yet suffered from damage that can occur through over-amplification from successive infection cycles. P1 virus was supplemented with 2% fetal bovine serum (FBS) and stored at 4°C, protected from light.

2.3.4 Virus amplification and test expression

Initial virus amplification was carried out using a 25 ml suspension culture (1.8 x 10^6 cells/ml) infected with 3 ml of P1 virus. This culture was incubated in 2L roller bottles (Corning) on the green sticky pads of a shaking incubator (InFors, at Edinburgh Protein Purification Facility, EPPF) at 27°C, 95 rpm for 48- 72 hours. Cells were spun (at 500 rcf, for 5 minutes) and the media containing the P2 virus was collected when the cell viability was around 75- 80 %, which was indicated using an automated cell counter (Countess, Invitrogen). The expression of the protein of interest was checked by SDS-

PAGE and revealed by western blot. Expression was also confirmed by observation of YFP activity in the cell cultures. P2 virus was then used to infect a larger culture to obtain a virus solution (P3) with a higher titer and volume to be used in the ultimate protein expression.

2.3.5 Protein expression

Sf9 cells were used during the bacmid transfection and virus amplifications since they tend to clump less than other cell lines (enabling better observation of the infection symptoms) and attach firmly to plate surfaces. Once we obtained the P1 virus, we switched to suspension culture that provides better aeration and reproduction rates. Although Sf9 cells are suitable for suspension cultures, they double only once in 72 hours whereas another insect cell line called High Five (Invitrogen) (kindly provided by Bill Earnshaw) has a much shorter doubling time (~18 hours). High Five cells are maintained in another media (ExpressFive, Gibco), but still could be infected with the virus released into Sf9 media. When High Five cells were initially transferred from tissue culture flasks to suspension culture, they started to form large aggregates of cells. Thus, 10 units/ ml Heparin (Heparin sodium salt from porcine intestinal mucosa, Sigma) was initially included in High Five media to prevent them from clumping, but removed before protein expression once clumping affected less than 10% of the total population. 500 ml of exponentially growing High Five cells (1.8 x 106 cells/ml, 98% viable) were infected with 10 ml of P3 virus. The cell pellet was harvested (spun at 5,000 rpm for 20 minutes) 48 – 60 hours after the infection (when 70-80 % of the cells appeared to express YFP) and washed with phosphate buffer saline (PBS) to remove insect cell media. Cell pellets were stored at – 20°C. In this way more than 20 g of insect cell pellet was collected to be used in the subsequent purification experiments.

2.3.6 Protein purification

Recombinant proteins expressed in the baculovirus and insect cell system carried a tag with two Strep II sites. A Strep II site is a short peptide (WSHPQFEK), which binds with high selectivity to Strep-Tactin, an engineered streptavidin. A tag with Strep II sites (strep-tag) allows affinity purification on immobilized Strep-tactin. Strep-tagged proteins bind to Strep-Tactin with a 100 times higher affinity (K_d = 1 μM) than to streptavidin. Then bound proteins are eluted using biotin (for magnetic beads) or desthiobiotin (for liquid chromotography). Desthiobiotin is a stable, reversibly binding analog of biotin, the natural ligand of streptavidin. Thawed insect cell pellets were re-suspended in 5x volume (v/w) of lysis buffer. Cells were lysed by sonication (8 minutes, 20% amplitude, 10 seconds on, 10 seconds off) and lysis efficiency was confirmed by checking the lysate under a bright-field microscope. Cell lysate was clarified by centrifuging at 22,000 rpm, 4°C for 40 minutes. Supernatant was collected and re-adjusted to pH 8.0 before filtering with a 4.5 μm filter (Millipore). Finally, recombinant protein was purified using magnetic beads.Pilot purification experiments involving relatively small pellets (<5 g) were performed using Strep-Tactin magnetic beads (Qiagen). The purification was carried out in the cold room. Magnetic bead suspension (70ul/ 1 g of pellet) was added to the cleared lysate and mixed on an end-over-end shaker for 2 hours at 4°C. The cell lysate – bead mixture was briefly centrifuged and the tube was placed on a magnetic separator for 2 minutes. The supernatant (flow-through) was removed and the beads were washed three times with 1 ml wash buffer in each time. A magnetic separator was used to remove supernatants. Then the beads were re-suspended in 100 μl elution buffer and incubated for 5 minutes. The tube was placed on a magnetic separator and the supernatant was transferred to a new tube. Beads were subjected to four rounds of elution and the supernatants collected. Finally samples from all steps were mixed with SDS sample buffer, boiled and analyzed by SDS-PAGE and western blotting.

Buffers used in the Strep-tactin magnetic-bead purification:

Strep-Tactin lysis buffer	50 mM NaH_2PO_4 pH 8.0, 0.3 M NaCl, 10% glycerol, 0.05% Tween 20, 10mM 2-mercaptoethanol, 1 Complete-Mini Protease Inhibitor Cocktail Tablet (EDTA-free) per 10 ml buffer, 0.5 mM Pefabloc, 0.4 ug/ml DNase
Strep-Tactin magnetic beads wash buffer	50 mM NaH_2PO_4 pH 8.0, 0.3 M NaCl, 10% glycerol, 0.05% Tween 20, 10mM 2-mercaptoethanol
Strep-Tactin magnetic beads elution buffer	50 mM NaH_2PO_4 pH 8.0, 0.3 M NaCl, 10% glycerol, 0.05% Tween 20, 10mM 2-mercaptoethanol, 20 mM biotin

2.4 DNA methods

Polymerase chain reaction

For cloning work, Phusion® 2X Master Mix (New England Biolabs) was used in accordance with the manufacturer's instructions. PCR products were visualised by agarose gel electrophoresis using ethidium bromide.

Restriction endonuclease digestion

All restriction enzymes were obtained from New England Biolabs and used in accordance with the manufacturer's instructions.

Ligation

Ligations were carried out using T4 Quick Ligase (New England Biolabs) in accordance with the manufacturer's instructions before transformation into *E. coli*

Ethanol precipitation of DNA

Three volumes of ice-cold 96 % ethanol and 1/10 volume 3 M sodium acetate solution was first added to one volume of DNA solution to precipitate DNA from aqueous solutions. After incubating on wet ice for 30 min., tubes were centrifuged at 14,000

rpm at 4 ºC for 15 min. Supernatant was aspirated and the pellet was washed with 500 µl of 70 % ethanol solution. The tubes were spun at 14,000 rpm at 4 ºC for 10 min. After removing the wash solution, tubes were air-dried for 5-10 min. before the pellet was re-suspended in TE buffer.

Site directed mutagenesis

Site-directed mutagenesis was carried out using the Quikchange II site-directed mutagenesis kit (Strategene) according to the manufacturer's instructions. Reaction volumes were reduced to 10 µl/reaction.

Gateway cloning

Gateway-based cloning was performed using the kit (LR Clonase II Enzyme Mix, Invitrogen) in accordance with the manufacturer's instructions. Reaction volumes were reduced to 5 µl/reaction.

Ethanol precipitation of DNA

Three volumes of ice-cold 100 % ethanol and 1/10 volume 3 M sodium acetate solution were added to one volume of DNA solution to precipitate DNA. After incubating it on ice for 30 min., tubes were centrifuged at 14,000 rpm at 4 ºC for 15 minutes. Then the supernatant was aspirated and the pellet was washed with 500 µl of cold 70 % ethanol solution. The tubes were spun at 14,000 rpm at 4 ºC for 10 minutes. After removing the wash solution, tubes were air-dried for 5-10 minutes, and the pellet was re-suspended in TE buffer.

2.4 Fission yeast methods

2.4.1 Yeast transformation

Electroporation

Yeast cells to be transformed were grown to mid-exponential phase (OD_{600} = 0.5) in YES overnight. Next day, cells were harvested (spun at 3000 rpm for 3 minutes), transferred to a pre-chilled microfuge tube and placed on ice. Then cells were washed once with ice-cold water, once with ice-cold 1 M sorbitol and re-suspended in ice-cold

sorbitol to a final density of 1 x 10^9 cells/ml. 40 µl of the cell suspension was mixed with 10 µl of transforming DNA (~1-2 µg) in a pre-chilled tube. The mixture was then transferred to a pre-chilled cuvette (0.2 cm gap) and incubated for 2 minutes on ice, followed by electroporation at 1.8 kV, 200 Ω, 25 µF capacitance using a BioRad electroporator. Immidiately after electroporation, 500 µl of ice-cold 1 M sorbitol was added onto the cells, incubated 2 minutes on ice and transferred to a sterile microfuge tube. Cells were then spun, washed with water and plated onto YES plates. Once a thick layer of cells appear on the YES plate (2-3 days), cells were replica plated onto selective plates.

2.4.2 Yeast genomic DNA extraction

Yeast was extracted using the single-tube LiOAc-SDS lysis method described in (Lõoke, Kristjuhan, & Kristjuhan, 2011).

2.4.3 Mitotic arrests

G2 arrests (*cdc25-22*) for synchronous mitotic time courses treated with microtubule depolymerizing drug carbendazim (CBZ)

Cells bearing the *cdc25-22* mutation were grown in YES medium at 25°C to mid-log phase and then shifted to 36°C for 4 hours to arrest them in G2 phase. Once all cells exhibited characteristics of G2 phase (long cells were checked under the microscope) they were released into a synchronous mitosis, by shifting the temperature back to 25°C in ice-water and then incubated at 25°C for 120-150 minutes. 20 mins after the G2 release into mitosis, the CBZ solution was spun at room temperature for 1 min at 4500 rpm, and the soluble phase added to liquid cultures at 100 µg/ml final concentration to activate the spindle assembly checkpoint (SAC). Cells were harvested, then either fixed in 100% methanol (to be stained with DAPI or calcofluor), or frozen in dry ice and stored at -80°C (to be lysed for protein extraction)

Preparation of the carbendazim (CBZ) solution

A carbendazim stock solution (3.75 mg/ml) was prepared by dissolving it in pre-warmed DMSO. This solution was vortexed and heated in a water bath set to 55°C for 3.5 hours. Then the solution was vortexed again and cooled down to room temperature before use.

Prolonged microtubule depolymerization via *nda3-KM311* block

Cells bearing the *nda3-KM311* cold sensitive tubulin mutation were grown at the permissive temperature (30°C) to mid-log phase and then shifted to the restrictive temperature (18°C) for 6-9 hours to depolymerize their microtubules and activate the spindle assembly checkpoint (SAC). Cells were harvested, fixed in 100% methanol and stained with DAPI (to detect DNA) or calcofluor (to detect septa).

SAC recovery assay

nda3-KM311 cells arrested at 18°C for 6 hours were shifted back to the permissive temperature (30°C), and incubated for 30 minutes to allow microtubule re-polymerization. Cells were harvested, fixed in 100% methanol and stained with DAPI (to detect DNA) or calcofluor (to detect septa).

Table 2.1 Fission yeast strains used in this study

Strain	Genotype	Source
OS118	*nda3-KM311 GFP-plo1::ura4*$^{+}$	Hardwick lab
OS165	*nda3-KM311 GFP-plo1::ura4*$^{+}$ *bub1Δ::NAT*	Hardwick lab
OS172	*nda3-KM311 GFP-plo1::ura4*$^{+}$ *bub1 K762R D900N*	This work
OS260	*cdc25-22 lid1-TAP::kan'mad2-GFP::his3 mad3-GFP::his3*	Hardwick lab
OS261	*cdc25-22 lid1-TAP::kan'mad2-GFP::his3 mad3-GFP::his3 bub1 K762R D900N*	Hardwick lab
OS216	*cdc25-22 lid1-TAP::kan'mad2-GFP::his3 mad3-GFP::his3 sgo2Δ::NAT*	This work
OS190	*cdc25-22 slp1-FLAG::hyg mad2-GFP::his3 mad3-GFP::his3 bub1 K762R D900N*	This work
OS20	*cdc25-22 slp1-FLAG::hyg mad3-GFP::his3*	This work
OS246	*cdc25-22 slp1-FLAG::hyg mad2-GFP::his3 mad3-GFP::his3 mph1-kd::NAT*	This work
OS191	*cdc25-22 lid1-TAP::kan' mad3-GFP::his3 slp1S482A::hyg*	This work
OS188	*cdc25-22 lid1-TAP::kan' mad3-GFP::his3 slp1S482A S483A S484A::hyg*	This work
OS210	*cdc25-22 lid1-TAP::kan' mad3-GFP::his3 S482E S483E S484E::hyg*	This work
OS201	*cdc25-22 lid1-TAP::kan' mad3-GFP::his3 mad2Δ::ura4+ leu1*	This work
OS213	*cdc25-22 lid1-TAP::kan' mad3-GFP::his3 S482E S483E S484E::hyg mad2Δ::ura4+ leu1*	This work
OS18	*cdc25-22 lid1-TAP::kan' mad3-GFP::his3 slp1-FLAG::hyg*	This work
OS184	*cdc25-22 lid1-TAP::kan' mad3-GFP::his3 slp1S482A-FLAG::hyg*	This work

Strain	Genotype	Source
OS154	*nda3-KM311 GFP-plo1::ura4⁺slp1S482A S483A S484A::hyg*	This work
OS123	*nda3-KM311 GFP-plo1::ura4⁺slp1S482E S483E S484E::hyg*	This work
OS129	*nda3-KM311 GFP-plo1::ura4⁺slp1R488E::hyg*	This work
OS119	*nda3-KM311 lid1-TAP::kan' mad3-GFP::his3*	Hardwick lab
OS134	*nda3-KM311 lid1-TAP::kan' mad3-GFP::his3 slp1S482E S483E S484E::hyg*	This work
OS135	*nda3-KM311 lid1-TAP::kan' mad3-GFP::his3 slp1R488E::hyg*	This work
OS287	*cdc25-22 lid1-TAP::kan' mad3-GFP::his3 slp1S482D::hyg*	This work
OS286	*cdc25-22 lid1-TAP::kan' mad3-GFP::his3 slp1S482D::hyg bub1 K762R D900N*	This work

Table 2.2 Plasmids used in this study

Name	Description	Source
OS11	pDONR201-Slp1-FLAG::hyg Gateway	This work
OS5	pFL-MCC-DN	David Barford
OS18	pFL-bub1	This work
OS19	pFL-bub1-kd	This work
OS7	pFL-MCC-FL	David Barford

Table 2.3 Primers used in this study

No.	Name	Sequence (5'–3')	Comments	Source
OS13	Slp1_1108Rev	CCATTGTGCCACCGCCTGTCG	Diagnostic PCR and sequencing	This work.
OS16	Slp1 938 FW	GTTCAGACGGTCTTCAGTTG	Diagnostic PCR and sequencing	This work.
OS17	Slp1 37bp downst FW	CGTCGAATCACTATGTTGC	Diagnostic PCR and sequencing	This work.
OS24	Slp1 upstream ApaI FW	GGGCCCCGCAGCATTACCATAAGCTG	Internal tag	This work.
OS34	Slp1 Hyg attB1 FW	TTGATGGCGAATCCGCTGCTATGAAATTGGTTG	Gateway cloning	This work.
OS35	Slp1 Hyg attB2 REV	CAACCAATTTCATAGCAGCGGATTCGCCATCAA	Gateway cloning	This work.
OS22	Slp1 upstream NaeI REV	TCACTAGAGAACGCGTTATATG	Internal tag	This work.
OS47	Slp1 S482D mutagenesis FW	CCAATTACCAAAACCCCGgacAGCAGCATAACAATCC	S1D mutation	This work.
OS48	Slp1 S482D mutagenesis REV	GGATTGTTATGCTGCTgtcCGGGGTTTTGGTAATTGG	S1D mutation	This work.
OS39	IE FW	CCCCGTCCAGCAGCATAACAATCgaaTGAACAACACC	IE mutation.	This work.
OS40	IE REV	GGTGTTGTTCAttcGATTGTTATGCTGCTGGACGGGG	IE mutation.	This work.
OS41	S3A FW	CCAAAACCCCGgcggctgccATAACAATCCG	S3A mutation	This work.
OS42	S3A REV	CGGATTGTTATggcagccgcCGGGGTTTTGG	S3A mutation	This work.
OS43	S3E FW	CCAAAACCCCGgaggaagagATAACAATCCG	S3E mutation	This work.
OS44	S3E REV	CGGATTGTTATctcttcctcCGGGGTTTTGG	S3E mutation	This work.

2.5 Protein methods

2.5.1 Immunoprecipitations

Anaphase promoting complex/cyclosome (APC/C) interaction

Proteins were extracted from harvested cells in lysis buffer (50 mM HEPES pH 7.5, 75 mM KCl, 1 mM MgCl2, 1 mM EGTA, 0.1% TritonX-100, 1 mM sodium vanadate, 0.1 µM microcystin, complete mini EDTA free, and 1 mM pefabloc). Cells were resuspended in lysis buffer and bead-beat twice for 30 seconds. Lysates were spun and cleared lysates were incubated for 45 min with IgG-coupled Dynabeads (Invitrogen), which bind to Apc4-TAP. The immunoprecipitated complexes were washed five times with lysis buffer and then analysed by immunoblotting with sheep anti-GFP antibody, sheep anti-Mad2 and Peroxidase anti-Peroxidase (PAP) antibodies.

$Cdc20^{Slp1}$ (mitotic checkpoint complex) interaction

The same steps described above were followed, except cells expressing $Cdc20^{Slp1}$-FLAG (instead of Apc4-TAP) were used, and the lysates from these cells were incubated with anti-FLAG-coupled Dynabeads, which bind to Cdc20-FLAG.

2.5.2 SDS-PAGE

Resolving gels were made following the recipe below:

	12.5 %
40 % acrylamide	4.7 ml
2 % Bis	0.75 ml
1.5 M Tris-HCl pH 8.8	3.75 ml
Water	to 15 ml

150 µl of 10 % ammonium persulfate (APS) and 20 µl TEMED were added to catalyse the polymerization of resolving gel. Once the gel solution was added between glass plates used to cast gels, it was overlaid with isopropanol and

allowed to set for 20 minutes. Then ispropanol was decanted, the gel was quickly rinsed and stacking gel solution was added.

Stacking gels were made following the recipe below:

40 % acrylamide	6.25 ml
2 % Bis	3.33 ml
1.0 M Tris-HCl pH 6.8	6.25 ml
Water	*to 50 ml*

Proteins were resolved for 60-120 minutes at a constant voltage (110-170 V) in SDS-PAGE running buffer (2 % SDS, 50 mM Tris, 384 mM glycine). After SDS-PAGE, proteins were transferred unto a nitrocellulose membrane (GE Healthcare) using a TE77 semi-dry transfer unit (Hoefer) at 135 mA for 120 min in semi-dry transfer buffer (25 mM Tris, 130 mM glycine, 10 % methanol).

2.5.3 Immunoblotting

Quality of the protein transfer was analyzed by Ponceau staining, and the membranes were blocked in blocking solution (1x PBS or TBS, 0.04 % Tween 20, 3-5 % w/v dried skimmed milk) for 30 minutes at room temperature and on a shaking platform, followed by overnight incubation with the primary antibody (diluted in blocking buffer) at 4 ^{o}C. Next day, membranes were washed with PBS or TBS + 0.04 % Tween 3 times for 5 minutes each, before being incubated with secondary antibody (diluted in blocking buffer) for 40 minutes at room temperature. Membranes were washed with PBS or TBS + 0.04 % Tween 3 times before protein visualisation by chemiluminescence using an ECL detection kit (SuperSignal West Pico or SuperSignal West Femto, Pierce) according to the manufacturer's instructions. Finally, membranes were exposed to X-ray films (Agfa Healthcare), which were subsequently developed using a SRX-101A Film Processor (Konica-Minolta).

Primary and secondary (HRP-conjugated) antibodies used in this study:

Antibody	Species	Dilution	Source
Anti-Mad2	Sheep	1:1000	Hardwick lab
Anti-FLAG M2	Mouse	1:1000	Sigma-Aldrich
Anti-Cdc20^{Slp1}	Rabbit	1:1000	Matsumoto lab
Anti-tubulin (TAT1)	Mouse	1:1000	Keith Gull
Anti-GFP	Sheep	1:1000	Hardwick lab
Anti-sheep, HRP conjugated*	Donkey	1:5000	Jackson Immuno-Research
Anti-mouse, HRP conjugated*	Donkey	1:5000	GE Healthcare
Anti-rabbit, HRP conjugated*	Sheep	1;5000	GE Healthcare

2.5.4 *In vitro* kinase assays

Fission yeast Bub1 and MCC (mitotic checkpoint complex) proteins, which were purified from insect cells (See chapter 4.1), were washed twice with 1 x kinase buffer (50 mM Hepes pH 7.5, 10 mM $MgCl_2$, 0.5 mM DTT). 25 µl of kinase reaction buffer (12.5 µl 2x kinase buffer (100 mM Hepes, pH7.5, 20 mM $MgCl_2$, 1 mM DTT), 0.5 µl P^{32} gamma-ATP, 0.5 µl 1 mM ATP, made up with substrate (MCC) and kinase (Bub1) in a final volume of 25 µl was then incubated at 30°C for 30 mins. Reactions were stopped by adding 2xSDS sample buffer, boiled and resolved in an SDS-PAGE gel. Then the gel was stained with Coomassie Blue, dried and phosphorylation signals were detected by exposing the gel to Typhoon phosphoimager. Cold kinase assays were carried out with 100 mM ATP and further analysed by mass spectrometry.

2.5.5 Mass-spectrometry

Cross-linking fission yeast MCC

Recombinant MCC was expressed in insect cells and the cell lysate was incubated with Strep magnetic beads to immobilize the MCC. Cross-linking was performed using two different cross-linkers: BS3 or EDC, each of them requiring different buffer conditions. Therefore, beads solution was split into two; one half was resuspended in HEPES (pH 8.0) for cross-linking with BS3, and the other half in MES (pH 6.0) for cross-linking with EDC. Cross-linking reactions were carried out on the beads by Angel Chen (from Juri Rappsilber lab), followed by trypsin digestion and mass spectrometry. Cross-linking data was visualized using Xi Network Viewer (Generated by Juri Rappsilber lab).

2.5.6 APC/C ubiquitination assays

Fission yeast genes E1 (Uba1) and E2s (Ubc1, 4 and 11) inserted in pMAL and pET16b vectors respectively were kindly provided by Hiro Yamano. These vectors were used to express the proteins in BL21 RIL cells. MBP-Uba1 and His-tagged E2s were then affinity purified using either amylose (NEB) or talon resins (Clonetech). MBP-Uba1 was further purified by size exclusion chromatography using a Sephadex S200 column. Full-length APC/C activator $Cdc20^{Slp1}$ and radiolabelled [Met ^{35}S] APC/C substrate, $securin^{cut2}$ were produced by *in vitro* translation using the TNT Quick Coupled Transcription/Translation kit (Promega) according to manufacturer's instructions using 1µg of pHY22-$Cdc20^{Slp1}$ and pHY22-$securin^{cut2}$ plasmids also provided by Hiro Yamano. Lid1-TAP APC/C was affinity purified using IgG agarose beads (GE Healthcare) from *S. pombe* cells carrying the ts *slp1-362* mutation to isolate the APC/C that is free from endogenous $Cdc20^{slp1}$.

In vitro APC/C ubiquitination assays were carried out following a method based on assays previously described for budding, fission yeast and human proteins (Foster & Morgan, 2012; Hwang et al., 1998). In brief, 0.05 mg/ml Uba1, 0.5mg/ml E2s (ubc1, ubc4 and ubc11) and 0.3 mM ATP were mixed with 1.5 mg/ml wild-type mono-ubiquitin (Sigma Aldrich), 2µM ubiquitin aldehyde (Boston Biochem) in a ubiquitination buffer containing 25 mM HEPES pH 7.5, 100 mM KCl, 3mM ATP, 2.5 mM $MgCl_2$, and 0.2 mM DTT. The ubiquitination mix was incubated at 23 °C for 20 min. 0.5 µM APC/C, 4 µl and 2 µl of $Cdc20^{Slp1}$ and $securin^{cut2}$ respectively were then added to the mix in a total reaction volume of 20 µl. Reactions were carried out at 23 °C for 45 min and stopped by adding 4xSDS sample buffer. Samples were subjected to SDS-PAGE electrophoresis and visualised by radiography using the Typhoon phosphoimager. The ubiquitination of $securin^{cut2}$ by APC/C was quantified using the ImageQuant software (GE Healthcare) to analyse the decrease in intensity of the unmodified securin band.

Chapter 3: Roles of Bub1 kinase activity in the spindle assembly checkpoint

3.1 Overview

During mitosis, equal chromosome segregation is crucial to maintain chromosomal stability throughout the cell division cycle. A cellular surveillance mechanism, known as the spindle assembly checkpoint (SAC) ensures chromosomal stability by delaying chromosome segregation (anaphase onset), until all sister kinetochores attain bi-orientation (Conly L. Rieder et al., 1995).

Bub1 kinase is one of the upstream enzymes of SAC signalling. Studies in various model organisms have reported two sets of Bub1 functions based on its structural domains:

1. Non-kinase related functions (mediated by the N-terminal and middle regions of Bub1), which are mainly functionaing as a scaffold at the unattached kinetochores to recruit downstream SAC proteins (Klebig et al., 2009; Rischitor et al., 2007; Shepperd et al., 2012a; Vanoosthuyse et al., 2004; Mathijs Vleugel et al., 2013).
2. Functions mediated by Bub1 kinase activity. Observations in various species have suggested two major roles for Bub1 kinase activity:
    (i) Ensuring chromosome bi-orientation by recruiting the Shugoshin protein (Sgo2 in fission yeast) to inner centromere through direct phosphorylation of H2A (Kawashima et al., 2010).
    (ii) Delaying premature anaphase onset (underlying mechanisms are currently unclear) to provide time for chromosome bi-orientation, which is the main focus of this chapter.

Unlike its chromosome bi-orientation roles described above, roles of Bub1 kinase activity for the SAC response are less well-understood. Even though its downstream pathways remain to be discovered, several lines of evidence have demonstrated the requirement of Bub1 kinase activity for a robust SAC response.

Several studies suggested that whilst the Bub1 kinase activity is not essential for the SAC response to many unattached kinetochores (generated by prolonged spindle

perturbation through *nda3-KM311* tubulin mutation or high dose of nocodazole), it is essential for the SAC response to a few unattached kinetochores (generated by low dose nocodazole) or lack of tension at sister kinetochores (generated by cohesion mutants) in budding yeast (Fernius & Hardwick, 2007), fission yeast (Kawashima et al., 2010) and *Xenopus* egg extracts (Chen, 2004). In addition, in fission yeast cells (Yamaguchi et al., 2003) that are exposed to an-anti microtubule drug (75µg/ml microtubule depolymerising drug carbendazim, CBZ) during synchronous mitosis, the ability of the 'kinase-dead' Bub1 mutant to delay anaphase onset is 25-30% less than that of wild type Bub1. Compared to *nda3-KM311* cold sensitive mutation, carbendazim (CBZ) treatment has been reported to cause relatively subtle spindle damage, as cells exposed to CBZ have been reported to retain short microtubule stubs associated with their spindle pole bodies (Petersen & Hagan, 2003). On the basis of these observations, we hypothesize that the SAC roles of Bub1 kinase activity may become more important to delay anaphase onset in response to relatively subtle and short spindle perturbation, rather than prolonged spindle damage.

The 'kinase-dead' Bub1 mutant (*bub1-K762R*), that was constructed by Yamaguchi and colleagues, has been reported to retain residual kinase activity *in vitro* and *in vivo* (Kawashima et al., 2010). On the other hand, Kawashima and colleagues have demonstrated that mutating the catalytic site (D900N) of Bub1 in addition to mutating its ATP binding motif (K762R) abolishes its kinase activity (Kawashima et al., 2010).

In this chapter, we aim to investigate roles of Bub1 kinase activity in SAC response using the *bub1-K762R D900N* allele (hereafter referred to interchangeably as *bub1-kd*) (Kawashima et al., 2010) and analysing its ability to:

- (i) Arrest at metaphase in response to relatively severe (*nda3-KM311* tubulin mutation) spindle damage (ii) recover from the SAC arrest upon re-polymerization of microtubules, and progress into anaphase.
- (i)Arrest at metaphase in response to relatively subtle (carbendazim treatment) spindle damage (ii) recruit two of the MCC components (Mad2 and Mad3) to kinetochores (iii) Assemble the MCC (iv) catalyse MCC-APC/C binding.

3.2 Analysis of Bub1 kinase function in response to microtubule depolymerisation by *nda3-KM311* allele

3.2.1 Analysis of Bub1 kinase function in maintaining SAC arrest at metaphase

In order to examine abilities of *wild type, bub1-kd* (Figure 3.1A) and *bub1* null cells to arrest at metaphase in response to depolymerised microtubules, we used the *nda3-KM311* cold sensitive tubulin mutation, by which microtubules are depolymerised at the restrictive temperature (18°C), and thereby the SAC is activated. Strains were grown overnight at the permissive temperature (30°C) to mid-logarithmic phase, and then shifted to the restrictive temperature (18°C) for 9 hours. Cell samples were collected 6 hours and 9 hours after the temperature shift, fixed in methanol and stained with DAPI to visualise DNA. In addition to scoring condensed DNA, we monitored localisation of polo kinase (Plo1-GFP) at spindle poles, which is another indication of a metaphase arrest (Bahler et al, 1998a; Mulvihill et al, 1999).

During the *nda3-KM311* block cells exhibited characteristics of three types of cell cycle stages (Figure 3.1D): the first type is late G2 cells, which have uncondensed DNA and relatively weak Plo1-GFP signal gradually accumulating on their spindle poles; the second type is metaphase arrested cells with condensed DNA and strong Plo1-GFP signal on spindle poles; the third type is the cut (**c**ell **u**ntimely **t**orn) cells, in which cells exit mitosis forming septa without symmetrical segregation of their sister chromatids. The cut phenotype correlates with defects in the SAC response, as in this case cells do not have a robust checkpoint machinery to delay mitotic exit when the spindle formation is perturbed (Yanagida, 1998).

Figure 3.1B and C show that after spending 6 hours with depolymerised microtubules, 52% of the wild type cells arrested at metaphase, 48% remained at late G2, and only 1% exhibited cut phenotype.

On the other hand, *bub1* null cells did not arrest at metaphase at all, however exhibited 41% cut and 59% late G2 phenotype. This result was expected since *bub1* null cells are known to be SAC deficient (Vanoosthuyse et al., 2004).

Despite having a fully functional Bub1 N-terminus, less *bub1-kd* cells arrested at metaphase (43%) than the wild type cells (52%). Moreover, Figure 3.1C shows that

after 6 hours of *nda3-KM311* block, 11% of the *bub1-kd* cells exhibited cut phenotype. In other words, 11% of the *bub1-kd* cells leaked through the metaphase arrest and exited mitosis without accurate chromosome segregation.

After 9 hours, Figure 3.1B displays that the difference between the abilities of *wild type* and *bub1-kd* in arresting at metaphase became more significant. While 76% of *wild type* cells arrested at metaphase, only 54% of *bub1-kd* cells were able to arrest. Furthermore, as shown in Figure 3.1C-D, *bub1-kd* cells exhibited the cut phenotype more frequently (12%) than wild type cells did (2%). In the absence of Bub1 protein, premature mitotic exit was even more frequent, which was indicated by 58% cut phenotype observed in *bub1* null cells.

These results suggest that the non-kinase region of Bub1 (N-terminal and the middle region) is essential for the SAC response, however its C-terminal kinase activity is still required for SAC maintenance during a prolonged and severe spindle perturbation (highly penetrant microtubule polymerisation) mediated by *nda3-KM311* mutation.

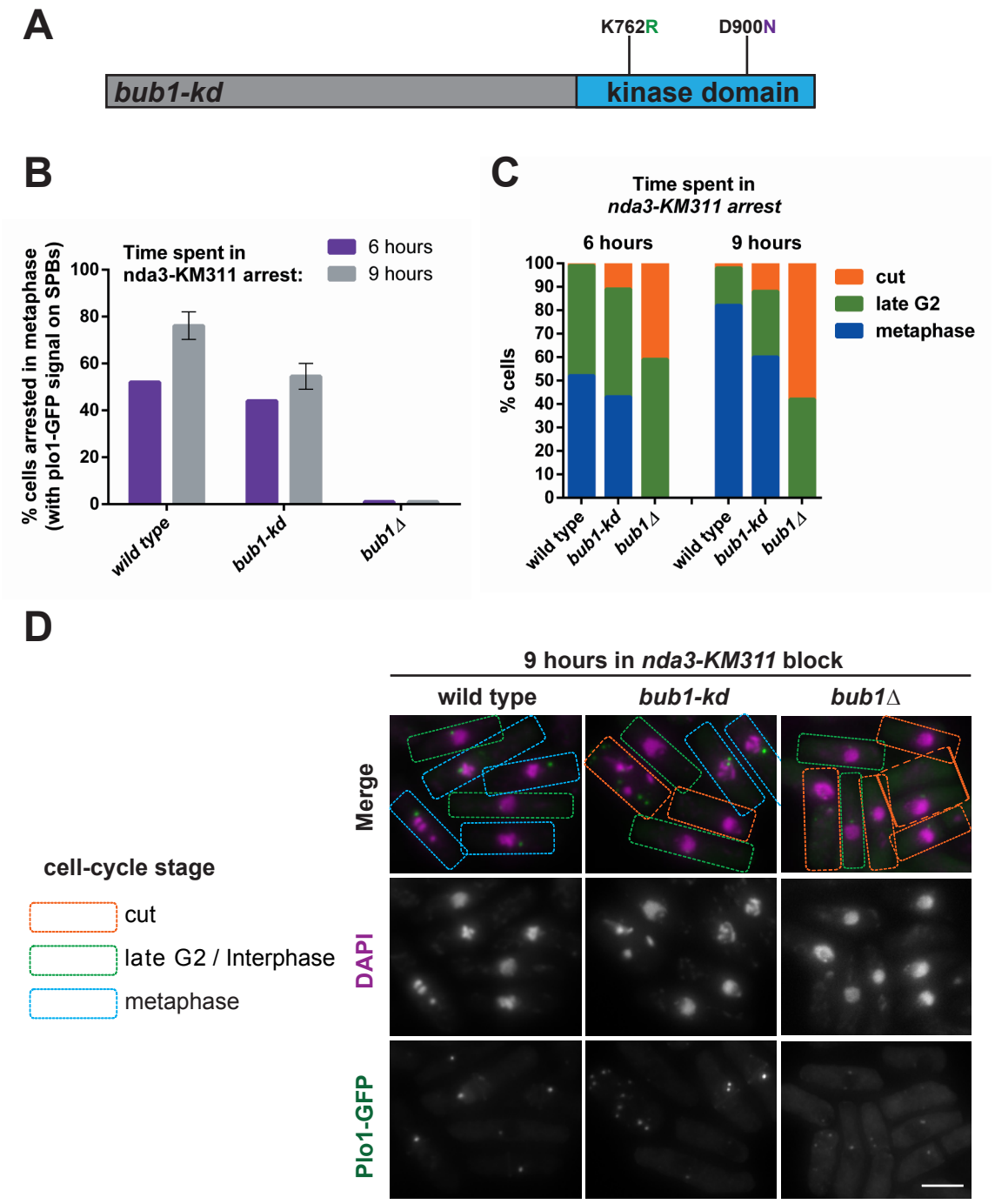

Figure 3.1 Bub1 kinase activity is required for maintaining the SAC in *nda3-KM311* block

(A) Cartoon illustrating *S. pombe bub1 kinase-dead (kd)* allele, in which the function of C-terminal kinase domain is abolished through two point mutations: K762R (ATP binding site) and D900N (catalytic site). **(B)** Wild type, *bub1-kd* and *bub1*Δ cells bearing *nda3-KM311* cold sensitive tubulin mutation were grown at the permissive temperature (30°C) and shifted to the restrictive temperature (18°C) for 9 hours. Cell samples were collected 6 hours and 9 hours after the temperature shift, fixed in methanol and stained with DAPI to visualize DNA. Graph plotting percentage of cells arrested at metaphase with condensed DNA and Plo1-GFP localization at their spindle pole bodies (SPBs). 9 hour results are the mean values of two independent experiments with the error bars represent standard error of the mean (SEM) (n=100 cells per time point). **(C)** Distribution of the cells described in B in terms of their cell cycle stage: late G2 cells (green) with uncondensed DNA and relatively weak or absent Plo1-GFP signal; metaphase arrested cells (blue) with condensed DNA and strong Plo1-GFP signal; cut cells (**c**ell **u**ntimely **t**orn) (orange) which exit mitosis forming septa, without equal chromatid segregation. **(D)** Representative images from 9 hours of *nda3-KM311* block, displaying the distribution of the cells in terms of their cell-cycle stage. Scale bar represents 5 microns.

3.2.2 Analysis of Bub1 kinase function in recovering from the SAC arrest at metaphase

In the previous section we demonstrated that Bub1 kinase function was important to fully activate the SAC response and arrest cells at metaphase when spindle formation was perturbed by *nda3-KM311* cold sensitive mutation. In its absence (in the case of *bub1-kd*), higher frequency of 'cut' phenotype was observed, in which the cells exited mitosis without ensuring equal segregation of their chromosomes.

In this section, we address whether Bub1 kinase activity has a role in recovering from the SAC-mediated metaphase arrest, upon formation of the spindle. To analyse this, we released *wild type* and *bub1-kd* cells (in the same experiment described in Figure 3.1) from 6 hours of *nda3-KM311* block at 18℃, shifting them back to the permissive temperature (32℃) to allow re-polymerisation of microtubules. Then we collected cell samples 10, 20 and 30 minutes after the temperature shift, and fixed them in methanol to process as described previously (Figure 3.1).

Following the release from metaphase arrest we observed that the cells exhibited characteristics of various cell-cycle stages (Figure 3.2A). The first type is late G2 cells, which have uncondensed DNA and relatively weak Plo1-GFP signal gradually accumulating on their spindle poles. The second type is metaphase arrested cells with condensed DNA and strong Plo1-GFP signal on spindle poles. Metaphase cells consist of two subtypes; the cells displaying overlapped Plo1-GFP signals (one spot) on two spindle poles that are very close to each other early in metaphase and the cells displaying separated Plo1-GFP signals late in metaphase (two spots). The third category is anaphase cells, which have their sister chromatids equally separated, and pulled to the opposite poles by re-polymerised microtubules. The fourth is 'cut' cells, which exit mitosis forming septa, without equal segregation of their sister chromatids, and become aneuploid.

On the basis of these criteria, Figure 3.2C shows that 10 minutes after the release from metaphase arrest 37% of initially arrested wild type cells exited mitosis by either progressing into normal anaphase (25%) or cut phenotype (12%) (mitotic exit without chromosome segregation) (Figure 3.2B). On the other hand, after 10 minutes 51% of

initially arrested *bub1-kd* cells exited mitosis, 30% of it progressing into normal anaphase and 21% exhibiting cut phenotype.

After 30 minutes (Figure 3.2C), 81% of initially arrested wild type cells exited mitosis, with 74% normal anaphase and 7% cut phenotype. However, after 30 minutes percentage of mitotic exit was 93% for *bub1-kd* cells, exhibiting 68% normal anaphase and 25% cut phenotype.

In order to compare mitotic exit rates of *wild type* and *bub1-kd* cells when spindle reformed, we plotted trend lines out of '% of initially arrested cells which exited mitosis upon microtubule re-polymerisation' data. Linear regression analysis of these lines demonstrated that SAC recovery (mitotic exit) rates of *wild type* and *bub1-kd* cells were not significantly different from each other, indicated by the result that neither the slopes (stability of a certain recovery rate), nor the elevations (recovery rates themselves) are significantly different.

In summary, (Figures 3.1A and B) upon re-polymerization of microtubules initially well-arrested wild type cells progressed into a normal anaphase with a low frequency of cut phenotype. On the other hand, *bub1-kd* cells did not only slip through the SAC arrest (with more frequent cut phenotype) throughout the *nda3-KM311* block, but also exhibited an increasing number of cut phenotype during the recovery from the SAC mediated arrest.

These results suggest that, Bub1 kinase function is important for both preventing premature mitotic exit when the spindle formation is perturbed, and ensuring equal segregation of chromosomes upon re-polymerization of microtubules.

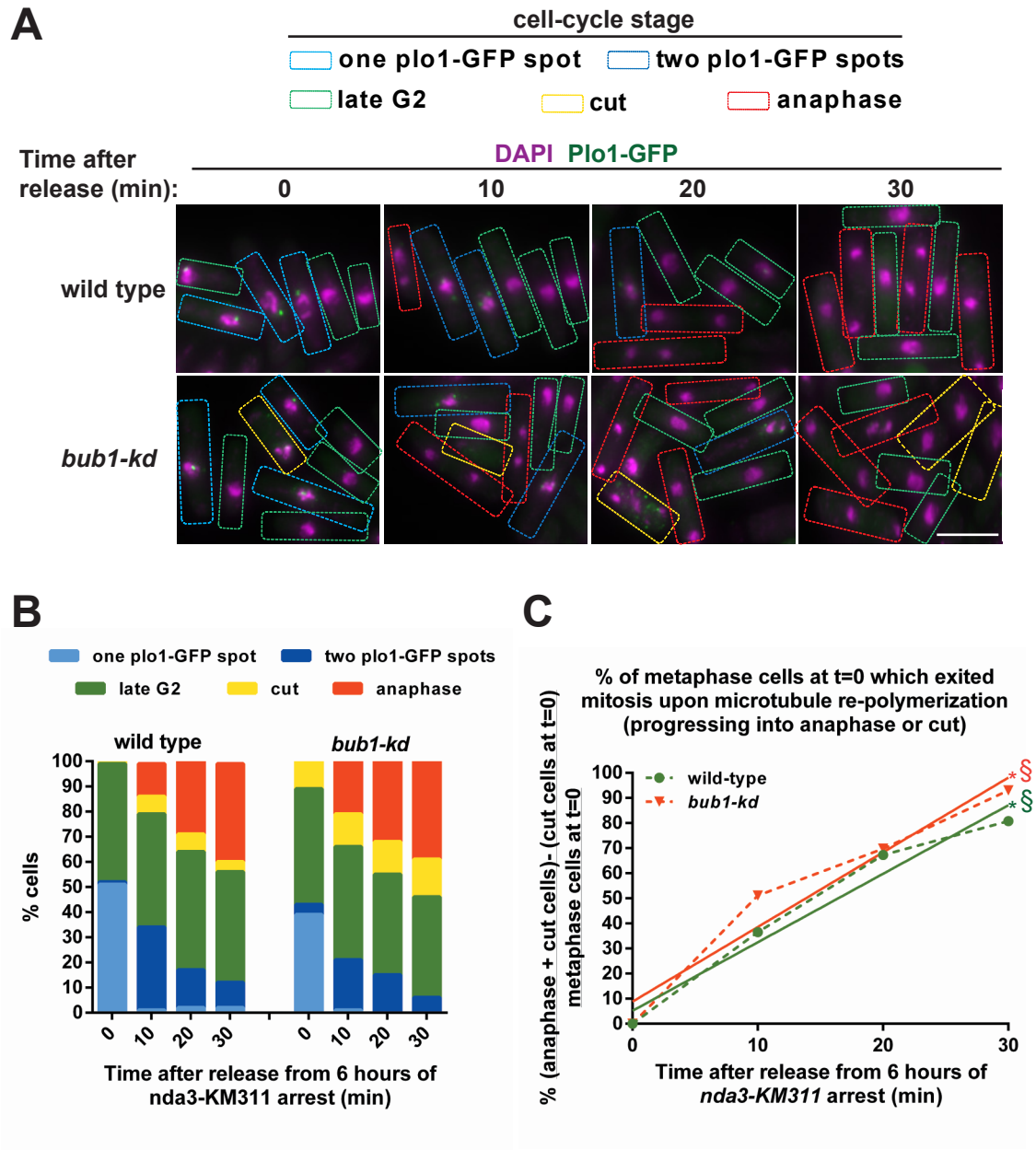

Figure 3.2 Bub1 kinase activity is required to ensure equal chromosome segregation

(A) Cells from the same experiment described in Figure 3.1 were blocked for 6 hours at 18°C with depolymerized microtubules through *nda3-KM311* tubuline mutation. Immidiately after taking the 0 minute samples, cells were shifted to the permissive temperature (32°C) to allow re-polymerization of microtubules, and subsequent recovery from the SAC. Cell samples were taken at each 10 minutes for 30 minutes after the release from *nda3-KM311* block, fixed in methanol, and stained with DAPI (purple) to visualize DNA, along with Plo1-GFP localisation at SPBs (green). Pictures demonstrate representative cell-cycle stages of the cells 0, 10, 20 and 30 minutes after the release. Observed mitotic stages are annotated with dashed rectangles as follows: cells at late G2 (green); metaphase cells with one (light blue) or two (dark blue) Plo1-GFP spots at SPBs; cut cells (yellow); and anaphase cells (red). Scale bar represents 5 microns. **(B)** Graph displaying the relative percentage of each cell-cycle stage for each strain throughout 30 minutes after the release (n=100 cells) **(C)** Graph plotting the percentage of metaphase cells at time=0, which progressed into anaphase or cut 0, 10, 20, 30 min after the release, using the following formula:

$$\% \ \frac{\text{(anaphase cells + cut cells at 0, 10, 20 or 30 min) - (cut cells at 0 min)}}{\text{metaphase cells at 0 min}}$$

Linear regression analysis of the trend lines was performed using GraphPad Prism software: * indicates lines with *slopes* that are not significantly different from each other; § indicates lines with *elevations* that are not significantly different from each other.

.

3.3 Analysis of Bub1 kinase function in response to microtubule depolymerisation by an anti-microtubule drug

In the preceding two sections, we have investigated possible roles of Bub1 kinase activity in activating (when microtubules depolymerized) and inactivating (when microtubules re-polymerized) the SAC, by employing *nda3-KM311* cold sensitive tubulin mutation. Using the n*da3-KM311* allele has multiple advantages and related downsides.

First, it provides a switch-like control on the polymerization of microtubules, which is reversible by switching between restrictive (18℃) and permissive (32℃) temperatures. However, *S. pombe* cells grow very slowly at 18℃. Therefore, once an asynchronous culture is shifted to 18℃, the whole population may not enter mitosis and be blocked at metaphase. This was observed in the previous experiment, in which 47% and 16% of the wild type cells were in late G2 after 6 and 9 hours of *nda3-KM311* block respectively. Second, because it is a genetic tool, spindle perturbation through *nda3-KM311* is much more penetrant than those obtained from anti-microtubule drugs. This is particularly useful to rule out possible outcomes of residual microtubule polymerization. On the other hand, this 'absolute' microtubule depolymerisation mediated by *nda3-KM311* results in activation of a very strong SAC response. In other words, a prolonged *nda3-KM311* block leaves all the kinetochores unattached for a considerably long period of time (6-9 hours), which leads to constant formation of high quantities of MCC. This is a condition, in which contributions from more subtle elements of the SAC machinery might be overlooked in the presence of excessive amount of MCC. Bub1 kinase activity may be playing such a subtle role in maintaining the SAC, compared to the direct involvement of MCC components (Cdc20, Mad2 and Mad3). Thus, in this section we investigate Bub1 kinase activity by employing a more subtle spindle perturbation that is mediated by an anti-microtubule drug called carbendazim (CBZ) (Petersen & Hagan, 2003). This way, we aim to dissect the roles of Bub1 kinase function under conditions where it might become more important for SAC activation.

To do this, we employ temperature sensitive *cdc25-22* mutant, which allows blocking the cells at G2 and releasing them into mitosis synchronously. To arrest cells in mitosis, they are treated with 100µg/ml CBZ 20 minutes after the G2 release (Note that cells have been observed not to enter mitosis if CBZ is added before 20 minutes, Jonathan Millar laboratory personal communication).

3.3.1 Analysis of mitotic progression rate and kinetochore localization of MCC components in the presence of an anti-microtubule drug

In the previously described *nda3-KM311* time courses we used *bub1* null allele as a negative control to examine *bub1-kd* allele in the context of the SAC. Although *bub1-kd* cells were not able to activate the SAC at wild type levels, they were not as defective as *bub1* null cells either. These results suggest that the N-terminal regulatory region of Bub1 is essential for the SAC, however C-terminal kinase function is still required for its maintenance during a prolonged spindle perturbation mediated by *nda3-KM311* mutation.

In this section, we investigate Bub1 kinase activity using *sgo2* null (Shugoshin2) as a control allele. *S. pombe* Sgo2 is required for loading the Aurora B complex (chromosome passenger complex) to centromeres, where it destabilizes erroneous attachments, and thereby activates the SAC (Vanoosthuyse, Hardwick, 2007). Bub1 kinase has been shown to recruit Sgo2 to centromere through direct phosphorylation of H2A-S121(Kawashima et al., 2010). It has also been observed that the centromeric localization of Sgo2 is abolished in *H2A-S121A* and *bub1-kd* cells, which impairs the recruitment of Aurora B. Moreover, *sgo2* null cells largely reproduced the defects of *bub1-kd* and *H2A-S121A* cells in ensuring accurate chromosome segregation, and delaying anaphase in the absence of sister chromatid cohesion. However, in an *nda3-KM311* block *sgo2* null cells activated the SAC like wild type cells did (Vanoosthuyse, Hardwick, 2007), whereas *bub1-kd* cells were more defective in that regard (Kawashima et al., 2010). This suggests that Bub1 kinase might have other substrates which are involved in the maintenance of the SAC response. Considering that *sgo2* null phenocopies *H2A-S121A* (lack of H2A phosphorylation by Bub1), it can serve as an ideal separation-of-function allele which would help distinguish from other possible roles of Bub1 kinase activity in SAC activation.

In order to investigate roles of Bub1 kinase function in regulating the progression rate of a mitosis with destabilized microtubules, wild type, *bub1-kd* and *sgo2* null cells bearing *cdc25-22* mutation were grown at 25°C to mid-log phase, and shifted to 36°C (restrictive temperature for the *cdc25-22* allele). After 4 hours at 36°C, cells were synchronously released from G2 phase into mitosis by shifting them back to the permissive temperature (25°C). Cells were treated with the anti-microtubule drug (CBZ) 20 minutes after the release. Samples were collected at 30 minute time points for 150 minutes, fixed in methanol, and then stained with calcofluor to detect septa. Septation was scored as a readout of anaphase onset/ mitotic exit (Yanagida, 1998), in order to determine mitotic progression rate. In addition, two of the MCC components Mad2-GFP and Mad3-GFP were visualized, as they are known to localise at kinetochores in metaphase arrested cells (S. Heinrich et al., 2012). Although the delay of anaphase onset (manifested as the absence of septation) and the kinetochore localization of MCC components are related events both occurring at the metaphase arrest, they might be regulated by different pathways. To be able to separately evaluate these pathways we scored kinetochore localisation of Mad2 and Mad3 only in the population of non-septating cells.

30 minutes after the G2 release (10 minutes after the CBZ treatment) all three strains (wild type, *bub1-kd* and *sgo2* null cells) arrested at metaphase with a low septation index (15-20%) (Figure 3.3A). Consistent with this, all three strains displayed kinetochore localization of Mad2 and Mad3 in roughly half (wild type 55%; *bub1-kd* 46%; and *sgo2* null; 54%) of their non-septating cells (Figure 3.4B).

60 minutes after the G2 release *bub1-kd* cells deviated from wild type and *sgo2* null cells. While wild type and *sgo2* null cells maintained a relatively robust SAC arrest indicated by only 41-45% septation, more than half of *bub1-kd* cells (66%) septated, as they could not delay anaphase onset (Figure 3.3A). Consistent with the maintenance of a SAC arrest, 90% of the non-septating wild type cells had Mad2 and Mad3 foci at unattached kinetochores. Although their SAC arrest (45% septation) was as robust as that of wild type cells (41% septation), a relatively small proportion of non-septating *sgo2* null cells (63%) exhibited kinetochore localization of the MCC components.

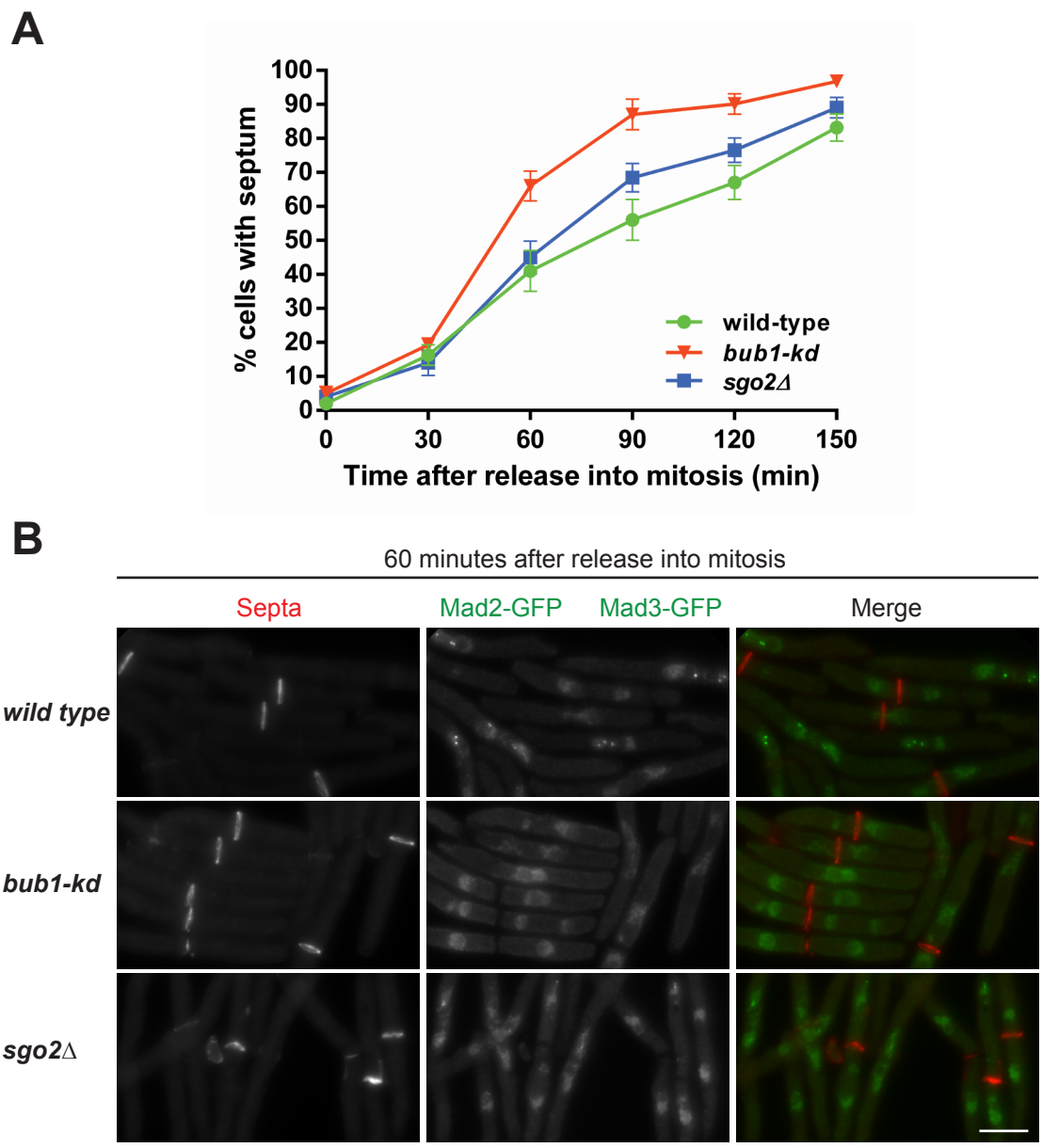

Figure 3.3 Bub1 kinase activity is required to delay premature anaphase in response to the microtubule drug CBZ

(A) *Cdc25-22* temperature sensitive cells (wild type, *bub1-kd* and *sgo2*Δ) were grown at the permissive temperature (25°C) until mid-log phase, then shifted to the restrictive temperature (36°C) for 4 hours to block in G2. Once all cells were blocked at G2-phase, they were shifted back to the permissive temperature (25°C) to be released into a synchronous mitosis (time=0). 20 minutes after the release, cells were treated with the microtubule depolymerising drug, 100 µg/ml carbendazim (CBZ) to activate the SAC response. Samples were collected at each 30 minutes time point. Graph plotting percentage of cells that formed septum (exited mitosis) throughout 150 minutes (n=100 cells). Results are the average of two independent experiments, and the values are expressed as mean ± SEM. **(B)** Representative images from 60 minutes after release into mitosis, displaying septation (in red) by calcofluor staining and Mad2-GFP, Mad3-GFP localisation (in green) at kinetochores. Scale-bar represents 5 microns.

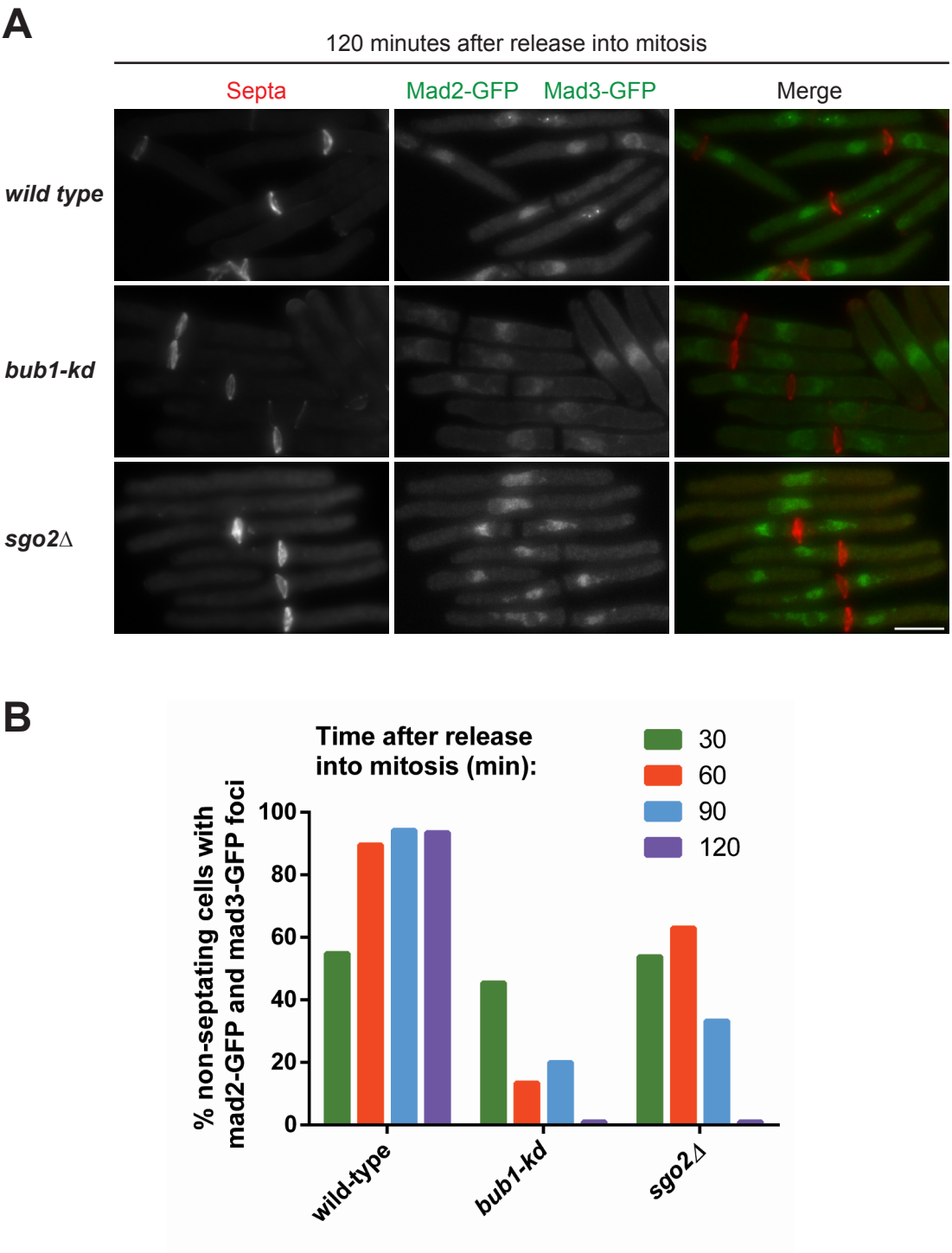

Figure 3.4 Bub1 kinase function is required to maintain the kinetochore localization of MCC components in response to CBZ

(A) Representative images at 120 minutes after release into mitosis, from the same experiment described in Figure 3.3, displaying septation (in red) by calcofluor staining and Mad2-GFP, Mad3-GFP localisation (in green) at kinetochores. Scale-bar represents 5 microns. **(B)** Graph plotting percentage of non-septating cells with Mad2-GFP and Mad3-GFP localized at kinetochores 30, 60, 90 and 120 min after the release into mitosis. (n= 30-80 cells).

Strikingly at 60 minutes, only 14% of non-septating *bub1-kd* cells displayed robust Mad2 and Mad3 localisation to unattached kinetochores (Figures 3.3B and 3.4B).

At the 90 minutes time point, abilities of wild type (56% septation) and *sgo2* null cells (68% septation) to delay anaphase onset became slightly different. On the other hand, a considerable proportion of *bub1-kd* cells (87% septation) slipped through the SAC arrest, and progressed into anaphase. Kinetochore localization of MCC components was observed in 94% of non-septating wild type cells, whereas that became even less frequent in *sgo2* null (33%) and remained low in *bub1-kd* cells (20%) (Figure 3.4B).

Towards the end of the time course at 120 minutes, almost all of the *bub1-kd* cells exited mitosis (90% septation), whereas wild type (67% septation) and *sgo2* null (77% septation) cells were more proficient at delaying anaphase onset. Despite the similar metaphase arrest profiles of wild type and *sgo2* null cells, their MCC kinetochore localization frequencies appeared to be dramatically different. Mad2 and Mad3 kinetochore foci were completely abolished in *sgo2* null and *bub1-kd* cells, whereas it was observed in 94% of the non-septating wild type cells (Figure 3.4 A and B)

These data suggest that at the early stages (30 minute) of a mitosis challenged with CBZ, Bub1 kinase activity is largely dispensable for both delaying anaphase onset and recruiting MCC components to kinetochores. However, at the later stages (60 minutes onward) it is required to maintain the SAC activity, to be able to sustain both the kinetochore recruitment of the MCC components and the anaphase delay. On the other hand, Bub1-mediated phosphorylation of H2A (*Sgo2+*) is not strictly required for either SAC activation or maintenance, as *sgo2* null cells exhibited a similar mitotic progression to wild type cells. However, although the SAC response was intact without it, the Bub1-H2A-Sgo2-Aurora B pathway appears to play a role in the kinetochore localization of the MCC components, given *sgo2* null cells became gradually defective in recruiting Mad2 and Mad3 after 30 minutes (Figure 3.4B).

Taken together, Bub1 kinase activity appears to be required for at least two main aspects of the SAC response:

1) Localization of Mad2, Mad3 (maybe even Cdc20) at unattached kinetochores, where they assemble to form MCC. This role of Bub1 kinase function appears to be partially mediated through the Bub1-H2A-Sgo2-Aurora B pathway.
2) Arresting at metaphase to delay anaphase onset, and provide cells time to correct erroneous microtubule-kinetochore attachments. This role of Bub1 kinase function appears to be largely mediated by another substrate(s) of Bub1, which may be directly involved in APC/C inhibition.

3.3.2 Analysis of MCC formation in an unperturbed mitosis

In the preceding section we proposed that Bub1 kinase activity maintains the anaphase delay in response to spindle perturbation through an unknown substrate(s) (and/or its autophosphorylation). Since this substrate(s) does not appear to be in the Bub1-H2A-Sgo2-Aurora B pathway, we hypothesize that it may be directly involved in the inhibition of APC/C.

Considering that the mitotic checkpoint complex (MCC) is the ultimate effector of the SAC (London & Biggins, 2014b; Sudakin et al., 2001), we addressed whether the Bub1 kinase activity has a role in MCC formation. To analyse that, wild type, *bub1-kd* and *mps1-kd* cells bearing c*dc25-22* mutation were grown at 25°C, and shifted to 36°C. After blocking cells at G2 phase for 4 hours, they were shifted back to 25°C to be released into an unperturbed mitosis (time 0). Cell samples were collected at 15 minute time points for 135 minutes. Then the samples were lysed, subjected to anti-FLAG (Cdc20) immunoprecipitation and processed for SDS-PAGE/western blotting, in which they were probed for two of the MCC components (Mad2 and Mad3). Note that, we used the SAC deficient Mps1 (Mph1 in fission yeast) kinase-dead (*mps1-kd*) allele as a negative control, because the kinase activity of Mps1 is required for MCC formation (unpublished data) and MCC-APC/C interaction (Zich et al., 2012).

Figure 3.5A shows that, consistent with the previous observations, MCC formation was somewhat compromised in *mps1-kd* cells, whereas *bub1-kd* cells exhibited MCC formation similar to wild type levels. It is worth to note that the mitotic appearance of Cdc20 (Stephanie Heinrich et al., 2013) was observed to be slightly delayed in *bub1-kd* cells (appearing at 45 minutes) compared to wild type (appearing at 30 minutes) (Figure 3.5B). This suggests that Bub1 kinase activity may be required for a timely mitotic entry after the G2 phase block.

These results suggest that unlike Mps1 kinase activity, Bub1 kinase activity is not necessary for MCC formation in an unperturbed mitosis.

A

IP: Cdc20 (FLAG)

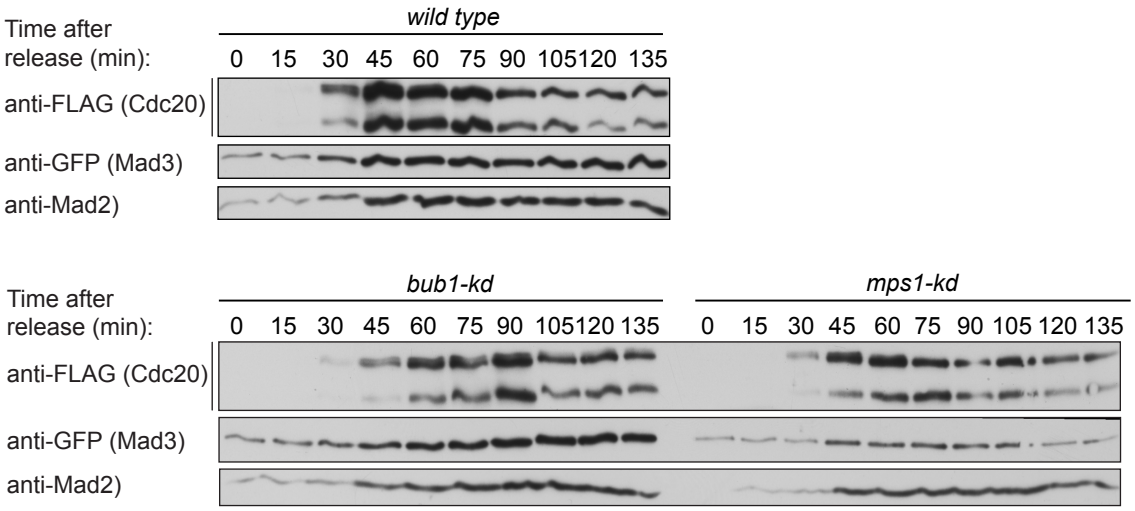

B

Input:

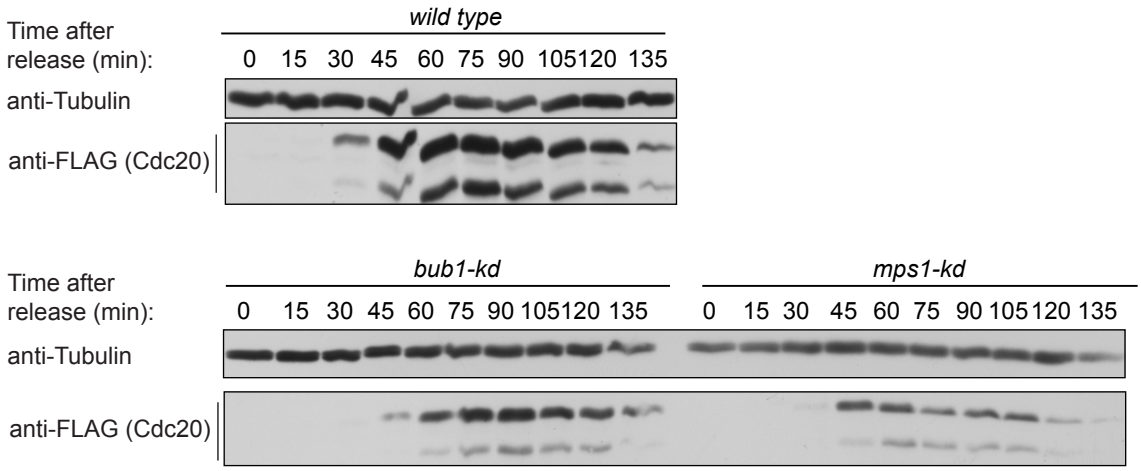

Figure 3.5 Bub1 kinase activity is not necessary for MCC formation in an unperturbed mitosis

Wild type, *bub1-kd* (kinase-dead Bub1) and *mps1-kd* (kinase-dead Mps1) cells were blocked in G2-phase for 4 hours through *cdc25-22* temperature sensitivity, and then released into an unperturbed mitosis at 0 minute. Cells were harvested at each 15 minutes time point throughout 135 minutes. Coimmunoprecipitation (IP) analysis of the MCC formation is shown. Cdc20 (FLAG) was immunoprecipitated from cell extracts. Levels of Mad3 (GFP) and Mad2 coimmunoprecipitated with Cdc20 (FLAG) were analyzed by immunoblotting using anti-GFP and anti-Mad2 antibodies. Tubulin (TAT1) levels were analyzed as loading control. Cdc20 (FLAG) is generally detected as two bands due to the cleavage of this fusion protein.

3.3.3 Analysis of MCC-APC/C interaction in the presence of an anti-microtubule drug

We demonstrated that *bub1-kd* cells can form MCC efficiently, therefore suggested that Bub1 kinase activity is not necessary for MCC formation in an unperturbed mitosis. However, formation of the MCC at wild type levels may not be sufficient to delay anaphase, considering the SAC maintenance defects of *bub1-kd* cells we previously observed in the presence of spindle damage (Figures 3.1, 3.3 and 3.4). Thus, we hypothesize that Bub1 kinase activity may have a role in MCC binding to the APC/C in response to spindle perturbation.

To determine that, wild type and *bub1-kd* cells bearing *cdc25-22* mutation were grown at 25°C, and shifted to 36°C. After blocking cells at G2 phase for 4 hours, they were shifted back to 25°C to release them into a synchronous mitosis (time 0), which was followed by CBZ treatment 20 minutes after the release. Cell samples were collected at 15 minute time points for 135 minutes. Then the samples were lysed, subjected to anti-TAP (APC4) immunoprecipitation and processed for SDS-PAGE/western blotting, in which they were probed for two of the MCC components (Mad2 and Mad3).

As demonstrated in Figure 3.6, Mad2 and Mad3 began binding the APC/C at 30 minutes after destabilisation of microtubules (20 minutes) in both wild type and *bub1-kd* cells, though amount of MCC components interacting with APC/C was less in *bub1-kd* cells. After 30 minutes, wild type cells maintained a detectable MCC-APC/C interaction until 120 minutes time point, whereas it was abolished at 60 minutes in *bub1-kd* cells.

Considering that the MCC-APC/C interaction is the ultimate inhibitory mechanism of the SAC (London & Biggins, 2014b), these results are consistent with our previous findings (Figures 3.1 and 3.3) that *bub1-kd* cells are not able to maintain an anaphase delay in response to microtubule depolymerisation. Thus, we conclude that Bub1 kinase activity contributes to the maintenance of anaphase delay, largely stabilizing MCC-APC/C interactions probably through phosphorylation of its unknown substrate(s).

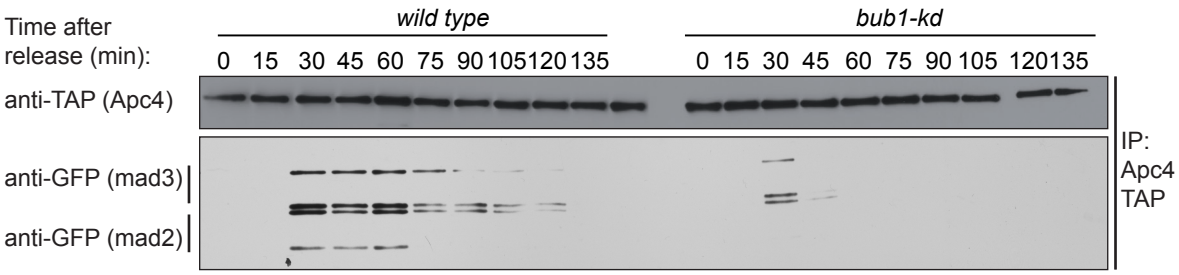

Figure 3.6 Bub1 kinase activity is required to maintain the MCC-APC/C interaction in response to the microtubule drug CBZ

Wild type and *bub1-kd* cells were blocked in G2-phase for 4 hours through *cdc25-22* temperature sensitivity, and then released into mitosis at 0 minute. At 20 minutes, cells were treated with the microtubule depolymerising drug CBZ to activate the SAC response. Cells were harvested at each 15 minutes time point throughout 135 minutes. Coimmunoprecipitation (IP) analysis of MCC-APC/C interaction is shown. Apc4 (TAP) was immunoprecipitated from cell extracts. Levels of Mad3 (GFP) and Mad2 (GFP) coimmunoprecipitated with Apc4 (TAP) were analyzed by immunoblotting using anti-GFP antibody. Apc4 levels were analyzed as loading control. Mad3 (GFP) and Mad2 (GFP) are commonly detected as two bands due to cleavage of these fusion proteins.

3.4 Discussion

In this chapter we investigated roles of fission yeast Bub1 kinase activity in SAC signalling under various spindle perturbation conditions: (i) severe (*nda3-KM311* tubulin mutation) or (ii) subtle (carbendazim treatment) microtubule depolymerisation.

3.4.1 Bub1 kinase activity is important but not necessary for the SAC response to prolonged spindle damage

In response to a prolonged exposure (9 hours) to severe (*nda3-KM311* tubulin mutation) microtubule depolymerisation we observed that the kinase-dead Bub1 mutant (*bub1-K762R D900N*) failed to maintain the SAC mediated metaphase arrest at wild type levels (22% less mitotic index than wild type), while exhibiting characteristics of the 'cut' phenotype (untimely mitotic exit with missing or aberrant chromosome segregation) more frequently (10% more than wild type), though not as frequently as *bub1* null exhibited (56% more than wild type).

Our observations are consistent with previous findings of (Kawashima et al., 2010), who constructed the kinase-dead Bub1 mutant allele (*bub1-K762R D900N*) that we have used in this study. (Kawashima et al., 2010) reported that in a 10 hours long *nda3-KM311* block, *bub1-K762R D900N* cells are 10% less efficient than wild type and *sgo2* null cells in arresting at metaphase. (comparable SAC proficiencies of wild type and *sgo2* null has been also reported by (Vanoosthuyse, Prykhozhij, & Hardwick, 2007)). This suggests, Kawashima and colleagues indicated that *bub1-K762R D900N* was not as SAC defective (10%) as we observed (22%). This phenotypical difference might have been due to using different criteria for scoring metaphase arrested cells. (Kawashima et al., 2010) have reported that they score all the cells displaying Plo1-GFP foci at spindle poles as metaphase arrested. However, weak yet detectible Plo1 localization in late G2 cells has been observed before, in which DNA is not condensed yet and exhibits the interphase-like morphology (crescent shape, with faint ribosomal DNA in the middle, see Figure 3.1D) (Mulvihill, Petersen, Ohkura, Glover, & Hagan, 1999). Therefore, in order to distinguish the genuine metaphase-arrested cells from the late G2 cells, we score only the ones (as metaphase arrested), which have both strong Plo1-GFP signal and condensed DNA (Figure 3.1D).

Taken together, these results confirm that the non-kinase region of Bub1 (N-terminal and the middle region) is essential for the SAC response to severe spindle damage. However, although not essential, C-terminal kinase activity of Bub1 is still required for SAC maintenance.

3.4.2 Bub1 kinase activity is necessary for chromosome bi-orientation

We next sought to determine whether Bub1 kinase activity has a role in recovering from the SAC-mediated metaphase arrest, upon reformation of the spindle. To examine this, we allowed re-polymerization of initially perturbed microtubules in the same experiment described in Figure 3.1, and analysed the abilities of wild type and *bub1-K762R D900N* cells to silence their SAC response and progress into anaphase.

Wild type and *bub1-kd* cells exited mitosis with similar rates (*bub1-kd* cells were slightly faster though), thus their abilities to recover from SAC recovery were comparable (Figure 3.C). However, while most of the wild type cells were progressing into a normal anaphase, *bub1-K762R D900N* cells exhibited an increasing frequency of cut phenotype during their recovery from the SAC arrest (Figure 3.2A and B). These observations are consistent with previous fission yeast studies which have reported that upon recovery from an *nda3-KM311* arrest, Bub1 kinase-dead cells (both *bub1-K762R D900N* (Kawashima et al., 2010) and *bub1-K762M* (Vanoosthuyse et al., 2009)) exhibit lagging chromosomes frequently, similar to *sgo2* null cells. The latter study (Vanoosthuyse et al., 2009) analysed chromosome bi-orientation of the *bub1-K762M* allele by monitoring the segregation of GFP-marked chromosome 2, which we should also carry out (ideally by live imaging) in order to accurately analyse the ability of *bub1-K762R D900N* allele in chromosome bi-orientation.

To sum, these results confirm that Bub1 kinase activity is necessary for bi-orientation and accurate segregation of chromosomes, and this role of Bub1 appears to be largely performed through the Bub1-H2A-Sgo2-Aurora B pathway.

3.4.3 Bub1 kinase activity is necessary to maintain anaphase delay and kinetochore recruitment of SAC proteins in response to the anti-microtubule drug CBZ

After confirming the published roles of Bub1 kinase activity (contributing to anaphase delay and playing a key role in chromosome bi-orientation) in response to prolonged spindle damage (*nda3-KM311*), we set out to determine whether it is also required under relatively subtle spindle perturbation. To analyse this, we monitored mitotic progression rates and the kinetochore recruitment of MCC components in wild type, *bub1-kd (bub1-K762R D900N)* and *sgo2* null cells, which all bear *cdc25-22* mutation and were exposed to microtubule depolymerising drug carbendazim (CBZ) 20 minutes after the release from G2 phase.

Abilities of wild type and *sgo2* null cells in delaying anaphase onset in response to spindle damage were comparable throughout the mitosis, whereas *bub1-K762R D900N* cells failed to maintain metaphase arrest, and they progressed into premature anaphase (Figure 3.3). Our results are in agreement with those of another fission yeast study (Yamaguchi et al., 2003). Yamaguchi and colleagues have reported that both the *bub1-K762R* allele and a Bub1 truncation allele lacking the entire kinase domain failed to delay anaphase onset in response to CBZ treatment. We observed that the *bub1-K762R D900N* mutant was capable of arresting like wild type and *sgo2* null early in mitosis (soon after the CBZ treatment), whereas after 60 minutes it leaked through the SAC arrest 25-30% more frequently than wild type and *sgo2* null cells did. Even though Yamaguchi and colleagues employed a different method to synchronize the cells in G2 phase (a Cdk1 temperature sensitive mutant), their results were consistent with ours. Similarly, their kinase-inactive Bub1 alleles were also able to arrest at metaphase soon after the CBZ treatment, however at later stages they failed to maintain that arrest, and entered anaphase 25% more frequently than wild type (Yamaguchi et al., 2003).

Taken together, soon after the CBZ treatment (30 minutes after the G2 release) Bub1 kinase activity is largely dispensable for delaying anaphase onset, whereas at the later stages of mitosis (60 minutes onward) it becomes necessary to maintain the SAC arrest. This role of Bub1 does not appear to be performed through the Bub1-H2A-

Sgo2-Aurora B pathway, because the absence of sgo2 does not significantly affect the mitotic progression rate, unlike the lack of whole Bub1 kinase activity does (Figure 3.3). Consequently, substrate(s) of Bub1 kinase, in addition to H2A, may be responsible for its anaphase delay role.

In addition to its role in delaying anaphase onset, we analysed the role of Bub1 kinase activity in recruiting MCC components (Mad2 and Mad3) to kinetochores independently from its anaphase delay role. As we previously demonstrated in Figure 3.3, the *bub1-K762R D900N* (*bub1-kd*) mutant has less cells arrested at metaphase. Therefore the *bub1-kd* mutant is expected to have a very low percentage of Mad2 and Mad3 kinetochore recruitment (within the whole *bub1-kd* population), which would be surely affected by its low mitotic index. However, this does not necessarily mean that the sub-population of *bub1-kd* cells, that are still arrested at metaphase (much fewer than wild type though), are defective in recruiting Mad2 and Mad3, in case its anaphase delay role is independent of the kinetochores (for instance, it may be mediated through a catalytic APC/C inhibition, via direct phosphorylation of it or one of its activators). In order to dissect these two possible roles of Bub1 kinase activity, we scored kinetochore localisation of Mad2 and Mad3 only in the population of non-septating cells (presumably arrested at metaphase).

Soon after the addition of CBZ (30 minutes after the G2 release), all three strains (wild type, *bub1-kd* and *sgo2* null cells) were able to recruit Mad2 and Mad3 to kinetochores at similar levels. However, later in mitosis (60 minutes onward) kinetochore recruitment abilities of *bub1-kd* and *sgo2* null cells gradually decreased (*bub1-kd* being more severe), while wild type cells maintained the kinetochore recruitment of Mad2 and Mad3 even at 120 minutes (where *bub1-kd* and *sgo2* null cells had no detectable kinetochore foci) (Figure 3.4). These results suggest that, soon after the CBZ treatment (30 minutes after the G2 release) Bub1 kinase activity is largely dispensable for the kinetochore recruitment of MCC components, whereas at the later stages of mitosis (60 minutes onward) it becomes more important to maintain their recruitment. This role of Bub1 appears to be partly mediated through the Bub1-H2A-Sgo2-Aurora B pathway, because the absence of sgo2 compromises Mad2 and Mad3 kinetochore localization 60 minutes onward, and becomes as defective as the lack of Bub1 kinase function at 120 minutes (Figure 3.4). This implies that another substrate(s) of Bub1

may be working in parallel with the Bub1-H2A-Sgo2-Aurora B pathway in performing the kinetochore recruitment (of the MCC components) role of Bub1 kinase activity.

On the basis of these observations, we propose a working model for the roles of Bub1 kinase activity in maintaining anaphase delay and kinetochore recruitment of MCC components in response to spindle damage (Figure 3.7). Soon after the CBZ treatment, its high concentration in the cells is presumably sufficient to depolymerise microtubules efficiently. This probably generates many unattached kinetochores. This experimental condition may mimic the cellular conditions in early prometaphase, in which most or all of the kinetochores are unattached (Chen, 2004; Pablo Lara-Gonzalez, Westhorpe, & Taylor, 2012). In the presence of relatively more unattached kinetochores, Bub1 "non-kinase activity" (kinetochore scaffolding) may suffice to recruit MCC components (Mad2, Mad3 and even Cdc20), and thereby promote the formation of "enough MCC molecules", that would efficiently inhibit Cdc20 even without Bub1 kinase activity. Although the two possible pathways mediating Bub1 kinase activity ((i) the H2A-Sgo2-Aurora B pathway and (ii) the additional "unknown" pathway) both contribute to the SAC response to a certain extent, they are largely dispensable under these conditions to maintain an average anaphase delay (Figure 3.7A).

On the other hand, in late prometaphase cells (mimicked by later stages of the time course, in which the CBZ concentration is probably lower due to being pumped out by cells (Goffeau et al., 1997)) probably fewer unattached kinetochores left. Under these conditions, lower number of unattached kinetochores may not be sufficient to stimulate enough MCC formation through the stoichiometric non-kinase activity of Bub1. Therefore, the sub-stoichiometric (catalytic) kinase activity of Bub1 may become more important for the few unattached kinetochores to maintain the "wait anaphase" signal until all kinetochores attach to microtubules (Figure 3.7).

This hypothesis is consistent with our observation that 30 and 60 minutes after the release into mitosis with CBZ (soon after the CBZ treatment), the ability of *sgo2* null cells to delay anaphase was identical to that of wild type, whereas at later stages (90 and 120 minutes) it slightly decreased (Figure 3.3A). This supports the notion that although the H2A-Sgo2-Aurora B pathway was not necessary to maintain anaphase

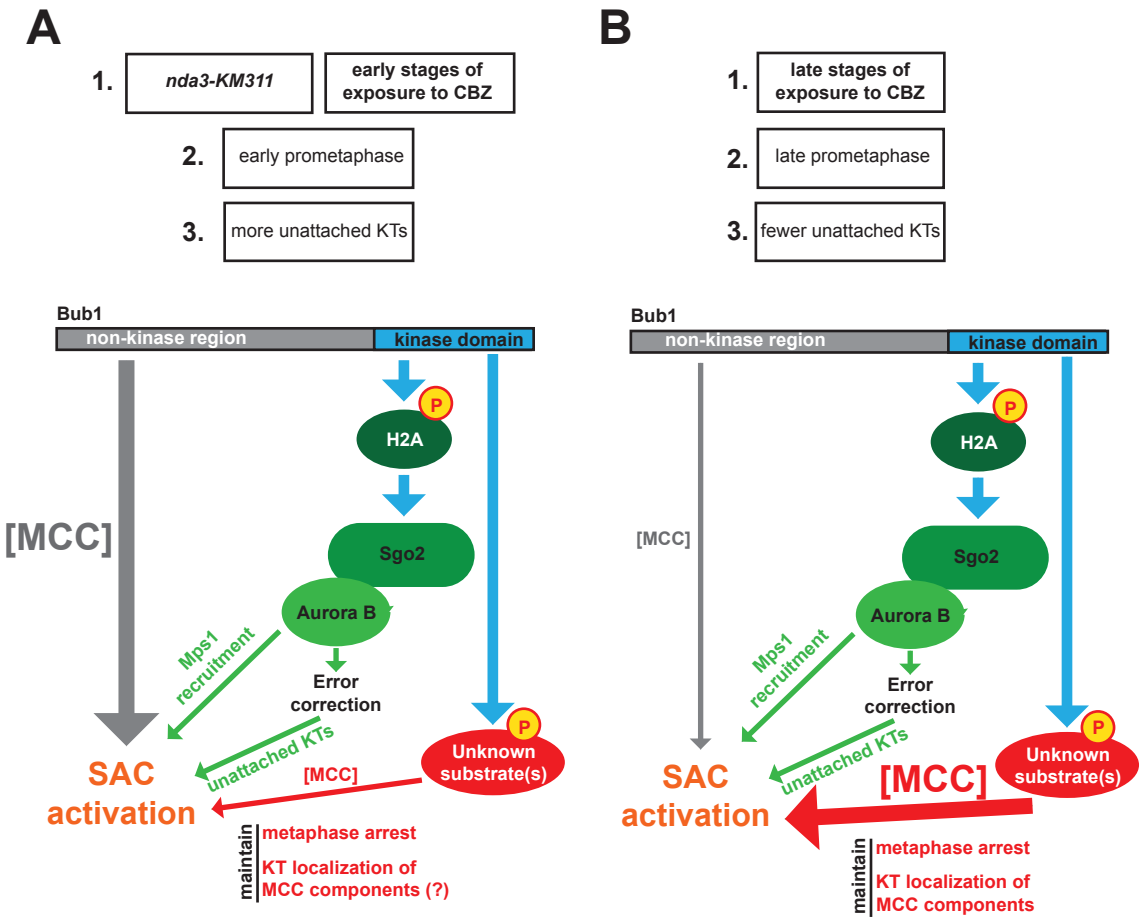

Figure 3.7 Speculative model for the regulation of SAC signalling by multiple factors in response to various degrees of spindle damage

Schematics illustrating the regulation of SAC response by multiple mechanisms, which are related to different structural domains of Bub1: C-terminal kinase domain (blue); N-terminal and middle non-kinase region (grey). Description boxes above the schematics denote: (1) various degrees of spindle damage that cells were exposed to in the time course experiments: prolonged mitotic arrest via the *nda3-KM311* tubulin mutation (relatively severe damage), early stages of exposure to the anti-microtubule drug CBZ when its at high concentrations in cells (relatively severe damage) and late stages of exposure to the anti-microtubule drug CBZ when its at relatively low concentrations in cells due to being pumped out over time(relatively subtle damage); (2) stages of prometaphase in an unperturbed mitosis mimicked by relatively severe damage (early prometaphase) or relatively subtle damage (late prometaphase) on the spindle; (3) hypothetical amounts of unattached kinetochores in early prometaphase (more) or late prometaphase (fewer). **(A)** In the presence of "more" unattached kinetochores (either in early prometaphase of an unperturbed mitosis or in a mitotic time course experiment in which cells are challenged by *nda3-KM311* or CBZ) the "non-kinase region" of Bub1 may be sufficient to promote "enough MCC molecules" ([MCC] indicates MCC concentration) to maintain the SAC response. Although the two possible pathways mediating Bub1 kinase activity, (i) the H2A-Sgo2-Aurora B pathway and (ii) the additional "unknown" pathway, both contribute to the SAC response to a certain extent, they are largely dispensable under these conditions. **(B)** In the presence of "fewer" unattached kinetochores (in late prometaphase of an unperturbed mitosis or in the later stages of a mitotic time course experiment in which cells have pumped out most of the CBZ), the "non-kinase region" of Bub1 may not be sufficient anymore to produce "enough MCC molecules", therefore Bub1 kinase activity may be required to promote (catalytically) the assembly of "enough MCC molecules" to maintain the SAC response.

delay at early stages, it becomes important, but not sufficient, to maintain the delay at later stages presumably through its contribution by (i) correcting erroneous attachments, and thereby generating more unattached kinetochores, and (ii) promoting recruitment of Mps1 to those unattached kinetochores (Figure 3.7). These roles of the H2A-Sgo2-Aurora B pathway are not sufficient, as there appears to be other roles (a parallel pathway) of Bub1 kinase activity that may be complementary to them (*bub1-kd* is significantly more SAC defective than *sgo2* null, Figure 3.3A).

This model is also in agreement with our findings in the *nda3-KM311* experiment (Figure 3.1B). In the presence of highly penetrant microtubule depolymerisation (similar to the early stages of CBZ treatment), Bub1 kinase function was not as important as it was in the late stages of CBZ treatment (Figure 3.3A). In addition, other *nda3-KM311* experiments in fission yeast have demonstrated that the H2A-Sgo2-Aurora B pathway is dispensable to maintain a robust metaphase arrest (Kawashima et al., 2010; Vanoosthuyse et al., 2007). This is sensible because when microtubules are depolymerised by *nda3-KM31,* presumably there are not enough intact microtubules (or only negligible amounts) in the cell to cause stochastic attachment errors. Under these conditions, "the error correction" role of the H2A-Sgo2-Aurora B pathway will be dispensable and is expected to contribute less to the SAC response**.**

In addition, our model is in agreement with observations in *Xenopus* egg extracts (Chen, 2004). Even though Bub1 kinase activity is dispensable in the presence of high dose nocodazole (when the "non-kinase Bub1 activity" is sufficient), it is required to maintain the SAC mediated metaphase arrest in the presence of low dose nocodazole. This suggests that the kinase activity of Bub1 probably does not function as an on-off switch of the SAC; instead, it modulates the strength of the SAC signal generated from each kinetochore, and appears to become more important for the maintenance of the SAC when the number of unattached kinetochores are presumably lower in the cell (mimicked by low dose of nocodazole). We hypothesize that Bub1 kinase activity may contribute to the maintenance of the "wait anaphase" signal through two likely mechanisms, which are not mutually exclusive:

(i) promoting MCC formation and/or MCC-APC/C interaction

(ii) inhibiting the APC/C via its kinase activity, independent of the MCC.

3.4.4 Bub1 kinase activity is not necessary for MCC assembly, yet essential to maintain MCC-APC/C interaction

We next sought to determine the inhibitory mechanism underlying the anaphase delay role of Bub1 kinase activity. We hypothesize that although the exact pathway is not known, it probably links Bub1 activity to the most downstream SAC effector, MCC, and its ultimate target, APC/C.

To test this, we analysed MCC formation in wild type and *bub1-kd,* and *mps1-kd* cells in an unperturbed mitosis. Results indicated that unlike Mps1 kinase activity, Bub1 kinase activity is not necessary for MCC formation in an unperturbed mitosis (Figure 3.5). However, this result is not sufficient conclude that MCC can assemble independent of Bub1 kinase activity, as we have tested the contribution of Bub1 activity to the SAC only in the presence of spindle damage. Therefore this experiment needs to be repeated in the presence of CBZ in order to reproduce the same conditions in which Bub1 kinase activity has been important for the SAC response.

Next, we hypothesize that Bub1 kinase activity may have a role in MCC binding to the APC/C in response to spindle perturbation. Analysis of wild type and *bub1-kd* cells in the presence of CBZ demonstrated that Bub1 kinase activity is essential to maintain MCC-APC/C interaction (Figure 3.6).

Considering that the MCC-APC/C interaction is the ultimate inhibitory mechanism of the SAC (London & Biggins, 2014b), these results are consistent with our previous findings (Figures 3.1 and 3.3) that *bub1-kd* cells are not able to maintain an anaphase delay in response to microtubule depolymerisation. Thus, we conclude that Bub1 kinase activity contributes to the maintenance of anaphase delay, largely stabilizing MCC-APC/C interactions probably through the phosphorylation of its unknown substrate(s) to be discovered, which is the main focus of chapter four.

Chapter 4: *In vitro* analysis of Bub1 kinase activity and interactions between the MCC components

4.1 Overview

In chapter three, we confirmed the requirement for Bub1 kinase activity for a robust SAC response to spindle damage, which has been reported by studies in budding yeast (Fernius & Hardwick, 2007; Roberts et al., 1994), fission yeast (Kawashima et al., 2010; Yamaguchi et al., 2003) and *Xenopus* egg extracts (Chen, 2004). We demonstrated that Bub1 kinase activity may contribute to the SAC response through another pathway that works parallel to the Bub1-H2A-Sgo2-Aurora B pathway. The upstream component of such a pathway is likely to be a substrate of Bub1 kinase, as our observations have suggested roles for its kinase activity (in addition to phosphorylating H2A) in maintaining kinetochore localization of the MCC components, MCC-APC/C interaction and ultimately anaphase delay in response to spindle perturbation. However, such a substrate of Bub1 other than H2A had not been implied until a report published in 2004 (Tang, Shu, et al., 2004). Tang and colleagues identified Cdc20 as a substrate of Bub1, and reported that Bub1-mediated phosphorylation of Cdc20 is required for a robust SAC response in response to spindle damage. In addition, they further supported this hypothesis by crystalizing the C-terminal kinase domain of Bub1, and demonstrating that Bub1 has a considerable specificity toward Cdc20 (Kang et al., 2008).

Considering our observations that Bub1 kinase activity promotes MCC-APC/C binding (Figure 3.6), we suggest that the unknown substrate of Bub1 may have a direct role in maintaining MCC-APC/C interaction in fission yeast. On the basis of human studies (Kang et al., 2008; Tang, Shu, et al., 2004; Yu & Tang, 2005), we hypothesize that maintenance of the SAC response through Bub1-mediated Cdc20 phosphorylation may be conserved among human and fission yeast.

In this chapter we aim to investigate this possibility by:

1. Purifying recombinant MCC components from insect cells, which will be used as substrates in a Bub1 kinase assay to analyse whether fission yeast Cdc20 (or other MCC components) are phosphorylated by Bub1 *in vitro.*
2. If phosphorylation takes place, identifying phosphorylated sites by mass spectrometry.
3. Analysing interactions between the recombinant MCC components to predict the roles of putative phosphorylation sites in the regulation of the SAC. Using this estimation to focus on the phosphorylation sites, which are more likely to be important for the SAC activity.
4. Engineering the cdc20+ gene at its endogenous locus (inserting an antibiotic resistance marker and an internal epitope tag) for using in subsequent experiments.
5. Generating phosphorylation mutants of Cdc20 to analyse its regulation through putative Bub1-phosphorylated sites.

4.2 Identification of Bub1 kinase substrates *in vitro*

4.2.1 Purification of Bub1 kinase and its putative substrates from insect cells

Previously in our lab there have been attempts to purify recombinant *S. pombe* Bub1 kinase and Cdc20 from competent *E. coli* cells (BL21) (data not shown). However, these attempts resulted in production of insoluble proteins. Although *E. coli* is a cheap and versatile host to produce recombinant proteins, it is likely that *S.pombe* Bub1 and Cdc20 proteins have particular requirements for chaperone systems or post-translational modifications that *E. coli* cannot support. Therefore, their recombinant production necessitates a eukaryotic expression system. The baculovirus/ insect cell system has recently become a method of choice in many laboratories for producing eukaryotic proteins. There are a number of reasons for that. First of all, large proteins with several hundred kilodalton molecular weight can be produced and authentically processed in insect cells, which contributes to their solubility. Moreover, this system does not require strict safety measures in the laboratories, as baculoviruses do not replicate in eukaryotic cells other than their insect cells hosts. Furthermore, subunits of multi-protein complexes can be simultaneously produced by infecting insect cells with a mixture of baculoviruses, each of which carries the gene encoding a particular subunit (Berger, Fitzgerald, & Richmond, 2004; Trowitzsch, Bieniossek, Nie, Garzoni, & Berger, 2010).

On the basis of these technical advantages, in this study we employed the baculovirus/ insect cell system to purify *S. pombe* Bub1 kinase and the mitotic checkpoint complex, which consists of Cdc20, Mad2 and Mad3 (Figure 4.1A), to be used in the subsequent experiments. Figure 4.2A summarises early steps of the protocol from cloning of the recombinant genes into a transfer vector to the first infection of insect cells. First, we cloned Bub1 or MCC components into a transfer vector (pFL) that is compatible with the baculovirus/ insect cell system Figure 4.2A and B. The transfer vector contains multiple baculovirus promoters (polyhedron and p10) followed by multiple cloning sites, consisting of several restriction enzyme sites. Using conventional cloning, coding sequences of Bub1 or the MCC components were inserted, whose expression would be driven by separate baculovirus promoters. *BUB1* gene was cloned in full length either as *wild type* or

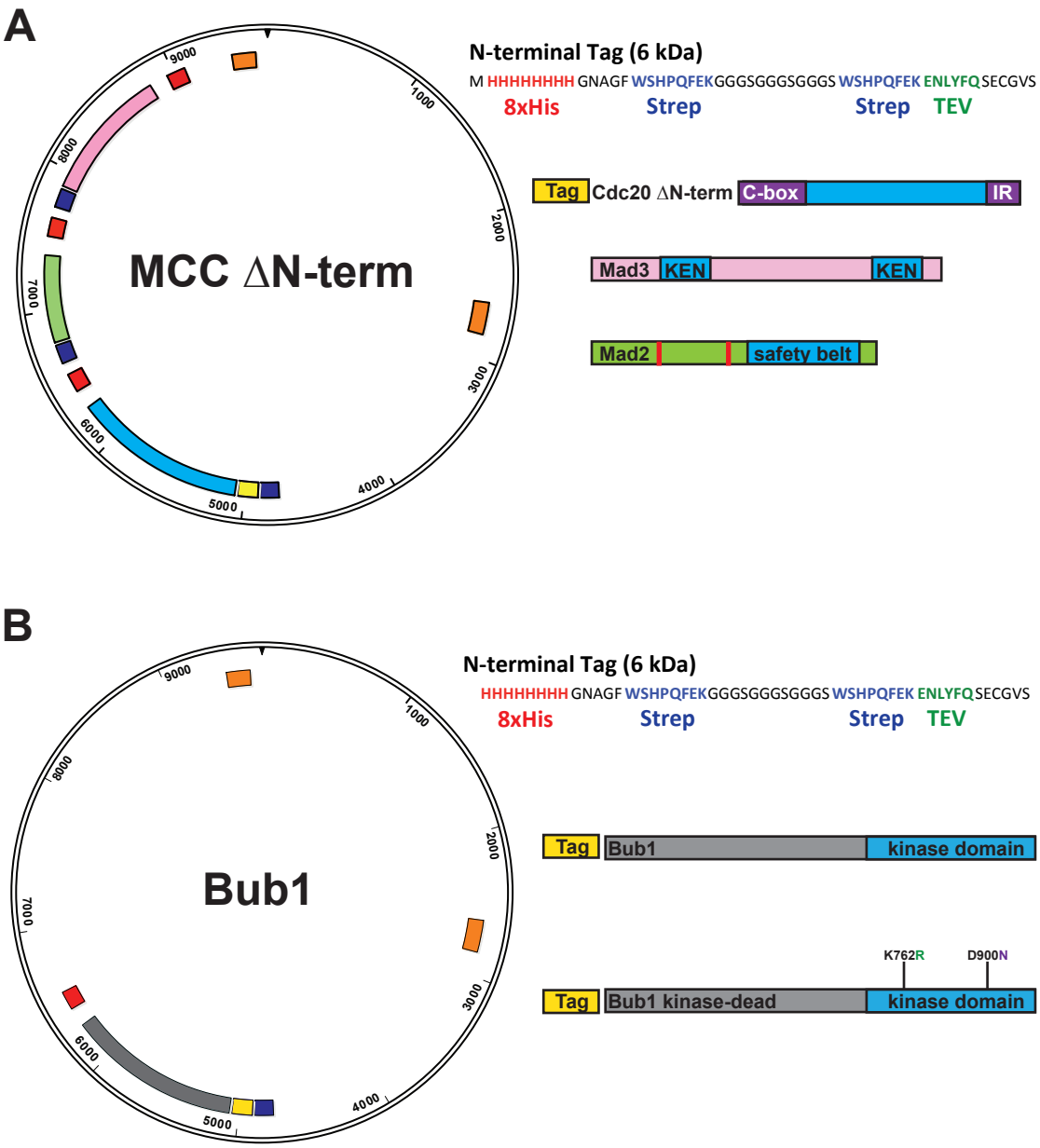

Figure 4.1 Baculovirus transfer vectors cloned with MCC ΔN-term or Bub1

(A) Schematic illustrating pFL baculovirus transfer vectors cloned with genes of the MCC ΔN-term components: Cdc20 ΔN, lacks its first 86 aminoacids and carries an N-terminal tag; Mad3 is full length and wild type; Mad2 double mutant (dm), bears two mutations, one (L12A) prevents it from dimerizing, and the other one (R133A) locks it into the closed-conformation. Sequence of the tag at the N-terminus of Cdc20 ΔN consists of 8xHis, two strep-tag II and a TEV protease recognition site. Dark blue boxes indicate baculovirus promoters, red boxes indicate terminator sequences and orange boxes indicate Tn7 transposon elements required for the transfer of recombinant genes into baculovirus genome. **(B)** Schematic illustrating pFL baculovirus transfer vectors cloned with genes of either of the following full length and N-terminally tagged Bub1 proteins: wild type Bub1 or Bub1 kinase-dead. The dark blue box indicates the baculovirus promoter, the red box indicates the terminator sequence, orange boxes indicate Tn7 transposon elements required for the transfer of recombinant genes into baculovirus genome. recombinant genes into baculovirus genome. Vector maps were constructed in and exported from Lasergene Seqbuilder Software.

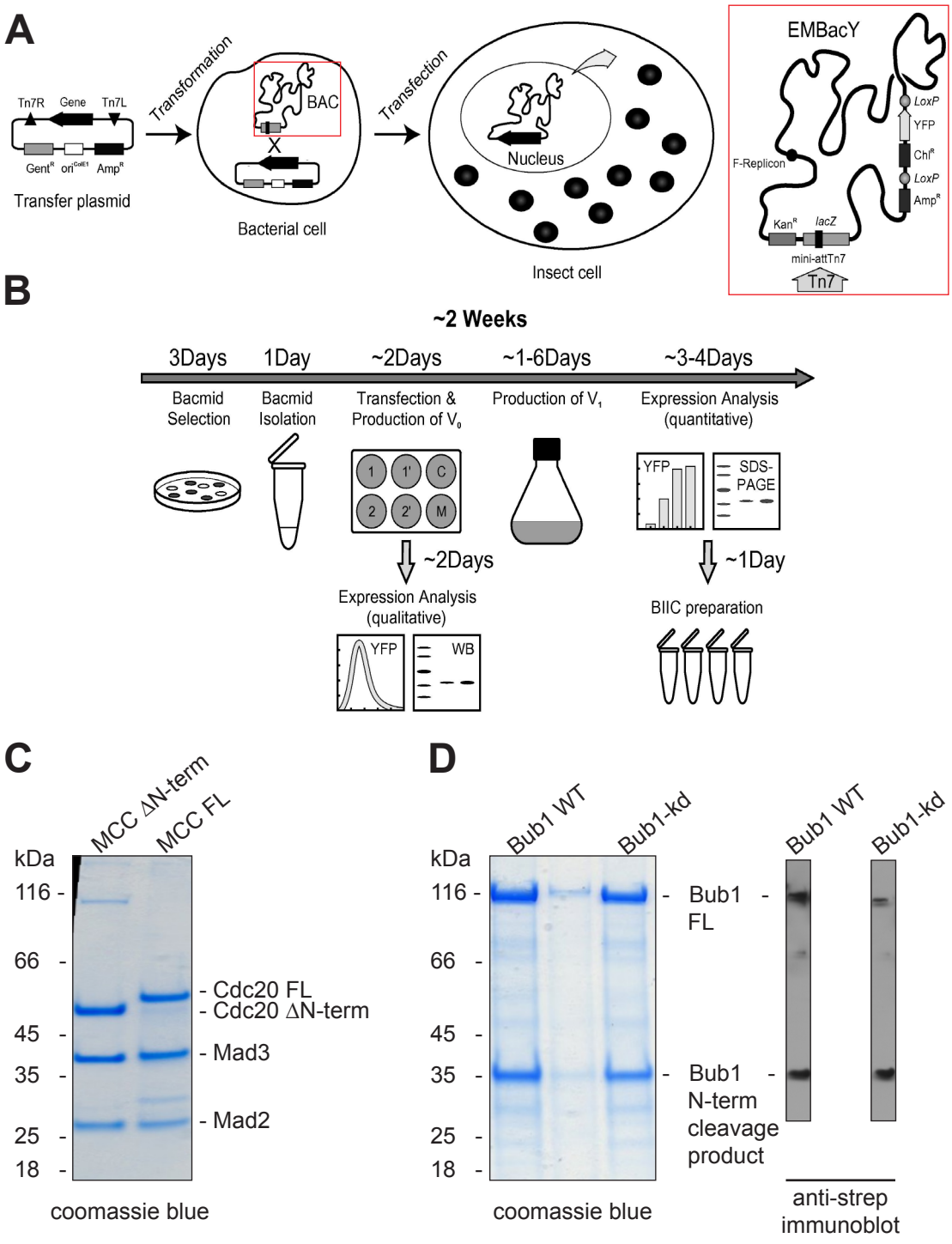

Figure 4.2 Purification of recombinant *S. pombe* SAC proteins from insect cells

(A) Schematic illustrating the early steps of producing recombinant proteins using baculovirus/ insect cell system. Genes of the recombinant proteins are cloned into a transfer plasmid (pFL), which is then used to transform bacterial cells containing the baculovirus genome (bacmid, indicated by the red rectangle and depicted in detail) in the form of a BAC. Once the recombinant genes are integrated into the bacmid, it is isolated and used in the transfection of insect cells. **(B)** Timetable for recombinant protein production in insect cells. Schematics in A and B were adapted from Trowitzsch et al. 2010 **(C)** Coomassie staining of purified recombinant mitotic checkpoint complexes (MCC); N-terminally truncated (MCC ΔN-term) and full length (MCC FL). **(D)** Coomassie staining and immunoblot (anti-Strep antibody) detection of purified recombinant Bub1 proteins tagged with a Strep tag at their N-terminus; wild type and kinase-dead (kd).

bub1-kd (Figure 4.1B). As for the MCC components (Figure 4.1A), MCC ΔN-term, containing a wild type Cdc20 ΔN that lacks its first 86 aminoacids, was cloned. By doing so, we aimed to compare MCC ΔN-term and full length MCC (provided by David Barford) to analyse whether the N-terminus of Cdc20 is phosphorylated by Bub1. MCC ΔN-term also contains (Figure 4.6A) a wild type full length Mad3 and a double mutant Mad2. The two mutations in the *MAD2-dm* gene prevent Mad2 from dimerizing (L12A) and lock it into the closed-conformation (R133A) that is active during the SAC response (Westhorpe et al., 2011). (The transfer vector containing MCC ΔN-term components was provided by David Barford, which was also used to purify the MCC and determine its crystal structure (Chao et al., 2012b). They used an N-terminally truncated Cdc20 because full length Cdc20 did not crystallize). Both Cdc20 and Bub1 carry an N-terminal tagging cassette that consists of eight tandem histidines, two strep-tag II and a TEV protease recognition site (Figure 4.1).

As illustrated in Figure 4.2A, the transfer vector also contains Tn7L and Tn7R sequence elements of the Tn7 transposon system flanking the foreign genes, which is later used in their integration into a baculoviral genome. Baculoviral genomic DNA (bacmid) isolated from native virus is engineered into an artificial bacterial chromosome (BAC) carried by competent *E. coli* cells. Integration of foreign genes into this BAC is accomplished *in vivo* via a Tn7 attachment site embedded in a lacZa gene on the BAC. A helper plasmid in the competent *E. coli* cells provides the Tn7 transposon enzyme complex for catalysing the transposition event (Berger et al., 2004).

Therefore, we transformed the competent *E. coli* cells, which contain baculovirus genome, with the transfer vector cloned with *BUB1* gene or the genes of MCC components. After a series of selections, Baculoviral genomic DNA (>130 kb) was purified from the correct *E. coli* transformants and used in the first round of infecting (transfection) insect cells (Figure 4.2A and B). In the transfection, purified bacmid was fused with a lipid-based transfection reagent and mixed into media of Sf9-type (*Spodoptera frugiperda)* insect cells that were cultured as monolayer in 6-well plates. In the next two days, the bacmid replicates itself in its host; propagating baculoviruses

burst insect cells, and are released into the insect cell growth medium. To monitor recombinant protein expression, a *YFP* gene is embedded in the bacmid, whose expression is controlled by the same promoter as that of the recombinant genes. Thus, two days after the transfection we monitored expression of our *S. pombe* genes using YFP expression as a readout. The first generation of baculoviruses were harvested from the medium and the extracts of remaining insect cells were analysed by immunoblotting to probe for Bub1 and MCC components. First generation baculoviruses were then used to infect a larger insect cell culture (50-100 ml) that was grown in suspension. After 3-4 days, expression levels were monitored as described above, and the second generation of baculovirus was obtained, which is expected to be concentrated enough to perform a large scale protein production. Ultimately, a larger culture (300-400 ml) was infected with baculovirus, followed by lysis of insect cells and purification of recombinant *S. pombe* proteins using Strep magnetic beads.

As displayed in Figure 4.2C, *S. pombe* MCC ΔN-term was purified at comparable concentration to that of the full length MCC. Figure 4.2D shows that wild type and kinase-dead versions of Bub1 were also purified at similar concentrations. Here, it is worth mentioning that a proportion of recombinant Bub1 is cleaved into two fragments. Since Bub1 was tagged at its N-terminus, the cleaved C-terminus, which bears the kinase domain, was not retained. Nevertheless, a band corresponding to the size of full length Bub1 was excised, and the presence of intact Bub1 was confirmed by mass spectrometry identification (collaboration with Juri Rappsilber's lab) for both wild type and kinase-dead versions. This was also confirmed by immunoblotting with anti-strep antibody, which detected N-terminally tagged intact Bub1 and N-terminal half of Bub1 cleavage product (Figure 4.2D).
In summary, the kinases (wild type and kinase-dead Bub1) and the substrates (MCC ΔN-term, MCC FL) were successfully prepared for *in vitro* Bub1 kinase assays.

4.2.2 *In vitro* Bub1 kinase assay

Initially, to test kinase functions of recombinant wild type and kinase-dead Bub1 proteins, we performed a preliminary kinase assay using an established substrate of Bub1, *S. pombe* H2A (Kawashima et al., 2010) (provided by Robin Allshire). Kinase assays were carried out with γ–^{32}P-ATP, run on SDS protein gels and phosphorylation was visualized by autoradiographs. Figure 4.3A demonstrates that H2A and Bub1 itself were phosphorylated only by wild type Bub1, whereas kinase-dead Bub1 was unable to phosphorylate either of them. This confirms that Bub1 kinase function has been completely abolished in the kinase-dead allele (Kawashima et al., 2010) and also suggests that our recombinant Bub1 preparations do not appear to contain any insect cell-originated contaminant kinases.

Next we carried out a Bub1 kinase assay using MCC ΔN-term and MCC FL as substrates. As displayed in Figure 4.3B, both full length and N-terminally truncated Cdc20 (Cdc20 ΔN-term) proteins were phosphorylated by the wild type Bub1 kinase, however not by kinase-dead Bub1. The N-terminus of Cdc20 has been found to be phosphorylated by Cdk1 in *X. laevis* (S50/T64/T68/ T79/S114/S165) (Labit et al., 2012) and Bub1 in *H. sapiens* (S41, S72, S92, S153, T157, S161) (Tang, Shu, et al., 2004). Our phosphorylation of N-terminally truncated Cdc20 suggests that Bub1 is able to phosphorylate downstream of the first 86 amino acids of Cdc20 as well. Moreover, Figure 4.3B confirms the Bub1 autophosphorylation observed in the previous experiment (Figure 4.3A). In addition to the autophosphorylation of Bub1 N-terminal cleavage product, somewhat slowly migrating Mad3 appears to be phosphorylated by wild type Bub1 too (more visible in the MCC ΔN-term lane). On the other hand, Mad2 does not appear to be phosphorylated by Bub1 *in vitro*, although it has been reported as a substrate of *S. pombe* Mph1 (Mps1 in budding yeast and higher eukaryotes) (Zich et al., 2012).

These data confirms that *S. pombe* Bub1 kinase auto-phosphorylates efficiently (Kawashima et al., 2010) and demonstrates that it phosphorylates Cdc20 directly. Unlike in *X. laevis,* phospho-modification of fission yeast Cdc20 is not restricted to its N-terminus.

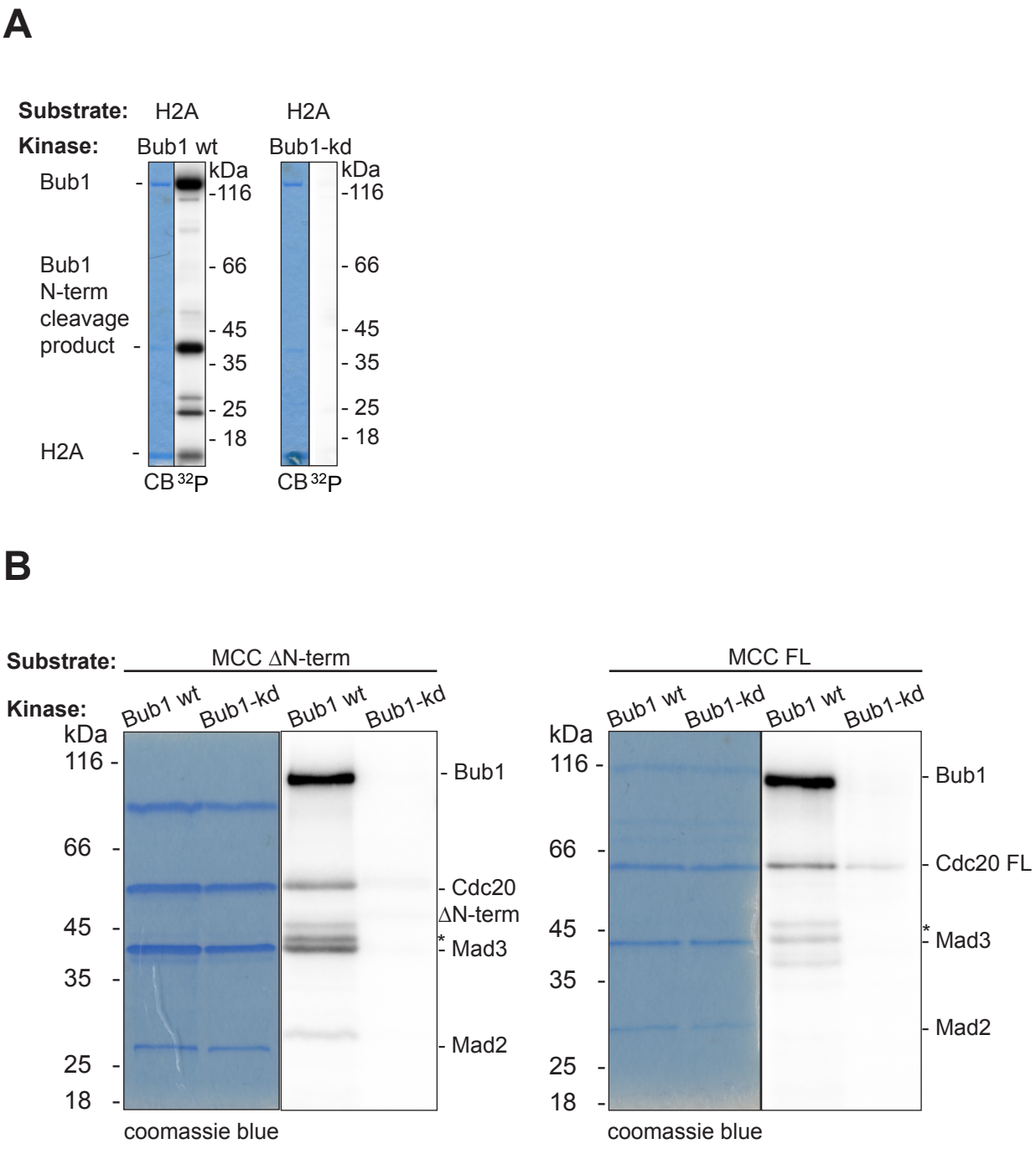

Figure 4.3 Bub1 kinase autophosphorylates and phosphorylates Cdc20 *in vitro*

(A) *S. pombe* H2A was incubated with recombinant *S. pombe* Bub1 (wild type or kinase-dead) in the presence of γ−32P-ATP. Protein loading was examined through Coomassie Blue (CB) staining, and incorporation of the radioactive phosphate group was visualized through autoradiography (32P). **(B)** Recombinant *S. pombe* MCCΔN-term and full length MCC (FL) were incubated with recombinant *S. pombe* Bub1 (wild type or kinase-dead) in the presence of γ−32P-ATP. Protein loading was examined through Coomassie Blue (CB) staining, and incorporation of the radioactive phosphate group was visualized through autoradiography (32P). Asterisk denotes phosphorylated Bub1 N-terminal cleavage product.

4.2.3 Identification of *in vitro* phosphorylation sites using mass spectrometry

In the previous section we demonstrated that Cdc20 is an *in vitro* substrate of Bub1. We observed that Bub1-mediated phosphorylation modified middle and/or C-terminal regions of Cdc20, as well as its N-terminal 86 amino acids that has been reported to be phospho-regulated *in vitro* and *in vivo* in other model organisms (Labit et al., 2012; Tang, Shu, et al., 2004).

In vivo phosphorylation of *S. pombe* Cdc20 had been analysed in our lab before by Sjaak van der Sar. Sjaak purified Mad3 and Apc4 proteins from either cycling or mitotically arrested (through *nda3-KM311* cold sensitive tubulin mutation) cells, and identified phosphorylated sites of their interactors by mass spectrometry analysis (in collaboration with John Yates' lab in Scripps Research Institute). These analyses showed that Cdc20 is phosphorylated at 10 serine or threonine residues *in vivo* (Figure 4.4A).

In this section, we aim to identify *in vitro* phosphorylated sites of Cdc20 by Bub1, and indicate which of those sites were previously found to be phosphorylated *in vivo.* For this purpose, we repeated the previously described Bub1 kinase assay (Figure 4.3B) using Cdc20 (full length or ΔN-term) and Bub1 kinase (wild type or kinase-dead) in the presence of non-radioactive ATP, and then identified *in vitro* phosphorylated sites by mass spectrometry analysis (in collaboration with Juri Rappsilber's lab). As listed in Figure 4.4A, wild type Bub1 was found to phosphorylate 14 sites of Cdc20 *in vitro,* 5 of which were also identified as *in vivo* phosphorylated sites in mitotically arrested cells. On the other hand, none of the Cdc20 sites were found to be phosphorylated by the kinase-dead Bub1, which confirms that the *in vitro* phosphorylation of Cdc20 was specific to Bub1. All together 19 different sites were indicated to be phosphorylated *in vivo* and/or *in vitro,* and 15 of them cluster around the N-terminal C-box motif. Several of these may be Cdk1 sites (S11, S28, T31, S76), as they are followed by a proline. (Figure 4.4B). The C-box motif has been reported to be required for APC/C activation (David Barford, 2011). Moreover, a study in *X. laevis* showed that Cdk1-mediated phosphorylation of the Cdc20 sites near the C-box (the majority of them are upstream the C-box) inhibits APC/C activation by Cdc20 (Labit et al., 2012). On the other hand, we observed a considerably strong phospho-signal given by Cdc20 ΔN-term *in vitro*

(Figure 4.3B), that lacks its N-terminal 86 amino acids, and starts from the C-box motif (included). This suggests that only five sites (S167, T359, T380, S399, S482) account for this signal. Importantly, one of these five sites (serine 482) was also identified as an *in vivo* phosphorylated residue in mitotically arrested cells, which is in very close proximity to the IR motif (**I**487 and **R**488). The IR motif has been shown to be required for Cdc20-APC/C interaction and subsequent activation of the APC/C (Izawa & Pines, 2012). Thus, phospho- modification of a nearby residue like serine 482 may be regulating Cdc20 activity.

Bub1, Cdk1 and Cdc20 proteins have several domains that are largely conserved from yeast to human. In order to determine which of the phosphorylation sites that we identified are well-conserved, we aligned the orthologs of Cdc20 protein from three fission yeast species (*S. pombe, S. octosporus, S. japonicus*), one budding yeast (*S.cerevisiae*) and two metazoans (*H. sapiens, X. laevis*) using ClustalWS algoritm in Jalview software. As demonstrated in Figure 4.5, four (S28, T31, S76 and S482) of the five residues, which were phosphorylated both *in vitro* by Bub1 and *in vivo* in mitosis, appear to be well-conserved at least among four of the six species. This strengthens the possibility that phospho- modification of these residues may play key roles in the regulation of Cdc20 throughout evolution.

In order to further narrow down the phosphorylated sites of Cdc20 with possible regulatory roles, we next determined the interacting sites of MCC components (Cdc20, Mad2 and Mad3) by crosslinking mass spectrometry (CLMS) analysis.

A

Phosphorylated residue	Peptides identified *in vitro*	Identified *in vitro*	Identified *in vivo*	Cell cycle stage (*in vivo*)
S7	MEIAGNSSTISPTFSTPTK	+		
S8	MEIAGNSSTISPTFSTPTK	+		
S11	MEIAGNSSTISPTFSTPTK	+	+	mitotic arrest and interphase
S15	MEIAGNSSTISPTFSTPTK	+		
S28	NLVFPNSPITPLHQQALLGR	+	+	mitotic arrest
T31	NLVFPNSPITPLHQQALLGR	+	+	mitotic arrest
S59	data N/A		+	mitotic arrest and interphase
T67	IDVVNTDWSIPLCGSPR	+		
S70	IDVVNTDWSIPLCGSPR	+		
S76	IDVVNTDWSIPLCGSPR	+	+	mitotic arrest and interphase
S93	data N/A		+	mitotic arrest
T97	data N/A		+	mitotic arrest
S104	data N/A		+	mitotic arrest
S116	data N/A		+	mitotic arrest
S167	FNTTPER	+		
T359	AVAWCPWQSNLLATGGGTMDK	+		
T380	QIHFWNAATGAR	+		
S399	VNTVDAGSQVTSLIWSPHSK	+		
S482	TPSSSITIR	+	+	mitotic arrest

B

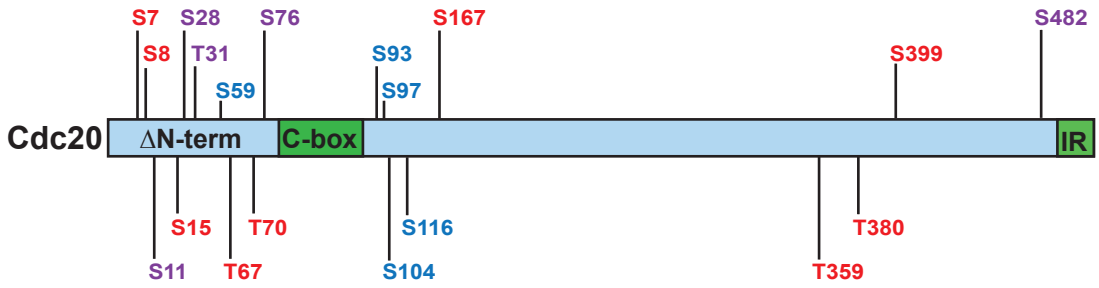

Figure 4.4 Cdc20 is phosphorylated *in vivo* during mitosis and *in vitro* by Bub1

(A) Table listing the phosphorylated sites of Cdc20; *in vitro* by Bub1(red), *in vivo* in mitotically arrested or cycling cells (blue) and both *in vitro* and *in vivo* (purple). Highlighted residues in the identified peptides correspond to the *in vitro* phoshorylated sites. **(B)** Cartoon illustrating distribution of the phosphorylated sites of Cdc20 along with its two domains important for APC/C activation: N-terminal C-box and C-terminal IR-motif.

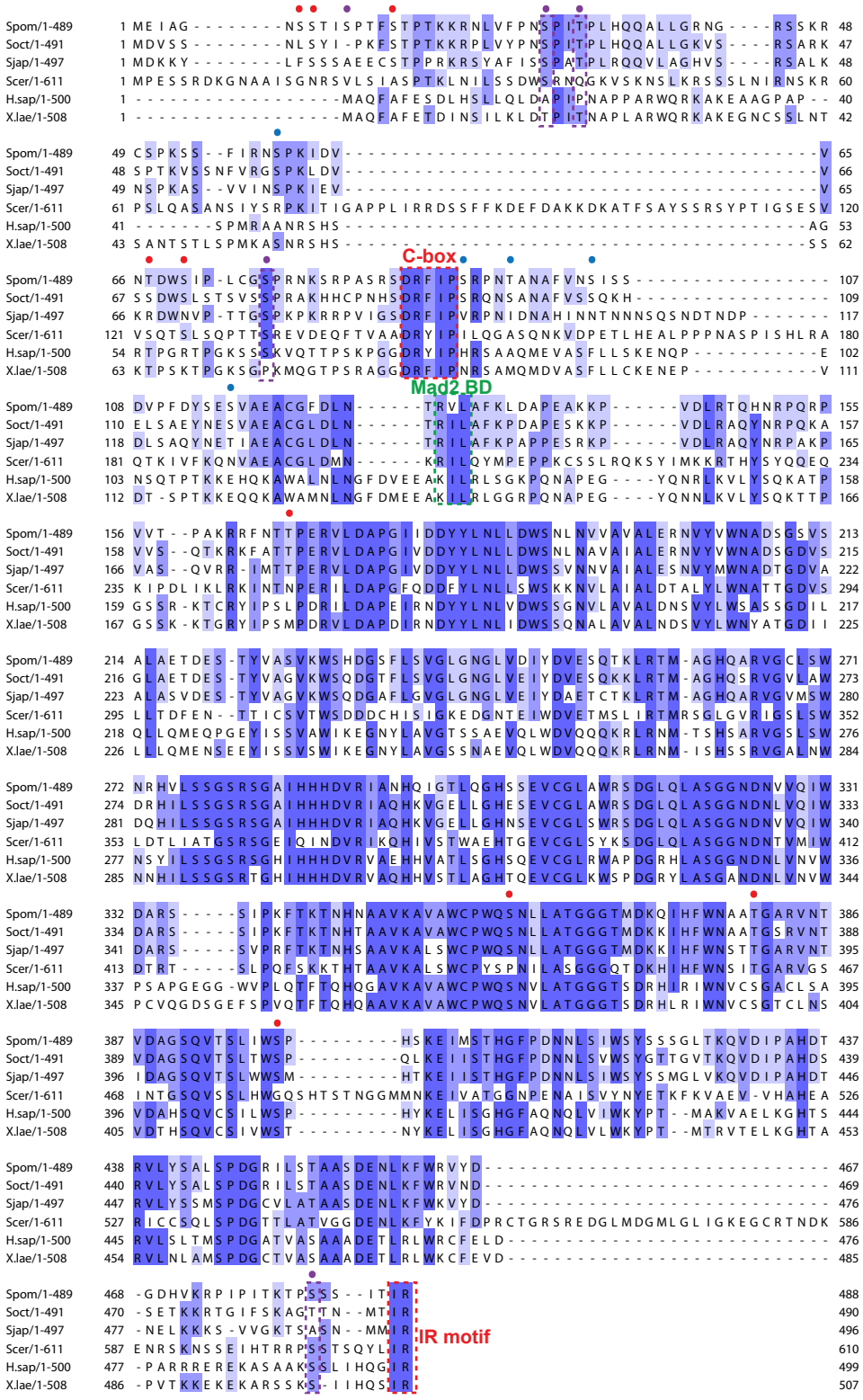

Figure 4.5 *In vivo* and *in vitro* phosphorylated Cdc20 sites are well-conserved

Alignment of Cdc20 orthologs from three fission yeast species (*S. pombe, S. octospo-rus, S. japonicus*), one budding yeast (*S. cerevisiae*) and two metazoans (*H. sapiens, X. laevis)* using ClustalWS algoritm in Jalview software. Red (*in vitro* by Bub1), blue (*in vivo* in mitotically arrested cells) and purple (*in vitro* and *in vivo*) dots indicate the phos-phorylated sites. Purple dashed rectangles denote well-conserved residues that are phosphorylated *in vitro* and *in vivo.* Red dashed rectangles annotate two domains of Cdc20 that are required for APC/C activation: C-box and IR-motif. The green dashed rectangle annotates the Mad2-binding domain.

4.3 Analysis of interactions between the recombinant MCC components: Cdc20, Mad2 and Mad3

As described in section 4.3.1 (Figure 4.6A), from insect cells we purified recombinant *S. pombe* MCC (MCC ΔN-term) that consists of; wild type Cdc20 ΔN-term (with an N-terminal strep-tag), lacking the first 86 amino acids; wild type full length Mad3; double mutant Mad2, that is prevented from dimerizing (L12A) and locked into the closed-conformation (R133A). Although, soluble Mad2 and Mad3 proteins have been efficiently purified from *E. coli* in our lab, Cdc20 has been insoluble in every attempt. This was the main reason for purifying the *S. pombe* MCC from insect cells, which provide a eukaryotic post-translational folding machinery. Therefore, before using recombinant MCC ΔN-term in crosslinking mass spectrometry (CLMS) analysis, we examined whether its components folded properly and assembled a functional complex, by testing its functionality as an APC/C inhibitor *in vitro.*

4.3.1 *In vitro* analysis of recombinant MCC as an APC/C inhibitor

An *in vitro* APC/C ubiquitination assay has been optimized (and carried out in this experiment) by Konstantinos Paraskevopoulos in our lab (Foe et al., 2011; Van Voorhis & Morgan, 2014). In this assay, we test the ability of APC/C (an E3 ubiquitin ligase) to add poly-ubiquitin chains to Securin, which is one of its mitotic targets (D. Barford, 2011). Moreover, this assay allows us to analyse the abilities of recombinant SAC proteins to inhibit APC/C activity *in vitro* (P. Lara-Gonzalez et al., 2011). In this experiment, we used wild type APC/C purified from the *Cdc20-362 S. pombe* strain, in which the temperature sensitive mutant Cdc20 was not able to bind APC/C (Matsumoto, 1997). This provides an APC/C preparation free from endogenous Cdc20. *S. pombe* full length Cdc20 was *in vitro* translated to be used as an APC/C activator. As the APC/C substrate, *S. pombe* Securin was translated *in vitro,* and radiolabelled with ^{35}S-methionine. As for the APC/C inhibitor proteins; full length Mad3 (wild type) and Mad2 (double mutant, see the description above) were purified from *E. coli*. In addition to single or double permutations of Mad2 and Mad3 proteins, we also used baculovirus produced MCC ΔN-term (described above) that contains Cdc20, Mad2 and Mad3.

Figure 4.6B and C show that Mad2 or Mad3 proteins partially inhibited APC/C activity to 77% and 55% respectively, when they were used alone. On the other hand, combination of Mad2 and Mad3 decreased the APC/C activity to 45%. Strikingly, MCC ΔN-term appeared to be the most potent inhibitor, as it almost completely abolished the APC/C activity (3%) towards Securin.

To sum up, recombinant MCC ΔN-term efficiently inhibits APC/C activity *in vitro.* This confirms that post-translational folding machinery in insect cells was sufficient to produce a functional *S. pombe* MCC. Moreover, these data demonstrate that although apo-Cdc20 is an APC/C activator, its presence in the MCC has a significant contribution to the inhibition of APC/C, which is in line with findings from a human study (P. Lara-Gonzalez et al., 2011).

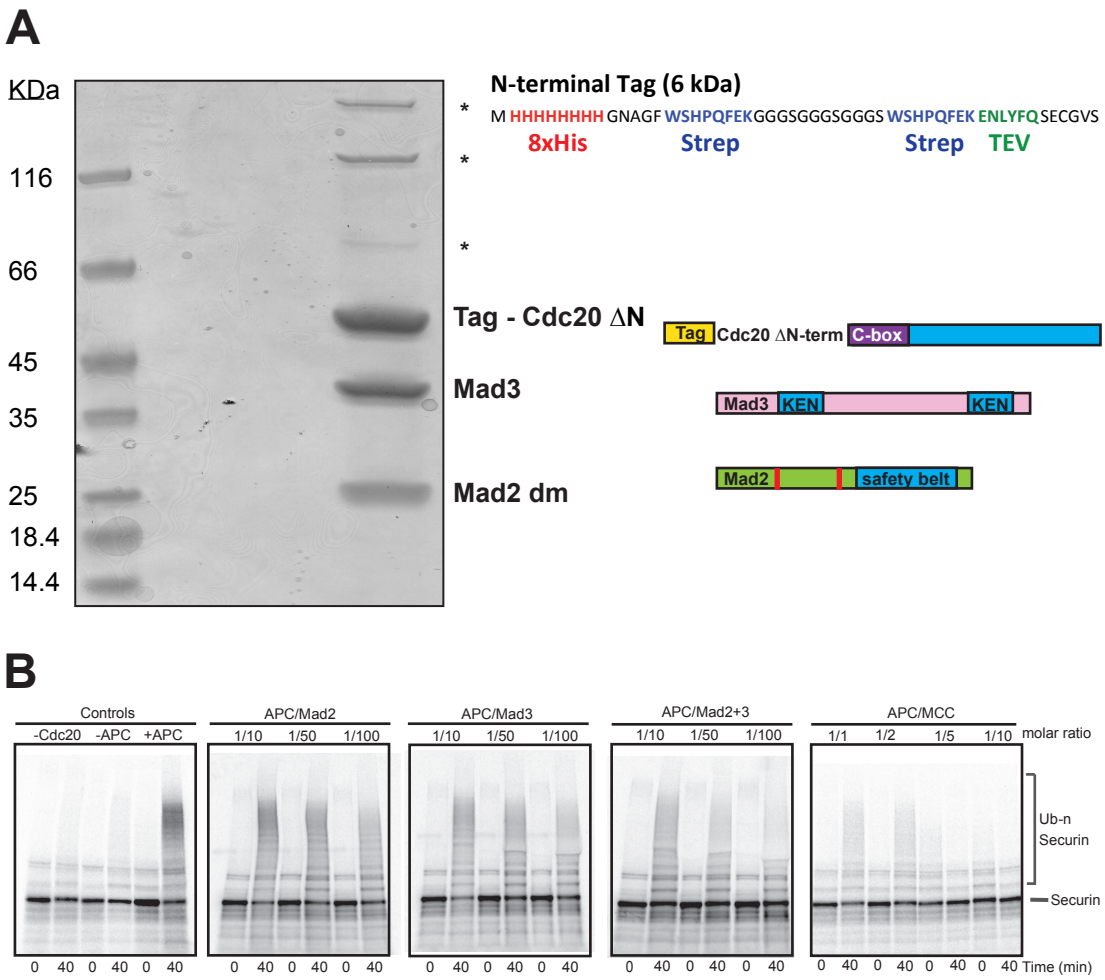

Figure 4.6 Recombinant MCC efficiently inhibits APC/C activity *in vitro*

(A) Coomassie stained gel shows *S. pombe* mitotic checkpoint complex (MCC) purified from Sf9 insect cells. (Asterisks denote contaminants, which are likely to be insect cell chaperones). Cartoon illustrates important domains of the purified MCC components: Cdc20 ΔN, lacks its first 86 aminoacids and carries an N-terminal tag; Mad3 is full length and wild type; Mad2 double mutant (dm), bears two mutations, one (L12A) prevents it from dimerizing, and the other one (R133A) locks it into the closed- conformation. Sequence of the tag at the N-terminus of Cdc20 ΔN consists of 8xHis, two strep-tag II and a TEV protease recognition site. **(B)** Autoradiography image shows results of an *in vitro* ubiquitination assay. Mad2, Mad3 (purified from *E.coli*) and MCC ΔN (purified from insect cells) were tested for their abilities to inhibit APC/C (purified from *S.pombe*) and Cdc20 (*S.pombe*, in vitro translated) mediated ubiquitination of Securin (*in vitro* translated with 35S-Methionine). Controls were as follows: '-Cdc20' was with APC/C and without Cdc20; '- APC' was without APC/C and with Cdc20; +APC was with both APC/C and Cdc20. Inhibitors were added as 10, 50 or 100 times more concentrated than APC/C. Half of each reaction was taken immidiately after mixing APC/C, Cdc20 and the inhibitors (0 min) and the other half after incubation (40 min). Samples were run on SDS gels, dried and visualized to detect ubiquitinated Securin **(C)** Graph plots the results (1/10 APC/inhibitor molar ratio) of the ubiquitination assay quantified by Image Quant software (measuring the signal decrease in the unmodified securin band). Results were normalized to the intensity of ubiquitinated-Securin in +APC control lane, considering it as 100% APC/C activity. Experiments shown in B and C were carried out by Konstantinos Paraskevopoulos.

4.3.2 Cross-linking mass spectrometry analysis of the interactions between the MCC components

A previous study has resolved the crystal structure of *S. pombe* MCC (Chao et al., 2012a). This finding has provided valuable insight into how Cdc20 is sequestered by Mad2 and Mad3, by revealing their key interacting domains. However, in order to optimize purification and crystallization steps Chao and his colleagues used 'MCC ΔN-term ΔC-term' comprising truncated components: Cdc20 ΔN-term lacking the first 86 amino acids (crystal structure lacks disordered last 22 amino acids 467-488 as well); Mad3 ΔC-term, lacking last 87 amino acids, 224-310; double mutant Mad2, that is prevented from dimerizing (L12A) and locked into the closed-conformation (R133A). Therefore, the crystal structure lacks some of the critical regulatory domains of Cdc20 (the N-terminus, where it is regulated by Cdk1 phosphorylation (Labit et al., 2012); the IR motif at the C-tail) and the Mad3 C-terminus, including the second KEN box, that is involved in the inhibition of APC/C substrate recruitment (P. Lara-Gonzalez et al., 2011). Considering that we have purified a recombinant MCC ΔN-term, which includes Mad3 C-terminus, we next sought to determine the interactions between its components by performing cross-linking mass spectrometry analysis (CLMS) in collaboration with Juri Rappsilber lab following the protocol in (Barysz et al., 2015). By using this method, we aimed to reveal interactions between (or within) the regions of MCC components that are in close proximity, which will be covalently bound by either of the two cross-linkers:

BS3 (bis(sulfosuccinimidyl)suberate) (11.4 Å spacer arm length)
EDC (1-ethyl-3-(3-dimethylaminopropyl)carbodiimide hydrochloride)
(0 Å spacer arm length)

For this purpose, we immobilized purified MCC ΔN-term on strep-magnetic beads through the strep-tag on the N-terminus of Cdc20 ΔN-term. This way it was more convenient to exchange the strep wash buffer with the buffers required by BS3 and EDC. Zhuo Angel Chen carried out the cross-linking reaction, mass spectrometry, and provided us with the CLMS data.

We identified two types of linkages from the CLMS data:

1. Linkages between the regions of MCC components that were resolved in the crystal structure (Figure 4.7 and Table 4.1).
2. Novel linkages between the regions of MCC components that were absent in the crystal structure (Figure 4.8 and Tables 4.2, 4.3).

Linkages that can be compared to the crystal structure

With the CLMS data, we plotted networks of cross-links and self-links between (or within) the MCC components (Figure 4.7) using XiNet Crosslink Viewer (Combe, Fischer, & Rappsilber, 2015). In the MCC crystal structure, Chao and his colleagues identified the major binding interfaces between Cdc20, Mad2 and Mad3, such as the first KEN box of Mad3 (KEN20) and its receptor in the WD40 domain of Cdc20, or the safety belt of Mad2 and the N-terminal Mad2 binding domain of Cdc20. In addition to these major regulatory contacts, the crystal structure reveals interactions between other regions of the MCC components, whose roles remain unknown. Therefore, we have annotated all of those interacting sites identified by the crystal structure in our CLMS data networks.

Linkages mediated by the BS3 cross-linker are demonstrated in Figure 4.7A (network) and Figure 4.8 (on the crystal structure), and listed in Table 4.1. The most prominent cross-links are between the Mad2 binding domain of Cdc20 (K133, K140, K141) and two sites of Mad2 (residues K43 and K66) which have been shown to interact with Cdc20 in the crystal structure (Figure 4.8A). Moreover, self-links form between those two sites (K43 and K61) of Mad2. This suggests, that particular region of Mad2 might be folding onto itself to bind (and perhaps to wrap) the Mad2 binding domain of Cdc20.

As for the Mad3 interactions, the N-terminus (K27) (near KEN20) and the middle region (K190, Y191) of Mad3 interact with the Mad2 binding domain of Cdc20 (K141) (Figure 4.7A, Figure 4.8B and Table 4.1). Furthermore, these two sites of Mad3 form a self-link. Taken together, these results imply that the sites of Mad2 and Mad3, which were found to interact with Cdc20, may be folding onto themselves in order to sequester Cdc20. Their binding interface (Mad2 binding domain of Cdc20) is only 34

Barford, 2011). Thus, sequestration of the Mad2 binding domain of Cdc20 by Mad2 and Mad3 may have a direct role in the inhibition of APC/C by MCC. Interestingly, a self-link within Cdc20 brings together its C-terminus region (K461) and an N-terminal region (T167), which is 27 amino acids downstream of its Mad2-binding domain (K140) (Figure 4.10). Because the C-terminal tail (last 22 amino acids) of Cdc20 is disordered, it was not resolved in the crystal structure. On that basis, assuming the last ordered (resolved) region of Cdc20 C-terminus (K461) folds onto the downstream (T167) of Cdc20's Mad2-binding domain (K140), this flexible C-terminal tail is likely to interact with the Mad2-binding domain itself, as it is exactly at the sufficient length to reach there (K461 to R488, and T167 to K140). Such a folding would bring the C-terminus of Cdc20 near its regulatory C-box motif, which may be required for APC/C activation (D. Barford, 2011). Moreover, the Mad2 binding domain of Cdc20 is also required for APC/C binding in humans (Izawa & Pines, 2012). This is intriguing because at the very end of its C-terminal tail Cdc20 has the IR motif (**I**487 and **R**488), which is also required for APC/C activation through interactions with its Cdc27 subunit (da Fonseca et al., 2011). This implies that, the Mad2 and Mad3 proteins may be targeting multiple regulatory domains of Cdc20 (C-box, Mad2 binding domain and IR-motif) that are responsible for APC/C activation.

Furthermore, linkages mediated by the EDC cross-linker are consistent with those identified through BS3 (Figure 4.7 A and Table 4.1). EDC cross-linking reproduced the interactions between the Mad2 binding domain of Cdc20 (K140, K141 and D144) and Cdc20 interacting sites of Mad2 (E40, K43 and E59).

Taken together, linkages between the regions of MCC components that were resolved in the crystal structure are in line with the interactions revealed by the MCC crystal structure. In addition, our findings suggest that when Cdc20 functions as an activator of APC/C, its IR motif in the flexible C-terminal region may come closer to the N-terminal C-box in order to synergistically activate APC/C. On the other hand, when the SAC is activated, MCC assembles in a way that Mad2 and Mad3 may sequester both C-box and IR-motif of Cdc20, in order to effectively block Cdc20's binding to and activation of the APC/C.

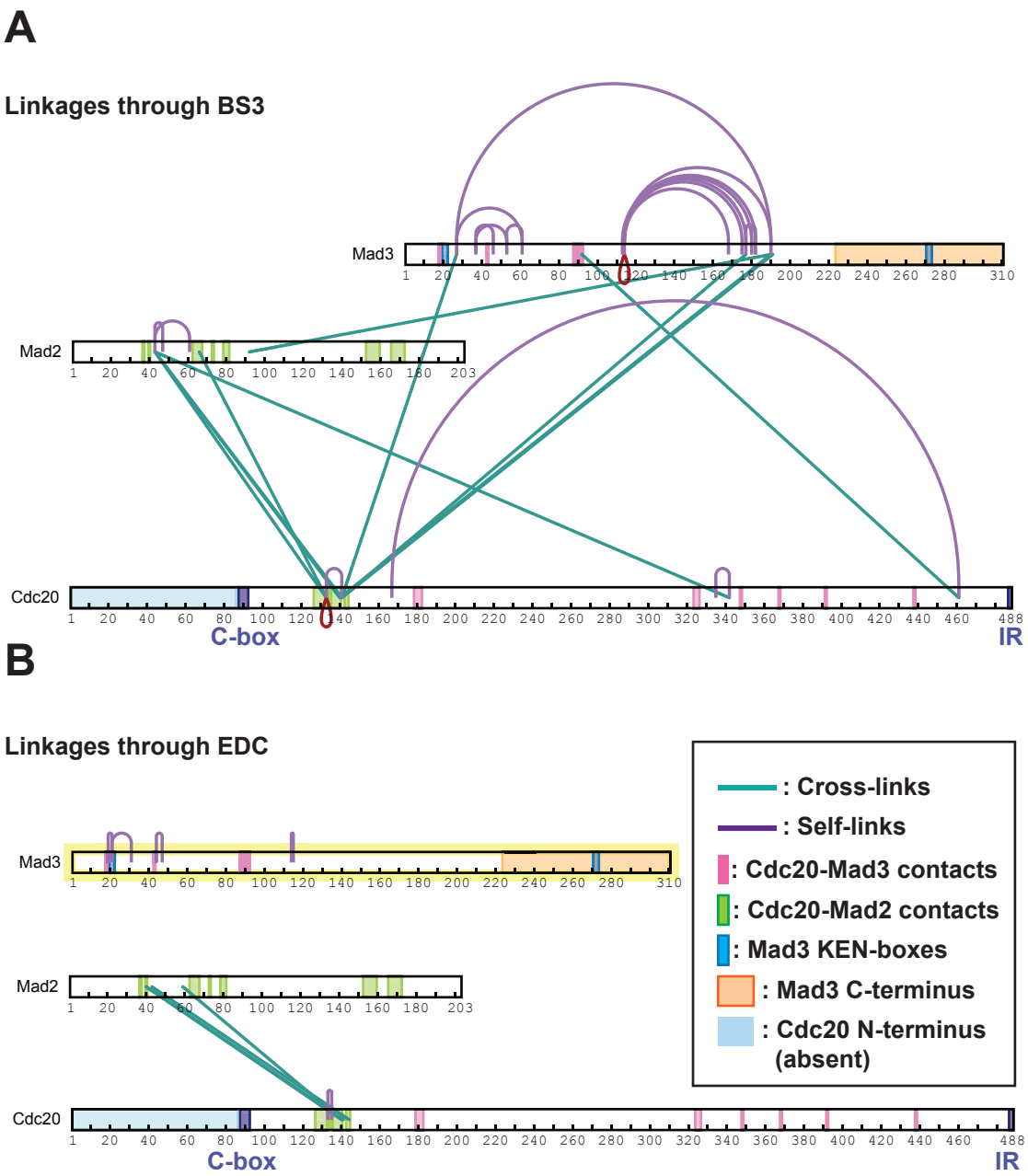

Figure 4.7 Linkages between the regions of MCC components which were resolved in the crystal structure

(A) Schematic illustrating the linkage network between MCC ΔN-term components mediated by BS3 (bis(sulfosuccinimidyl)suberate) crosslinker. MCC ΔN-term components: Cdc20 ΔN-term, lacking the first 86 amino acids; wild type full length Mad3; double mutant Mad2, that is prevented from dimerizing (L12A) and locked into the closed-conformation (R133A). C-alpha distances and Cdc20-Mad3, Cdc20-Mad2 contacts were obtained from *S. pombe* MCC crystal structure (4AEZ.pdb). Different from the crystal structure, cross-linked MCC ΔN-term used here contains Mad3 C-terminus (last 87 amino acids; 224-310) and disordered C-tail region of Cdc20 (last 22 amino acids; 467-488). **(B)** Schematic illustrating the linkages between MCC ΔN-term components mediated by EDC (1-ethyl-3-(3-dimethylaminopropyl)carbodiimide hydrochloride) crosslinker. Networks of cross-links and self-links were constructed using XiNet Crosslink Viewer (Combe, Fischer, & Rappsilber, 2015).

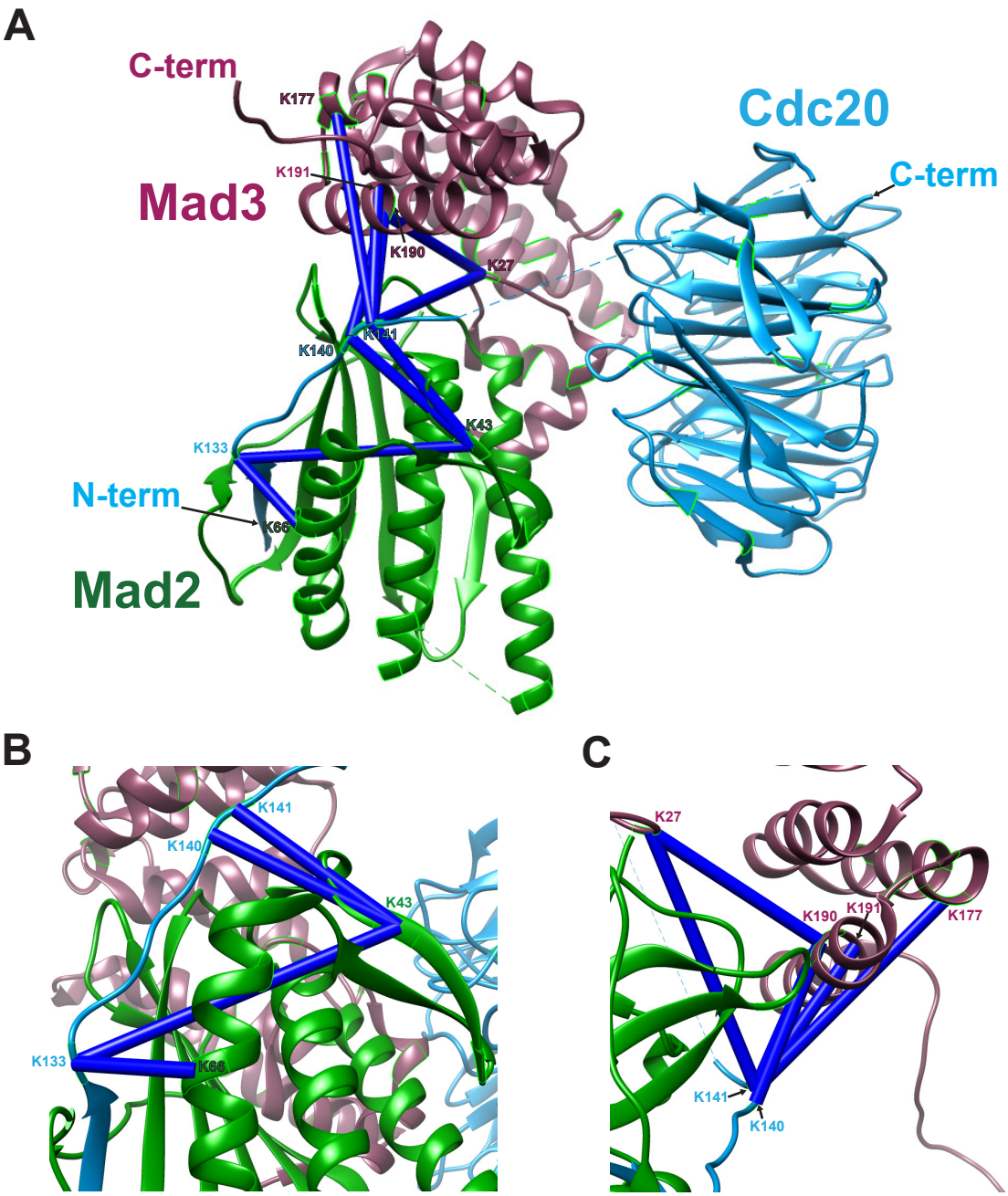

Figure 4.8 MCC cross-linking data are consistent with the MCC crystal structure

(A) Cartoon representation of the "MCC ΔN-term ΔC-term" crystal structure with the prominent BS3-mediated cross-links (indicated by dark blue lines) between its components: Cdc20 ΔN-term lacking the first 86 amino acids (crystal structure lacks disordered last 22 amino acids 467-488 as well); Mad3 ΔC-term, lacking last 87 amino acids, 224-310; double mutant Mad2, that is prevented from dimerizing (L1 2A) and locked into the closed-conformation (R133A). N-terminal end of Cdc20 ΔN-term starts with the C-box. Mad2 binding domain of Cdc20 is between K133 and K141. **(B)** Details of the linkages between Mad2 (K43 and K66) and the Mad2 binding domain of Cdc20 (K133, K140 and K141), shown in A. **(C)** Details of the linkages between Mad3 (K27, K177, K190 and K191) and the Mad2 binding domain of Cdc20 (K140 and K141), shown in A. Lysines of the proteins are highlighted, between which the BS3 crosslinker formed covalent bonds. Cartoon representations were generated using X-link Analyser tool in UCSF Chimera Software.

Linkages through BS3

Protein 1	Linkage site 1	Protein 2	Linkage site 2	Match count	C-α distance in 4AEZ (Å)
Mad2	K43	Mad2	K47	7	12.3
Mad2	K43	Mad2	K61	2	12.1
Mad2	K43	Cdc20	K133	2	C-α
Mad2	K43	Cdc20	K140	2	15.8
Mad2	K43	Cdc20	K141	5	16.8
Mad2	K43	Cdc20	K342	4	25.8
Mad2	K66	Cdc20	K133	2	11.3
Mad2	S92	Mad3	K190	1	15.3
Mad3	Y113	Mad3	K177	2	21.5
Mad3	K114	Mad3	K114	17	0
Mad3	K114	Mad3	K168	4	24.3
Mad3	K114	Mad3	K175	3	17.2
Mad3	K114	Mad3	K180	3	15.6
Mad3	K114	Mad3	K182	14	13.9
Mad3	K114	Mad3	K190	4	22.3
Mad3	K177	Mad3	K180	2	4.8
Mad3	K177	Mad3	K182	7	9.5
Mad3	K177	Cdc20	K141	1	21.5
Mad3	K190	Cdc20	K140	4	15.1
Mad3	K190	Cdc20	K141	9	12.6
Mad3	Y191	Cdc20	K141	1	13.5
Mad3	K27	Mad3	K190	5	16.5
Mad3	K27	Mad3	K61	1	27.3
Mad3	K27	Cdc20	K141	4	23.1
Mad3	K37	Mad3	K46	10	14.8
Mad3	K37	Mad3	K53	37	16.5
Mad3	K53	Mad3	K61	3	12.6
Mad3	K92	Cdc20	K461	3	15.7
Cdc20	K133	Cdc20	K133	2	0
Cdc20	K133	Cdc20	K141	3	24.5
Cdc20	T167	Cdc20	K461	1	9.5
Cdc20	S335	Cdc20	K342	1	17.1

Linkages through EDC

Protein 1	Linkage site 1	Protein 2	Linkage site 2	Match count	C-α distance in 4AEZ (Å)
Mad2	E40	Cdc20	K140	1	10.2
Mad2	E40	Cdc20	K141	5	10.1
Mad2	K43	Cdc20	D144	1	13.4
Mad2	E59	Cdc20	K140	1	10.7
Mad3	K114	Mad3	D115	1	3.8
Mad3	S19	Mad3	E21	1	5.7
Mad3	E21	Mad3	S31	1	15.5
Mad3	T44	Mad3	E47	2	5.2
Cdc20	K133	Cdc20	D135	2	6.5

Table 4.1 Linkages between the regions of MCC components which were resolved in the crystal structure

List of linkages between MCC ΔN-term components mediated through BS3 or EDC cross-linkers. C-alpha distances were obtained from *S. pombe* MCC crystal structure (4AEZ.pdb). Linkages listed in this table were identified between the regions of MCC Δ N-term components which are present in the crystal structure. Within-length distances (~28Å for BS3; ~15Å for EDC) were calculated as follows: spacer arm length of the crosslinker + lengths of the side chains of linked residues + 2Å for displacement of carbon-alpha atoms.

Novel linkages that can be complementary to (were absent in) the crystal structure

In this subsection, we describe the CLMS data that indicates novel interactions of Mad3 C-terminus and Cdc20 C-tail, which were absent in the MCC crystal structure.

Novel linkages mediated by the BS3 cross-linker are demonstrated in Figure 4.9A and listed in Table 4.2. We observed two major clusters of cross-links mediated by BS3. The first cluster is the cross-links between the Mad2 binding domain of Cdc20 (K133 and K141) and the C-terminus of Mad3 (K271, K288 and K292). It is worth noting that K271 is the lysine of the C-terminal (second) KEN box of Mad3. It has been previously shown that fission yeast KEN271 (Sczaniecka et al., 2008), and its counterpart in budding yeast (Janet L. Burton & Solomon, 2007; King et al., 2007) are essential for a SAC response. In addition, a recent study has reported that the human counterpart of KEN271 is required for the inhibition of substrate recruitment to APC/C (P. Lara-Gonzalez et al., 2011).

The second cluster of cross-links mediated by BS3 is the one between C-terminus of Mad3 (K271, K288 and K292) and the C-terminal tail of Cdc20 (K461, K472 and K479) (Figure 4.9A and Table 4.2). Importantly, the flexible C-terminal tail of Cdc20 (K472 and K479) also forms self-links with the Mad2 binding domain of Cdc20 (K133 and K141), which supports our hypothesis that the IR-motif in the C-tail may come closer to the N-terminal C-box (Figure 4.10).

Taken together, the novel linkages mediated by BS3 suggest that the C-terminal Mad3 KEN271 may be inhibiting substrate recruitment to APC/C, through its interaction with the Mad2 binding domain of Cdc20, where the C-box and IR-motif (which are responsible for substrate recruitment and APC/C activation) come closer (Figure 4.10).

Novel linkages mediated by EDC cross-linker are consistent with those identified through BS3 (Figure 4.9B and Table 4.3), as numerous linkages show that C-terminus of Mad3 interacts with the C-terminal tail and the Mad2 binding domain of Cdc20. What is more, both the C-terminal Mad3 KEN271 and the C-terminal Cdc20 IR-motif (R488) interact with two very same regions of Mad2 N-terminus (K13) and C-terminus (D177 and E179) (see two V shaped linkages meeting at Mad2 in Figure 4.9B). These

findings strengthen the possibility that Mad2 may cooperate with both the N-terminal KEN20 (see Figure 4.7A), and the C-terminal KEN271 (see Figure 4.9B) of Mad3 to sequester the C-box, and especially the IR-motif of Cdc20 for effective inhibition of APC/C, likely through blocking substrate recruitment (Figure 4.10).

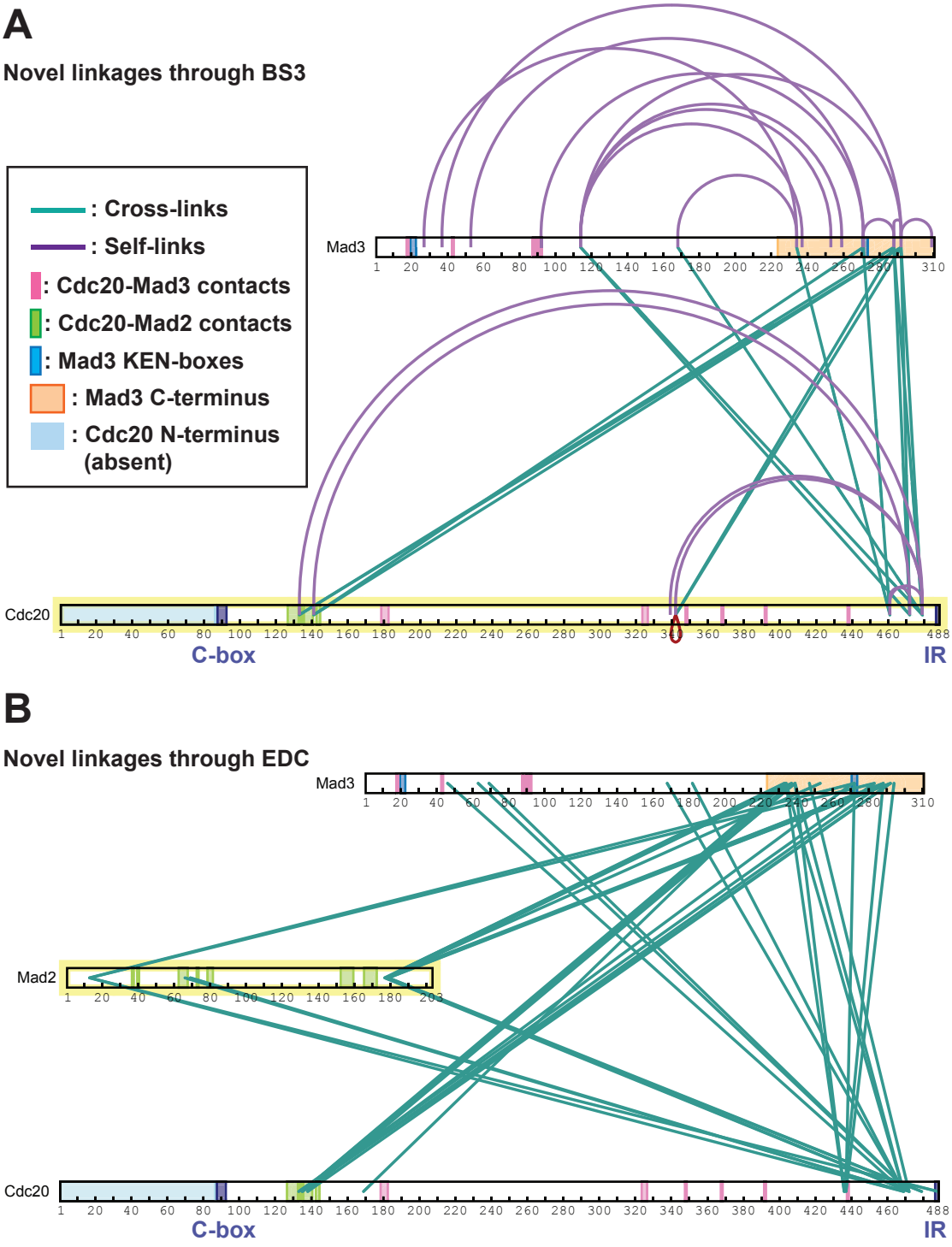

Figure 4.9 Novel linkages between the regions of MCC components which were absent in the crystal structure

(A) Schematic illustrating novel linkages between MCC ΔN-term components mediated by BS3 (bis(sulfosuccinimidyl)suberate) crosslinker. MCC ΔN-term components: Cdc20 ΔN-term, lacking the first 86 amino acids; wild type full length Mad3; double mutant Mad2, that is prevented from dimerizing (L12A) and locked into the closed-conformation (R133A). C-alpha distances and Cdc20-Mad3, Cdc20-Mad2 contacts were obtained from *S. pombe* MCC crystal structure (4AEZ.pdb). Different from the crystal structure, cross-linked MCC ΔN-term used here contains Mad3 C-terminus (last 87 amino acids; 224-310) and disordered C-tail region of Cdc20 (last 22 amino acids; 467-488). The linkages illustrated in A and B represent interactions of these regions that are absent in the crystal structure. **(B)** Schematic illustrating novel linkages between MCC ΔN-term components mediated by EDC (1-ethyl-3-(3-dimethylaminopropyl)carbodiimide hydrochloride) crosslinker. Self-links identified by EDC cross-linking are not presented here, as BS3 self-link data are representative of both of them. Networks of cross-links and self-links were constructed using XiNet Crosslink Viewer (Combe, Fischer, & Rappsilber, 2015).

Linkages through BS3

Protein 1	Linkage site 1	Protein 2	Linkage site 2	Match count	C-α distance in 4AEZ (Å)
Mad3	114	Mad3	237	1	N/A
Mad3	114	Mad3	253	3	N/A
Mad3	114	Mad3	259	4	N/A
Mad3	114	Mad3	292	2	N/A
Mad3	114	Cdc20	472	1	N/A
Mad3	114	Cdc20	479	2	N/A
Mad3	168	Mad3	234	2	N/A
Mad3	168	Cdc20	479	1	N/A
Mad3	234	Cdc20	461	1	N/A
Mad3	27	Mad3	234	2	N/A
Mad3	271	Mad3	288	4	N/A
Mad3	271	Cdc20	141	1	N/A
Mad3	271	Cdc20	461	7	N/A
Mad3	288	Mad3	292	2	N/A
Mad3	288	Cdc20	133	1	N/A
Mad3	288	Cdc20	342	2	N/A
Mad3	288	Cdc20	472	2	N/A
Mad3	288	Cdc20	479	1	N/A
Mad3	292	Mad3	309	2	N/A
Mad3	292	Cdc20	133	4	N/A
Mad3	292	Cdc20	141	3	N/A
Mad3	292	Cdc20	342	4	N/A
Mad3	292	Cdc20	472	5	N/A
Mad3	292	Cdc20	479	12	N/A
Mad3	37	Mad3	292	1	N/A
Mad3	53	Mad3	271	1	N/A
Mad3	92	Mad3	271	4	N/A
Cdc20	133	Cdc20	479	1	N/A
Cdc20	141	Cdc20	472	2	N/A
Cdc20	339	Cdc20	479	1	N/A
Cdc20	342	Cdc20	342	7	N/A
Cdc20	342	Cdc20	479	7	N/A
Cdc20	461	Cdc20	472	2	N/A
Cdc20	461	Cdc20	479	1	N/A

Table 4.2 Novel linkages through BS3 between the regions of MCC components which were absent in the crystal structure

List of novel linkages between MCC ΔN-term components mediated through BS3 cross-linker. C-alpha distances are not available, as the linkages listed in this table were identified between the regions of MCC ΔN-term components which are absent in *S. pombe* MCC crystal structure (4AEZ.pdb). Those regions which were present only in the crosslinked MCC ΔN-term are as follows: Mad3 C-terminus (last 87 amino acids; 224-310) and disordered C-tail region of Cdc20 (last 22 amino acids; 467-488).

Linkages through EDC

Protein 1	Linkage site 1	Protein 2	Linkage site 2	Match count	C-α distance in 4AEZ (Å)
Mad2	108	Mad2	119	1	N/A
Mad2	11	Mad2	179	2	N/A
Mad2	13	Mad2	110	2	N/A
Mad2	13	Mad3	272	1	N/A
Mad2	13	Mad3	283	1	N/A
Mad2	13	Cdc20	469	1	N/A
Mad2	13	Cdc20	488	2	N/A
Mad2	177	Mad3	233	1	N/A
Mad2	177	Mad3	234	1	N/A
Mad2	177	Mad3	237	2	N/A
Mad2	177	Mad3	253	1	N/A
Mad2	177	Mad3	288	3	N/A
Mad2	177	Mad3	292	2	N/A
Mad2	177	Cdc20	472	3	N/A
Mad2	177	Cdc20	479	1	N/A
Mad2	179	Mad3	234	1	N/A
Mad2	179	Mad3	237	2	N/A
Mad2	179	Mad3	288	2	N/A
Mad2	179	Mad3	292	2	N/A
Mad2	179	Cdc20	472	1	N/A
Mad2	179	Cdc20	479	3	N/A
Mad2	66	Cdc20	469	1	N/A
Mad2	69	Cdc20	469	1	N/A
Mad3	101	Mad3	237	1	N/A
Mad3	101	Mad3	292	1	N/A
Mad3	168	Mad3	247	2	N/A
Mad3	168	Cdc20	469	2	N/A
Mad3	171	Mad3	239	3	N/A
Mad3	171	Mad3	288	1	N/A
Mad3	171	Mad3	292	1	N/A
Mad3	175	Mad3	247	1	N/A
Mad3	182	Cdc20	469	1	N/A
Mad3	21	Mad3	239	1	N/A
Mad3	233	Cdc20	138	1	N/A
Mad3	233	Cdc20	169	1	N/A
Mad3	234	Cdc20	135	2	N/A
Mad3	234	Cdc20	138	2	N/A
Mad3	234	Cdc20	436	2	N/A
Mad3	234	Cdc20	469	3	N/A
Mad3	237	Mad3	272	1	N/A
Mad3	237	Cdc20	135	4	N/A
Mad3	239	Mad3	247	2	N/A
Mad3	239	Mad3	249	1	N/A
Mad3	239	Mad3	254	1	N/A
Mad3	239	Cdc20	135	1	N/A
Mad3	239	Cdc20	138	1	N/A
Mad3	239	Cdc20	436	1	N/A
Mad3	239	Cdc20	469	1	N/A
Mad3	241	Mad3	254	4	N/A
Mad3	243	Mad3	254	1	N/A
Mad3	245	Mad3	254	1	N/A
Mad3	246	Mad3	254	2	N/A
Mad3	247	Mad3	288	2	N/A
Mad3	247	Cdc20	472	1	N/A
Mad3	249	Mad3	292	1	N/A
Mad3	251	Mad3	254	2	N/A
Mad3	254	Mad3	271	2	N/A
Mad3	254	Mad3	288	2	N/A
Mad3	254	Mad3	292	1	N/A
Mad3	271	Cdc20	135	2	N/A
Mad3	272	Mad3	288	1	N/A
Mad3	272	Mad3	292	1	N/A
Mad3	272	Cdc20	437	1	N/A
Mad3	283	Mad3	288	3	N/A
Mad3	283	Mad3	292	3	N/A
Mad3	283	Cdc20	133	6	N/A
Mad3	288	Cdc20	135	3	N/A
Mad3	288	Cdc20	436	2	N/A
Mad3	292	Cdc20	135	5	N/A
Mad3	292	Cdc20	138	2	N/A
Mad3	294	Cdc20	437	1	N/A
Mad3	46	Cdc20	469	1	N/A
Mad3	63	Mad3	292	1	N/A
Mad3	63	Cdc20	472	1	N/A
Mad3	69	Mad3	234	2	N/A
Mad3	69	Mad3	288	4	N/A
Mad3	69	Mad3	292	1	N/A
Mad3	69	Cdc20	472	2	N/A
Mad3	70	Mad3	239	1	N/A
Cdc20	135	Cdc20	472	1	N/A
Cdc20	135	Cdc20	479	1	N/A
Cdc20	138	Cdc20	472	2	N/A
Cdc20	141	Cdc20	469	1	N/A
Cdc20	169	Cdc20	472	1	N/A
Cdc20	342	Cdc20	469	1	N/A
Cdc20	436	Cdc20	472	5	N/A
Cdc20	458	Cdc20	472	1	N/A

Table 4.3 Novel linkages through EDC between the regions of MCC components which were absent in the crystal structure

List of novel linkages between MCC ΔN-term components mediated through EDC cross-linker. C-alpha distances are not available, as the linkages listed in this table were identified between the regions of MCC ΔN-term components which are absent in *S. pombe* MCC crystal structure (4AEZ.pdb). Those regions which were present only in the crosslinked MCC ΔN-term are as follows: Mad3 C-terminus (last 87 amino acids; 224-310) and disordered C-tail region of Cdc20 (last 22 amino acids; 467-488).

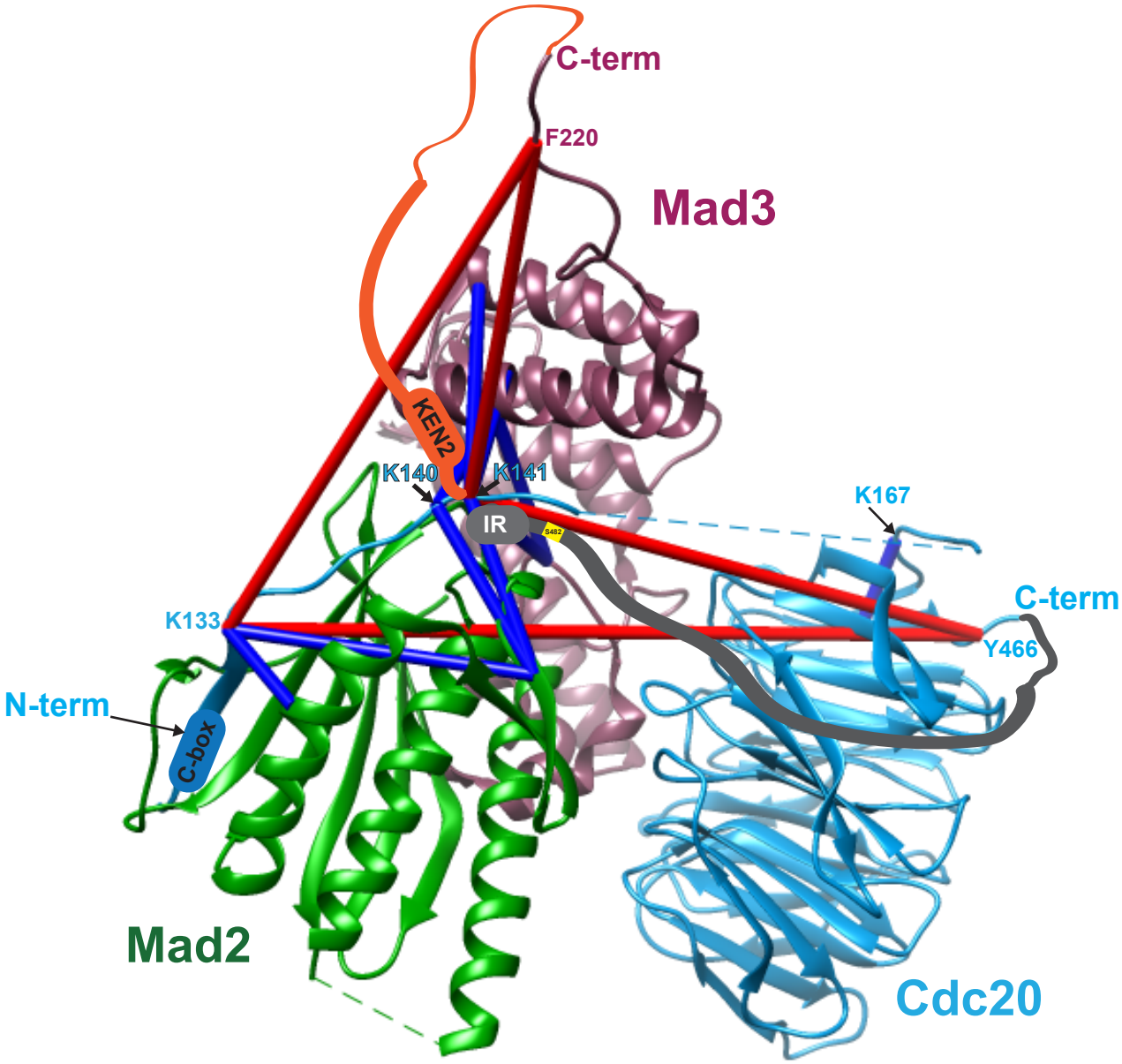

Figure 4.10 Mad2 and Mad3 may cooperate to sequester the APC/C activation domains of Cdc20

Cartoon representation of the "MCC ΔN-term ΔC-term" crystal structure with the prominent BS3-mediated cross-links (indicated by dark blue lines) between its components. Red lines denote the novel interactions between the Mad2 binding domain of Cdc20 (K133 and K141) and C-terminal tails of Cdc20 and Mad3 (which were absent in the crystal structure since they are disordered). Here Cdc20 K133 and K141 are linked (through red lines) to Cdc20 Y466 and Mad3 F220 (last ordered residues of Cdc20 and Mad3 C-termini) in order to show the direction of the novel interactions identified by cross-linking. Grey (Cdc20 C-tail) and orange (Mad3 C-tail) drawings emanating from the C-terminal ends (that were available in the crystal structure) of Cdc20 and Mad3 represent possible interactions of the flexible (disordered) C-terminal tails of Cdc20 and Mad3 respectively. Both C-tails were found to interact with the Mad2 binding domain of Cdc20 (K133, K140 and K141) by cross-linking. KEN2 denotes the second KEN box (KEN271) of Mad3. IR denotes the IR-motif of Cdc20 (its last two residues) that is required for binding to and activation of APC/C. The yellow box denotes the conserved phosphorylation site of Cdc20, serine 482 (S482), that is 4 aminoacids upstream of the IR-motif. Cartoon representations were generated using X-link Analyser tool in UCSF Chimera Software.

4.4 Marking of cdc20+ gene with an antibiotic resistance and inserting an internal tag

As described in the previous sections we have identified phosphorylation sites of Cdc20 and novel interactions between MCC components. In order to investigate roles of these sites *in vivo,* we needed a selection marker in its endogenous locus, so we would be able to select for the Cdc20 alleles that we will generate. We initially had an attempt to mark the *cdc20* gene locus at its 5' UTR with the hygromycin B resistance gene. However, this led to a severe benomyl and temperature sensitivity, which might be due to the presence of a non-coding RNA sequence at that region. In addition, modification of 5' UTR might have affected a complex Cdc20 promoter. To test these possibilities, RNA levels of Cdc20 could be analysed performing reverse transcriptase polymerase chain reaction (RT-PCR). Therefore, we inserted the hygromycin B resistance gene at its 3' UTR, 460 bp downstream of *cdc20* stop codon (Figure 4.11A). Analysis of benomyl and temperature sensitivities indicated that marking *cdc20* gene at its 3' UTR does not cause any detectable phenotypes (data not shown).

To be able to track the Cdc20 protein in our immunoprecipitation and immunoblotting experiments we needed to couple it with an epitope tag. Previously in our lab, Cdc20 had been coupled with several tags (GFP, HA and myc) at its C-terminal end by Matylda Sczaniecka. These tags had been inserted between the IR motif and the stop codon of Cdc20, which has been reported to involve in APC/C activation. Subsequent functionality analyses indicated that tagging Cdc20 at its C-terminus led to benomyl sensitivity and inability to hold a fully functional checkpoint arrest upon depolymerisation of microtubules by *nda3-KM311* cold sensitivity. This could be caused by a possible perturbation of the IR-motif function and Cdc20-APC/C interaction due to the location of the tag. On the other hand, N-terminal tagging did not seem to be a viable solution either, since at that region Cdc20 has been found to bear several regulatory phosphorylation sites (Labit et al., 2012) and the C-box (David Barford, 2011), which have been reported to have roles in the APC/C activation. Moreover, similar difficulties in tagging $Cdc20^{Slp1}$ has been reported by other groups before (Hiro Yamano and Silke Hauf personal communication).

Cdc20 function. Thus we decided to use three tandem repeats of FLAG tag (DYKDDDDK; 1012 Da). Figure 4.111C illustrates the process of inserting an internal 3xFLAG tag, which consists of three steps. First, we amplified from the genomic DNA a sequence cassette with flanking restriction enzyme sites, which consists of the *cdc20* ORF and its 3'UTR followed by the hygromycin resistance gene and 527 base pair-long 3'UTR downstream of the resistance marker. This ~500 base pair sequence was aimed to serve during homologous recombination of the final product into the yeast genome. Then we inserted this sequence cassette into Gateway pDONR201 vector using conventional cloning. Second, we ordered a synthetic Cdc20 DNA (nucleotides 1-363) sequence (5' end of the ORF), which contains the internal 3xFLAG tag. This sequence was incorporated into *cdc20* ORF using conventional cloning in the Gateway vector. Third, we released the whole sequencing cassette, including the internal 3xFLAG tag inside *cdc20* ORF using restriction enzyme digestion, and transformed it into haploid *S. pombe* cells, followed by selection of the right isolates through hygromycin B resistance, and further analysis by PCR amplification and DNA sequencing.

Next, we analysed *cdc20*-FLAG cells in terms of benomyl and temperature sensitivity and observed that they grow similarly to untagged *cdc20* cells. Moreover, analyses in terms of mitotic progression rate in an unperturbed mitosis (using *cdc25-22* block in G2 phase and synchronous release into mitosis) and *nda3-KM311* mediated SAC activation indicated that internal tagging of Cdc20 protein does not lead to a detectable defect unlike the previously tried C-terminal tags (data not shown). Thus, we conclude that the internal FLAG tag is a relatively physiological tool to examine Cdc20 regulation in our following experiments.

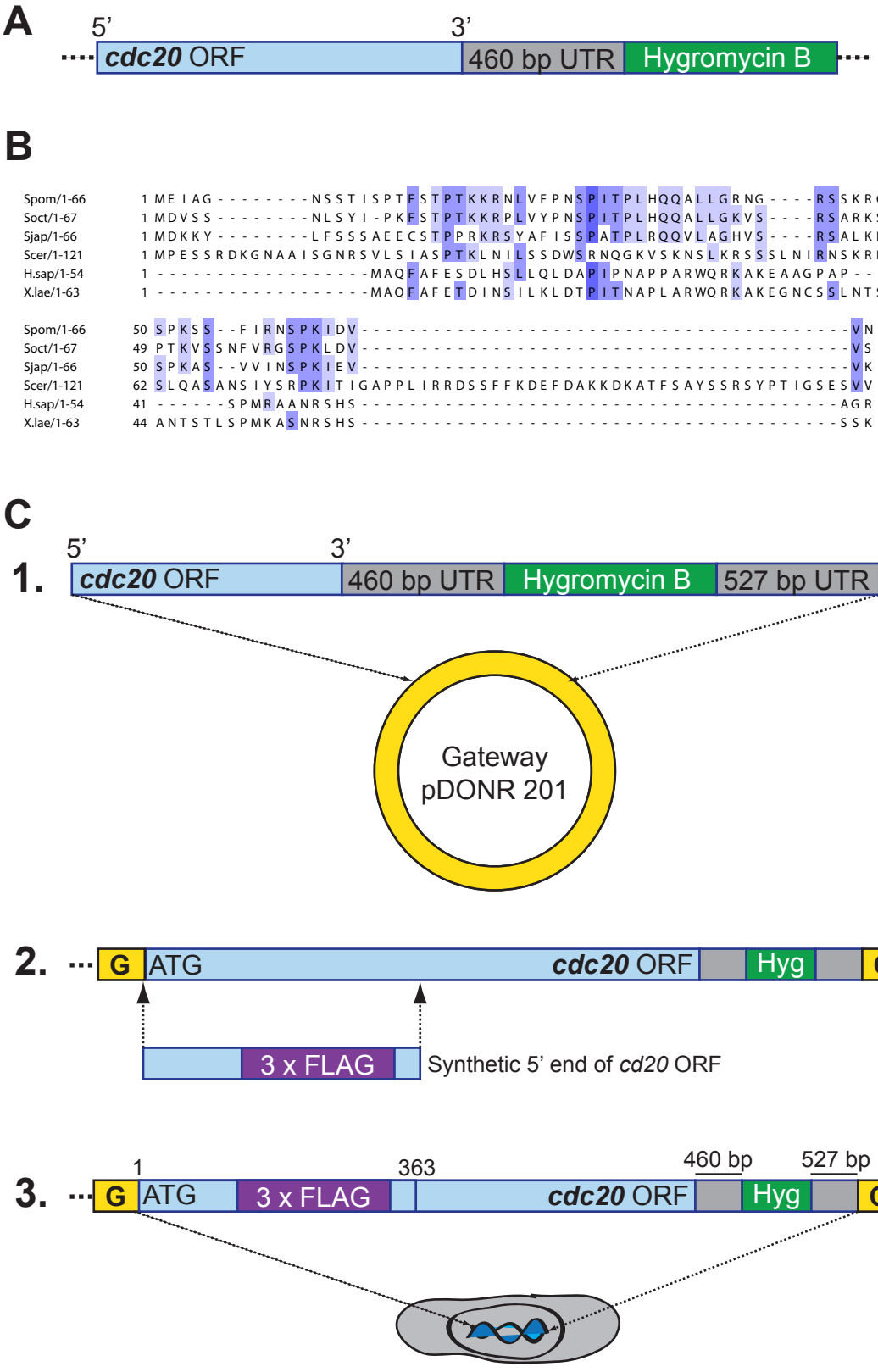

Figure 4.11 Marking of cdc20+ gene with an antibiotic resistance gene and inserting an internal tag

(A) Schematic illustrating the marking of 3' UTR of *cdc20* gene with Hygromycin B resistance gene, using the 'two-step PCR based gene modification' method. **(B)** Alignment of Cdc20 N-terminus from three fission yeast species (*S. pombe, S. octosporus, S. japonicus*), one budding yeast (*S.cerevisiae*) and two metazoans (*H. sapiens, X. laevis*), performed in Jalview software using ClustalWS algoritm. The internal tag (3 x FLAG) was inserted between two valine residues (V64 and V65) flanking the gap **(C)** Schematic illustrating three-steps of inserting an internal 3 x FLAG tag into Cdc20 ORF, and transformation of haploid fission yeast with the final product. See the text for details.

4.5 Generating phosphorylation site mutants of Cdc20

In the previous sections, by performing kinase assays we identified Cdc20 as a substrate of Bub1 kinase *in vitro* (Figure 4.3B). Subsequently, mapping of Cdc20's *in vitro* phosphorylated sites by Bub1 indicated that five of those sites (S11, S28, T31, S76 and S482) overlap with the *in vivo* phosphorylated sites of Cdc20 in mitotically arrested cells (Figure 4.4A). Alignment of the Cdc20 orthologs from three fission yeast species (*S. pombe, S. octosporus, S. japonicus*), one budding yeast (*S.cerevisiae*) and two metazoans (*H. sapiens, X. laevis*) indicated that four (S28, T31, S76 and S482) of these five residues are well-conserved among these species (Figure 4.5). This strengthens the possibility that phospho- modification of these residues may play a role in the regulation of Cdc20 throughout evolution. In order to investigate this possibility, we categorised the putative phosphorylation sites in two groups: N-terminal sites S28, T31, S76 and S59 (instead of S11 that is not well-conserved); and the C-terminal site S482. Initially, we began to examine the N-terminal phosphorylation sites by mutating them to alanine, generating the phospho-deficient *cdc20 4A* allele. Analysis of *cdc20 4A* cells in mitosis under unperturbed conditions or spindle perturbation by CBZ demonstrated that *cdc20 4A* was not expressed at the endogenous levels (data not shown). Because this phenotype would make interpretation of the results difficult, we have decided to split the *cdc20 4A* allele by generating two *cdc20 2A* alleles (S28, T31 and S59, S76), which will be studied in the future.

I next chose to focus on the C-terminal site S482. There are four reasons that I chose to analyse the serine 482 site in particular:

1. In the Cdc20 alignments, serine 482 appears to be fairly well-conserved among *S. pombe, S. cerevisiae, X. laevis* and *H.sapiens* (Figure 4.5 and Figure 4.12A), in which phospho-regulation of Cdc20 has been demonstrated before (Chung & Chen, 2003; Labit et al., 2012; Pan & Chen, 2004; Tang, Shu, et al., 2004; Vanoosthuyse & Hardwick, 2005; Yu & Tang, 2005). This suggests that phospho-modification of Cdc20 through S482 may be evolutionarily conserved.

2. Serine 482 is the only '*in vivo* and *in vitro'* phosphorylated residue among the five sites of Cdc20 ΔN-term which were phosphorylated by Bub1 *in vitro* (Figure 4.3B). This increases the possibility that S482 may be phosphorylated by Bub1 *in vivo.*

3. Serine 482 is only four residues away from the IR-motif (Figure 4.12A), that is required for APC/C activation (D. Barford, 2011). The study (Labit et al., 2012) that demonstrated the Cdk1-mediated inhibition of *X. laevis* APC/C^{Cdc20}, attributed this regulation to the close proximity of the N-terminal phosphorylation sites to the C-box, which is the other APC/C activating domain of Cdc20 (David Barford, 2011). This implies that likewise the C-box motif, the IR-motif of Cdc20 may also be regulated by phosphorylation of a nearby residue, like serine 482.

4. Cross-linking mass spectrometry analysis (Figures 4.10) showed that Mad2 and Mad3 proteins interact with the C-terminus of Cdc20, and are therefore in close proximity (numerous linkages were observed to K479) to serine 482. This strengthens the possibility that C-terminus of Cdc20 may be phospho-regulated in the context of an active SAC, in which the activity of Bub1 kinase and the assembly of Mad2, Mad3 and Cdc20 (as the MCC) coincide.

Therefore, to analyse lack of phosphorylation (phospho - deficiency) at this site we mutated this putative Bub1 site, serine 482, (or two adjacent serine residues as well; serine 482, serine 483 and serine 484) to alanine, in order to generate phospho – deficient mutants of Cdc20 C-terminal *cdc20 S1A* and *cdc20 S3A* (Figure 4.12B). In addition to mutating only serine 482, we mutated two adjacent serines as well, although they were not mapped. This was because of the high proximity of these three serines and the possibility that the mass spectrometry mapping could be misleading. Therefore, if any of these three sites is phosphorylated *in vivo* (and if this is important for the cell cycle), it would be indicated through the *cdc20 S3A* allele.

On the other hand, to analyse constitutive phosphorylation of serine 482, we mutated it to glutamate to generate a phospho – mimicking allele, *cdc20 S3E*. We generated another phospho – mimic mutant of Cdc20 as well, mutating serine 482 to aspartate (*cdc20 S1D*), that we examine in the last section of chapter 5. Besides the C-terminal phosphorylation site mutants, we also mutated arginine 488 of the IR motif to glutamate, in order to generate the *cdc20 IE* mutant (Figure 4.12B).

In addition to investigating the function of the IR-motif in *S. pombe,* we used the *Cdc20 IE* allele as a control, which was thought to help us interpret the behaviour of our Cdc20 phosphorylation mutants with respect to the following aspects:

1. Deletion of the IR motif or its mutation into IE have been reported to impair Cdc20's activator function and MCC-APC/C interaction (Izawa & Pines, 2012). In our case, substitution of serine(s) by alanine or glutamate/ aspartate in close proximity to the IR motif might affect Cdc20 functions in this regard.

2. In the case of phospho – mimic mutations (*cdc20 S3E* and *cdc20 S1D*) additional negative charge(s) would be constitutively introduced in close proximity to the IR motif. Substitution of the arginine 488 by glutamate in the case of *cdc20 IE* may help us evaluate whether changes in charge impair functions of the C-terminus, regardless of their roles in phospho – regulation of Cdc20.

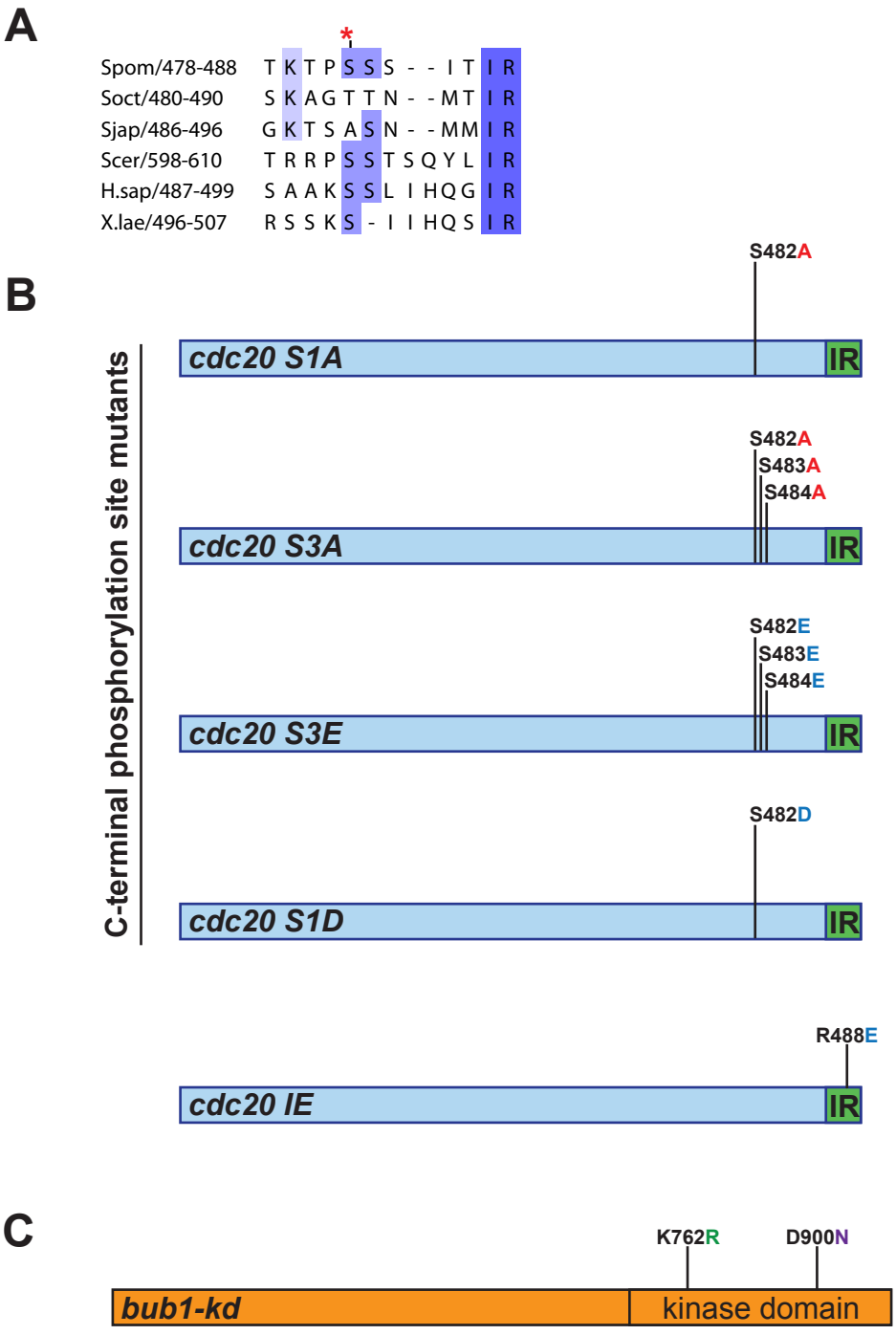

Figure 4.12 Cdc20 C-terminal mutants and the *bub1 kinase-dead (kd)* mutant used in this study.

(A) Allignment of Cdc20 C-terminus from three fission yeast species (*S. pombe, S. octosporus, S. japonicus*), one budding yeast (*S.cerevisiae*) and two metazoans (*H. sapiens, X. laevis*), performed in Jalview software using ClustalWS algoritm. The red asterisk annotates serine 482 that was found to be phosphorylated *in vitro* by Bub1 and *in vivo* in mitotically arrested cells. **(B)** Schematic illustrating the C-terminal pshosphorylation site mutants (phospho-deficient *cdc20 S1A* and *cdc20 S3A*; phospho-mimicking *cdc20 S3E* and *cdc20 S1D*) and IR motif mutant (*cdc20 IE*) of Cdc20 with their mutated sites. **(C)** Schematic illustrating the kinase-dead mutant of Bub1 (*bub1-kd*) with two point mutations in its kinase domain.

Chapter 5: Roles of Cdc20^{Slp1} phospho-regulation in the SAC

5.1 Overview

Phospho-regulation of Cdc20 by different kinases has been reported in different species. In *Xenopus* egg extracts, phosphorylation of Cdc20 by Cdk1 (D'Angiolella et al., 2003; Yudkovsky et al., 2000) and MAPK (Chung & Chen, 2003) is required for its interaction with the other two MCC components (Mad2 and Mad3/BubR1). Another *Xenopus* study has reported that phosphorylation of Cdc20 N-terminus by Cdk1 decreases it affinity for the APC/C in early mitosis, which is later (at metaphase-anaphase transition) reversed through its dephosphorylation by PP2A to promote Cdc20-APC/C binding, and thereby promote anaphase onset (Labit et al., 2012). In addition, phosphorylation of Cdc20 N-terminus by Bub1 has been reported in a human study for the first time (Tang, Shu, et al., 2004) suggesting that, this phosphorylation is required for a robust SAC response. Furthermore, the same group (Kang et al., 2008) has further supported this hypothesis by crystalizing the C-terminal kinase domain of Bub1, and demonstrating that Bub1 has a considerable specificity toward Cdc20 (see page 26 for details).

In chapter three, we confirmed the observations of previous studies (Chen, 2004; Fernius & Hardwick, 2007; Kawashima et al., 2010; Roberts et al., 1994; Yamaguchi et al., 2003) that Bub1 kinase activity is necessary for bi-orientation and required to have a robust SAC response to spindle damage, in order to ensure accurate chromosome segregation. We demonstrated that Bub1 kinase activity contributes to delaying premature anaphase onset by maintaining kinetochore recruitment of the MCC components (Mad2 and Mad3), and MCC-APC/C interaction until the later stages of prometaphase. In addition, by using the *sgo2* null strain, we attempted to separate possible SAC roles of Bub1 kinase activity from its relatively better established chromosome biorientation (and indirect SAC activation) role through the Bub1-H2A-Sgo2-Aurora B pathway. We observed that its roles in maintaining the MCC components on kinetochores (partly shared by the Bub1-Aurora B pathway), and sustaining a robust anaphase delay may be mediated by another substrate.

In chapter four, we confirmed that *S. pombe* Bub1 auto-phosphorylates efficiently (Kawashima et al., 2010) and demonstrated for the first time that it phosphorylates

fission yeast Cdc20 directly (*in vitro*). Identification of the phosphorylated Cdc20 sites (*in vitro* by Bub1 and *in vivo* in mitotically arrested cells) revealed that this modification of fission yeast Cdc20 is not restricted to its N-terminal region, unlike it has been reported in *Xenopus* egg extracts (Labit et al., 2012) and allegedly in human cells (Tang, Shu, et al., 2004). Unlike Tang and colleagues proposed, mutating six N-terminal Bub1 sites (to alanine) on human Cdc20 does not appear to abolish its Bub1 mediated phosphorylation *in vitro* (see the residual phosphorylation signal of the "nonphosphorylatable" Cdc20 mutant in (Tang, Shu, et al., 2004)). This suggests that Bub1 may phosphorylate Cdc20 at its other regions which might be important for mitotic regulation.

By using crosslinking mass spectrometry (CLMS) analysis, we confirmed already known interactions between the MCC components (Cdc20, Mad and Mad3) (Chang et al., 2015; Chao et al., 2012b; Izawa & Pines, 2012), and demonstrated new ones between the flexible C-terminal tails of Cdc20 and Mad3, which were not determined in the MCC crystal structure (Chao et al., 2012b). These novel interactions suggest that, Mad2 and Mad3 may inhibit APC/C activity by binding to the C-terminal tail of Cdc20 where the regulatory IR-motif (da Fonseca et al., 2011) and a highly conserved phosphorylation site, serine 482, (revealed in both *in vitro* and *in vivo* analyses) are found. In other words, sequestration of Cdc20 IR motif by Mad2 and Mad3 may inhibit the activation of APC/C by Cdc20. On the basis of these observations, we generated phosphorylation mutants of Cdc20, either refractory to C-terminal phosphorylation (phospho-deficient) or mimicking constitutive phosphorylation of this site (phospho-mimicking).

In this chapter, we aim to:

1. Examine the mitotic behaviour of the C-terminal Cdc20 phosphorylation mutants to determine whether they still retain the mitotic functions of Cdc20 under unperturbed conditions: (i) activating APC/C to promote anaphase onset, (ii) maintaining MCC assembly and (iii) MCC-APC/C interaction.

2. Analyse whether lack of C-terminal Cdc20 phosphorylation or its constitutive phosphorylation have any functional consequences on the abilities of cells in recruiting the MCC components to kinetochores and maintaining the MCC-APC/C interaction, thus delaying anaphase onset in response to various degrees of spindle perturbation. In addition, we aim to assess the abilities of Cdc20 phosphorylation mutants in satisfying the SAC (chromosome biorientation) and subsequently recovering from the SAC mediated metaphase arrest (SAC silencing), upon spindle reformation.

3. Finally, combine the phospho-mimicking Cdc20 mutants with the *bub1-kd* mutant to analyse whether the constitutive phosphorylation of Cdc20 C-terminus can rescue the SAC defects observed in the absence of Bub1 kinase activity. By performing this rescue experiment, we aim to provide *in vivo* evidence for the possibility that Bub1-mediated phosphorylation of Cdc20 (that we observed *in vitro*) is important for the mitotic regulation in fission yeast.

5.2 Analysis of Cdc20 C-terminal phosphorylation mutants under unperturbed conditions

In this section we aim to analyse whether the phospho-deficient (*cdc20 S1A* and *cdc20 S3A*) or phospho-mimicking (*cdc20 S3E*) mutations affect its functions under unperturbed conditions. To determine this, we analyse the abilities of C-terminal Cdc20 phosphorylation mutants in progressing into anaphase, assembling the MCC and maintaining MCC-APC/C interaction in an unperturbed mitosis.

5.2.1 Progression through an unperturbed mitosis

In this experiment we aimed to analyse whether Cdc20 phosphorylation mutations (*cdc20 S3E, cdc20 S1A* and *cdc20 S3A*) affect its APC/C activator function. If this was impaired, then we would expect the cells to have defects in anaphase onset, despite the absence of any microtubule perturbation (Izawa & Pines, 2012; Nilsson et al., 2008).

In order to track progression of the Cdc20 mutants through an unperturbed mitosis, temperature sensitive *cdc25-22* mutant was used to synchronize cells in G2 phase. In addition, SAC deficient *mad2* null allele (Vanoosthuyse et al., 2009) was used as a negative control and crossed with wild type and *cdc20 S3E,* to be able to test if the results depend on the presence of a functional SAC machinery. Cells were grown at 25°C to mid-log phase, and then the temperature was shifted to 36°C (restrictive temperature for *cdc25-22* allele), in order to arrest them in G2 phase. After 4 hours, cells were synchronously released into mitosis by shifting the temperature back to the permissive temperature of 25°C. Samples were collected at 15 minute time points for 120 minutes, and fixed in methanol. Fixed samples were then stained with calcofluor to detect septation, which was scored as a readout of mitotic exit (Vanoosthuyse et al., 2009; Yanagida, 1998). The Mad3-GFP fusion protein was also visualized as it is known to localise to kinetochores of prometaphase arrested cells (Rischitor et al., 2007; Sczaniecka et al., 2008).

It is evident from the results (Figure 5.1A) that at 60 minutes, 80-90% of the cells from all strains exited mitosis (septated) without any detectable Mad3-GFP localization to kinetochores. As can be seen in Figure 5.1B, septation scores of all Cdc20 phosphorylation mutants, both phospho-deficient and phospho-mimicking ones, are similar to that of wild type throughout the time course. At the end of two hours 90-100% cells of all strains exited mitosis with an almost equal timing. Moreover, the *mad2* null mutant and the *mad2* null, *cdc20 S3E* double mutant do not significantly deviate from this mitotic timing. (Figure 5.1B). This result implies that the effect of a functional SAC machinery on the timing of an unperturbed mitosis is negligible (Movies have demonstrated that unperturbed mitosis is only 1-2 minutes shorted in the absence of Mad2, Kevin Hardwick personal communication).

These results suggest that *cdc20 S3E, cdc20 S1A* and *cdc20 S3A* mutants can activate APC/C as efficiently as wild type *cdc20* does. In other words the Cdc20 activator function is not significantly affected by either absent (*cdc20 S1A* and *cdc20 S3A*) or constitutive phosphorylation (*cdc20 S3E*) of its C-terminal tail.

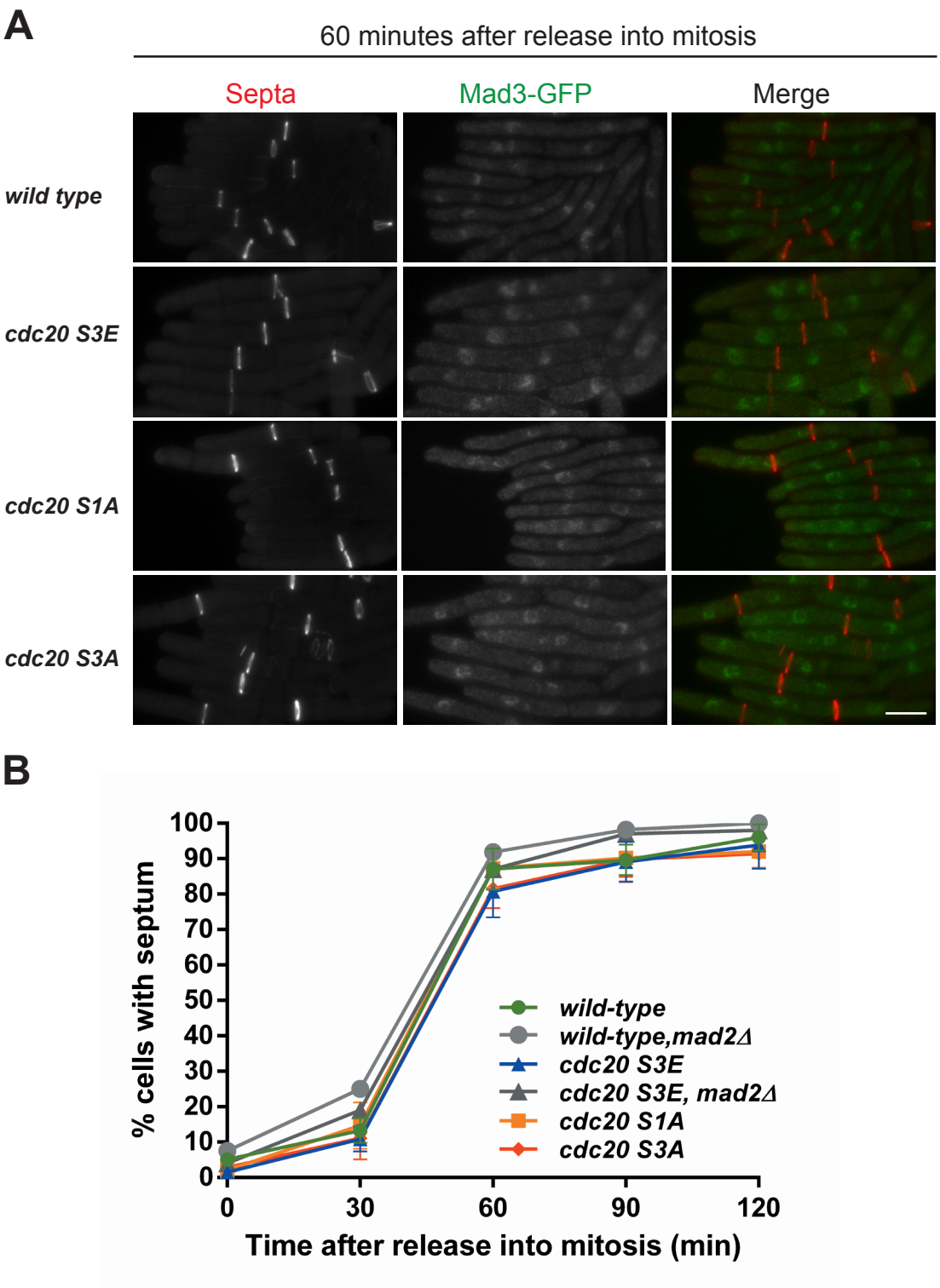

Figure 5.1 APC/C activating function of Cdc20 is not affected by either absent or constitutive phosphorylation of its C-terminus in an unperturbed mitosis.

(A) Representative images from 60 minutes, displaying septation (in red) by calcofluor staining and Mad3-GFP localisation (in green) in the cells expressing wild type *cdc20*, *cdc20 S3E, cdc20 S1A or cdc20 S3A,* following 4 hours of *cdc25-22* block at G2-phase and release into an unperturbed mitosis (time zero). Scale-bar represents 5 microns **(B)** Graph plotting percentage of cells that formed septum (exited mitosis) with respect to time. Results are the average of two independent experiments. Error bars representing standard error.

5.2.2 MCC formation in an unperturbed mitosis

In the previous section we reported that mitotic progression rates of Cdc20 phosphorylation mutants were comparable to that of wild type. This result was accompanied by the finding that mitotic progression of *mad2* null double mutants were not significantly faster. In other words, although cells with a functional SAC machinery (+Mad2 strains) were able to form MCC, this did not delay their mitotic timing dramatically. We hypothesize that in an unperturbed mitosis, random microtubule-kinetochore attachment errors may still occur, which leads to MCC formation to a certain extent. However, those errors are likely to be corrected without a long delay, which leads to silencing of the SAC and subsequent disassembly of the MCC. Thus, in the next experiment, we aimed to analyse MCC formation in the cells expressing wild type *cdc20* or *cdc20 S3A* in an unperturbed mitosis. Cells were released into a synchronous mitosis employing *cdc25-22* temperature sensitivity as described previously. Cell samples were collected at 15 minute time points for 135 minutes. Then the samples were lysed, subjected to anti-FLAG (Cdc20) immunoprecipitation and processed for SDS-PAGE/western blotting, in which they were probed for Cdc20, Mad2 and Mad3 to monitor MCC formation.

As shown in Figure 5.2A, wild type *cdc20* and *cdc20 S3A* total protein levels were largely similar overall, although there may be a slight delay in the decline of *cdc20 S3A* levels compared to that of wild type *cdc20.* Nevertheless, Figure 5.2B shows that comparable amount of MCC components (Mad2 and Mad3) are pulled-down by wild type *cdc20* and *cdc20 S3A.*

These data suggest that lack of the phosphorylation of Cdc20 C-terminus (as in the case of *cdc20 S3A*) does not significantly affect MCC formation during an unperturbed mitosis.

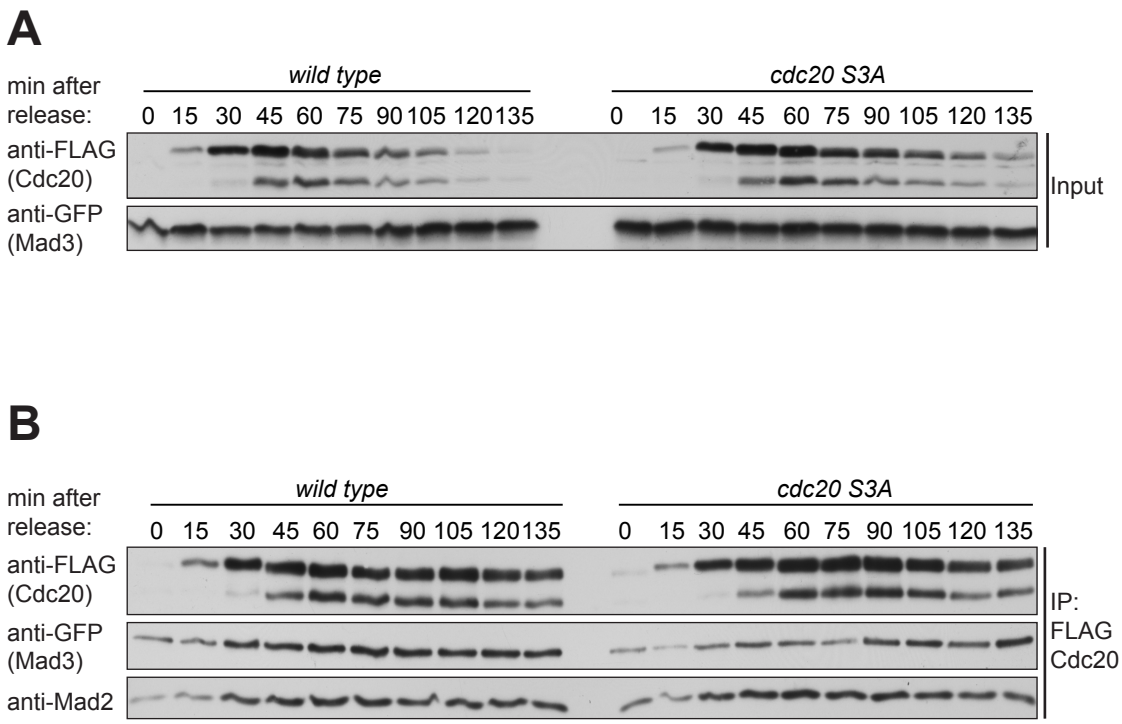

Figure 5.2 MCC formation is not affected by the absence of Cdc20 C-terminus phosphorylation in an unperturbed mitosis

(A) Total levels of Cdc20 (FLAG) and Mad3 (GFP) were analyzed by immunoblotting in whole cell extracts from cells blocked at G2-phase (*cdc25-22*), and released into unperturbed mitosis for 135 minutes. Mad3 levels were used as loading control. **(B)** Coimmunoprecipitation (IP) analysis of mitotic checkpoint complex (MCC) formation. Cdc20 (FLAG) was immunoprecipitated from the extracts described in A. Levels of Mad3 (GFP) and Mad2 coimmunoprecipitated with Cdc20 (FLAG) were analyzed by immunoblotting. Cdc20 (FLAG) commonly appears as two bands due to the cleavage of Cdc20 (FLAG) fusion protein. Results are representative of three independent experiments.

5.2.3 MCC-APC/C interaction in an unperturbed mitosis

Having shown previously that phosphorylation of Cdc20 C-terminus affects neither the mitotic progression rate nor the MCC formation abilities of cells significantly, next we sought to determine whether it influenced their MCC-APC/C interaction. To analyse that we employed *cdc25-22* temperature sensitivity assay that enables us to release cells into an unperturbed mitosis. Cell samples were collected at 15 minute time points for 135 minutes. Then the samples were lysed, subjected to anti-TAP (APC4) immunoprecipitation and processed for SDS-PAGE/western blotting, in which they were probed for MCC components.

As Figure 5.3A shows that total levels of wild type *cdc20* and *cdc20 S3A* were fairly similar despite *cdc20 S3A* being slightly more stabilised towards the end of mitosis. This subtle stabilisation of *cdc20 S3A* levels is consistent with the previous finding (Figure 5.2A).

As for the MCC-APC/C interaction, Figure 5.3B displays that comparable amounts of Cdc20, Mad2 and Mad3 bound to APC/C in wild type *cdc20* and *cdc20 S3A* cells.

This result is consistent with the previous findings that wild type *cdc20* and *cdc20 S3A* cells progress through mitosis with almost the same rate (Figure 5.1B) as they form similar amounts of MCC (Figure 5.2B).

To sum up, lack of Cdc20 phosphorylation at its C-terminus (as in the case of *cdc20 S3A*) does not significantly affect MCC formation, MCC-APC/C interaction or the progression rate of cells in an unperturbed mitosis.

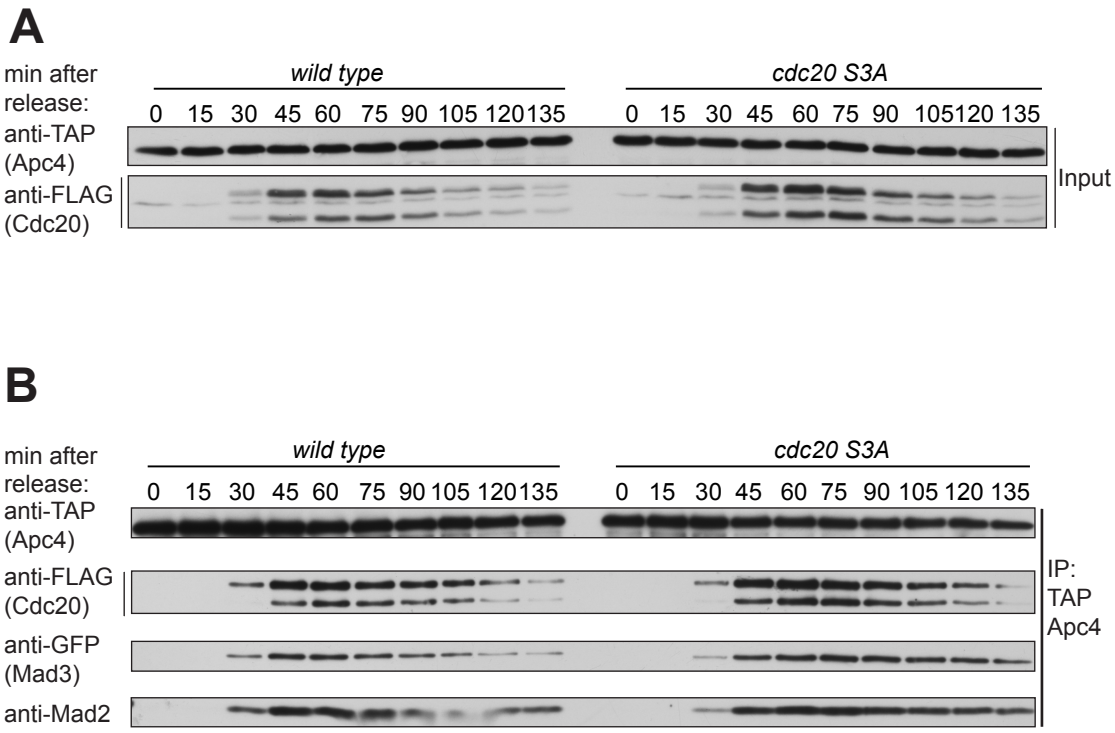

Figure 5.3 MCC-APC/C interaction is not affected by the absence of Cdc20 C-terminus phosphorylation in an unperturbed mitosis

(A) Total levels of Cdc20 (FLAG) and Apc4 (TAP) were analyzed by immunoblotting in whole cell extracts from cells blocked at G2-phase (*cdc25-22*), and released into unperturbed mitosis for 135 minutes. Apc4 levels were used as loading control. **(B)** Coimmunoprecipitation (IP) analysis of MCC-APC/C interaction. Apc4 (TAP) was immunoprecipitated from the extracts described in A. Levels of Cdc20 (FLAG), Mad3 (GFP) and Mad2 coimmunoprecipitated with Apc4 (TAP) were analyzed by immunoblotting. Apc4 levels were used as loading control. Cdc20 (FLAG) commonly appears as two bands due to the cleavage of Cdc20 (FLAG) fusion protein. Results are representative of three independent experiments.

5.3 Analysis of Cdc20 C-terminal phosphorylation site mutants in the context of the SAC activated by an anti-microtubule drug

Our previous findings show that C-terminal phospho-modification of Cdc20 does not appear to affect cells' mitotic timing, MCC formation and MCC-APC/C interaction in an unperturbed mitosis. In this section we aim to investigate whether this is also true in the context of a perturbed mitosis with destabilised spindle microtubules, activating the SAC. To investigate this, we released cells into a synchronous mitosis, employing *cdc25-22* temperature sensitivity followed by treatment with the microtubule depolymerising drug carbendazim (CBZ) at 20 minutes after the release. Using this method, we aim to determine whether C-terminal phospho-modification of Cdc20 is involved in the regulation of mitotic progression rate and MCC-APC/C interaction, when the SAC is activated by depolymerised microtubules.

5.3.1 Analysis of mitotic timing and Mad3 kinetochore localisation in the presence of an anti-microtubule drug

Following their release into synchronous mitosis with CBZ treatment, cell samples were collected at 15 minute time points for 150 minutes, and fixed in methanol. Later, fixed cells were stained to detect septa, which was visualised by microscopy along with Mad3-GFP localisation at unattached kinetochores.

Figure 5.4A and B demonstrate that after 60 minutes into mitosis, 56% of wild type cells exited mitosis (indicated by septation), and the remaining 44% still arrested at metaphase through the SAC response activated upon microtubule depolymerisation. However, this arrest did not occur anymore when Mad2 is deleted, as indicated by 94 % septation index of the *mad2* null strain. This result suggests that the observed metaphase arrest depends on a functional SAC machinery in the presence of spindle damage, which is abolished by deletion of Mad2 (Vanoosthuyse et al., 2009). Septation indexes of the phospho-deficient Cdc20 mutants *cdc20 S1A* and *cdc20 S3A* were similar to that of wild type, being 51% and 47% respectively. This result indicates that there is only a slight delay in the mitotic progression of phospho-deficient Cdc20 mutants compared to that of wild type.

On the other hand, phospho-mimicking Cdc20 mutant *cdc20 S3E* displayed a dramatically lower septation index (13%) (and higher arrest profile (87%)). Importantly, when Mad2 was deleted, *cdc20 S3E* cells were not able to delay anaphase onset anymore, as indicated by a very high septation index (88%) exhibited by *cdc20 S3E, mad2* null cells.

Figure 5.4B shows that the relative proportions of mitotic progression rates indicated at 60 minutes (Figure 5.4A) were largely maintained by the strains throughout the time course. At 150 minutes, ~80% of wild type and phospho-deficient Cdc20 cells (*cdc20 S1A* and *cdc20 S3A*) septated, whereas the septation index of phospho-mimic Cdc20 mutant *cdc20 S3E* was as low as 39%. This excessive arrest phenotype of *cdc20 S3E* was reversed in the absence of Mad2, indicated by 98% septation index of *cdc20 S3E, mad2* null cells, which is almost identical to that of *wild type, mad2* null strain (100%).

In addition to examining mitotic exit, we monitored localisation of Mad3-GFP to unattached kinetochores, which is another indicator of metaphase arrest. To be able to separately evaluate abilities of cells to regulate either mitotic timing (indicated by septation index) or localisation of MCC components to unattached kinetochores (indicated by Mad3-GFP foci), we scored Mad3-GFP kinetochore localisation only in the population of non-septating cells.

Figure 5.5 displays that at 30 minutes 66% of the non-septating wild type cells exhibited Mad3-GFP kinetochore foci, which was followed by phospho-deficient cells *cdc20 S1A* (54%) and *cdc20 S3A* (64%) with similar scores. However, only 17% of non-septating *wild type, mad2* null cells could display kinetochore foci, suggesting that Mad2 is required to maintain the recruitment of MCC components to unattached kinetochores in wild type cells. On the other hand, non-septating *cdc20 S3E* cells exhibited a significantly high percentage of Mad3-GFP kinetochore foci (86%). Interestingly unlike *wild type, mad2* null, removal of Mad2 from *cdc20 S3E* cells did not abolish kinetochore localisation of Mad3-GFP at 30 minutes, which is indicated by fairly high percentage of kinetochore foci exhibited by *cdc20 S3E, mad2* null cells (64%). This result suggests that, *cdc20 S3E* phospho-mimicking mutation can rescue the Mad3 recruitment defect in the absence of Mad2, and restores it almost to the wild type levels (66%). However, this rescue phenotype was not maintained throughout the

time course, as at 60 minutes the percentage of Mad3- GFP kinetochore foci in *cdc20 S3E, mad2* null cells (4.5%) became as low as that in *wild type, mad2* null cells (5%), and eventually both of them became zero at 90 and 120 minutes (Figure 5.5B).

This suggests that although *cdc20 S3E* mutation promotes kinetochore localisation of Mad3 at early stages of metaphase (30 min), Mad2 is still required in a functional SAC to maintain Mad3 recruitment until the later stages of mitosis (60, 90, 120 min). As for the other strains, Figure 5.5B shows that non-septating wild type, *cdc20 S1A* and *cdc20 S3A* cells exhibited Mad3 foci similar to each other throughout the time course, indicated as ~80% (60 min), ~90% (90 min) and ~60% (120 min). On the other hand the ability of *cdc20 S3E* maintain Mad3 at kinetochores remained higher than that of others, especially towards the end of time course (94% at 120 min).

These results suggest that in the presence of a microtubule depolymerising drug (CBZ), lack of C-terminal Cdc20 phosphorylation (as in the case of *cdc20 S1A* and *cdc20 S3A*) does not significantly affect either the mitotic timing or the recruitment of Mad3. On the other hand, constitutive phosphorylation of Cdc20 C-terminus (mimicked by *cdc20 S3E*) leads to an significantly strong metaphase arrest that is dependent on Mad2 protein.

Moreover, constitutive phosphorylation of the Cdc20 C-terminus (mimicked by *cdc20 S3E*) not only enhances the kinetochore localisation of Mad3 throughout mitosis, but also rescues the defect of *mad2* null allele in this regard at the early (30 minutes), but not late stages (60, 90, 120 minutes) of metaphase.

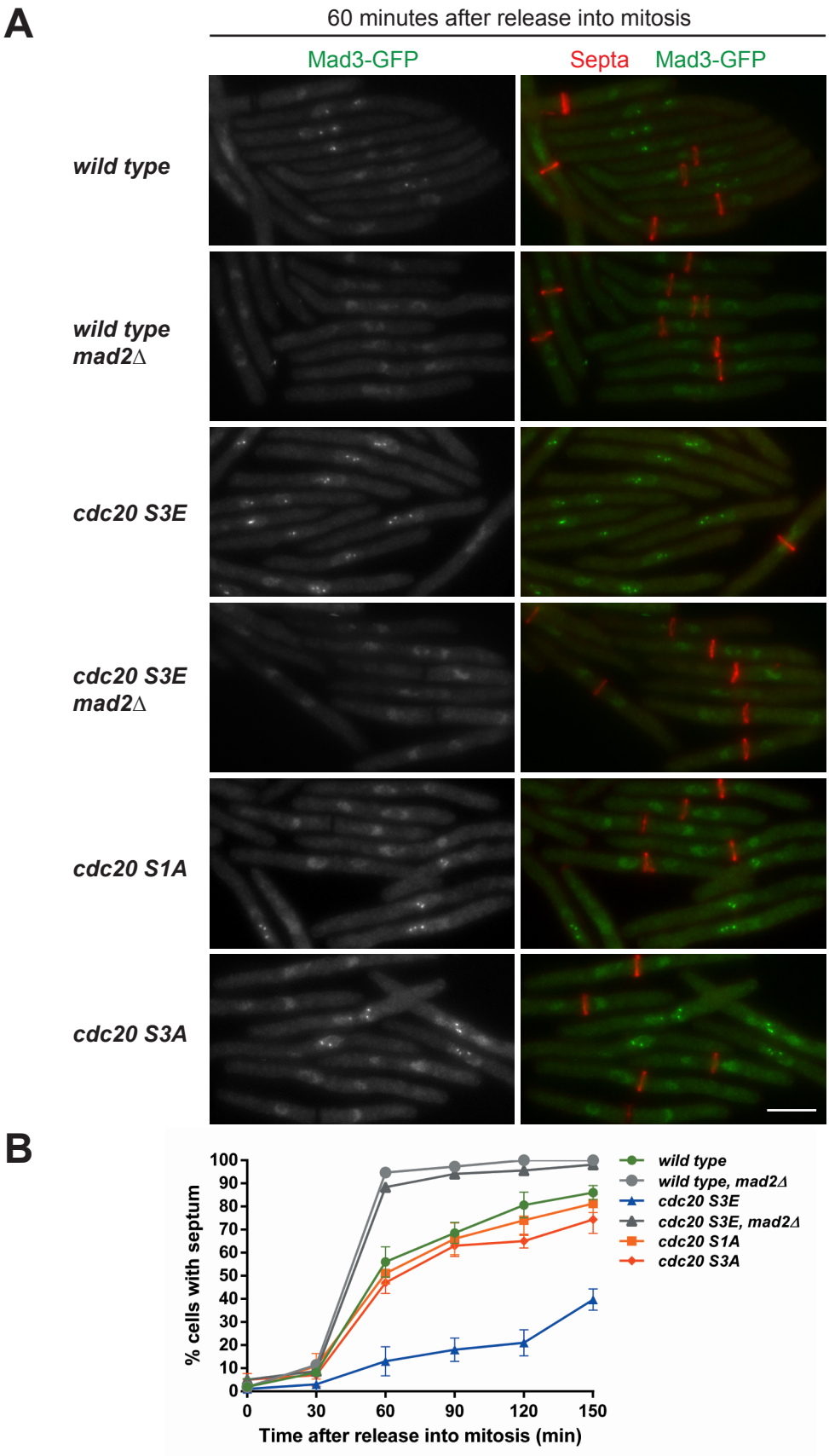

Figure 5.4 Mimicking constitutive phosphorylation of Cdc20 C-terminus results in a hyperactivated SAC response that is dependent on Mad2

(A) Representative images from 60 minutes, displaying septation (in red) by calcofluor staining and Mad3-GFP localisation (in green). Scale-bar represents 5 microns. **(B)** Cells were blocked in G2-phase for 4 hours through *cdc25-22* temperature sensitivity, and then released into mitosis at 0 minute. At 20 minutes, cells were treated with the microtubule depolymerising drug CBZ to activate SAC response. Samples were collected at each 30 minutes time point. Graph plotting percentage of cells that formed septum (exited mitosis) with respect to time. Results are the average of two experiments. Error bars representing standard error.

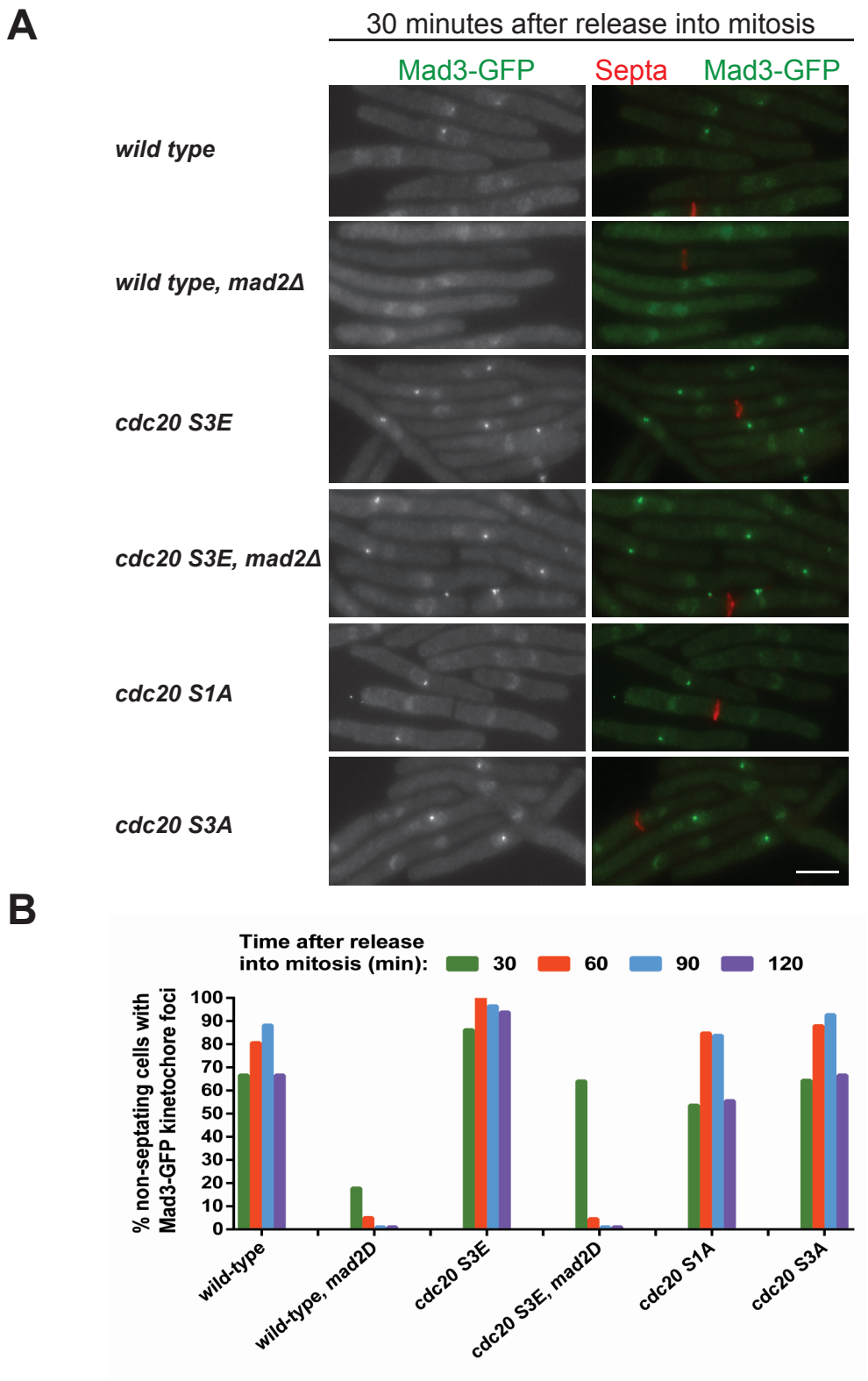

Figure 5.5 Constitutive phosphorylation of Cdc20 C-terminus significantly increases the frequency of Mad3 kinetochore recruitment

(A) Representative images from 30 minutes of the same experiment described in Figure 5.6, displaying septation (in red) by calcofluor staining and Mad3-GFP localisation (in green). Scale-bar represents 5 microns. **(B)** Graph plotting percentage of non-septating cells (still in mitosis) that exhibit Mad3-GFP kinetochore localisation at 30, 60, 90 and 120 minutes after release into mitosis.

5.3.2 Analysis of the MCC-APC/C interaction in the presence of an anti-microtubule drug

In the previous section we demonstrated that mitotic exit of cells is strongly delayed due to constitutive phosphorylation of Cdc20 C-terminus (mimicked by *cdc20 S3E*), whereas that is not significantly affected by the lack of this phosphorylation (as in the case of *cdc20 S1A* and *cdc20 S3A*). This reproducible anaphase delay is likely to be an outcome of strengthened APC/C inhibition, since this E3 ligase is the ultimate target of SAC (P. Lara-Gonzalez et al., 2011). Thus, we hypothesize that constitutive phosphorylation of the Cdc20 C-terminus (mimicked by *cdc20 S3E*) may lead to a stronger MCC-APC/C interaction, whereas lack of this phosphorylation (as in the case of *cdc20 S1A* and *cdc20 S3A*) is expected to result in an interaction similar to wild type levels. To investigate a possible link between Cdc20 C-terminal phospho-modification and MCC-APC/C binding, we carried out time course experiments as described in the previous section. Following the release into a synchronous mitosis with CBZ treatment (20 minutes after the release), cell samples were collected at 15 minute time points for 150 minutes. Then the samples were lysed, subjected to anti-TAP (APC4) immunoprecipitation and processed for SDS-PAGE/western blotting, in which they were probed for MCC components.

As displayed in Figure 5.6A, total levels of wild type Cdc20 and *cdc20 S3A* were almost identical in the presence of CBZ. Figure 5.6B shows that, this similarity was also observed in the amount of MCC components (Cdc20, Mad2 and Mad3) pulled-down by APC4 in wild type and *cdc20 S3A* cells. Moreover, this result is supported by the observation (Figure 5.6A) that wild type and *cdc20 S3A* cells exhibited highly comparable Cyclin B levels throughout the time course.

These results suggest that wild type and *cdc20 S3A* cells inhibited APC/C to a comparable extent by binding similar amounts of MCC to it, which is consistent with their comparable mitotic timing that we reported previously (Figure 5.4B).

On the other hand, comparison of wild type and phospho-mimicking *cdc20 S3E* cells appeared to be rather different. Figure 5.7B demonstrates that, *cdc20 S3E* cells exhibited significantly high amount of MCC-APC/C binding compared to that in wild type cells. Furthermore, the MCC-APC/C interaction in *cdc20 S3E* cells lasted longer

than it did in wild type cells. In wild type cells MCC components began disassembling from the APC/C at 60 minutes into mitosis, whereas in *cdc20 S3E* cells the decline of the MCC-APC/C interaction was not observed until the 120 minutes time point (Figure 5.7B).

As Figure 5.7A shows, wild type Cdc20 and *cdc20 S3E* levels were similar until 45 minutes after release into mitosis. However, from 45 minutes onwards wild type Cdc20 levels began to decrease, while *cdc20 S3E* levels increased until 90 minutes. Moreover, although Cyclin B degradation began at 15 minutes in both strains, *cdc20 S3E* cells stabilized their Cyclin B levels at a significantly higher level than wild type cells did until the end of the time course.

These results suggest that upon microtubule depolymerisation beginning at 20 minutes, *cdc20 S3E* cells activate a more potent SAC response than the wild type cells do, which probably leads to formation of more MCC molecules that inhibit the APC/C more efficiently. Due to this stronger inhibition, higher amounts of Cyclin B are stabilised in *cdc20 S3E* cells, which results in an extended metaphase arrest consistent with our previous findings (Figure 5.4B). In this case, the extended mitotic state of *cdc20 S3E* cells explains their relatively more stabilised Cdc20 levels, whose expression is sustained by Cdk1 in budding yeast mitosis (Liang et al., 2011; Vernieri, Chiroli, Francia, Gross, & Ciliberto, 2013). Taken together, our results suggest that the lack of C-terminal Cdc20 phosphorylation (as in the case of *cdc20 S3A*) does not appear to affect either MCC-APC/C interaction or mitotic timing significantly. However, constitutive phosphorylation of Cdc20 C-terminus (mimicked by *cdc20 S3E*) leads to a stronger and longer MCC-APC/C interaction, which delays anaphase onset. This stronger MCC-APC/C interaction may be a direct result of higher amounts of MCC formed in *cdc20 S3E* cells, which can be tested by co-immunoprecipitation of *Cdc20 S3E*-FLAG and the other MCC components. In addition, in the previous section (Figure 5.5) we reported that *cdc20 S3E* allele rescued the kinetochore recruitment of Mad3 in the absence of Mad2 at the early stages of mitosis. In order to assess the Mad2 dependency for a tight MCC formation, this experiment should be carried out along with the *mad2* null, *Cdc20 S3E*-FLAG strain.

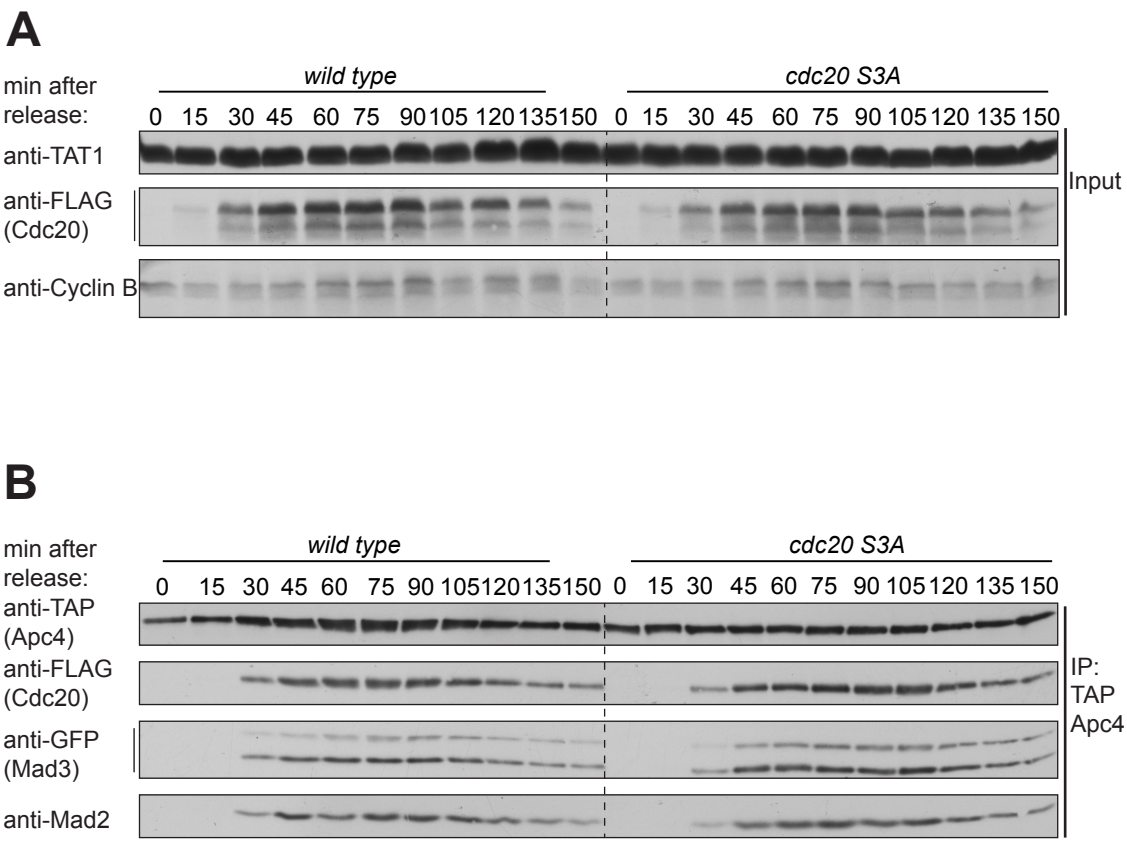

Figure 5.6 MCC-APC/C interaction is not affected by the absence of Cdc20 C-terminus phosphorylation in response to the microtubule drug CBZ

(A) Total levels of tubulin (TAT1), Cdc20 (FLAG) and Cyclin B were analyzed by immunoblotting in whole cell extracts at each 15 minute time points from cells blocked at G2-phase (*cdc25-22*), and released into mitosis (0 minutes) followed by CBZ (100 µg/ml) treatment at 20 minutes. TAT1 levels were used as loading control. Cdc20 (FLAG) commonly appears as two bands due to the cleavage of Cdc20 (FLAG) fusion protein. **(B)** Coimmunoprecipitation (IP) analysis of MCC-APC/C interaction. Apc4 (TAP) was immunoprecipitated from the extracts described in A. Levels of Cdc20 (FLAG), Mad3 (GFP) and Mad2 coimmunoprecipitated with Apc4 (TAP) were analyzed by immunoblotting. Apc4 levels were used as loading control. Mad3 (GFP) is commonly detected as two bands due to the cleavage of the fusion protein. Results are representative of two independent experiments.

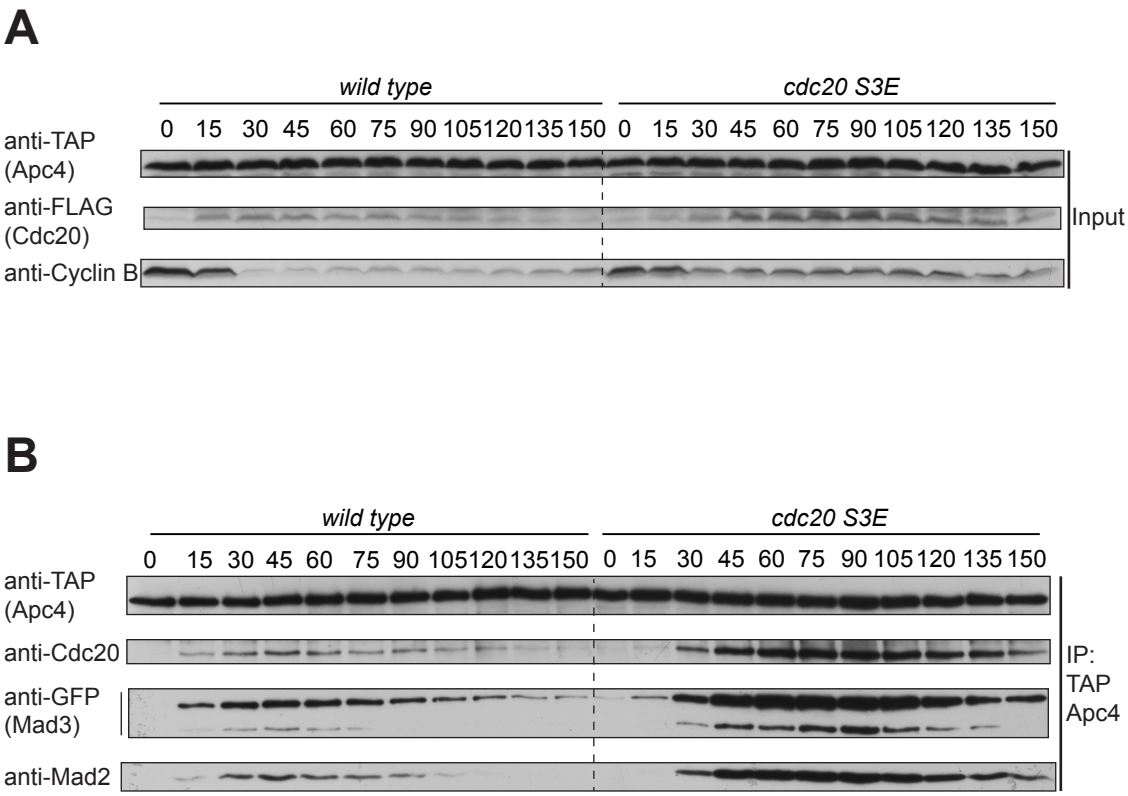

Figure 5.7 Constitutive phosphorylation of Cdc20 C-terminus enhances MCC-APC/C interaction in response to the microtubule drug CBZ

(A) Total levels of Apc4 (TAP), Cdc20 (FLAG) and Cyclin B were analyzed by immunoblotting in whole cell extracts collected at each 15 minute time points from cells blocked at G2-phase (*cdc25-22*), and released into mitosis (0 minutes) followed by CBZ (100 µg/ml) treatment at 20 minutes. Apc4 levels were used as loading control. **(B)** Coimmunoprecipitation (IP) analysis of MCC-APC/C interaction. Apc4 (TAP) was immunoprecipitated from the extracts described in A. Levels of Cdc20 (FLAG), Mad3 (GFP) and Mad2 coimmunoprecipitated with Apc4 (TAP) were analyzed by immunoblotting. Apc4 levels were used as loading control. Mad3 (GFP) is commonly detected as two bands due to cleavage of the fusion protein.

5.4 Analysis of Cdc20 C-terminal phosphorylation mutants under *nda3-KM311*-mediated microtubule depolymerisation

In the preceding sections, we described how phospho-modification of the Cdc20 C-terminus can affect MCC formation, MCC-APC/C interaction, kinetochore localisation of MCC components and progression rate in an unperturbed mitosis. In addition, to examine the same cellular events in the context of an activated SAC, we treated cells with the microtubule depolymerising drug carbendazim (CBZ). For both of these experiments, we used *cdc25-22* temperature sensitivity to be able to arrest the cells in G2-phase, and release them into a synchronous mitosis. As described in the third chapter, there is another method of enriching cells in mitosis that employs the *nda3-KM311* cold sensitive allele, by which microtubules are completely depolymerised, thereby the SAC is activated upon shifting cells to the restrictive temperature. In this section we present experiments in which we examined the mitotic behaviour of Cdc20 C-terminal phosphorylation mutants along with *bub1-kd* and *bub1* null alleles with regards to their abilities to activate and recover from the SAC, using *nda3-KM311* cold sensitivity.

5.4.1 Metaphase arrest mediated by *nda3-KM311*

In order to examine abilities of the Cdc20 C-terminal mutants and the Bub1 mutants to arrest at metaphase in response to depolymerised microtubules, we carried out *nda3-KM311* time course experiments. Cells were grown overnight at the permissive temperature (30°C), and the next day log phase cultures were shifted to the restrictive temperature (18°C) for 9 hours. Cell samples were collected 6 hours and 9 hours after the temperature shift, fixed in methanol and stained with DAPI to visualise DNA. In addition to scoring condensed DNA, we monitored localisation of polo kinase (Plo1-GFP) to spindle poles, which is another indication of metaphase arrest (Bahler et al, 1998a; Mulvihill et al, 1999). Cdc20 C-terminal mutants examined in this experiment were phospho-deficient *cdc20 S3A*, phospho-mimic *cdc20 S3E* and *cdc20 IE* alleles (where the arginine of the C-terminal IR motif is mutated to glutamate); Bub1 mutants were *bub-kd* and *bub1 null* (negative control) alleles.

After spending 6 hours with depolymerised microtubules (Figure 5.8), 52% of wild type cells arrested in metaphase, followed by *cdc20 S3A* with a similar arrest profile (49%). As expected from the negative control, *bub1 null* cells did not arrest at all, since they are known to be defective in the SAC response. *Bub1-kd* cells exhibited a lower arrest profile (44%) than the *wild type* cells did. On the other hand, higher (62%) proportion of *cdc20 S3E* cells arrested in metaphase. Interestingly, *cdc20 IE* cells also appeared to arrest with a rather high percentage (61%).

After 9 hours, (Figure 5.8) arresting proportions of *wild type* (76%), *cdc20 S3A* (76%) and became comparable, that were higher than *cdc20 IE* (68%) cells. On the other hand, *Cdc20 S3E* cells (84%) were observed to have the highest arrest frequency than the other strains. However, *bub1-kd* cells exhibited a significant arrest defect (54%) compared to wild type cells (76%).

These results suggest that, in a prolonged and relatively more penetrant spindle perturbation (6-9 hours), constitutive phosphorylation of Cdc20 C-terminus (mimicked by *cdc20 S3E*) leads to a strengthened SAC arrest, although the difference is not as big as in the case of a less penetrant spindle perturbation by CBZ treatment for a relatively short period (130 min) (Figure 5.4B). Lack of C-terminal Cdc20 phosphorylation (as in the case of *cdc20 S3A*) results in a slightly weaker SAC arrest than wild type cells only after 6 hours, but not 9 hours. On the other hand, lack of the Bub1 kinase activity (as in the case of *bub1-kd*) compromises the SAC response significantly, especially after 9 hours of spindle damage. This result is consistent with previous observations in fission yeast (Kawashima et al., 2010; Yamaguchi et al., 2003).

Interestingly, *cdc20 IE* cells arrested more frequently than wild type cells after 6 hours, although *cdc20 IE* mutation was expected to impair the Cdc20-APC/C interaction as it has been reported in human cells (Izawa & Pines, 2012). This might have been due to two possibilities; (i) *cdc20 IE* mutation either leads to a more potent SAC response or (ii) it impairs the activator function of Cdc20 so that the *cdc20 IE* cells cannot progress into anaphase.

To determine this we analysed the amount of Mad3 that is bound to the APC/C in wild type, *cdc20 S3E* and *cdc20 IE* cells, which were blocked at metaphase for 6 hours by *nda3-KM311* mutation. Figure 5.9A-B display that *cdc20 S3E* cells exhibited a slightly higher Mad3-APC/C interaction than wild type cells (the difference was much higher in response to CBZ), whereas it is noticeably lower in *cdc20 IE* cells. This result suggests that, the "strong arrest" phenotype of *cdc20 IE* cells observed in the previous experiment (Figure 5.8) is probably not due to a more potent SAC response. In contrast, a more likely explanation is that *cdc20 IE* mutation may impair the activator function of Cdc20, and this leads to a defective anaphase onset, which was manifested as a prolonged anaphase delay. In order to better understand functional consequences of the IR-motif mutation, the mitotic progression rate of *cdc20 IE* cells should be analysed in an unperturbed mitosis, to determine whether their ability to progress into anaphase is compromised.

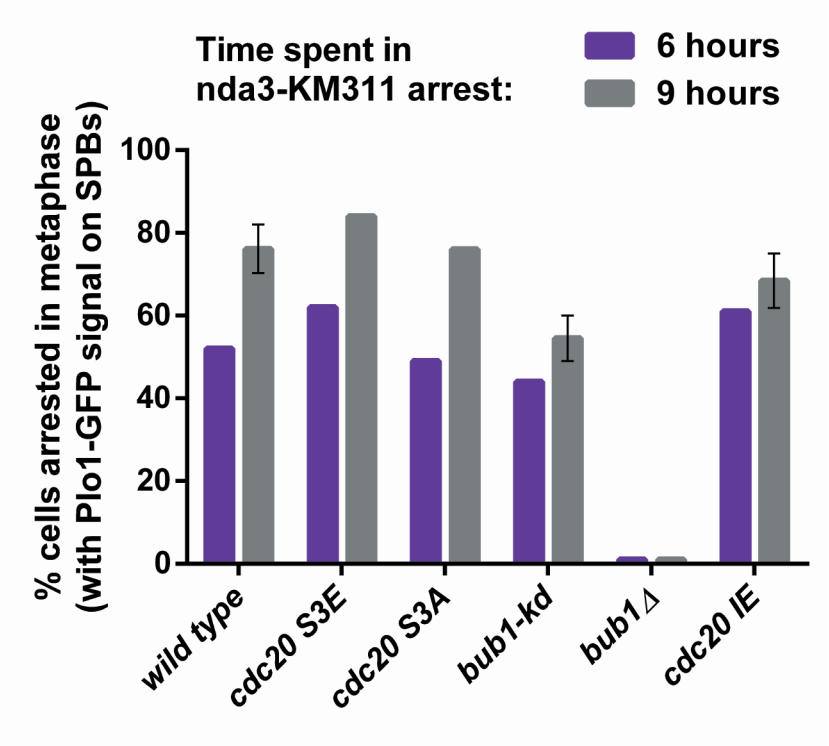

Figure 5.8 Constitutive phosphorylation of Cdc20 C-terminus slightly enhances SAC activity in response to *nda3-KM311* block

Graph plotting percentage of cells arrested at metaphase indicated by Plo1-GFP signal at spindle pole bodies (SPBs) after 6 or 9 hours at the restrictive temperature (18°C) with depolymerised microtubules (*nda3-KM311* cold sensitivity). Results of wild type, *bub1-kd* and *cdc20 IE* cells are the average of two independent experiments. Error bars representing standard error.

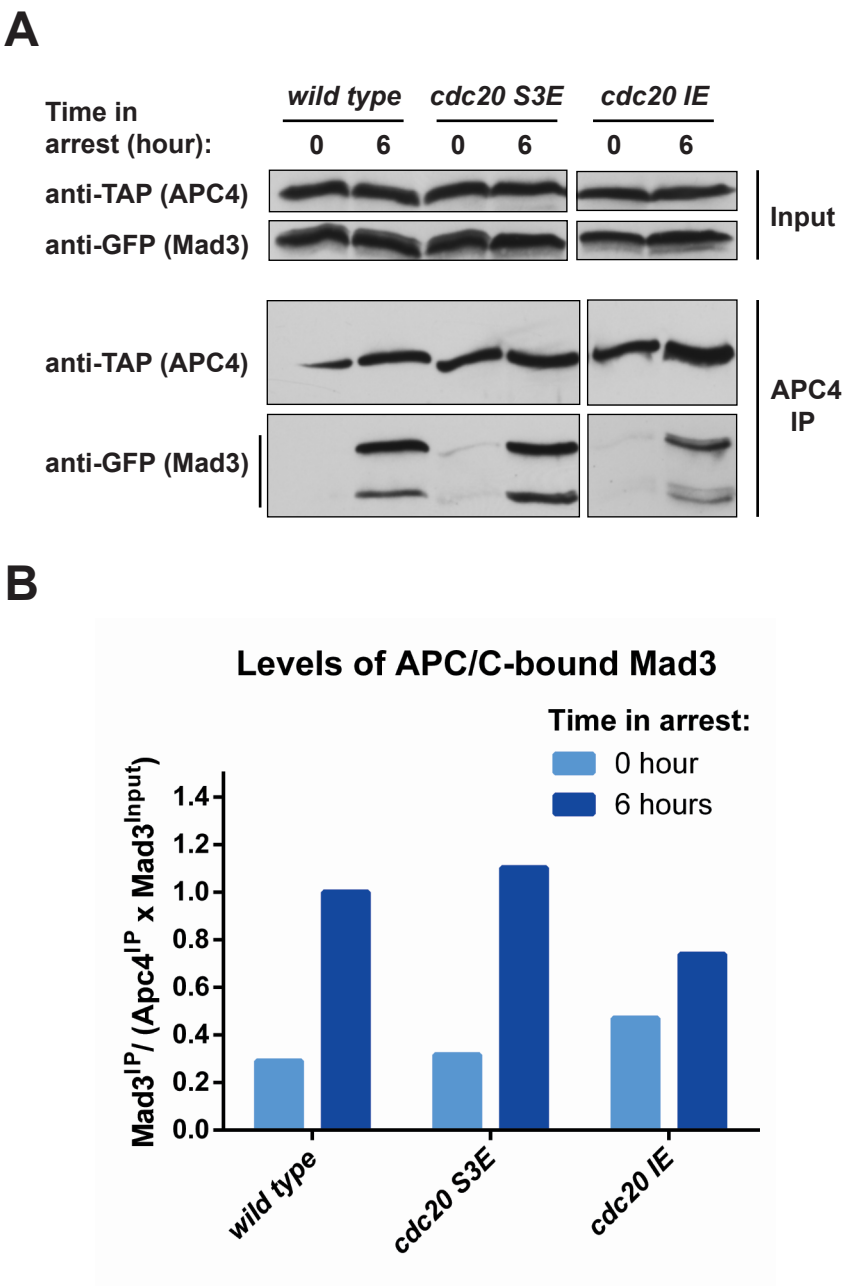

Figure 5.9 IR-motif of Cdc20 is required for an efficient Mad3-APC/C interaction

(A) Coimmunoprecipitation analysis of Mad3-APC/C interaction in cells arrested at metaphase for 6 hours through *nda3-KM311* allele. Mad3-APC/C interactions of wild type, *cdc20 S3E and cdc20 IE* cells were compared by immunoprecipitating Apc4 (TAP), immunoblotting against Mad3 (GFP). **(B)** Graph displaying the quantification of the results in A. APC/C-bound Mad3 intensities were measured by Image J and normalized to immunoprecipitated Apc4 levels and total Mad3 levels.

5.4.2 Recovery from *nda3-KM311*-mediated metaphase arrest

Having compared the Cdc20 C-terminal phosphorylation mutants and *bub1-kd* allele in terms of their abilities to arrest at metaphase in response to depolymerised microtubules, in this section we investigate how efficiently these mutants are able to extinguish the SAC-mediated 'wait anaphase' signal, and progress into anaphase upon re-polymerisation of microtubules. In order to examine this, we released the cells from the same experiment described in the previous section, from 6 hours of metaphase arrest at 18℃ by shifting them back to the permissive temperature (32℃) to allow re-polymerisation of microtubules. Then we collected cell samples at 10, 20 and 30 minutes after the release, and fixed them in methanol to process as described previously. Following the release from metaphase arrest we observed that cells exhibited characteristics of various cell cycle stages (Figure 5.10A). The first type is late G2 cells, which have uncondensed DNA and relatively weak Plo1-GFP signal gradually accumulating on their spindle poles. The second type is metaphase arrested cells exhibiting condensed DNA and strong Plo1-GFP signal on spindle poles. This category consists of two subtypes; (i) early metaphase cells displaying overlapped Plo1-GFP signals (appear as one spot) on two spindle poles that are very close to each other and (ii) late metaphase cells displaying separated Plo1-GFP signals (appear as two spots). The third category is anaphase cells, which have their sister chromatids symmetrically separated, and pulled to the opposite poles by anaphase spindles. The forth and the last category is 'cut' (**c**ell **u**ntimely **t**orn) cells, which form septa without symmetrical segregation of their sister chromatids, and become aneuploidy eventually (Yanagida, 1998).

On the basis of these criteria, (Figure 5.10 C) 10 minutes after the release 37% of "initially (at time zero) arrested wild type cells" exited mitosis by either progressing into normal anaphase (25%) or exhibiting cut phenotype (12%) (Figure 5.10 A and B). However, after 10 minutes 51% of "initially arrested *bub1-kd* cells" exited mitosis with the proportions of 30% normal anaphase and 21% cut phenotype.

30 minutes after the release (Figure 5.10C), 81% of initially arrested wild type cells exited mitosis, with 74% normal anaphase and 7% cut phenotype. However, after 30 minutes percentage of mitotic exit was as high as 93% for *bub1-kd* cells, exhibiting 68% normal anaphase and 25% cut phenotype.

Phospho – deficient *Cdc20 S3A* cells exhibited a fairly comparable SAC recovery pattern to wild type cells at the early stages after the release. Figure 5.10C plots that 10 minutes after the release, 31% of the initially arrested *Cdc20 S3A* cells exited mitosis, by either progressing into normal anaphase (25%) or cut phenotype (6%). After 30 minutes, 92% of initially arrested *Cdc20 S3A* cells exited mitosis, with 83% normal anaphase and 9% cut phenotype. Although, frequency of cut phenotype was comparable to that of wild type (7%), *Cdc20 S3A* cells progressed into anaphase faster than wild type (74%) at the later stages of the release from *nda3-KM311* block (Figure 5.10 B).

Phospho – mimetic *Cdc20 S3E* cells recovered from the SAC slightly slower than wild type cells did (Figure 5.10 B and C). 10 minutes after the release, 21% of initially arrested *Cdc20 S3E* cells exited mitosis (wild type 37%), almost of them progressing into normal anaphase (20%). After 30 minutes, mitotic exit index of initially arrested *Cdc20 S3E* cells was 77% which became similar to that of wild type (81%). Strikingly 20% of those cells exhibited cut phenotype (wild type 7%), which largely accounts for this increase in the mitotic exit, whereas the cells progressing into a normal anaphase were only 57% of it.

On the other hand, *Cdc20 IE* cells exhibited a rather different SAC rescue pattern. Figure 5.10B shows that, *Cdc20 IE* cells exhibited an arrest profile (63%) as high as *Cdc20 S3E* cells did (62%) immediately before the release. However, unlike *Cdc20 S3E* cells, a considerable portion of *Cdc20 IE* cells remained arrested at metaphase even at 10 (54%), 20 (45%) and 30 minutes (43%) after the release. Consistent with this, as low as 36% of initially arrested *Cdc20 IE* cells could exit mitosis at 30 minutes time point (Figure 5.10C), which is significantly lower than the SAC recovery rates of wild type (81%) and *Cdc20 S3E* (77%).

In order to compare the mitotic exit (SAC recovery) rates of these strains when spindle reformed, (other than *Cdc20 IE*, that was significantly slower than the others) we plotted trend lines out of '% of initially arrested cells which exited mitosis upon microtubule re-polymerisation' data (Figure 5.10 C). Linear regression analysis demonstrates that slopes and elevation (magnitude) values of the lines plotting mitotic exit rates of *wild type, bub1-kd* and *cdc20 S3A* cells are not significantly different from each other. In other words, the variance of mitotic exit rates among their own time points (0, 10, 20, 30 minutes) (represented by the slope of a line) and the levels of mitotic exit rates relative to each other (represented by the elevation of a line) were both statistically indistinguishable. On the other hand, the line plotting the mitotic exit rate of *Cdc20 S3E* cells has the same slope as the other three above, but with a lower elevation value. This suggests that *Cdc20 S3E* cells were able to maintain 'a constant rate of recovery from the SAC' (represented by the slope) as efficiently as *wild type, bub1-kd* and *cdc20 S3A* cells. However, that "constant rate" of SAC recovery was lower for *Cdc20 S3E* cells (represented by the elevation) than the other three.

Taken together, these data suggest that the SAC recovery rate does not appear to be significantly affected by either lack of C-terminal Cdc20 phosphorylation by presumably Bub1 kinase (as in the case of *cdc20 S3A*) or lack of the whole Bub1 kinase function (as in the case of *bub1-kd*), albeit it is faster than wild type in both cases. However, constitutive phosphorylation of Cdc20 C-terminus by Bub1 kinase (mimicked by *cdc20 S3E*) slightly slows down the SAC recovery rate, yet does not impair the activation of APC/C by Cdc20, which takes place when the spindle reforms. This result is in line with our previous findings that *cdc20 S3E* retains its Cdc20 function as an APC/C activator (It progresses through mitosis similar to wild type in an unperturbed mitosis (Figure 5.1) or when the SAC was shut down (*mad2* null) in the presence of CBZ (Figure 5.4)).

In contrast, mutation of the arginine residue of the Cdc20 IR motif to glutamate (as in the case of *cdc20 IE*) dramatically delays the SAC recovery. This result suggests that the *cdc20 IE* allele fails to fully perform the APC/C activator function of Cdc20, therefore is not able to trigger anaphase onset even after the re-polymerisation of microtubules.

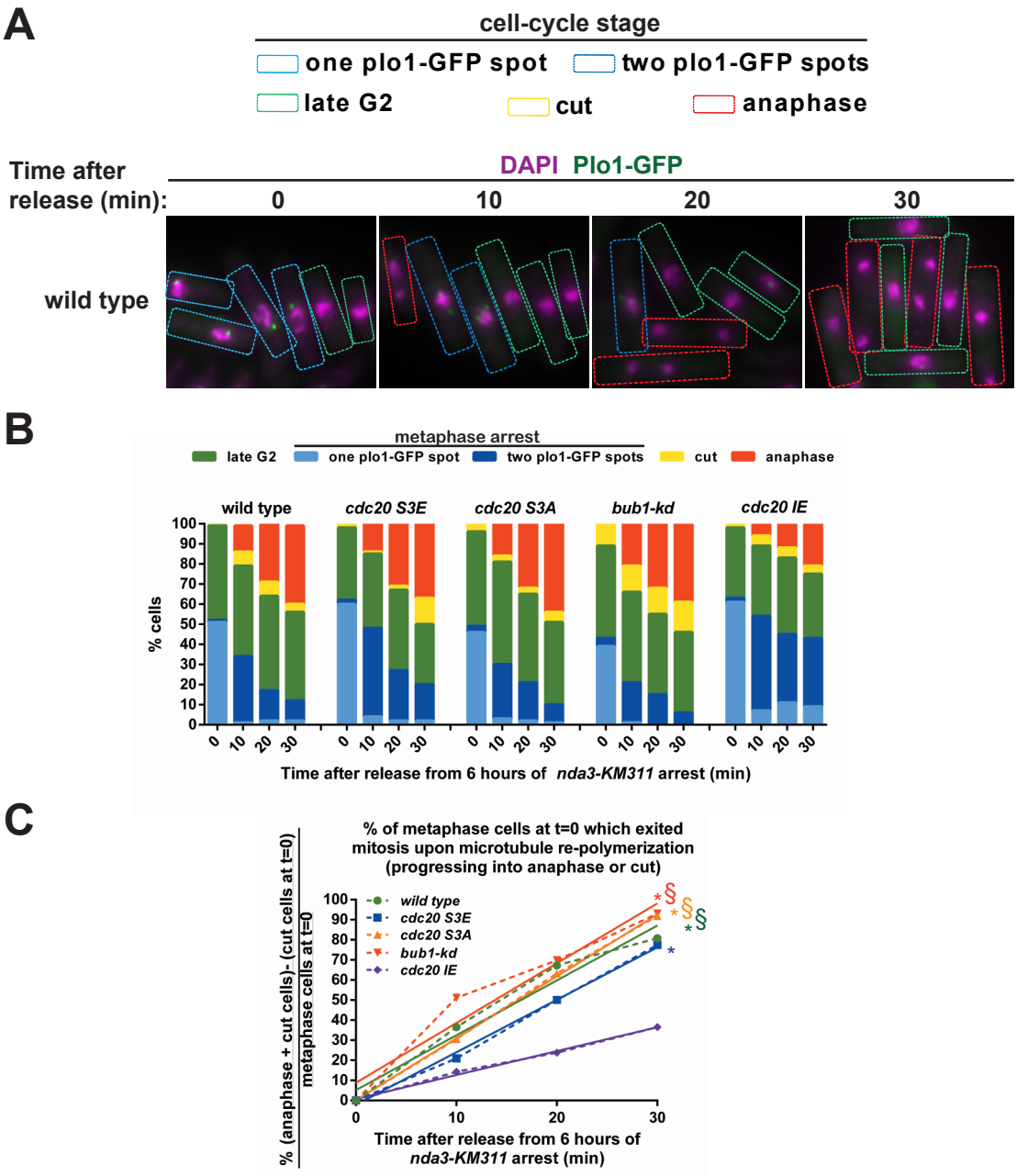

Figure 5.10 Constitutive phosphorylation of Cdc20 C-terminus does not impair Cdc20 function, yet slows down the SAC recovery

(A) Cells from the same experiment described in Figure 3.1 were blocked for 6 hours at 18°C with depolymerized microtubules through *nda3-KM311* tubuline mutation. Immidiately after taking the 0 minute samples, cells were shifted to the permissive temperature (32°C) to allow re-polymerization of microtubules, and subsequent recovery from the SAC. Cell samples were taken at each 10 minutes for 30 minutes after the release from *nda3-KM311* block, fixed in methanol, and stained with DAPI (purple) to visualize DNA, along with Plo1-GFP localisation at SPBs (green). Pictures demonstrate representative cell-cycle stages of the cells 0, 10, 20 and 30 minutes after the release. Observed mitotic stages are annotated with dashed rectangles as follows: cells at late G2 (green); metaphase cells with one (light blue) or two (dark blue) Plo1-GFP spots at SPBs; cut cells (yellow); and anaphase cells (red). Scale bar represents 5 microns. **(B)** Graph displaying the relative percentage of each cell-cycle stage for each strain throughout 30 minutes after the release (n=100 cells) **(C)** Graph (dashed lines) plotting the percentage of metaphase cells at time=0, progressed into anaphase or cut 0, 10, 20, 30 min after the release, using the following formula:

$$\% \ \frac{\text{(anaphase cells + cut cells at 0, 10, 20 or 30 min) - (cut cells at 0 min)}}{\text{metaphase cells at 0 min}}$$

Linear regression analysis of the trend lines (solid lines) was performed using GraphPad Prism software:

* indicates lines with *slopes* that are not significantly different from each other; § indicates lines with *elevations* that are not significantly different from each other.

5.4.3 Turnover rates of Cdc20 phospho – mutants during *nda3-KM311*-mediated metaphase arrest

Above we described how C-terminal phosphorylation of Cdc20 may affect activation of and recovery from the SAC arrest. Abilities of cells to arrest at metaphase, or recover from that were not affected much by the lack of this phosphorylation (*cdc20 S3A*). However, constitutive phosphorylation of Cdc20 C-terminus (*cdc20 S3E*) resulted in a more potent metaphase arrest and slower recovery from that. In order to address whether these C-terminal phosphorylation mutations affect levels of Cdc20 during a SAC mediated arrest, we analysed turnover rates of Cdc20 during the *nda3-KM311* block.

First, we analysed the phospho – deficient *cdc20 S1A* cells. Following 6 hours of *nda3-KM311* arrest as described before, we treated wild type and *cdc20 S1A* cells either with cycloheximide (CHX) or DMSO. Cycloheximide was used to inhibit synthesis of new proteins, and thereby to monitor the degradation rate of Cdc20. We collected cell samples immediately before and 15, 30, 45, 60 minutes after the treatment. Then the samples were lysed, processed for SDS-PAGE/western blotting, in which they were probed for Cdc20 and Bip1 (loading control).

As demonstrated in Figure 5.11A, Cdc20 levels decreased only in the cycloheximide treated samples, which indicates that the decrease in the protein levels was due to the inhibition of protein synthesis and continued protein turnover. Quantification of the turnover rates shows that (Figure 5.11B) the degradation rates of wild type Cdc20 and *cdc20 S1A* proteins were almost identical when synthesis of new Cdc20 proteins was inhibited by cycloheximide. However, turnover dynamics of *cdc20 S3E* were rather different than that of *cdc20 S1A*. Figure 5.12 displays that the cycloheximide treatment affected levels of only wild type Cdc20, whereas *Cdc20 S3E* levels remained stable, which is similar to the DMSO treatment group.

Taken together, these results suggest that during an *nda3-KM311* arrest, lack of C-terminal phosphorylation of Cdc20 does not significantly affect its turnover dynamics. On the other hand, constitutive phosphorylation of Cdc20 C-terminus stabilizes its turnover rate during the SAC arrest mediated by *nda3-KM311*.

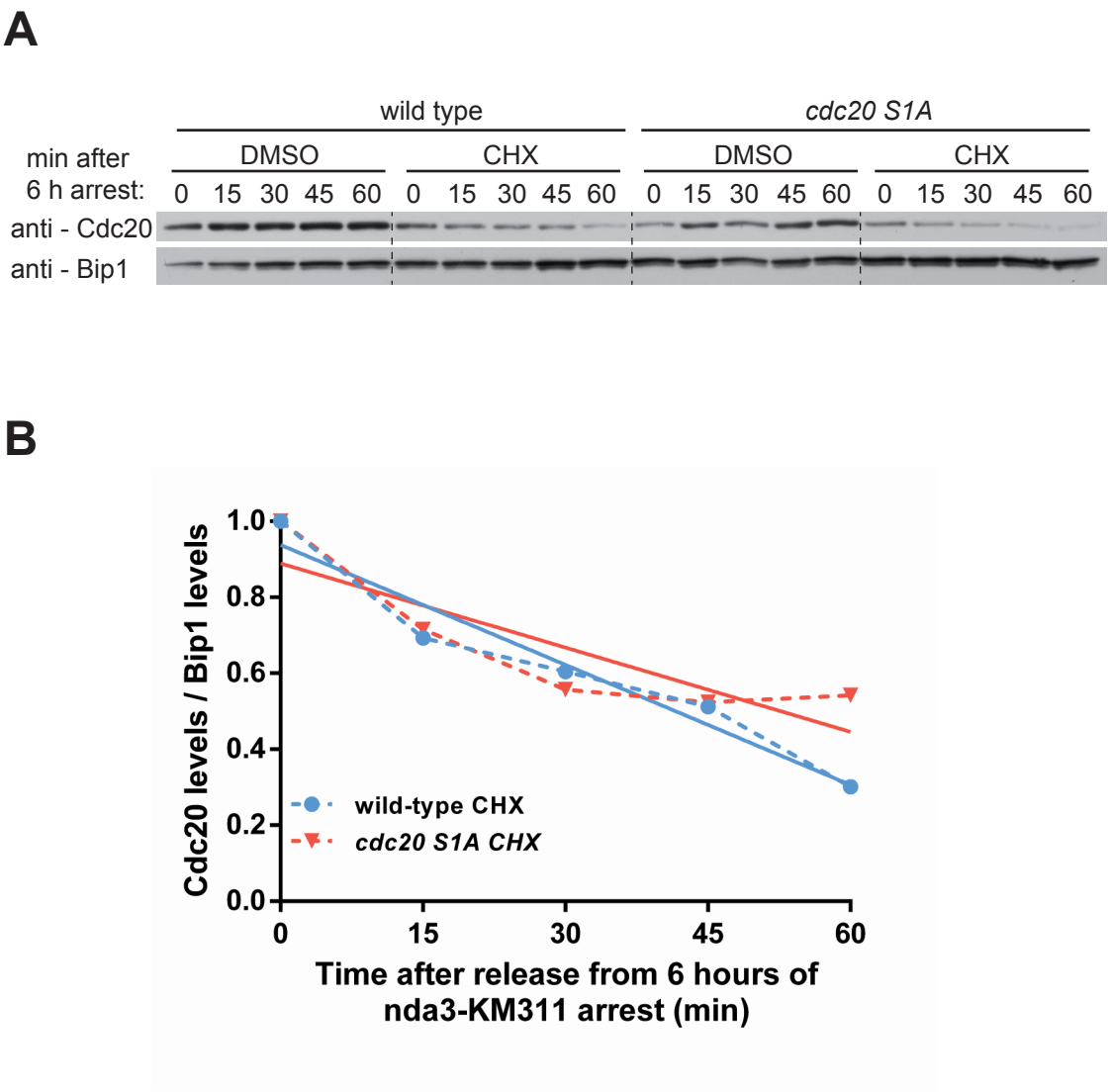

Figure 5.11 Lack of Cdc20 C-terminus phoshorylation does not affect Cdc20 turnover rate during metaphase arrest

(A) Wild type and *cdc20 S1A* cells were shifted to the restrictive temperature to arrest them for 6 hours in metaphase through *nda3-KM311* allele. After 6 hours cell samples were taken (0 minute), and immediately after the cells were treated with cycloheximide (CHX) to inhibit protein synthesis, or with DMSO (negative control). Samples were taken at each 15 minutes for one hour. Extracts from the lysed cells were immunoblotted with Cdc20 and Bip1 antibodies (loading control) to analyse Cdc20 turnover rates. **(B)** Graph demonstrating Cdc20 turnover rates quantified using ImajeJ software and normalized to Bip1 levels. All values were normalized to the '0 minute' value of their CHX treatment group. Trendlines were plotted to demonstrate corresponding turnover rates represented by the slope of each line.

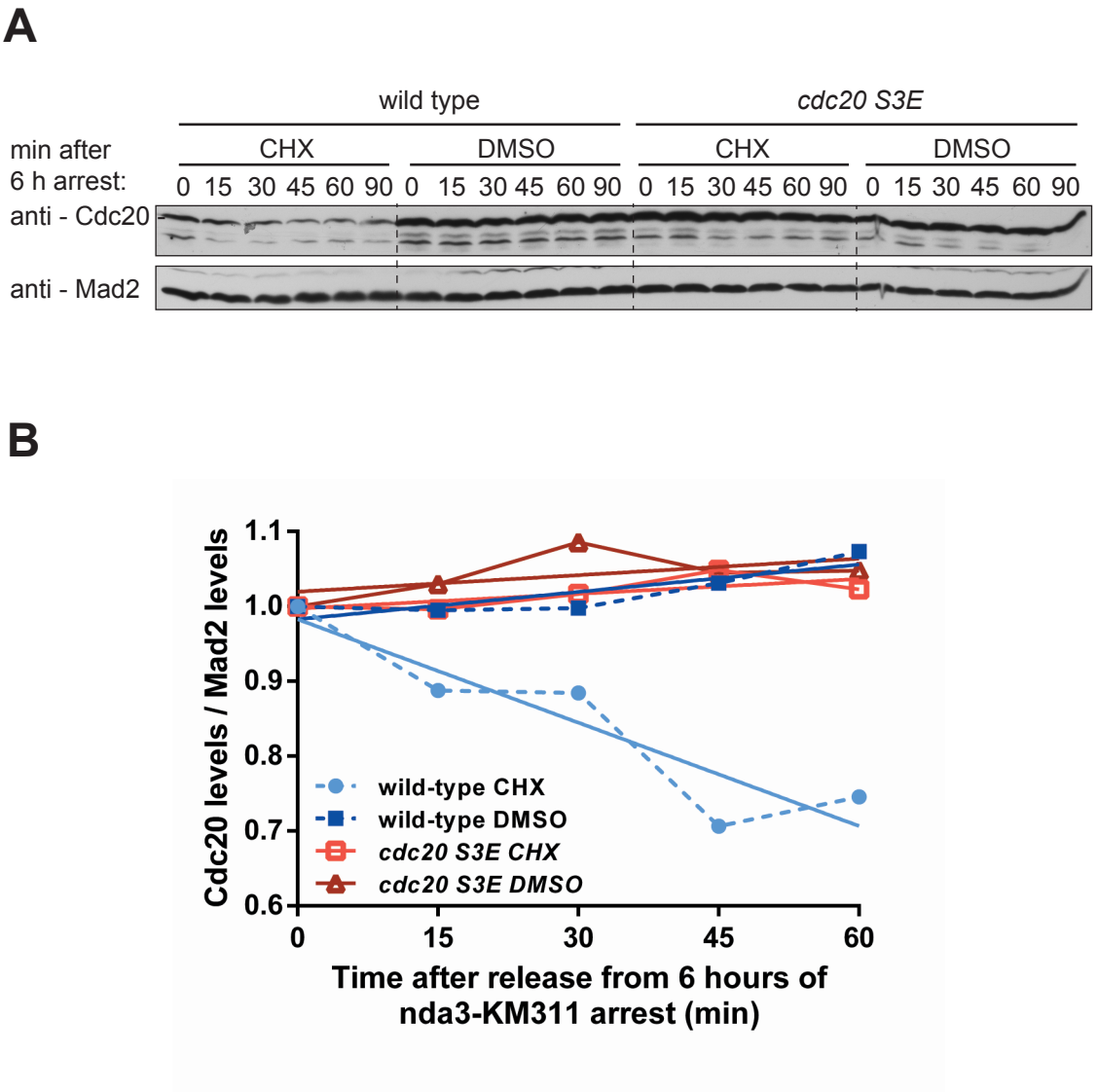

Figure 5.12 Constitutive phoshorylation of Cdc20 C-terminus decreases Cdc20 turnover rate during metaphase arrest

(A) Wild type and *cdc20 S3E* cells were shifted to the restrictive temperature to arrest them for 6 hours in metaphase through *nda3-KM311* allele. After 6 hours cell samples were taken (0 minute), and immediately after the cells were treated with cycloheximide (CHX) to inhibit protein synthesis, or with DMSO (negative control). Samples were taken at each 15 minutes for 90 minutes. Extracts from the lysed cells were immunoblotted with Cdc20 and Mad2 antibodies (loading control) to analyse Cdc20 turnover rates. **(B)** Graph demonstrating Cdc20 turnover rates quantified using ImajeJ software and normalized to Mad2 levels. All values were normalized to the '0 minute' value of their treatment group (CHX or DMSO). Trendlines were plotted to demonstrate corresponding turnover rates represented by the slope of each line.

5.5 Can the Cdc20 C-terminal phospho-mimicking mutation rescue the SAC defects of *bub1-kd* allele?

In the third chapter, we reported that cells expressing the kinase-dead mutant of Bub1 (*bub1-kd*) are partially defective in arresting at metaphase and thereby delaying anaphase onset upon depolymerisation of their microtubules by either a microtubule poison (CBZ) or *nda3-KM311* cold sensitive mutant. Furthermore, this SAC defect of *bub1-kd* cells is accompanied by significantly decreased kinetochore localisation of MCC components and defective MCC-APC/C interaction when their spindle is perturbed by CBZ.

In the fourth chapter, we showed by *in vitro* kinase assays that the two point mutations in the *bub1-kd* allele completely abolish its kinase function, which accounts for the *in vivo* SAC defects of *bub1-kd* described above. Moreover, we demonstrated that Cdc20 is a substrate of Bub1 kinase *in vitro.* Identification of *in vitro* phosphorylated sites of Cdc20 revealed that some of those sites overlap with the sites phosphorylated *in vivo* in mitotically arrested cells. Among those overlapping sites, particularly C-terminal serine 482 is well-conserved among fission yeast, budding yeast, *X. laevis* and *H.sapiens*. Moreover, cross-linking mass spectrometry results we described in the fourth chapter indicated that Mad2 and Mad3 proteins interact with C-terminus of Cdc20, which is in close proximity to Serine 482. Therefore, we mutated this putative Bub1 site, (or adjacent two serine residues as well; serine 482, serine 483 and serine 484) to generate phospho – deficient (*cdc20 S1A* and *cdc20 S3A*) and phospho – mimicking (*cdc20 S3E*) mutants of Cdc20. In the previous sections of this chapter, we showed that the phospho – deficient mutants of Cdc20 (*cdc20 S1A* and *cdc20 S3A*) behave similarly to wild type in terms of their mitotic progression, MCC formation, MCC-APC/C interaction, Cdc20 turnover rate and kinetochore localisation of the MCC components during unperturbed and perturbed (through CBZ or *nda3-KM311*) mitoses. On the other hand, the phospho – mimicking mutant (*cdc20 S3E)* behaves rather differently under the conditions activating the SAC, although it is similar to wild type during unperturbed mitosis. Upon depolymerisation of microtubules by CBZ, cells expressing *cdc20 S3E* arrest at metaphase for much longer, which is accompanied by more abundant and prolonged kinetochore localisation of the MCC components.

Moreover, this acquired SAC potency of *cdc20 S3E* correlates with a stronger and longer MCC-APC/C interaction in mitosis.

On the basis of these findings, we hypothesize that *cdc20 S3E*, which mimics C-terminal phosphorylation of Cdc20, may rescue the SAC defects of *bub1-kd,* if this site of Cdc20 is modified by Bub1 kinase *in vivo*.

First, in order to address this possibility more accurately, we generated another phospho – mimicking mutant of Cdc20 (*cdc20 S1D*) by mutating serine 482 to aspartate. Subsequently, we crossed the phospho – mimicking mutants (*cdc20 S3E* or *cdc20 S1D*) with *bub1-kd,* and analysed these double-mutants in a synchronous mitosis using *cdc25-22* allele, in which microtubules were depolymerised by CBZ. Cell samples were collected at 30 minute time points for 150 minutes, and fixed in methanol. In order to determine their mitotic progression rate, fixed cells were stained with calcofluor to detect septa, or DAPI to detect DNA. Kinetochore localization of the MCC components was analysed visualising Mad3-GFP localisation at unattached kinetochores. As described in Chapter 3.3.1 (Figure 3.4B), to be able to evaluate the anaphase delay mechanisms, which may be independent of the kinetochore recruitment of MCC components, we scored kinetochore localisation of Mad3 only in the population of cells that arrested at metaphase exhibiting condensed DNA (similar to the non-septating cells we considered previously in Figure 3.4B).

The strains used in this experiment are: wild type, *cdc20 S1D, cdc20 S1D bub1-kd, cdc20 S3E, cdc20 S3E bub1-kd*, *bub1-kd** and wild type*. It should be noted that all the strains express Mad3-GFP; in addition *bub1-kd** and wild type* strains express Mad2-GFP as well (annotated throughout the text with an asterisk). Moreover, *mps1-kd* results from an independent experiment under identical conditions were used as a negative control, as *mps1-kd* is known to be defective in the SAC (Shepperd et al., 2012b; Yamagishi et al., 2012; Zich et al., 2012)).

30 minutes after the release into mitosis (10 minutes after the CBZ treatment) only a small portion of the strains progressed into anaphase, that is indicated by a low septation index (%5-10) (Figure 5.13 A). Consistent with this, all the strains had a high percentage (83-92%) of metaphase arrested cells displaying condensed DNA (Figure 5.14 A and C).

In order to analyse the abilities of the strains to recruit the MCC components to unattached kinetochores, regardless of their abilities to delay anaphase, we scored the percentage of metaphase arrested cells, which also exhibit kinetochore foci of MCC components (Figure 5.14 A and D). Within the population of metaphase arrested ones, 60-66% of wild type, *bub1-kd** and wild type* cells recruited Mad3-GFP to kinetochores (*bub1-kd** and wild type* cells recruited Mad2-GFP as well). Hereafter Mad3 and/or Mad2 localization will be referred to interchangeably as 'kinetochore localization of the MCC components' as their localization dependencies are very similar (S. Heinrich et al., 2012)). As expected, none of the *mps1-kd* cells could recruit the MCC components, although they were at metaphase like the other strains at this time point. On the other hand, both phospho – mimicking mutants (*cdc20 S1D, cdc20 S3E)* and their double mutant alleles, which also bear *bub1-kd* mutation, (*cdc20 S1D bub1-kd, cdc20 S3E bub1-kd*) exhibited kinetochore foci of the MCC components more frequently (80-95%) than wild type and *bub1-kd* cells did (60%) (Throughout this experiment, *cdc20 S1D* phenocopied *cdc20 S3E;* and *cdc20 S1D bub1-kd* phenocopied *cdc20 S3E bub1-kd.* Therefore hereafter, the functional consequences of phospho – mimicking mutations will be described by referring to *cdc20 S1D* and *cdc20 S1D bub1-kd* alleles).

60 minutes after the release into mitosis, the septation indexes of the strains deviated from each other depending on their abilities to maintain the SAC response. Wild type strains (wild type and wild type*) maintained a robust SAC response indicated by 44% of septation (Figure 5.13 A and B). However, *bub1-kd** cells could not delay anaphase onset, as 71% of them septated. The inability of *bub1-kd* cells to hold a robust arrest was similar to that of *mps1-kd* (87% septation). On the other hand, *cdc20 S1D* cells maintained a very strong SAC response, and only 10% of them septated. Strikingly, although *cdc20 S1D bub1-kd* cells lacked Bub1 kinase activity, they maintained a robust SAC response (only 25% septation) that was significantly stronger than that of *bub1-kd** (71%) and wild type (44%) cells (Figure 5.13 A and B).

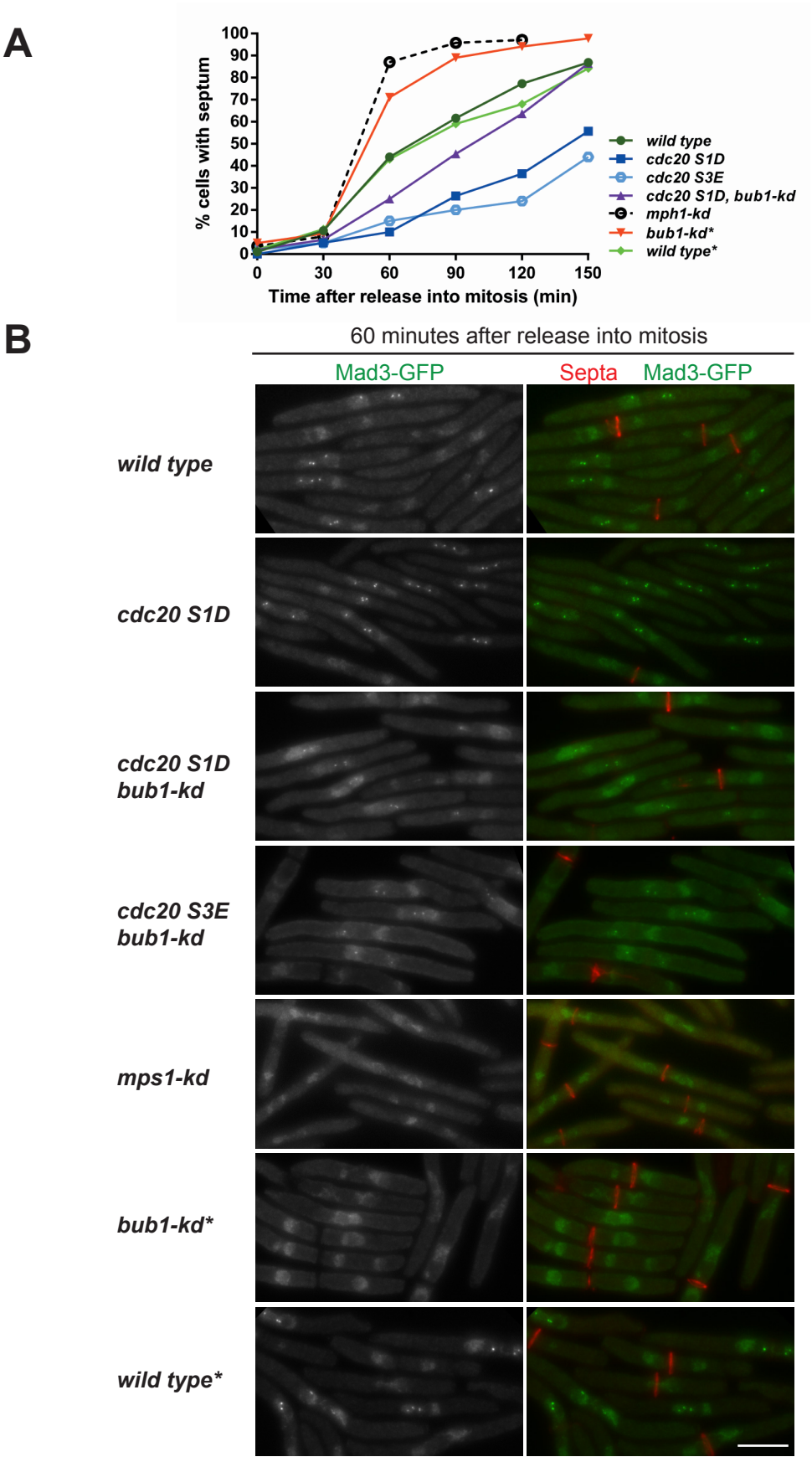

Figure 5.13 Mimicking the phosphorylation of a putative Bub1 site in Cdc20 C-terminus rescues the anaphase delay defect of *bub1-kinase dead*

(A) Cells were blocked in G2-phase for 4 hours through *cdc25-22* temperature sensitivity, and then released into mitosis at 0 minute. At 20 minutes, cells were treated with the microtubule depolymerising drug CBZ to activate SAC response. Samples were collected at each 30 minutes time point. Graph plotting percentage of cells that formed septum (exited mitosis) throughout 150 minutes. Mph1-kd result was taken (dashed black line) from another experiment with the identical conditions. **(B)** Representative images from 60 minutes, displaying septation (in red) by calcofluor staining and Mad3-GFP localisation (in green). Scale-bar represents 5 microns. All of the seven strains express Mad3-GFP. The two strains (annotated with an asterisk), bub1-kd* and wild type* express Mad2-GFP as well as Mad3-GFP.

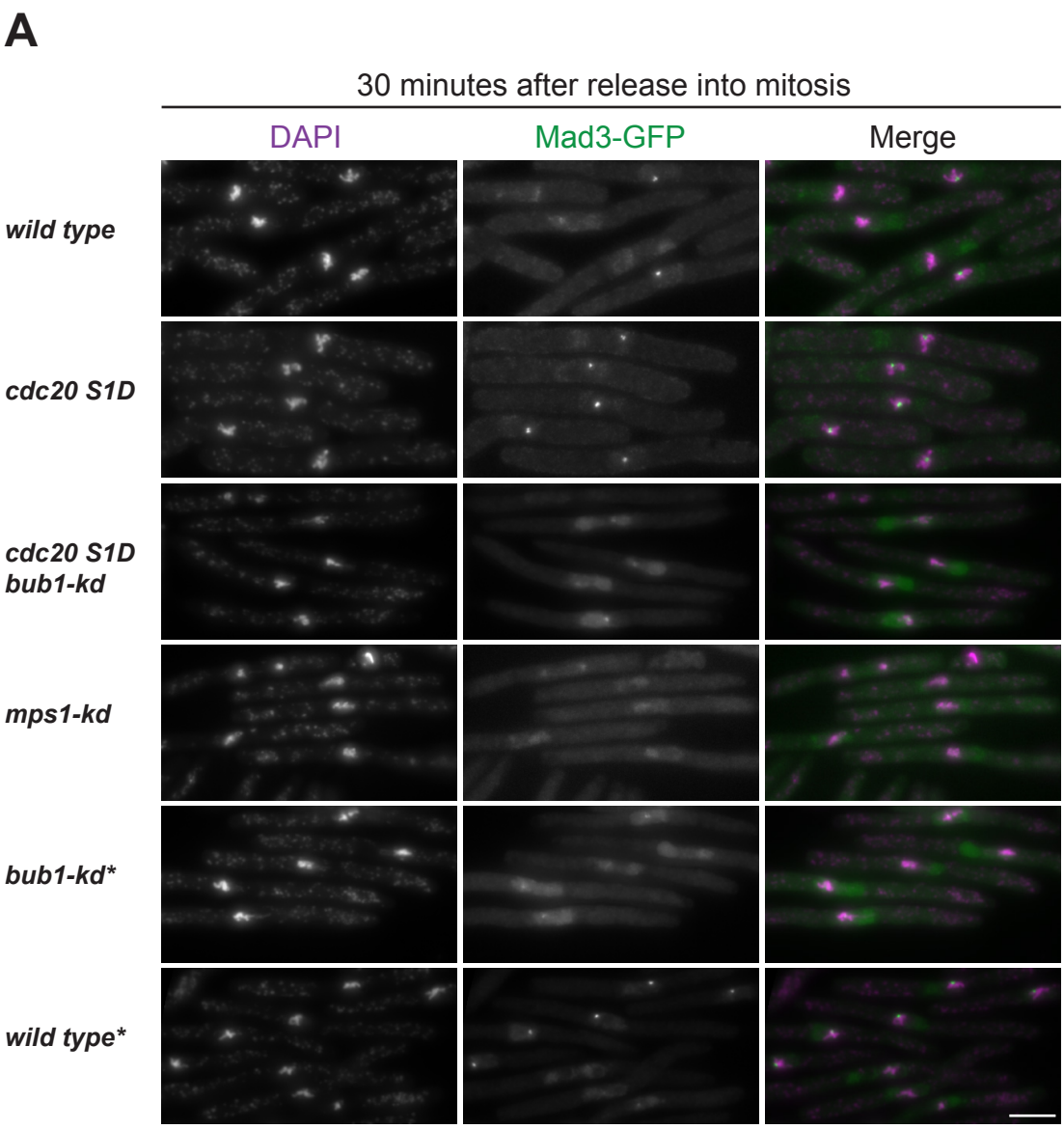

Figure 5.14 Mimicking the phosphorylation of a putative Bub1 site in Cdc20 C-terminus rescues the Mad3 kinetochore localization defect of *bub1-kinase dead*

The strains are from the same experiment described in Figure 5.15. All of the seven strains express Mad3-GFP. The two strains (annotated with an asterisk), bub1-kd* and wild type*, express Mad2-GFP as well as Mad3-GFP.
(A) Representative images from 30 minutes, displaying DNA (in purple) by DAPI staining and Mad3-GFP (Mad3-GFP and Mad2-GFP in the cells annotated with *) localisation at kinetochores (in green). Scale-bar represents 5 microns.
(B) Representative images from 60 minutes, displaying DNA (in purple) by DAPI staining and Mad3-GFP (Mad3-GFP and Mad2-GFP in the cells annotated with *) localisation at kinetochores (in green). Scale-bar represents 5 microns.
(C) Graph plotting 'percentage of metaphase cells' (indicated by scoring condensed DNA) at 30 and 60 minutes after release into mitosis.
(D) Graph plotting 'percentage of metaphase cells exhibiting Mad3-GFP kinetochore foci at 30 and 60 minutes after release into mitosis.

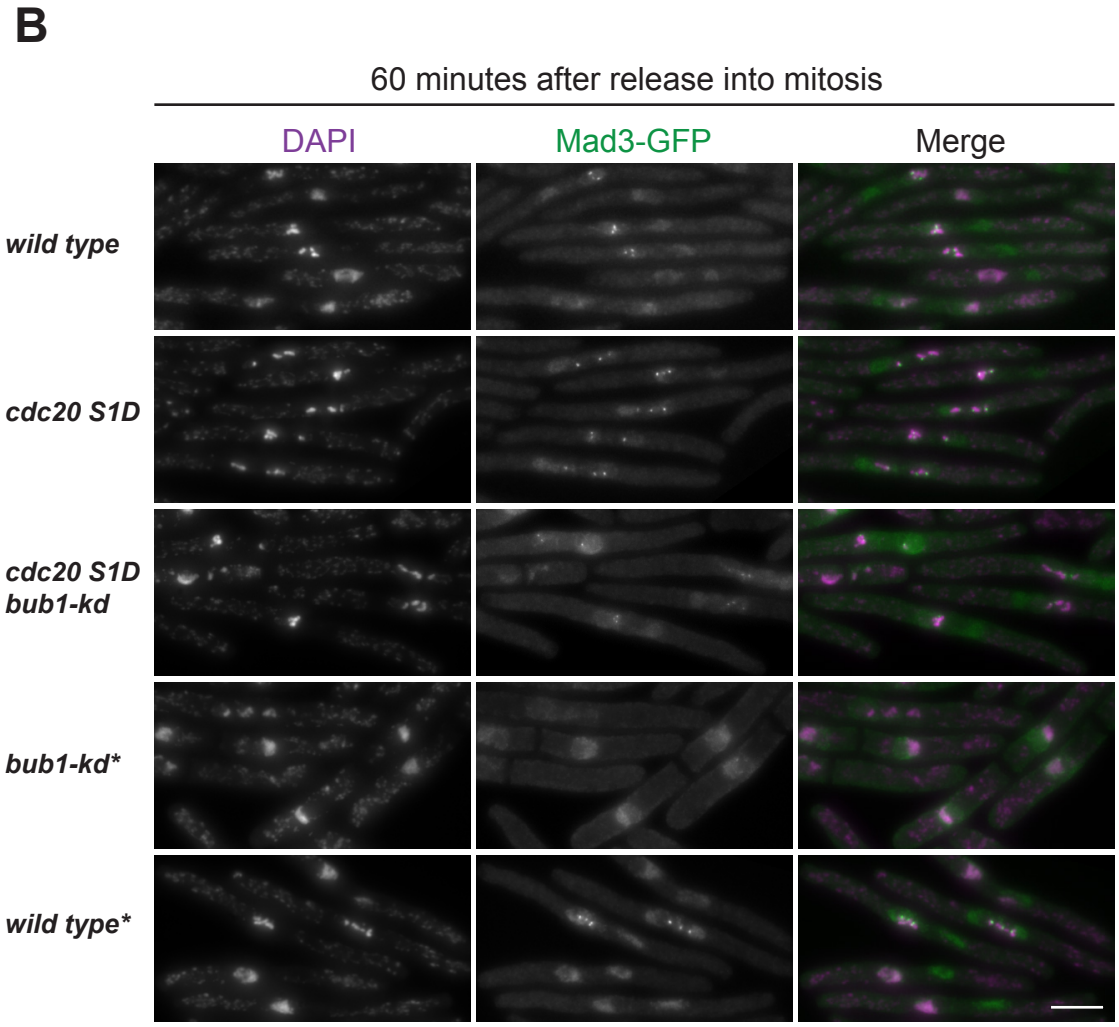
B
60 minutes after release into mitosis
DAPI
Mad3-GFP
Merge
wild type
cdc20 S1D
cdc20 S1D bub1-kd
bub1-kd*
wild type*

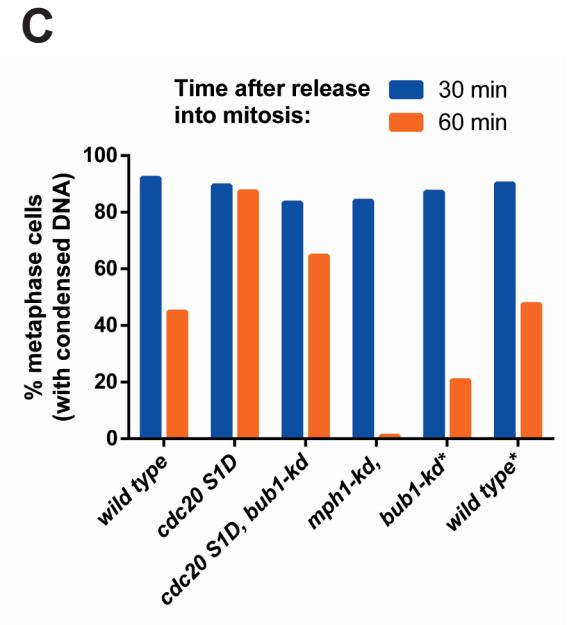
C
Time after release into mitosis:
30 min
60 min
% metaphase cells (with condensed DNA)
100
80
60
40
20
0
wild type
cdc20 S1D
cdc20 S1D, bub1-kd
mph1-kd,
bub1-kd*
wild type*

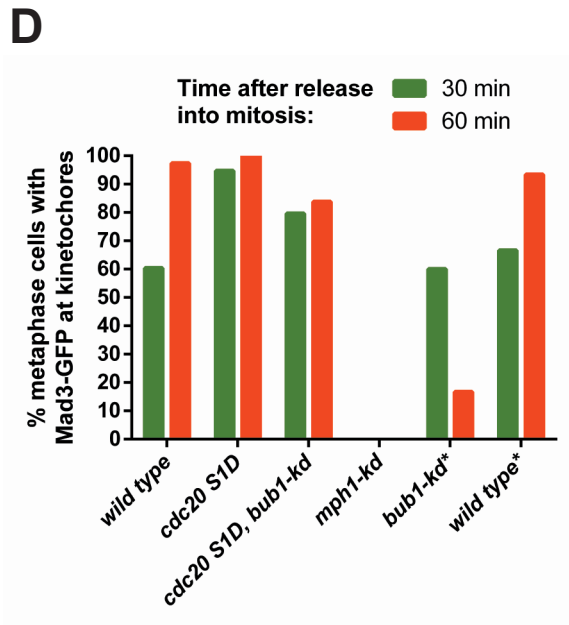
D
Time after release into mitosis:
30 min
60 min
% metaphase cells with Mad3-GFP at kinetochores
100
90
80
70
60
50
40
30
20
10
0
wild type
cdc20 S1D
cdc20 S1D, bub1-kd
mph1-kd
bub1-kd*
wild type*

As for the proportions of the cells arresting at metaphase with condensed DNA 60 minutes after the release into mitosis, 45-47% of the wild type strains were observed to have condensed DNA (Figure 5.14 B and C). It should be noted that at 60 minutes the wild type strains had 56% non-septating cells (44% septation), which are expected to arrest at metaphase. This slight discrepancy suggests that there were cells, which de-condensed their DNA, but have not fully septated yet.

Consistent with its inability to delay anaphase onset, only 21% of *bub1-kd** cells had condensed DNA, which was closer to that of the SAC deficient *mps1-kd* (1%). In contrast, phospho – mimicking *cdc20 S1D* (87%) and double mutant *cdc20 S1D bub1-kd* (65%) strains had more cells with condensed DNA, which is in line with their lower septation indexes (Figure 5.14 B and C).

As for the proportions of metaphase arrested cells displaying kinetochore foci of the MCC components at 60 minutes, Figure 5.14 B and D demonstrate that the Mad3 localization increased in wild type strains (93-97%) to the levels of the phospho – mimicking mutant *cdc20 S1D* (100%). However, the double mutant *cdc20 S1D bub1-kd* (84%) was not able to recruit Mad3 as efficiently as wild type, although it had more metaphase arrested cells with condensed DNA. On the other hand, even though *bub1-kd* recruited the MCC components to kinetochores at wild type levels at 30 minutes, at 60 minutes the proportion of (metaphase arrested) *bub1-kd* cells exhibiting kinetochore foci dropped to as low as 17%. This defect of *bub1-kd* appears to be close to that of the SAC deficient *mps1-kd*, in which no kinetochore localization of the MCC components was observed.

At the later stages of mitosis, differences between septation indexes of the strains largely followed the proportions observed at 60 minutes (Figure 5.13 A): wild type strains (with or without Mad2-GFP expression) were similar, and ~85% of them septated at 150 minutes. *Bub1-kd* remained as the highest septating strain throughout the time course, and exhibited a very high septation index (95-98%) 120 minutes onward, which was identical to that of the SAC deficient *mps1-kd* (97% at 120 minutes). On the other hand, phospho – mimicking *cdc20 S1D* cells maintained their strong metaphase arrest throughout mitosis, and only 56% of them septated at 150 minutes. Interestingly, although double mutant *cdc20 S1D bub1-kd* had a lower

septation index than wild type throughout the mitosis, it septated (86%) at wild type levels at 150 minutes.

These data suggest that at the early stages (30 minute) of a mitosis challenged with CBZ, Bub1 kinase function is not essential for (initial activation of the SAC) either delaying anaphase onset or kinetochore recruitment of MCC components. However, at the later stages (60 minutes onward) Bub1 activity is required to maintain a robust SAC response, to be able to delay premature anaphase and sustain localization of the MCC components at unattached kinetochores of metaphase arrested cells.

In chapter three we proposed that the role of Bub1 kinase activity to delay premature anaphase appeared to be only partially mediated through the Bub1-H2A-Sgo2-Aurora B pathway, as the *sgo2* null cells exhibited a similar septation index to wild type when microtubules were depolymerized. We hypothesized that this role of Bub1 kinase activity may be mediated through phosphorylating Cdc20, and thereby inhibiting the APC/C. Indeed, here we demonstrate that mimicking the constitutive phosphorylation of Cdc20 C-terminus (which was phosphorylated *in vitro* by Bub1) rescued the anaphase delay defect observed in the absence of Bub1 kinase activity and brought it at least to the wild type levels (as in the case of the double mutant *cdc20 S1D bub1-kd*). According to these findings we conclude that the anaphase delaying role of Bub1 kinase activity may be largely mediated through the phosphorylation of Cdc20 C-terminus (serine 482).

In addition, we also suggested in Chapter three that the role of Bub1 kinase activity to recruit Mad2, Mad3 (maybe even Cdc20) to unattached kinetochores appears to be partly mediated through the Bub1-H2A-Sgo2-Aurora B pathway, since it was partially compromised in *sgo2* null cells (27% less compared to wild type, see Figure 3.4) 60 minutes after the release into the mitosis challenged with carbendazim. This implies that there may be another pathway(s) working in parallel with the Bub1-H2A-Sgo2-Aurora B pathway in mediating the kinase activity of Bub1 towards kinetochore recruitment of the MCC components.

Consistent with this possibility, mimicking Bub1 kinase activity on Cdc20 C-terminus was able to significantly rescue the Mad3 kinetochore localization defect in the absence of Bub1 kinase function (*cdc20 S1D bub1-kd*) to a level slightly below (13% less than wild type) that of wild type at the same time point (60 minutes). Note that the double mutant could not rescue the kinetochore recruitment of Mad3 at exact wild type levels probably because in *cdc20 S1D bub1-kd* cells both H2A-S121 (Bub1-H2A-Sgo2-Aurora B pathway) and other putative phosphorylation sites of Cdc20 failed to be phosphorylated, which may further contribute to the kinetochore localisation of Mad3. On the basis of these findings we conclude that Cdc20 C-terminus (serine 482) and H2A C-terminus (serine 121) may be the two main mediators of Bub1 kinase activity for promoting the kinetochore recruitment of MCC components when the spindle formation is perturbed.

Chapter 6: Final discussion

In chapter three, we investigated the roles of Bub1 kinase activity in maintaining the SAC response. In chapter four, we demonstrated that fission yeast $Cdc20^{Slp1}$ is an *in vitro* substrate of Bub1, and identified its phosphorylated sites. In addition, we revealed novel interactions between the MCC components that may be relevant to the regulation of the SAC through Cdc20 phosphorylation. In chapter five we investigated possible roles of fission yeast $Cdc20^{Slp1}$ C-terminal phosphorylation (that we identified in the chapter four) in mitosis. For this purpose, we analysed the phosphorylation mutants of Cdc20, either refractory to C-terminal phosphorylation (phospho-deficient) or mimicking constitutive phosphorylation of this site (phospho-mimicking) under various mitotic conditions given below:

1. In an unperturbed mitosis, to determine whether the phosphorylation mutants of Cdc20 retain their mitotic functions in the absence of spindle damage:
    - APC/C activation and subsequent anaphase onset
    - MCC assembly
    - MCC-APC/C interaction

2. In the presence of prolonged spindle damage mediated by the cold sensitive tubulin mutant *nda3-KM311*, to examine whether the phosphorylation mutants of Cdc20 are capable of:
    - Maintaining a robust metaphase arrest mediated by the SAC
    - Recovering from the SAC arrest upon reformation of the spindle, and segregating their chromosomes equally

3. In the presence of spindle damage caused by the microtubule depolymerising drug carbendazim (CBZ), to examine whether the phosphorylation mutants of Cdc20 are capable of:
    - Recruiting the MCC components (Mad2 and Mad3) to kinetochores
    - Maintain MCC-APC/C interaction
    - Delay premature anaphase onset

4. In the absence of Bub1 kinase activity, to determine whether the phospho-mimicking Cdc20 mutant can rescue the SAC defects observed in the absence of Bub1 kinase activity (which would provide *in vivo* evidence for a potential Bub1- Cdc20 pathway, in addition to the existing Bub1-H2A-Sgo2-Aurora B pathway)

6.1 Cdc20 C-terminal phosphorylation mutants retain their mitotic functions in an unperturbed mitosis

Phosphorylation of Cdc20 has been implicated to affect its mitotic functions, independent of the SAC. In *Xenopus* egg extracts, Cdk1 mediated phosphorylation of Cdc20 N-terminus blocks its binding to and activation of the APC/C, by inhibiting the interaction of Cdc20 C-box (N-terminal APC/C interaction domain) with Apc8. This phosphorylation needs to be reversed by PP2A for anaphase onset (Labit et al., 2012).

APC/C activation and anaphase onset

Another conserved APC/C interaction domain of Cdc20 is the C-terminal IR-motif, whose mutation compromises the Cdc20- APC/C interaction (Izawa & Pines, 2012). Our mutated sites are in close proximity to the IR-motif (4 amino acids upstream of the IR). This raises the possibility that our C-terminal phosphorylation mutations might affect the Cdc20 function mediated by the IR-motif.

In order to determine whether the C-terminal phosphorylation mutations on Cdc20 affect its APC/C activating function, we analysed abilities of the mutants in progressing into anaphase, assembling the MCC and maintaining MCC-APC/C interaction in an unperturbed mitosis. We demonstrated that the cells expressing phospho-deficient (*cdc20 S1A* and *cdc20 S3A*) or phospho-mimicking (*cdc20 S3E*) Cdc20 mutants are capable of activating APC/C, and promote anaphase onset as efficiently as wild type cells do. Thus we suggest that the APC/C activator functions of the Cdc20 C-terminal phosphorylation mutants are not affected by the mutations, despite their proximity to the regulatory IR-motif. To further conform this, we intend to express the Cdc20 mutants *in vitro*, and test them in *in vitro* APC/C assays to determine whether they can activate the APC/C efficient.

MCC formation and MCC-APC/C interaction

In addition, we showed that the lack of Cdc20 C-terminus phosphorylation (as in the case of *cdc20 S3A*) does not significantly affect the MCC formation or the MCC-APC/C interaction during an unperturbed mitosis. At the time we carried out these two assays, anti-Cdc20 antibody was not available. Therefore we used the internally FLAG-tagged *cdc20 S3A* strain to perform Cdc20-FLAG immunoprecipitations (to analyse MCC formation) or Cdc20-FLAG immunoblotting following Apc4 immunoprecipitations (to analyse MCC-APC/C interaction).

However, the internally FLAG-tagged *cdc20 S3E* strain has become available only recently. Though considering its comparable mitotic progression rate to that of wild type and phospho-deficient mutants, we expect the phospho-mimicking *cdc20 S3E* to exhibit similar MCC formation and MCC-APC/C interaction. Nevertheless, we will need to carry out these experiments using *cdc20 S3E* to be able to fully confirm that all of its mitotic functions are as intact as those of wild type and *cdc20 S3A.*

6.2 Constitutive phosphorylation of Cdc20 C-terminus slightly enhances the SAC arrest in response to penetrant spindle damage (*nda3-KM311*)

In chapter five, we confirmed that the non-kinase region of Bub1 (N-terminal and the middle region) is essential for the SAC response to severe spindle damage (*bub1* null is SAC deficient) (Kadura, He, Vanoosthuyse, Hardwick, & Sazer, 2005; Kiyomitsu et al., 2007), and although not essential, its C-terminal kinase activity is required for maintaining a robust SAC (*bub1-kd* is compromised in the SAC) (Figure 5.8) (Fernius & Hardwick, 2007; Kawashima et al., 2010; Yamaguchi et al., 2003).

In addition, we demonstrated that constitutive phosphorylation of Cdc20 C-terminus (*cdc20 S3E*) leads to a slightly enhanced SAC arrest, whereas lack of this phosphorylation (*cdc20 S3A*) results in a slightly weaker SAC response than wild type cells (Figure 5.8, especially after 6 hours of *nda3-KM311* block). These results are consistent with our hypothesis that Bub1 may be at least one of the kinases phosphorylating serine 482 (*in vivo*) in mitotically arrested cells (Figure 4.4), as well as in our *in vitro* kinase assay (Figure 4.3). We believe that lack of S482

phosphorylation should phenocopy the lack of Bub1 kinase activity (toward serine 482) to an extent, indicated by the slight SAC deficiency of *cdc20 S3A*. Moreover, constitutive phosphorylation of serine 482 indeed improved the SAC response, which strengthens the possibility that Bub1 may phosphorylate serine 482 to promote the SAC.

On the other hand, introducing a negative charge on the regulatory IR-motif (*cdc20 IE*) impaired the interaction between APC/C and Mad3. Even though a compromised MCC-APC/C interaction is expected to result in leakage through mitosis, *cdc20 IE* cells exhibited a mitotic index that is similar to wild type. Considering *cdc20 IE* cells are not expected to inhibit the APC/C efficiently, we hypothesized that their high mitotic index could be due to a compromised Cdc20 function, as an APC/C activator. In order to test this possibility we next analysed abilities of the C-terminal Cdc20 mutants in activating the APC/C (recovering from the SAC) and promoting anaphase onset upon reformation of the spindle.

6.3 IR-motif of Cdc20 is required for recovering from the SAC arrest (*nda3-KM311*) and progressing into anaphase

Once the cells are released from a *nda3-KM311* block, microtubules re-polymerize, chromosomes are bi-oriented (SAC is satisfied), and cells recover from the SAC (activating the APC/C), which results in progression into anaphase (Vanoosthuyse et al., 2009). However, this was not the case for *cdc20 IE* cells. Despite the spindle reformation (30 minutes after the release from metaphase arrest), a considerable portion of *Cdc20 IE* cells (43%) remained arrested at metaphase; in fact some them were even stuck at early metaphase indicated by Plo1-GFP localisation (“one spot”) to the spindle pole bodies which had not separated yet (Figure 5.10B) (Mulvihill et al., 1999). This result suggests that the *cdc20 IE* mutant fails to fully perform its APC/C activating function, therefore is not able to trigger anaphase onset even after the re-polymerisation of microtubules. To be able to further characterize roles of the IR-motif, we need to analyse the mitotic progression rate of *cdc20 IE* cells in an unperturbed mitosis (using *cdc25-22* mediated G2 arrest), to determine the degree of their inability in progressing into anaphase.

Constitutive phosphorylation of Cdc20 C-terminus slightly decreases the rate of SAC recovery

Other C-terminal (phosphorylation) Cdc20 mutants recovered from the SAC more normally than the *cdc20 IE* cells did, yet with some variance depending on their mutation.

Although the overall SAC recovery trends (Figure 5.10C displays the line representing the average mitotic exit at 10, 20 and 30 minutes) were comparable throughout the release, kinase inactive *bub1-kd* cells exited mitosis faster than wild type, especially at the later stages (30 minutes) of the release from metaphase. Interestingly, phospho-deficient (at the C-terminus) *cdc20 S3A* cells phenocopied this, which is indicated by their slightly accelerated mitotic exit compared to wild type cells. According to this observation our hypothesis is as follows:

Phosphorylation of SAC proteins (yet to be discovered) by Bub1 may promote SAC maintenance during spindle damage. Once the spindle reforms (and the SAC is satisfied), the sites phosphorylated by Bub1 may need to be dephosphorylated to recover from the SAC and activate APC/C (similar to the SAC silencing activity of PP1 (Liu et al., 2010; Meadows et al., 2011)).

Accordingly, when the Bub1 kinase activity is absent (*bub1-kd*), it may be quicker to recover from the SAC arrest. Consistent with this hypothesis, lack of one of those Bub1 sites (as in the case of *cdc20 S3A*) may lead to a slightly accelerated SAC response (Figure 5.10C). If this hypothesis is true, then the phosphorylation and dephosphorylation of Cdc20 serine 482 may contribute to the regulation of SAC maintenance and the subsequent recovery from it respectively. Such a mechanism is not very unlikely, as threonine 79 (T79) of *Xenopus* Cdc20 has been shown to be in a dynamic state of phosphorylation and dephosphorylation mediated by Cdk1 and PP2A, respectively, which regulate the APC/C activation by Cdc20 in metaphase (Labit et al., 2012). In order to test whether the serine 482 phosphorylation has a key regulatory role in the context of SAC, we should analyse phosphatases, such as PP1 and PP2A, which may possibly reverse the phospho-modification of this residue.

Consistent with this hypothesis, constitutive (non-reversible) phosphorylation of serine 482 (*cdc20 S3E*) resulted in a slightly slower SAC recovery (Figure 5.10C). This suggest that dephosphorylation of serine 482 is not essential for the mitotic exit upon spindle reformation, yet it contributes to the rate of SAC recovery. Intriguingly, at the later stages of the release from the arrest, *cdc20 S3E* cells exhibited the "cut" phenotype more frequently than wild type and *cdc20 S3A* cells did (Figure 5.10B). In other words, more c*dc20 S3E* cells failed to segregate their chromosomes equally before the septation began. This might be due to a possible defect in microtubule-kinetochore attachment and/or chromosome bi-orientation caused by the non-reversible phosphorylation of serine 482. Hypothetically, the phosphorylation of serine 482 may be promoting the SAC, and thereby contributing to ensuring accurate chromosome segregation in the absence of kinetochore-microtubule attachments (or in the presence of spindle damage in our experiment). However, once microtubules attach to kinetochores (the spindle reforms, in our experiment), serine 482 may need to be dephosphorylated (that does not happen in *Cdc20 S3E*) to allow proper SAC recovery. Thus, the relatively slower and detectably inaccurate chromosome segregation in *Cdc20 S3E* cells suggest possible mechanisms for the regulation of SAC arrest and recovery through of phosphorylation and dephosphorylation of Cdc20 C-terminus.

Alternatively, slower SAC recovery (APC/C activation) might be due to a possible destabilisation of the *cdc20 S3E* levels, therefore depletion of the APC/C activator during the SAC arrest. We next analysed whether phospho-deficient or phospho-mimicking mutations affect the Cdc20 turnover rate during an active SAC arrest.

Effects of constitutive phosphorylation of Cdc20 C-terminus on its levels during the SAC arrest mediated by *nda3-KM311*

By inhibiting the biosynthesis of new Cdc20 (using the translation inhibitor cycloheximide) we showed that *cdc20 S1A* had the same turnover rate as the wild type Cdc20 (Figure 5.11), whereas the *cdc20 S3E* degradation rate appeared to be reduced during the *nda3-KM311* block (Figure 5.12). On the other hand, the *cdc20 S3E* cells treated with DMSO had the same levels of *cdc20 S3E* as wild type Cdc20, suggesting that total *cdc20 S3E* levels (the net result of expression and degradation, which are not affected in DMSO) are similar to wild type. Thus, the relatively slow SAC recovery rate of *cdc20 S3E* cells was probably not due to destabilisation of the *cdc20 S3E* levels during the SAC arrest. Instead, the slower SAC recovery rate of *cdc20 S3E* cells may be related to their reduced degradation rate. MCC (comprising Cdc20, Mad2 and Mad3) has been reported to dynamically assemble and disassemble during the SAC arrest, through Cdc20 ubiquitination mediated by Apc15 in budding yeast (Foster & Morgan, 2012) and humans (Uzunova et al., 2012). Reduced degradation rate of *cdc20 S3E* may have resulted from their reduced ubiquitination by the APC/C, which leads to a slower MCC disassembly during the SAC arrest. Accordingly, slower MCC disassembly would result in delayed APC/C activation, which may explain the SAC recovery delay of *cdc20 S3E* cells (Figure 5.10C).

6.4 Constitutive phosphorylation of Cdc20 C-terminus enhances the SAC response to the microtubule depolymerising drug CBZ

In addition to the spindle damage mediated by *nda3-KM311* block, we tested the C-terminal Cdc20 phosphorylation mutants also under the spindle damage caused by the microtubule depolymerising drug CBZ, in synchronous mitotic time courses (Figure 5.4). As we discussed previously, while the *nda3-KM311* cold sensitive mutation leads to a prolonged (9-10 hours (Kawashima et al., 2010)) and highly penetrant microtubule depolymerisation, CBZ concentrations in the cell probably reduce in time (due to the efflux pumps in yeast (Goffeau et al., 1997)) as even the fully SAC proficient wild type cells do not arrest in CBZ as long as in the *nda3-KM311* block (Yamaguchi et al., 2003). Therefore, the gradually decreasing spindle damage mediated by CBZ may

mimic the early and late stages of metaphase arrest, in terms of the amount of unattached kinetochores in the cell.

Soon after the CBZ treatment (at 30 minutes), both phospho-deficient (*cdc20 S3A* and *cdc20 S1A*) and phospho-mimicking (*cdc20 S3E*) cells arrested at metaphase like wild type (Figure 5.4B). At this early stage, phospho-deficient cells (*cdc20 S3A* and *cdc20 S1A*) were capable of localizing Mad3 to kinetochores at wild type levels. In wild type cells, Mad3 recruitment was Mad2 dependent, as it was abolished when Mad2 was deleted (Figure 5.5A and B). On the other hand, significantly more *cdc20 S3E* cells exhibited Mad3 kinetochore foci than wild type. Interestingly, unlike wild type cells, *cdc20 S3E* cells were able to rescue Mad3 recruitment in the absence of Mad2, at the early (30 minutes), but not late (60 minutes) stages of mitosis (in Figure 5.5B, compare *mad2* null strains: wild type Cdc20 and *cdc20 S3E*). This suggest that phosphorylation of Cdc20 C-terminus at early stages (which may be happening much later in wild type cells) might have strengthened the interaction between Mad3 and Cdc20, which presumably accounts for the enhancement (by *cdc20 S3E*) or the compensation of Mad2 deletion (by *cdc20 S3E mad2* null) in terms of Mad3 kinetochore localization. However, constitutive phosphorylation of Cdc20 C-terminus is not sufficient, and requires Mad2, to maintain this interaction at later stages. Such an interaction between Mad3 and Cdc20 may be possible, as we identified cross-links between Cdc20 C-terminus (K479, two residues upstream the mutated phospho-site serine 482) and Mad3 (mainly C-terminus, near its second KEN box) described in chapter four (Figure 4.9 and 4.10). Thus a transient negative charge on Cdc20 C-terminus (by phosphorylation and subsequent dephosphorylation) may be regulating the recruitment of MCC components at different stages of mitosis.

Later in mitosis (at 60 minutes), abilities of the phospho-deficient cells (*cdc20 S3A* and *cdc20 S1A*) to delay anaphase onset remained similar to that of wild type cells, suggesting that lack of Cdc20 C-terminus phosphorylation does not affect the SAC response significantly (Figure 5.4A and B). The delay of anaphase onset in response to spindle damage was Mad2 dependent, as the wild type cells could not delay anaphase anymore when Mad2 was deleted. On the other hand, significantly more *cdc20 S3E* cells delayed anaphase onset, which correlated with their more frequent Mad3 localization at kinetochores. This enhanced SAC response in *cdc20 S3E* cells

was completely dependent on Mad2, as the deletion of Mad2 abolished their arrest, and *cdc20 S3E mad2* null cells exited mitosis as frequently as *mad2* null cells did (Figure 5.4A and B). This result further confirms that *cdc20 S3E* retains the APC/C activating function of Cdc20, as it is as efficient as wild type Cdc20 to progress into anaphase in the absence of a functional SAC machinery (*mad2* null). In addition, this Mad2 dependency and the enhanced Mad3 recruitment (even in the lack of Mad2) of the phospho-mimicking *cdc20 S3E* mutant suggest that its strengthened SAC activity is probably mediated by the MCC, possibly through the direct inhibition of the APC/C. To gain more insight into interactions between the MCC components and how these interactions may contribute to their kinetochore recruitment, we intend to carry out several related experiments as follows:

- Repeat the same experiment in Mad2-GFP, *mad3* null background, to determine whether phosphorylation of Cdc20 C-terminus (*cdc20 S3E*) can enhance Cdc20-Mad2 interactions as well, and promote the kinetochore recruitment of Mad2.

- Replace the internal FLAG tag of Cdc20 with a GFP tag, to analyse how phosphorylation of Cdc20 may affect its cellular localization, especially at the kinetochores.

Mimicking the C-terminus Cdc20 phosphorylation enhances the MCC-APC/C interaction

We next demonstrated that in the presence of spindle damage caused by CBZ, lack of C-terminal Cdc20 phosphorylation (as in the case of *cdc20 S3A*) does not affect the MCC-APC/C interaction significantly, whereas constitutive phosphorylation of Cdc20 C-terminus (mimicked by *cdc20 S3E*) leads to a stronger and longer MCC-APC/C interaction. This result strengthens the possibility that the phosphorylation of Cdc20 C-terminus contributes to the SAC response through the MCC mediated inhibition of the APC/C. As we discussed in section 5.3.2, this enhanced MCC-APC/C interaction may be the outcome of multiple reasons (which are not mutually exclusive) as follows:

- ***cdc20 S3E* cells may form higher amounts of MCC**, which saturate and efficiently inhibit the APC/C molecules, leading to the enhanced anaphase delay (Figure 5.4). This mechanism is likely to occur, as the cells expressing *cdc20 S3E* have more abundant, and longer-lasting Mad3-GFP kinetochore localization, which may catalyse formation of more MCC molecules at the unattached kinetochores (presumably through more abundant Cdc20 and Mad2 recruitment as well). We intend to test this hypothesis by performing co-immunoprecipitation of *Cdc20 S3E*-FLAG and Mad2/ Mad3 to compare how efficiently the MCC is formed in this strain.

- ***cdc20 S3E* cells may have slower MCC disassembly**, resulting in MCC accumulation, and thereby excessive APC/C inhibition. As described before, MCC has been shown to dynamically assemble and disassemble during the SAC arrest, through Cdc20 ubiquitination mediated by Apc15 in in budding yeast (Foster & Morgan, 2012) and humans (Uzunova et al., 2012), and p31 in humans (Miniowitz-Shemtov et al., 2012; Westhorpe et al., 2011). This can be investigated by (i) analysing how efficiently the C-terminal Cdc20 mutants (expressed *in vitro*) are ubiquitinated in APC/C assays (ii) analysing the biophysical features of MCC molecules produced in insect cells (including different Cdc20 mutants), to determine whether the reduced MCC disassembly is caused by tighter interactions (due to Cdc20 C-terminus phosphorylation) within the MCC.

- ***cdc20 S3E* cells may assemble more potent MCC molecules which inhibit APC/C more efficiently, regardless of their amounts.** This possibility is also worth considering, as the enhanced APC/C inhibition in *cdc20 S3E* cells is strictly dependent on Mad2 (Figure 5.4). According to this hypothesis, *cdc20 S3E* requires Mad2 and Mad3 molecules to form an MCC molecule that can inhibit APC/C more efficiently, presumably through increased affinity of C-terminally phosphorylated Cdc20 (*cdc20 S3E*) towards the APC/C. In order to test this possibility, we intend to compare abilities of the MCC molecules, containing different Cdc20 mutants, to inhibit the APC/C *in vitro.*

6.5 Mimicking phosphorylation of Cdc20 C-terminus by Bub1 rescues the SAC defects in the absence of Bub1 kinase activity

Finally in the absence of Bub1 kinase activity (*bub1-kd*) we analysed *cdc20 S3E* and *cdc20 S1D*, mimicking constitutive phosphorylation of Cdc20 serine 482, that was identified as an *in vivo* phosphorylated site and an *in vitro* target of Bub1 kinase. (Hereafter we will refer to the *cdc20 S1D* allele to describe functional consequences of the phospho – mimicking mutation for two reasons: (i) the *S1D* mutation has successfully phenocopied the *S3E* mutation, (ii) the *S1D* mutation may be a more reliable allele as only this particular serine residue (S482D) was identified in the mass spectrometry analysis).

We demonstrated that mimicking the constitutive phosphorylation of a putative Bub1 site on Cdc20 (*cdc20 S1D*) significantly restored *two prominent SAC defects* in the cells, which lack Bub1 kinase activity and were exposed to a microtubule depolymerising drug: (i) delay of premature anaphase onset (Figure 5.13), (ii) kinetochore recruitment of the MCC components (Mad2, Mad3 and Cdc20) (Figure 5.14). In order to further characterize this phenotype, we intend to clarify its certain aspects by carrying out a series of experiments in the future as follows:

Is the compromised MCC-APC/C interaction in *bub1-kd* allele restored by *cdc20 S1D*?

We aim to address whether *cdc20 S1D* rescued the anaphase delay defect of *bub1-kd* (Figure 5.13), through restoring its highly defective MCC-APC/C interaction (Figure 3.6). To determine this, we intend to repeat the synchronous mitotic time course experiment in the presence of CBZ. Considering the enhanced kinetochore recruitment of Mad3 in *cdc20 S1D, bub1-kd* cells, we expect them to exhibit also a stronger and longer-lasting MCC- APC/C interaction than *bub1-kd* cells.

In addition, carrying out this experiment without CBZ may also provide insights into whether Bub1 kinase activity is required in an unperturbed mitosis, to maintain the relatively transient MCC-APC/C interaction observed in wild type cells (Zich et al., 2012); moreover this experiment may reveal whether *cdc20 S1D* allele (that appeared to have a comparable progression rate to wild type in an unperturbed mitosis, similar to *cdc20 S3E* in Figure 5.1) would affect the mitotic progression rate of *bub1-kd.*

Is the rescue phenotype (restored anaphase delay) dependent on kinetochores?

Previously (in section 5.6.4) we discussed that the enhancement of anaphase delay and MCC-APC/C interaction observed in the phospho – mimicking Cdc20 mutants may have resulted from assembly of more MCC molecules at the kinetochores. Considering *cdc20 S1D* significantly restored the Mad3 localisation defect of the *bub1-kd* allele, we hypothesize that this recruitment, which may be mediated by Cdc20 C-terminal phosphorylation, might have an upstream role in its contribution to anaphase delay. To address this hypothesis, we aim to assess the dependency of this rescue phenotype on kinetochore recruitment of Mad2 and Mad3. For this purpose, we will repeat the same experiment (Figure 5.13 and 14) in *bub3* null background, which abolishes the kinetochore recruitment of Bub1 and Mad3 (S. Heinrich et al., 2012; Shepperd et al., 2012b; Yamagishi et al., 2012).

Is Cdc20 phosphorylated by Bub1 at serine 482 *in vivo*?

Although the mutated phospho – site in *cdc20 S1D* (serine 482) was identified as an *in vivo* phosphorylated site (in mitotically arrested cells) and an *in vitro* target of Bub1 kinase, this possibility needs to be further analysed. In order to support the possibility that serine 482 is phosphorylated by Bub1 *in vivo*, we aim to perform several experiments as follows:

a) Analyse Cdc20+ (wild type) proteins from Bub1+ (wild type) or *bub1-kd* cells to determine whether lack of Bub1 kinase activity leads to a mobility shift of Cdc20 on Phos-tag protein gels, which have been reported to improve the detection of minor mobility shifts resulted from phospho – modification (Godfrey, Kuilman, & Uhlmann, 2015).

b) Purify Cdc20+ (wild type) proteins from Bub1+ (wild type) or *bub1-kd* cells, and identify which of the previously phosphorylated Cdc20 sites (by Bub1+) change in the absence of Bub1 kinase activity (especially serine 482).

c) Purify the C-terminal Cdc20 phospho – deficient mutants (*cdc20 S3A* and *cdc20 S1A*) from insect cells and use them in an *in vitro* Bub1 kinase assay, to determine whether lack of Cdc20 phosphorylation by Bub1 at these specific sites decrease its total phosphorylation signals. Previously we have attempted to express these Cdc20 mutants *in vitro* in rabbit reticulocyte system, however the proteins were not pure enough to detect subtle changes in the phosphorylation signal (data not shown).

d) Purify the C-terminal Cdc20 mutants (*cdc20 S1D, cdc20 S3E, cdc20 S3A* and *cdc20 S1A*) along with Cdc20+, to incubate with recombinant Mad2, Mad3 (to assemble the MCC) and Bub1+ kinase *in vitro*, and analyse their abilities to inhibit the APC/C activity (towards securin). This assay may provide direct evidence for whether Bub1 mediated Cdc20 C-terminal phosphorylation (either phosphorylation itself, or mimicking it via aspartate or glutamate mutations) inhibits APC/C directly. For this purpose, purification of the Cdc20 mutants using *in vitro* in rabbit reticulocyte system may be sufficient, as the products of this system have been shown to work successfully in *in vitro* APC/C assays (Foe et al., 2011; Foster & Morgan, 2012).

Does *cdc20 S1D* really rescue the *bub1-kd* phenotype or it has a dominant-positive effect on the SAC response?

By performing the experiments listed above, we expect to provide further evidence for the our hypothesis that C-terminal Cdc20 may be regulated by Bub1 kinase activity; yet we will need to rule out the possibility that the rescue phenotype (*cdc20 S1D, bub1-kd*) may be due to a dominant-positive effect of the *cdc20 S1D* allele rather than specifically restoring Bub1 kinase activity toward Cdc20 C-terminus. To investigate this possibility, we intend to determine whether the *cdc20 S1D* allele can restore the SAC defects of the alleles given below:

- ***bub1* null**, is SAC deficient due to lack of its functions described in chapter 1.
- ***mps1-kd,*** is severely defective in the SAC mainly because its kinase activity is required to localise the SAC proteins at kinetochores (London et al., 2012; Shepperd et al., 2012a; Yamagishi et al., 2012) and to promote the SAC response through Mad2 phosphorylation (Zich et al., 2012).
- ***mad3 KEN271AAA,*** is a Mad3 allele that lacks its second KEN-box function, and is not able to maintain anaphase delay or MCC-APC/C interaction, although it can assemble the MCC efficiently (Sczaniecka et al., 2008). This allele would especially be useful to determine whether Cdc20 C-terminus phosphorylation (*cdc20 S1D*) promotes the MCC-APC/C interaction independently of MCC assembly.

Understanding these aspects of Cdc20 C-terminus phosphorylation will hopefully strengthen our hypothesis that in addition to the Bub1-H2A-Sgo2-Aurora B pathway, a Bub1-Cdc20 mediated pathway may further promote the SAC response to ensure accurate chromosome segregation.

6.6 Relevance of Bub1 kinase activity and Cdc20 to therapeutic approaches

Loss of Bub1 kinase activity has been reported to cause significant aneuploidy and male subfertility in mice (Ricke, Jeganathan, Malureanu, Harrison, & Van Deursen, 2012). Together with several other studies, our findings imply that a possible Bub1-Cdc20 pathway (in addition to the Bub1-Aurora B pathway) may contribute to genome stability in higher eukaryotes considering the observations as follows:

- Bub1 kinase activity maintains the SAC response through direct phosphorylation of Cdc20 in humans (Tang, Shu, et al., 2004)
- Human Bub1 has a considerable specificity toward Cdc20, through its extended substrate recognition loop in the non-kinase region (Kang et al., 2008)
- Phosphorylation of human Cdc20 by Bub1 *in vitro* is not restricted to its N-terminus (Tang, Shu, et al., 2004), which suggests a possible phosphorylation of the C-terminus as well.
- C-terminal phosphorylation site of Cdc20 (serine 482) is conserved among higher eukaryotes, including humans (Figure 4.5)
- Mimicking C-terminal phosphorylation of fission yeast Cdc20 restores SAC related defects in the absence of Bub1 kinase activity (Figures 5.13 and 14)

On the basis of these findings, investigation of Bub1 kinase activity towards Cdc20 in vertebrates may increase our understanding of the underlying mechanisms by which it ensures genome stability. Furthermore, these studies may lead to novel cancer therapeutic strategies, considering that targeting Cdc20 may be a better approach than using the anti-mitotics (Huang, Shi, Orth, & Mitchison, 2009).

References

Adams, I. R., & Kilmartin, J. V. (2000). Spindle pole body duplication: a model for centrosome duplication? *Trends in Cell Biology*, *10*(8), 329–35. Retrieved from http://www.ncbi.nlm.nih.gov/pubmed/10884685

Barford, D. (2011). Structural insights into anaphase-promoting complex function and mechanism. *Philosophical Transactions of the Royal Society B: Biological Sciences*, *366*(1584), 3605–3624. http://doi.org/10.1098/rstb.2011.0069

Barford, D. (2011). *Structure, function and mechanism of the anaphase promoting complex (APC/C). Quarterly reviews of biophysics* (Vol. 44). http://doi.org/10.1017/S0033583510000259

Barysz, H., Kim, J. H., Chen, Z. A., Hudson, D. F., Rappsilber, J., Gerloff, D. L., … Earnshaw, W. C. (2015). Three-dimensional topology of the SMC2 / SMC4 subcomplex from chicken condensin I revealed by cross-linking and molecular modelling.

Berger, I., Fitzgerald, D. J., & Richmond, T. J. (2004). Baculovirus expression system for heterologous multiprotein complexes. *Nature Biotechnology*, *22*(12), 1583–1587. http://doi.org/10.1038/nbt1036

Brady, D. M., & Hardwick, K. G. (2000). Complex formation between Mad1p, Bub1p and Bub3p is crucial for spindle checkpoint function. *Current Biology*, *10*(11), 675–678. http://doi.org/10.1016/S0960-9822(00)00515-7

Burton, J. L., & Solomon, M. J. (2001). D box and KEN box motifs in budding yeast Hsl1p are required for APC-mediated degradation and direct binding to Cdc20p and Cdh1p. *Genes and Development*, *15*(18), 2381–2395. http://doi.org/10.1101/gad.917901

Burton, J. L., & Solomon, M. J. (2007). Mad3p, a pseudosubstrate inhibitor of APCCdc20 in the spindle assembly checkpoint. *Genes and Development*, *21*(6), 655–667. http://doi.org/10.1101/gad.1511107

Buschhorn, B. a, Petzold, G., Galova, M., Dube, P., Kraft, C., Herzog, F., … Peters, J.-M. (2011). Substrate binding on the APC/C occurs between the coactivator Cdh1 and the processivity factor Doc1. *Nature Structural & Molecular Biology*, *18*(1), 6–13. http://doi.org/10.1038/nsmb.1979

Chang, L., Zhang, Z., Yang, J., McLaughlin, S. H., & Barford, D. (2015). Atomic structure of the APC/C and its mechanism of protein ubiquitination. *Nature*. http://doi.org/10.1038/nature14471

Chao, W. C. H., Kulkarni, K., Zhang, Z., Kong, E. H., & Barford, D. (2012a). Structure of the mitotic checkpoint complex. *Nature*, *484*(7393), 208–213. http://doi.org/10.1038/nature10896

Chao, W. C. H., Kulkarni, K., Zhang, Z., Kong, E. H., & Barford, D. (2012b). Structure of the mitotic checkpoint complex. *Nature*, *484*(7393), 208–213. http://doi.org/10.1038/nature10896

Chen, R.-H. (2004). Phosphorylation and activation of Bub1 on unattached chromosomes facilitate the spindle checkpoint. *The EMBO Journal*, *23*(15), 3113–3121. http://doi.org/10.1038/sj.emboj.7600308

Cheryl D. Warren, † D. Michelle Brady, Johnston, R. C., Joseph S. Hanna, K. G. H., & Spencer*‡, and F. A. (2003). Distinct Chromosome Segregation Roles for Spindle Checkpoint Proteins. *Molecular Biology of the Cell*, *14*(June), 2559–2569. http://doi.org/10.1091/mbc.E02

Chung, E., & Chen, R.-H. (2003). Phosphorylation of Cdc20 is required for its inhibition by the spindle checkpoint. *Nature Cell Biology*, *5*(8), 748–753. http://doi.org/10.1038/ncb1022

Combe, C. W., Fischer, L., & Rappsilber, J. (2015). xiNET: Cross-link Network Maps With Residue Resolution. *Molecular & Cellular Proteomics*, *14*(4), 1137–1147. http://doi.org/10.1074/mcp.O114.042259

D'Angiolella, V., Mari, C., Nocera, D., Rametti, L., & Grieco, D. (2003). The spindle checkpoint requires cyclin-dependent kinase activity. *Genes & Development*, *17*(20), 2520–2525. http://doi.org/10.1101/gad.267603

D'Arcy, S., Davies, O. R., Blundell, T. L., & Bolanos-Garcia, V. M. (2010). Defining the molecular basis of BubR1 kinetochore interactions and APC/C-CDC20 inhibition. *Journal of Biological Chemistry*, *285*(19), 14764–14776. http://doi.org/10.1074/jbc.M109.082016

Da Fonseca, P. C. a, Kong, E. H., Zhang, Z., Schreiber, A., Williams, M. a, Morris, E. P., & Barford, D. (2011). Structures of APC/C(Cdh1) with substrates identify Cdh1 and Apc10 as the D-box co-receptor. *Nature*, *470*(7333), 274–278. http://doi.org/10.1038/nature09625

David, R. (2010). Cell cycle: dissecting mitosis. *Nature Reviews. Molecular Cell Biology*, *11*(5), 310. http://doi.org/10.1038/nrm2892

De Antoni, A., Pearson, C. G., Cimini, D., Canman, J. C., Sala, V., Nezi, L., … Musacchio, A. (2005). The Mad1/Mad2 complex as a template for Mad2 activation in the spindle assembly checkpoint. *Current Biology : CB*, *15*(3), 214–25. http://doi.org/10.1016/j.cub.2005.01.038

Diffley, J. F. X. (2004). Regulation of early events in chromosome replication. *Current Biology : CB*, *14*(18), R778–86. http://doi.org/10.1016/j.cub.2004.09.019

Elmore, Z. C., Beckley, J. R., Chen, J.-S., & Gould, K. L. (2014). Histone H2B ubiquitination promotes the function of the anaphase-promoting complex/cyclosome in Schizosaccharomyces pombe. *G3 (Bethesda, Md.)*, *4*(8), 1529–38. http://doi.org/10.1534/g3.114.012625

Elowe, S., Dulla, K., Uldschmid, A., Li, X., Dou, Z., & Nigg, E. a. (2010). Uncoupling of the spindle-checkpoint and chromosome-congression functions of BubR1. *Journal of Cell Science*, *123*(Pt 1), 84–94. http://doi.org/10.1242/jcs.056507

Enoch, T., & Nurse, P. (1990). Mutation of fission yeast cell cycle control genes abolishes dependence of mitosis on DNA replication. *Cell*, *60*(4), 665–73. Retrieved from http://www.ncbi.nlm.nih.gov/pubmed/2406029

Fang, G., Yu, H., & Kirschner, M. W. (1998). The checkpoint protein MAD2 and the mitotic regulator CDC20 form a ternary complex with the anaphase-promoting complex to control anaphase initiation. *Genes and Development*, *12*(12), 1871–1883. http://doi.org/10.1101/gad.12.12.1871

Fattaey, A., & Booher, R. N. (1997). Myt1: a Wee1-type kinase that phosphorylates Cdc2 on residue Thr14. *Progress in Cell Cycle Research*, *3*, 233–40. Retrieved from http://www.ncbi.nlm.nih.gov/pubmed/9552418

Fernius, J., & Hardwick, K. G. (2007). Bub1 kinase targets Sgo1 to ensure efficient chromosome biorientation in budding yeast mitosis. *PLoS Genetics*, *3*(11), 2312–2325. http://doi.org/10.1371/journal.pgen.0030213

Foe, I. T., Foster, S. a., Cheung, S. K., Deluca, S. Z., Morgan, D. O., & Toczyski, D. P. (2011). Ubiquitination of Cdc20 by the APC occurs through an intramolecular mechanism. *Current Biology*, *21*(22), 1870–1877. http://doi.org/10.1016/j.cub.2011.09.051

Foster, S. a., & Morgan, D. O. (2012). The APC/C Subunit Mnd2/Apc15 Promotes Cdc20 Autoubiquitination and Spindle Assembly Checkpoint Inactivation. *Molecular Cell*, *47*(6), 921–932. http://doi.org/10.1016/j.molcel.2012.07.031

Fraschini, R., Beretta, A., Sironi, L., Musacchio, A., Lucchini, G., & Piatti, S. (2001). Bub3 interaction with Mad2, Mad3 and Cdc20 is mediated by WD40 repeats and does not require intact kinetochores. *EMBO Journal*, *20*(23), 6648–6659. http://doi.org/10.1093/emboj/20.23.6648

Gassmann, R., Holland, A. J., Varma, D., Wan, X., Filiz, C., Oegema, K., … Desai, A. (2010). controls spindle checkpoint silencing in human cells Removal of Spindly from microtubule- attached kinetochores controls spindle checkpoint silencing in human cells, 957–971. http://doi.org/10.1101/gad.1886810

Godfrey, M., Kuilman, T., & Uhlmann, F. (2015). Nur1 Dephosphorylation Confers Positive Feedback to Mitotic Exit Phosphatase Activation in Budding Yeast. *PLoS Genetics*, *11*(1), e1004907. http://doi.org/10.1371/journal.pgen.1004907

Goffeau, A., Park, J., Paulsen, I. T., Jonniaux, J. L., Dinh, T., Mordant, P., & Saier, M. H. (1997). Multidrug-resistant transport proteins in yeast: Complete inventory and phylogenetic characterization of yeast open reading frames within the major facilitator superfamily. *Yeast*, *13*(1), 43–54. http://doi.org/10.1002/(SICI)1097-0061(199701)13:1<43::AID-YEA56>3.0.CO;2-J

Hardwick, K. G., Johnston, R. C., Smith, D. L., & Murray, A. W. (2000). MAD3 encodes a novel component of the spindle checkpoint which interacts with Bub3p, Cdc20p, and Mad2p. *Journal of Cell Biology*, *148*(5), 871–882. http://doi.org/10.1083/jcb.148.5.871

Hartwell, L. H., Culotti, J., Pringle, J. R., & Reid, B. J. (1974). Genetic control of the cell division cycle in yeast. *Science*, *183*, 46–51. http://doi.org/10.1126/science.183.4120.46

Hartwell, L. H., & Weinert, T. A. (1989). Checkpoints: controls that ensure the order of cell cycle events. *Science (New York, N.Y.)*, *246*(4930), 629–634. http://doi.org/10.1126/science.2683079

He, X., Patterson, T. E., & Sazer, S. (1997). The Schizosaccharomyces pombe spindle checkpoint protein mad2p blocks anaphase and genetically interacts with the anaphase-promoting complex. *Proceedings of the National Academy of Sciences of the United States of America*, *94*(15), 7965–7970. http://doi.org/10.1073/pnas.94.15.7965

Heinrich, S., Geissen, E.-M., Kamenz, J., Trautmann, S., Widmer, C., Drewe, P., … Hauf, S. (2013). Determinants of robustness in spindle assembly checkpoint signalling. *Nature Cell Biology*, *15*(11), 1328–39. http://doi.org/10.1038/ncb2864

Heinrich, S., Windecker, H., Hustedt, N., & Hauf, S. (2012). Mph1 kinetochore localization is crucial and upstream in the hierarchy of spindle assembly checkpoint protein recruitment to kinetochores. *Journal of Cell Science*, 4720–4727. http://doi.org/10.1242/jcs.110387

Herzog, F. (2009). Mitotic Checkpoint Complex. *Science*, *1985*(March), 1477–1481.

Holland, A. J., & Taylor, S. S. (2006). Cyclin-B1-mediated inhibition of excess separase is required for timely chromosome disjunction. *Journal of Cell Science*, *119*(Pt 16), 3325–36. http://doi.org/10.1242/jcs.03083

Howell, B. J., McEwen, B. F., Canman, J. C., Hoffman, D. B., Farrar, E. M., Rieder, C. L., & Salmon, E. D. (2001). Cytoplasmic dynein/dynactin drives kinetochore

protein transport to the spindle poles and has a role in mitotic spindle checkpoint inactivation. *Journal of Cell Biology*, *155*(7), 1159–1172. http://doi.org/10.1083/jcb.200105093

Howell, B. J., Moree, B., Farrar, E. M., Stewart, S., Fang, G., & Salmon, E. D. (2004). Spindle checkpoint protein dynamics at kinetochores in living cells. *Current Biology : CB*, *14*(11), 953–64. http://doi.org/10.1016/j.cub.2004.05.053

Huang, H. C., Shi, J., Orth, J. D., & Mitchison, T. J. (2009). Evidence that Mitotic Exit Is a Better Cancer Therapeutic Target Than Spindle Assembly. *Cancer Cell*, *16*(4), 347–358. http://doi.org/10.1016/j.ccr.2009.08.020

Izawa, D., & Pines, J. (2012). Mad2 and the APC/C compete for the same site on Cdc20 to ensure proper chromosome segregation. *Journal of Cell Biology*, *199*(1), 27–37. http://doi.org/10.1083/jcb.201205170

Kadura, S., He, X., Vanoosthuyse, V., Hardwick, K. G., & Sazer, S. (2005). The A78V mutation in the Mad3-like domain of Schizosaccharomyces pombe Bub1p perturbs nuclear accumulation and kinetochore targeting of Bub1p, Bub3p, and Mad3p and spindle assembly checkpoint function. *Molecular Biology of the Cell*, *16*(1), 385–95. http://doi.org/10.1091/mbc.E04-07-0558

Kalantzaki, M., Kitamura, E., Zhang, T., Mino, A., Novák, B., & Tanaka, T. U. (2015). Kinetochore-microtubule error correction is driven by differentially regulated interaction modes. *Nature Cell Biology*, *17*(4), 421–33. http://doi.org/10.1038/ncb3128

Kang, J., Yang, M., Li, B., Qi, W., Zhang, C., Shokat, K. M., … Yu, H. (2008). Structure and Substrate Recruitment of the Human Spindle Checkpoint Kinase Bub1. *Molecular Cell*, *32*(3), 394–405. http://doi.org/10.1016/j.molcel.2008.09.017

Kawashima, S. a, Yamagishi, Y., Honda, T., Ishiguro, K., & Watanabe, Y. (2010). Phosphorylation of H2A by Bub1 prevents chromosomal instability through localizing shugoshin. *Science (New York, N.Y.)*, *327*(5962), 172–177. http://doi.org/10.1126/science.1180189

King, E. M. J., van der Sar, S. J. a, & Hardwick, K. G. (2007). Mad3 KEN boxes mediate both Cdc20 and Mad3 turnover, and are critical for the spindle checkpoint. *PLoS ONE*, *2*(4). http://doi.org/10.1371/journal.pone.0000342

Kiyomitsu, T., Obuse, C., & Yanagida, M. (2007). Human Blinkin/AF15q14 Is Required for Chromosome Alignment and the Mitotic Checkpoint through Direct Interaction with Bub1 and BubR1. *Developmental Cell*, *13*(5), 663–676. http://doi.org/10.1016/j.devcel.2007.09.005

Klebig, C., Korinth, D., & Meraldi, P. (2009). Bub1 regulates chromosome segregation in a kinetochore-independent manner. *Journal of Cell Biology*, *185*(5), 841–858. http://doi.org/10.1083/jcb.200902128

Kraft, C., Herzog, F., Gieffers, C., Mechtler, K., Hagting, A., Pines, J., & Peters, J. M. (2003). Mitotic regulation of the human anaphase-promoting complex by phosphorylation. *EMBO Journal*, *22*(24), 6598–6609. http://doi.org/10.1093/emboj/cdg627

Kramer, E. R., Scheuringer, N., Podtelejnikov, a V, Mann, M., & Peters, J. M. (2000). Mitotic regulation of the APC activator proteins CDC20 and CDH1. *Molecular Biology of the Cell*, *11*(5), 1555–1569.

Krenn, V., Overlack, K., Primorac, I., Van Gerwen, S., & Musacchio, A. (2014). KI motifs of human Knl1 enhance assembly of comprehensive spindle checkpoint complexes around MELT repeats. *Current Biology*, *24*(1), 29–39. http://doi.org/10.1016/j.cub.2013.11.046

Labit, H., Fujimitsu, K., Bayin, N. S., Takaki, T., Gannon, J., & Yamano, H. (2012). Dephosphorylation of Cdc20 is required for its C-box-dependent activation of the APC/C. *The EMBO Journal*, *31*(15), 3351–3362. http://doi.org/10.1038/emboj.2012.168

Lara-Gonzalez, P., Scott, M. I. F., Diez, M., Sen, O., & Taylor, S. S. (2011). BubR1 blocks substrate recruitment to the APC/C in a KEN-box-dependent manner. *Journal of Cell Science*.

Lara-Gonzalez, P., & Taylor, S. S. (2012). Cohesion Fatigue Explains Why Pharmacological Inhibition of the APC/C Induces a Spindle Checkpoint-Dependent Mitotic Arrest. *PLoS ONE*, *7*(11). http://doi.org/10.1371/journal.pone.0049041

Lara-Gonzalez, P., Westhorpe, F. G., & Taylor, S. S. (2012). The spindle assembly checkpoint. *Current Biology*, *22*(22), R966–R980. http://doi.org/10.1016/j.cub.2012.10.006

Lau, D. T. C., & Murray, A. W. (2012). Mad2 and Mad3 cooperate to arrest budding yeast in mitosis. *Current Biology*, *22*(3), 180–190. http://doi.org/10.1016/j.cub.2011.12.029

Li, Y., Gorbea, C., Mahaffey, D., Rechsteiner, M., & Benezra, R. (1997). MAD2 associates with the cyclosome/anaphase-promoting complex and inhibits its activity. *Proceedings of the National Academy of Sciences of the United States of America*, *94*(23), 12431–12436. http://doi.org/10.1073/pnas.94.23.12431

Liang, H., Lim, H. H., Venkitaraman, A., & Surana, U. (2011). Cdk1 promotes kinetochore bi-orientation and regulates Cdc20 expression during recovery from

spindle checkpoint arrest. *The EMBO Journal*, *31*(2), 403–416. http://doi.org/10.1038/emboj.2011.385

Liu, D., Vleugel, M., Backer, C. B., Hori, T., Fukagawa, T., Cheeseman, I. M., & Lampson, M. a. (2010). Regulated targeting of protein phosphatase 1 to the outer kinetochore by KNL1 opposes Aurora B kinase. *Journal of Cell Biology*, *188*(6), 809–820. http://doi.org/10.1083/jcb.201001006

London, N., & Biggins, S. (2014a). Mad1 kinetochore recruitment by Mps1-mediated phosphorylation of Bub1 signals the spindle checkpoint. *Genes and Development*, *28*(2), 140–152. http://doi.org/10.1101/gad.233700.113

London, N., & Biggins, S. (2014b). Signalling dynamics in the spindle checkpoint response. *Nature Reviews Molecular Cell Biology*, *15*(11), 736–748. http://doi.org/10.1038/nrm3888

London, N., Ceto, S., Ranish, J. a., & Biggins, S. (2012). Phosphoregulation of Spc105 by Mps1 and PP1 regulates Bub1 localization to kinetochores. *Current Biology*, *22*(10), 900–906. http://doi.org/10.1016/j.cub.2012.03.052

Lõoke, M., Kristjuhan, K., & Kristjuhan, A. (2011). Extraction of genomic DNA from yeasts for PCR-based applications. *BioTechniques*, *50*(5), 325–328. http://doi.org/10.2144/000113672

Maldonado, M., & Kapoor, T. M. (2011). Constitutive Mad1 targeting to kinetochores uncouples checkpoint signalling from chromosome biorientation. *Nature Cell Biology*, *13*(4), 475–482. http://doi.org/10.1038/ncb2223

Matsumoto, T. (1997). A Fission Yeast Homolog of CDC20 / p55 CDC / Fizzy Is Required for Recovery from DNA Damage and Genetically Interacts with p34 cdc2, *17*(2), 742–750.

Mchedlishvili, N., Wieser, S., Holtackers, R., Mouysset, J., Belwal, M., Amaro, a. C., & Meraldi, P. (2012). Kinetochores accelerate centrosome separation to ensure faithful chromosome segregation. *Journal of Cell Science*, *125*(4), 906–918. http://doi.org/10.1242/jcs.091967

Meadows, J. C., Shepperd, L. a., Vanoosthuyse, V., Lancaster, T. C., Sochaj, A. M., Buttrick, G. J., … Millar, J. B. a. (2011). Spindle checkpoint silencing requires association of PP1 to both Spc7 and kinesin-8 motors. *Developmental Cell*, *20*(6), 739–750. http://doi.org/10.1016/j.devcel.2011.05.008

Millband, D. N., & Hardwick, K. G. (2002). Fission yeast Mad3p is required for Mad2p to inhibit the anaphase-promoting complex and localizes to kinetochores in a Bub1p-, Bub3p-, and Mph1p-dependent manner. *Molecular and Cellular Biology*, *22*(8), 2728–2742. http://doi.org/10.1128/MCB.22.8.2728-2742.2002

Miniowitz-Shemtov, S., Eytan, E., Ganoth, D., Sitry-Shevah, D., Dumin, E., & Hershko, a. (2012). Role of phosphorylation of Cdc20 in p31comet-stimulated disassembly of the mitotic checkpoint complex. *Proceedings of the National Academy of Sciences*, *109*(21), 8056–8060. http://doi.org/10.1073/pnas.1204081109

Moyle, M. W., Kim, T., Hattersley, N., Espeut, J., Cheerambathur, D. K., Oegema, K., & Desai, A. (2014). A Bub1-Mad1 interaction targets the Mad1-Mad2 complex to unattached kinetochores to initiate the spindle checkpoint. *Journal of Cell Biology*, *204*(5), 647–657. http://doi.org/10.1083/jcb.201311015

Mulvihill, D. P., Petersen, J., Ohkura, H., Glover, D. M., & Hagan, I. M. (1999). Plo1 kinase recruitment to the spindle pole body and its role in cell division in Schizosaccharomyces pombe. *Molecular Biology of the Cell*, *10*(8), 2771–2785.

Musacchio, A., & Salmon, E. D. (2007). The spindle-assembly checkpoint in space and time. *Nature Reviews. Molecular Cell Biology*, *8*(5), 379–393. http://doi.org/10.1038/nrm2163

Nilsson, J., Yekezare, M., Minshull, J., & Pines, J. (2008). The APC/C maintains the spindle assembly checkpoint by targeting Cdc20 for destruction. *Nature Cell Biology*, *10*(12), 1411–1420. http://doi.org/10.1038/ncb1799

Pan, J., & Chen, R. H. (2004). Spindle checkpoint regulates Cdc20p stability in Saccharomyces cerevisiae. *Genes and Development*, *18*(12), 1439–1451. http://doi.org/10.1101/gad.1184204

Petersen, J., & Hagan, I. M. (2003). S. pombe Aurora Kinase/Survivin Is Required for Chromosome Condensation and the Spindle Checkpoint Attachment Response. *Current Biology*, *13*(7), 590–597. http://doi.org/10.1016/S0960-9822(03)00205-7

Primorac, I., Weir, J. R., Chiroli, E., Gross, F., Hoffmann, I., van Gerwen, S., … Musacchio, A. (2013). Bub3 reads phosphorylated MELT repeats to promote spindle assembly checkpoint signaling. *eLife*, *2013*(2), 1–20. http://doi.org/10.7554/eLife.01030

Qi, W., & Yu, H. (2007). KEN-box-dependent degradation of the Bub1 spindle checkpoint kinase by the anaphase-promoting complex/cyclosome. *Journal of Biological Chemistry*, *282*(6), 3672–3679. http://doi.org/10.1074/jbc.M609376200

Ricke, R. M., Jeganathan, K. B., Malureanu, L., Harrison, A. M., & Van Deursen, J. M. (2012). Bub1 kinase activity drives error correction and mitotic checkpoint control but not tumor suppression. *Journal of Cell Biology*, *199*(6), 931–949. http://doi.org/10.1083/jcb.201205115

Rieder, C. L., Cole, R. W., Khodjakov, A., & Sluder, G. (1995). The checkpoint delaying anaphase in response to chromosome monoorientation is mediated by an inhibitory signal produced by unattached kinetochores. *Journal of Cell Biology*, *130*(4), 941–948. http://doi.org/10.1083/jcb.130.4.941

Rieder, C. L., Cole, R. W., Khodjakov, A., & Sluder, G. (1995). The checkpoint delaying anaphase in response to chromosome monoorientation is mediated by an inhibitory signal produced by unattached kinetochores. *The Journal of Cell Biology*, *130*(4), 941–8. Retrieved from http://www.pubmedcentral.nih.gov/articlerender.fcgi?artid=2199954&tool=pmcentrez&rendertype=abstract

Rischitor, P. E., May, K. M., & Hardwick, K. G. (2007). Bub1 is a fission yeast kinetochore scaffold protein, and is sufficient to recruit other spindle checkpoint proteins to ectopic sites on chromosomes. *PLoS ONE*, *2*(12), 1–6. http://doi.org/10.1371/journal.pone.0001342

Roberts, B. T., Farr, K. a, & Hoyt, M. a. (1994). The Saccharomyces cerevisiae checkpoint gene BUB1 encodes a novel protein kinase. *Molecular and Cellular Biology*, *14*(12), 8282–8291. http://doi.org/10.1128/MCB.14.12.8282.Updated

Ruchaud, S., Carmena, M., & Earnshaw, W. C. (2007). Chromosomal passengers: conducting cell division. *Nature Reviews. Molecular Cell Biology*, *8*(10), 798–812. http://doi.org/10.1038/nrm2257

Rudner, A. D., & Murray, A. W. (2000). Phosphorylation by Cdc28 activates the Cdc20-dependent activity of the anaphase-promoting complex. *Journal of Cell Biology*, *149*(7), 1377–1390. http://doi.org/10.1083/jcb.149.7.1377

Sazer, S., Lynch, M., & Needleman, D. (2014). Deciphering the evolutionary history of open and closed mitosis. *Current Biology : CB*, *24*(22), R1099–103. http://doi.org/10.1016/j.cub.2014.10.011

Sczaniecka, M., Feoktistova, A., May, K. M., Chen, J. S., Blyth, J., Gould, K. L., & Hardwick, K. G. (2008). The spindle checkpoint functions of Mad3 and Mad2 depend on a Mad3 KEN box-mediated interaction with Cdc20-anaphase-promoting complex (APC/C). *Journal of Biological Chemistry*, *283*(34), 23039–23047. http://doi.org/10.1074/jbc.M803594200

Sharp-Baker, H., & Chen, R. H. (2001). Spindle checkpoint protein Bub1 is required for kinetochore localization of Mad1, Mad2, Bub3, and CENP-E, independently of its kinase activity. *Journal of Cell Biology*, *153*(6), 1239–1249. http://doi.org/10.1083/jcb.153.6.1239

Shepperd, L. a., Meadows, J. C., Sochaj, A. M., Lancaster, T. C., Zou, J., Buttrick, G. J., … Millar, J. B. a. (2012a). Phosphodependent recruitment of Bub1 and Bub3 to Spc7/KNL1 by Mph1 kinase maintains the spindle checkpoint. *Current Biology*, *22*(10), 891–899. http://doi.org/10.1016/j.cub.2012.03.051

Shepperd, L. a., Meadows, J. C., Sochaj, A. M., Lancaster, T. C., Zou, J., Buttrick, G. J., … Millar, J. B. a. (2012b). Phosphodependent recruitment of Bub1 and Bub3 to Spc7/KNL1 by Mph1 kinase maintains the spindle checkpoint. *Current Biology*, *22*(10), 891–899. http://doi.org/10.1016/j.cub.2012.03.051

Sherlock, G., & Rosamond, J. (1993). Starting to cycle: G1 controls regulating cell division in budding yeast. *Journal of General Microbiology*, *139*(11), 2531–41. Retrieved from http://www.ncbi.nlm.nih.gov/pubmed/8277239

Sudakin, V., Chan, G. K., & Yen, T. J. (2001). Checkpoint inhibition of the APC/C in HeLa cells is mediated by a complex of BUBR1, BUB3, CDC20, and MAD2. *The Journal of Cell Biology*, *154*(5), 925–36. http://doi.org/10.1083/jcb.200102093

Sullivan, M., & Morgan, D. O. (2007). Finishing mitosis, one step at a time. *Nature Reviews. Molecular Cell Biology*, *8*(11), 894–903. http://doi.org/10.1038/nrm2276

Tang, Z., Bharadwaj, R., Li, B., & Yu, H. (2001). Mad2-Independent Inhibition of APCCdc20 by the Mitotic Checkpoint Protein BubR1. *Developmental Cell*, *1*(2), 227–237. http://doi.org/10.1016/S1534-5807(01)00019-3

Tang, Z., Shu, H., Oncel, D., Chen, S., & Yu, H. (2004). Phosphorylation of Cdc20 by Bub1 provides a catalytic mechanism for APC/C inhibition by the spindle checkpoint. *Molecular Cell*, *16*(3), 387–397. http://doi.org/10.1016/j.molcel.2004.09.031

Tang, Z., Sun, Y., Harley, S. E., Zou, H., & Yu, H. (2004). Human Bub1 protects centromeric sister-chromatid cohesion through Shugoshin during mitosis. *Proceedings of the National Academy of Sciences of the United States of America*, *101*(52), 18012–18017. http://doi.org/10.1073/pnas.0408600102

Taylor, S. S., & McKeon, F. (1997). Kinetochore localization of murine Bub1 is required for normal mitotic timing and checkpoint response to spindle damage. *Cell*, *89*(5), 727–735. http://doi.org/10.1016/S0092-8674(00)80255-X

Thornton, B. R., Ng, T. M., Matyskiela, M. E., Carroll, C. W., Morgan, D. O., David, P., & Toczyski, D. P. (2006). An architectural map of the anaphase-promoting complex An architectural map of the anaphase-promoting complex, *1*, 449–460. http://doi.org/10.1101/gad.1396906

Trowitzsch, S., Bieniossek, C., Nie, Y., Garzoni, F., & Berger, I. (2010). New baculovirus expression tools for recombinant protein complex production. *Journal of Structural Biology*, *172*(1), 45–54. http://doi.org/10.1016/j.jsb.2010.02.010

Uhlmann, F., Wernic, D., Poupart, M. A., Koonin, E. V, & Nasmyth, K. (2000). Cleavage of cohesin by the CD clan protease separin triggers anaphase in yeast.

Cell, *103*(3), 375–86. Retrieved from http://www.ncbi.nlm.nih.gov/pubmed/11081625

Uzunova, K., Dye, B. T., Schutz, H., Ladurner, R., Petzold, G., Toyoda, Y., … Peters, J.-M. (2012). APC15 mediates CDC20 autoubiquitylation by APC/CMCC and disassembly of the mitotic checkpoint complex. *Nature Structural & Molecular Biology*, (September), 1–10. http://doi.org/10.1038/nsmb.2412

Van Voorhis, V. a., & Morgan, D. O. (2014). Activation of the APC/c ubiquitin ligase by enhanced E2 efficiency. *Current Biology*, *24*(13), 1556–1562. http://doi.org/10.1016/j.cub.2014.05.052

Vanoosthuyse, V., & Hardwick, K. G. (2005). Bub1 and the multilayered inhibition of Cdc20-APC/C in mitosis. *Trends in Cell Biology*, *15*(5), 231–233. http://doi.org/10.1016/j.tcb.2005.03.003

Vanoosthuyse, V., Meadows, J. C., van der Sar, S. J. A., Millar, J. B. A., & Hardwick, K. G. (2009). Bub3p facilitates spindle checkpoint silencing in fission yeast. *Molecular Biology of the Cell*, *20*(24), 5096–105. http://doi.org/10.1091/mbc.E09-09-0762

Vanoosthuyse, V., Prykhozhij, S., & Hardwick, K. G. (2007). Shugoshin 2 regulates localization of the chromosomal passenger proteins in fission yeast mitosis. *Molecular Biology of the Cell*, *18*(5), 1657–69. http://doi.org/10.1091/mbc.E06-10-0890

Vanoosthuyse, V., Valsdottir, R., Javerzat, J.-P., & Hardwick, K. G. (2004). Kinetochore targeting of fission yeast Mad and Bub proteins is essential for spindle checkpoint function but not for all chromosome segregation roles of Bub1p. *Molecular and Cellular Biology*, *24*(22), 9786–9801. http://doi.org/10.1128/MCB.24.22.9786-9801.2004

Vernieri, C., Chiroli, E., Francia, V., Gross, F., & Ciliberto, A. (2013). Adaptation to the spindle checkpoint is regulated by the interplay between Cdc28/Clbs and PP2ACdc55. *Journal of Cell Biology*, *202*(5), 765–778. http://doi.org/10.1083/jcb.201303033

Vink, M., Simonetta, M., Transidico, P., Ferrari, K., Mapelli, M., De Antoni, A., … Musacchio, A. (2006). In Vitro FRAP Identifies the Minimal Requirements for Mad2 Kinetochore Dynamics. *Current Biology*, *16*(8), 755–766. http://doi.org/10.1016/j.cub.2006.03.057

Vleugel, M., Hoek, T. a., Tromer, E., Sliedrecht, T., Groenewold, V., Omerzu, M., & Kops, G. J. P. L. (2015). Dissecting the roles of human BUB1 in the spindle assembly checkpoint. *Journal of Cell Science*, *128*(16), 2975–2982. http://doi.org/10.1242/jcs.169821

Vleugel, M., Tromer, E., Omerzu, M., Groenewold, V., Nijenhuis, W., Snel, B., & Kops, G. J. P. L. (2013). Arrayed BUB recruitment modules in the kinetochore scaffold KNL1 promote accurate chromosome segregation. *The Journal of Cell Biology*, *203*(6), 943–955. http://doi.org/10.1083/jcb.201307016

von Schubert, C., Cubizolles, F., Bracher, J. M., Sliedrecht, T., Kops, G. J. P. L., & Nigg, E. A. (2015). Plk1 and Mps1 Cooperatively Regulate the Spindle Assembly Checkpoint in Human Cells. *Cell Reports*, *12*(1), 66–78. http://doi.org/10.1016/j.celrep.2015.06.007

Westhorpe, F. G., Tighe, a., Lara-Gonzalez, P., & Taylor, S. S. (2011). p31comet-mediated extraction of Mad2 from the MCC promotes efficient mitotic exit. *Journal of Cell Science*, *124*(22), 3905–3916. http://doi.org/10.1242/jcs.093286

Windecker, H., Langegger, M., Heinrich, S., & Hauf, S. (2009). Bub1 and Bub3 promote the conversion from monopolar to bipolar chromosome attachment independently of shugoshin. *EMBO Reports*, *10*(9), 1022–1028. http://doi.org/10.1038/embor.2009.183

Yamagishi, Y., Yang, C.-H., Tanno, Y., & Watanabe, Y. (2012). MPS1/Mph1 phosphorylates the kinetochore protein KNL1/Spc7 to recruit SAC components. *Nature Cell Biology*, *14*(7), 746–752. http://doi.org/10.1038/ncb2515

Yamaguchi, S., Decottignies, A., & Nurse, P. (2003). Function of Cdc2p-dependent Bub1p phosphorylation and Bub1p kinase activity in the mitotic and meiotic spindle checkpoint. *EMBO Journal*, *22*(5), 1075–1087. http://doi.org/10.1093/emboj/cdg100

Yanagida, M. (1998). Fission yeast cut mutations revisited: control of anaphase. *Trends in Cell Biology*, *8*(4), 144–9. Retrieved from http://www.ncbi.nlm.nih.gov/pubmed/9695827

Yu, H., & Tang, Z. (2005). Bub1 multitasking in mitosis. *Cell Cycle*, *4*(2), 262–265. http://doi.org/10.4161/cc.4.2.1487

Yudkovsky, Y., Shteinberg, M., Listovsky, T., Brandeis, M., & Hershko, a. (2000). Phosphorylation of Cdc20/fizzy negatively regulates the mammalian cyclosome/APC in the mitotic checkpoint. *Biochemical and Biophysical Research Communications*, *271*(2), 299–304. http://doi.org/10.1006/bbrc.2000.2622

Zich, J., Sochaj, A. M., Syred, H. M., Milne, L., Cook, A. G., Ohkura, H., … Hardwick, K. G. (2012). Kinase activity of fission yeast Mph1 Is required for Mad2 and Mad3 to stably bind the anaphase promoting complex. *Current Biology*, *22*(4), 296–301. http://doi.org/10.1016/j.cub.2011.12.049

Acknowledgements

I would like to thank everyone who has contributed to make the last four years nice and memorable for me, but I am especially grateful to…

My supervisor Kevin. Thank you very much for giving me the opportunity to work in your lab, for providing excellent guidance and continuous motivation throughout my project, and for everything you have taught me in my PhD. It has been a pleasure to work with you and learn from our conversations.

Karen, for your positive attitude and generosity in sharing your fission yeast knowledge no matter how busy you were. I will miss our conversations during the tea time and lab meetings.

Ivan, for being helpful throughout our stay in the lab. Considering we started more or less the same time, we have learned many things together and it has been great to exchange ideas with you. I wish you all the best for your next step.

Ioanna, you have joined us recently but quickly adapted with your cheerful mood. I hope Bub1 will make you happy very soon.

Adele, Ken and Malcolm for providing very useful feedback throughout my PhD.

Marston lab people, for the traditional Friday afternoon music and making the lab a fun place to work.

Members of Ohkura group, for nice conversations during our traditional cake sessions and all the fruit flies you set free!

My family, for their encouragement and support.

Finally, Edinburgh University, for kindly funding my PhD. This has been a life changing opportunity, and I really appreciate that.